PHOTOFERMENTATIVE HYDROGEN PRODUCTION FROM MOLASSES IN TUBULAR PHOTOBIOREACTOR WITH pH CONTROL

A THESIS SUBMITTED TO
THE GRADUATE SCHOOL OF NATURAL AND APPLIED SCIENCES
OF
MIDDLE EAST TECHNICAL UNIVERSITY

BY

FATMA BETÜL OFLAZ

IN PARTIAL FULFILLMENT OF THE REQUIREMENTS
FOR
THE DEGREE OF MASTER OF SCIENCE
IN
CHEMICAL ENGINEERING

JULY 2019

Approval of the thesis:

PHOTOFERMENTATIVE HYDROGEN PRODUCTION FROM MOLASSES IN TUBULAR PHOTOBIOREACTOR WITH PH CONTROL

submitted by **FATMA BETÜL OFLAZ** in partial fulfillment of the requirements for the degree of **Master of Science in Chemical Engineering Department, Middle East Technical University** by,

Prof. Dr. Halil Kalıpçılar
Dean, Graduate School of **Natural and Applied Sciences** _____

Prof. Dr. Pınar Çalık
Head of Department, **Chemical Engineering** _____

Assist. Prof. Dr. Harun Koku
Supervisor, **Chemical Engineering, METU** _____

Examining Committee Members:

Prof. Dr. Pınar Çalık
Chemical Engineering, METU _____

Assist. Prof. Dr. Harun Koku
Chemical Engineering, METU _____

Assoc. Prof. Dr. Çağdaş Son
Biology, METU _____

Assoc. Prof. Dr. Eda Çelik Akdur
Chemical Engineering, Hacettepe University _____

Assist. Prof. Dr. Yasemin Dilşad Yılmazel
Environmental Engineering, METU _____

Date: 25.07.2019

I hereby declare that all information in this document has been obtained and presented in accordance with academic rules and ethical conduct. I also declare that, as required by these rules and conduct, I have fully cited and referenced all material and results that are not original to this work.

Name, Surname: Fatma Betül Oflaz

Signature:

ABSTRACT

PHOTOFERMENTATIVE HYDROGEN PRODUCTION FROM MOLASSES IN TUBULAR PHOTOBIOREACTOR WITH PH CONTROL

Oflaz, Fatma Betül
Master of Science, Chemical Engineering
Supervisor: Assist. Prof. Dr. Harun Koku

July 2019, 240 pages

Biological hydrogen production has the potential to supply hydrogen from various wastes as feedstock and operation under ambient conditions. In order to obtain cost effective production, photobioreactors (PBRs) that can operate for long durations while utilizing waste are necessary. Two primary issues limiting the duration are decrease in pH and the non-optimal C/N ratio. The main aim of this study was to construct and operate a pH control system for a pilot scale photobioreactor (20 L) to achieve prolonged outdoor hydrogen production from molasses by *R. capsulatus* by stabilizing pH during operation.

Optimum C/N ratio was also investigated for molasses utilization by *R. capsulatus* for indoor and simulated outdoor conditions in small scale photobioreactors in batch mode. Simulated outdoor conditions for day and night cycle were designed as indoor experiments with changing temperature and light/dark cycle. Effects of constant pH under indoor were investigated to increase molasses utilization in small scale.

Long-term outdoor hydrogen production on diluted molasses in a pilot-scale PBR using photofermentative bacteria was demonstrated. The experiment lasted 48 days and carried out on August 16 and October 2, 2017. PID control system was chosen to

control pH and it was successfully implemented. The highest productivity was 0.69 mol $H_2/(m^3.h)$.

For small-scale experiments, the C/N ratio was decided as 45 and the highest productivities were 0.38 and 0.69 mol $H_2/(m^3.h)$, under indoor and simulated outdoor conditions, respectively. With constant pH conditions, molasses concentration could be increased to 15 from 5 mM with better productivity.

Keywords: Photofermentation, pH control, Rhodobacter capsulatus, Molasses, C/N ratio, Outdoor

ÖZ

pH KONTROLÜ İLE TÜBÜLER FOTOBİYOREAKTÖRDE MELASTAN FOTOFERMENTATİF HİDROJEN ÜRETİMİ

Oflaz, Fatma Betül
Yüksek Lisans, Kimya Mühendisliği
Tez Danışmanı: Dr. Öğr. Üyesi Harun Koku

Temmuz 2019, 240 sayfa

Biyolojik hidrojen üretimi, çeşitli atıkların hammadde olarak kullanılmasını ve çevre koşullarında çalışılarak hidrojen eldesini sağlama potansiyeline sahiptir. Ekonomik bir üretim elde etmek için, atık kullanarak uzun süreler çalışabilen fotobiyoreaktörler (PBR) gereklidir. Süreyi sınırlayan iki ana konu, pH değerindeki azalma ve optimal olmayan C/N oranıdır. Bu çalışmanın temel amacı, pH'ı stabilize ederek atık şekerden *R. capsulatus* ile uzun süreli dış mekan hidrojen üretimi elde etmek için pilot ölçekli bir fotobiyoreaktöre (20 L) bir pH kontrol sistemi eklemek ve işletmektir.

Optimum C/N oranı, küçük ölçekli fotobiyoreaktörlerde iç ve dış mekân koşullarında *R. capsulatus* ile melas kullanımında da incelenmiştir. Gündüz ve gece döngüsü için simüle edilmiş dış ortam koşulları, değişen sıcaklık ve aydınlık / karanlık döngüsüyle iç mekân denemesi olarak tasarlanmıştır. Oda koşullarında pH sabit tutularak küçük ölçek deneyleri artan melas miktarları ile ayrıca denenmiştir.

Pilot ölçekli PBR'de seyreltilmiş melasta uzun süreli dış mekan hidrojen üretimi gösterilmiştir. Deney 48 gün sürmüştür. pH kontrolü için PID kontrol sistemi seçilmiş ve başarıyla uygulanmıştır. En yüksek hidrojen üretim hızı 0.69 mol $H_2/(m^3.h)$ olarak elde edilmiştir.

C/N oranına iç ve dış mekan simülasyonları için 45 optimum olarak bulunmuştur, en yüksek hidrojen üretim hızı sırasıyla 0,38 ve 0,69 mol $H_2/(m^3.h)$ olarak belirlenmiştir. Sabit pH koşullarında, melas konsantrasyonu 5 mM'den 15'e yükseltilmiş ve hidrojen üretim hızı arttırılmıştır.

Anahtar Kelimeler: Fotofermentasyon, pH kontrolü, Rhodobacter capsulatus, Melas, C / N oranı, Dış mekan

To my family,

ACKNOWLEDGEMENTS

I would like to express my sincere gratitude to my supervisor Assist. Prof. Dr. Harun Koku for his continuous support, guidance, motivation and generous advice throughout my master studies. His immense knowledge and experiences influenced my perspective on science deeply.

I would like to give my special thanks to Prof. Dr. Meral Yücel and Prof. Dr. İnci Eroğlu for their precious suggestions and help. Their invaluable feedback on my research enlightened my point of view. I thank Assoc. Prof. Dr. Çağdaş Son for his help in the images of the bacteria, and Assoc. Prof. Dr. Serkan Kıncal for help in the process control systems.

I thank Dr. Muazzez Gürgan Eser and Dr. Emrah Sağır for their help in the biological preparation experiments and my labmate Dilan Savaştürk.

I would like to thank the technical staff of the chemical engineering department, İsa Çağlar and Gazi Saranay, for their technical help and support.

I would like to express my special thanks to Öznur Doğan and Duygu Sezen Polat for their friendship and support. They were always ready to help and motivate me. I am thankful to my roommates; Selda Odabaşı, Ezgi Gözde and Ahmet Fırat Taşkın and my groupmate Özge Demirdoğan for their kind friendship. Their friendships were irreplaceable.

I sincerely thank all members of my family, especially my parents for their help, support and love in all my life. I have no words to describe my mother's love, care, and support. I am thankful to my sweet father for his understanding and patience. I owe a lot to my precious sister Merve Derya Oflaz for her limitless support and encouragement. She is my sister and best friend who always watching my back.

I would like to thank deeply my cousin Seçil Tanrıverdi for her endless concern and support. There are so many memories that we had and so many that we will.

TABLE OF CONTENTS

LIST OF TABLES

TABLES

LIST OF FIGURES

FIGURES

LIST OF ABBREVIATIONS

ABBREVIATIONS	
PNSB	Purple non-sulfur bacteria
HPM	Hydrogen production medium
C/N	Carbon to nitrogen ratio
R. capsulatus	*Rhodobacter capsulatus*
hup^-	Uptake Hydrogenase Deficient
VFA	Volatile fatty acids
ADP	Adenosine di-Phosphate
ATP	Adenosine tri-Phosphate
CoA	Coenzyme A
PFL	Pyruvate formate lyase
FHL	Formate hydrogen lyase
PFOR	Pyruvate ferredoxin oxidoreductase
TCA	Citric acid cycle
G-6-P	Glucose 6-phosphate
F-6-Pf	Ructose 6-phosphate
6-PG	6-phosphogluconate
KDPG	2-keto-3-deoxy-6-phosphogluconate
KDG	2-keto-3-deoxygluconate
F-1-P	Fructose-1-phosphate

DHAP	Dihydroxyacetone phosphate
3PGAL	Glyceraldehyde 3-phosphate
3-PGA	3-phosphoglyceric acid,
PHB	Poly-β-hydroxybutyrate,
PEP	Phosphoenolpyruvate.
PS	Photosystem
Fd	Ferredoxin
ICM	Intracytoplasmic membrane
PRK	Phosphoribulokinase
RubisCO	Ribulose 1,5-bisphosphate carboxylase
etfp	Electron-transfer flavoprotein
PMF	Proton motive force
Glu	Glutamate
Arg	Arginine
Lys	Lysine
CFA	Cyclopropane fatty acids
UFA	Unsaturated fatty acids
GABA	γ-aminobutyric acid
EGSB	Expanded granular sludge bed
PID	Proportional-integral-derivative
STR	Stirred-tank reactor

CSTR	Continuous stirred-tank reactor
PBR	Photobioreactor
MPYE	Mineral–peptone–yeast extract
OD	Optical density
HPLC	High-Performance Liquid Chromatography
RI	Refractive index
lc	Culture liter
gdcw	Gram dry cell weight of bacteria

LIST OF SYMBOLS

SYMBOLS	
e(t)	Error value
r(t)	Set point
y(t)	Process output
u(t)	Controller output
d(t)	Disturbance signal
$\bar{u}$	Bias (steady-state) value
K	Process gain
τ	Time constant
θ	Time delay
K_c	Controller gain
τ_I	Integral time
τ_D	Derivative time

CHAPTER 1

INTRODUCTION

Today, global energy is supplied mostly by fossil fuel sources. The finite nature of these resources, coupled to pollution and large scale emissions of greenhouse gases due to their consumption, have intensified the demand for renewable energy. Hydrogen is one of the most promising energy carriers since it has a high heating value (12.7 kJ/m^3) and produces only water upon combustion (Das and Veziroğlu 2001). Moreover, the conversion efficiency of hydrogen to electricity can be improved by using fuel cells (Arooj et al. 2008), and it can be stored as gas metal hydrides (Ramachandran and Menon 1998).

Hydrogen is one of the most promising energy carriers with the highest energy content of any known fuels by weight as 142 MJ/kg, nearly two times of natural gas (55 MJ/kg) and three times of gasoline (46 MJ/kg) (World Nuclear Association 2016). Hydrogen has been used as an energy carrier for a long time. Hydrogen was used for street lightening and to supply home energy need in many countries from the 1960s. With the development of fuel cell technology around 1990s, hydrogen has attracted considerable attention (Wietschel and Ball 2009). Nowadays, 700 billion Nm^3 hydrogen is being produced and this amount can meet the need of 600 billion fuel cell cars (Staffell et al. 2019). Chemical and petrochemical industries utilize most of the produced hydrogen.

Natural gas reforming, gasification, and water electrolysis are the main hydrogen production methods. Hydrogen was produced 48% from natural gas, 30% from heavy oils and naphtha, and 18% from coal and 4% from electrolysis (Kothari, Buddhi, and Sawhney 2008; Nikolaidis and Poullikkas 2017). Natural gas reforming is the cheapest hydrogen production method with low CO_2 emission among other methods utilizing

fossil fuel (Kalamaras and Efstathiou 2013). However, water electrolysis is a sustainable and renewable hydrogen production source by utilizing wind power, hydropower or photovoltaics. Such methods typically require high production costs. Biological hydrogen production is a potential solution for cost effective process utilizing solar energy and wastes (Androga et al. 2014).

Direct and indirect biophotolysis, dark fermentation, and photofermentation are the main biological hydrogen production methods. In direct and indirect biophotolysis, hydrogen can be produced directly from the water with the utilization of sunlight. In dark fermentation, carbon sources including organic wastes could be utilized to produce hydrogen in the absence of oxygen. In photofermentation, carbon sources including organic acids and wastes can be utilized to produce hydrogen under anoxygenic conditions and existence of light (Nath and Das 2004).

Photofermentative production using purple non-sulfur bacteria (PNSB) is favorable because of its high theoretical conversion yield, high purity of produced hydrogen, the capability of PNSB to use a wide portion of the light spectrum (from 300 to 1000 nm), lack of O_2 evaluation which inhibits enzymes responsible for H_2 production, and their ability to utilize agricultural and food wastes among several biohydrogen production routes (Budiman and Wu 2018; Koku et al. 2002).

PNSB are commonly used in photofermentation studies. The optimum temperature of these bacteria is between 30^{o}C and 35 ^{o}C, while the optimum pH for hydrogen production is typically between 6.8 and 7.2 (Fang, Liu, and Zhang 2005; Sasikala, Ramana, and Raghuveer Rao 1991). Öztürk improved the hydrogen production by deleting the gene coding for the uptake hydrogenases, which is responsible for hydrogen consumption, of *Rhodobacter capsulatus* YO3 (hup^-) (Ozturk et al. 2006).

Sugar-containing substances can be readily used as the carbon source for PNSB. For example, thick juice and sugar beet molasses are potential feedstocks (Sagir et al. 2017). In particular, sugar beet molasses, a thick syrup formed as a byproduct of sucrose crystallization contains a high amount of sucrose (50% w/w) as the primary

carbon source. Also, various amino acids and trace elements promoting hydrogen production activity such as iron and molybdenum (Sagir et al. 2018). Small (Sagir et al. 2017) and pilot-scale runs with PNSB (Kayahan, Eroglu, and Koku 2017; Savasturk, Kayahan, and Koku 2018) have yielded promising hydrogen production results when sucrose from beet molasses was utilized by PNSB with single-stage photofermentation. However, the productivity and duration of production are still limited and several factors such as pH, nutrient and ion concentrations (Na^+ and NH^{4+}), the carbon-to-nitrogen (C/N) ratio, and bacterial strain capacities remain to be optimized for stable, prolonged hydrogen production. This is especially an issue in large-scale outdoor runs, in which the daily fluctuation of temperature and light intensity introduces additional variability.

Temperature, pH, C/N ratio, inoculated cell age, inoculation ratio and concentration of Mo-Fe are some key parameters that affect hydrogen production significantly.

For continuous, long-term photofermentative hydrogen production, one challenge for long-term is the optimization of the carbon-to-nitrogen (C/N) ratio. Hydrogen production by PNSB is mainly through the action of the (Mo-Fe) nitrogenase, which catalyzes the formation of ammonium. An abundance of nitrogen sources relative to the carbon content of the nutrient medium may also promote ammonia formation, which then suppresses the activity of nitrogenase. Thus the selection and regulation of the optimal carbon-to-nitrogen (C/N) ratio has been found to be critical for hydrogen production (Androga, Özgür, et al. 2011a; Eroglu et al. 1999; Savasturk, Kayahan, and Koku 2018; Shi and Yu 2005). A low C/N ratio reduces lag and promotes high initial rates of hydrogen production but also results in a shorter period of hydrogen production (Eroglu et al. 1999; Savasturk, Kayahan, and Koku 2018), whereas a high value results in long lag times and unstable operation (Kayahan, Eroglu, and Koku 2017).

pH also has a substantial effect on fermentative hydrogen production, and modifies the enzyme activity, the diversity of the side products and the toxicity of harmful

substances as demonstrated in many studies (Akhlaghi et al. 2017; Braz Romão et al. 2018; Fang and Liu 2002; Hwang et al. 2004; Khanal et al. 2004; I. S. Kim et al. 2004; B. F. Liu et al. 2010; Shi and Yu 2005; Xie et al. 2010). Accumulation of fermentation products such as acetic, lactic, propionic, butyric and formic acids decreases the pH of the medium. While the optimum pH for photofermentative hydrogen production is typically between 6.8 and 7.2 (Fang, Liu, and Zhang 2005; Sasikala, Ramana, and Raghuveer Rao 1991), it has been reported in the fermentation of molasses that the pH decreases steadily to values as low as 4, with concomitant termination of hydrogen production (Kayahan, Eroglu, and Koku 2016, 2017; Keskin and Hallenbeck 2012; J. Li et al. 2007; Ren et al. 2006; Sagir et al. 2017). This behavior is consistent with the optimal range of nitrogenase activity, reported as 6.5-7.5 for both in vivo and in vitro experiments (Koku et al. 2002; Peng et al. 1987; Pham and Burgess 1993). To mitigate the effects of decreasing pH, various strategies have been suggested, such as starting with a slightly higher value of pH (Khanal et al. 2004; Sinha and Pandey 2011), increased buffer concentrations (B. F. Liu et al. 2010; Özgür, Mars, et al. 2010) or modulating the feed pH (Jianzheng et al. 2002; Kayahan, Eroglu, and Koku 2016, 2017; J. Li et al. 2007). However, the initial pH has to be limited to 6-9, the range favorable for bacterial growth (Sasikala et al. 1993), so this measure is not sufficient for long-term operations. A high initial buffer concentration is not feasible either due to economic and environmental aspects. It has been observed that increasing the buffer concentration from 20 mM to 50 mM did not eliminate the decrease in pH (Sagir et al. 2017) and higher buffer concentrations could be inhibitory for growth. A third option is the modulation of the feed pH to restore the optimal range of the medium pH, but it has been observed that once hydrogen production stops, it cannot be recovered simply by the readjustment of the pH (Jianzheng et al. 2002; Kayahan, Eroglu, and Koku 2016, 2017; J. Li et al. 2007). Thus, an automated pH control seems to be necessary for long-term photofermentative hydrogen production. This might be straightforward in small-scale conventional systems, where small volumes allow uniform control due to good mixing. On the other hand, large volumes require custom-

built complex geometries such as tubular designs which provide a high surface to volume ratio (Palamae et al. 2018).

In addition to ammonium, alkali cations such as Na^{+}, K^{+} and Ca^{+2}, which are in fact necessary for bacterial growth, have been reported to affect hydrogen production negatively when at higher concentrations (Argun, Kargi, and Kapdan 2009; Guwy et al. 2011; D. Kim, Kim, and Shin 2009; Uygur and Kargı 2004). Medium dilution has been employed as a strategy in two-stage fermentation to prevent inhibition by feeding ammonium and alkali ions (Chen et al. 2010).

In this study, optimum concentration and C/N ratio were also investigated for molasses utilization by *R. capsulatus* for indoor small scale experiments in batch mode. Optimum C/N ratio under outdoor conditions was also investigated. Simulated outdoor conditions for day and night cycle were designed as indoor experiments with changing temperature and light/dark cycle. Effects of constant pH for small scale experiment under indoor conditions were investigated in order to observe the effect of pH on molasses utilization in small scale.

If photobiological hydrogen is to be a feasible option in the future, the stability, and the duration of large-scale, outdoor runs have to be demonstrated. Therefore, the goal of this study was to achieve prolonged outdoor hydrogen production from molasses by *R. capsulatus* in a 20 L outdoor photobioreactor (PBR). To this end, we addressed the two primary issues limiting the duration, namely the decrease in pH and the non-optimal C/N ratio. Although small-scale batch type pH-controlled studies with various species (Arooj et al. 2008; Braz Romão et al. 2018; Wang and Jin 2009) and PNSB (Zagrodnik and Laniecki 2015) are available under indoor conditions and controlled environment, to our knowledge, this is the first time continuous pH adjustment has been employed for a pilot-scale, outdoor tubular PBR with PNSB.

Optimum molasses concentration was obtained under indoor outdoor condition. C/N ratio was optimized for indoor and simulated outdoor conditions. pH effect on

increase molasses utilization was investigated and high molasses concentration was found more effective. A pH control system was installed to the PBR, tuned and operated to maintain the pH close to optimum during continuous operation. The duration of continuous hydrogen production was increased by applying new strategies of C/N ratio adjustment, dilution, and artificial illumination.

The rest of the thesis is organized as follows: a literature survey on photobiological hydrogen production and pH control is presented in Chapter 2. The materials and methods for all experimental runs are summarized in Chapter 3. The results for all sets of experimental studies, i.e. pH controller tuning, small-scale hydrogen production runs, and pilot-scale hydrogen production runs are presented in Chapter 4. Finally, the conclusions are listed in Chapter 5.

CHAPTER 2

LITERATURE SURVEY

2.1. Energy Carrier Hydrogen

Currently, the increasing energy demand of the world is mostly met by fossil fuels. The finite nature of these resources, coupled to pollution and large scale emissions of greenhouse gases, is not sufficient due to their rapid consumption. Alternative renewable energy sources draw great interest since they are clean and cheap and can eventually replace fossil fuels. Global energy demand will continue to grow because of the rising incomes and word population. According to the new policies scenario of international energy agency, it is expected that energy demand will grow by more than 25% until 2040 in Figure 2.1 (International energy agency, 2019).

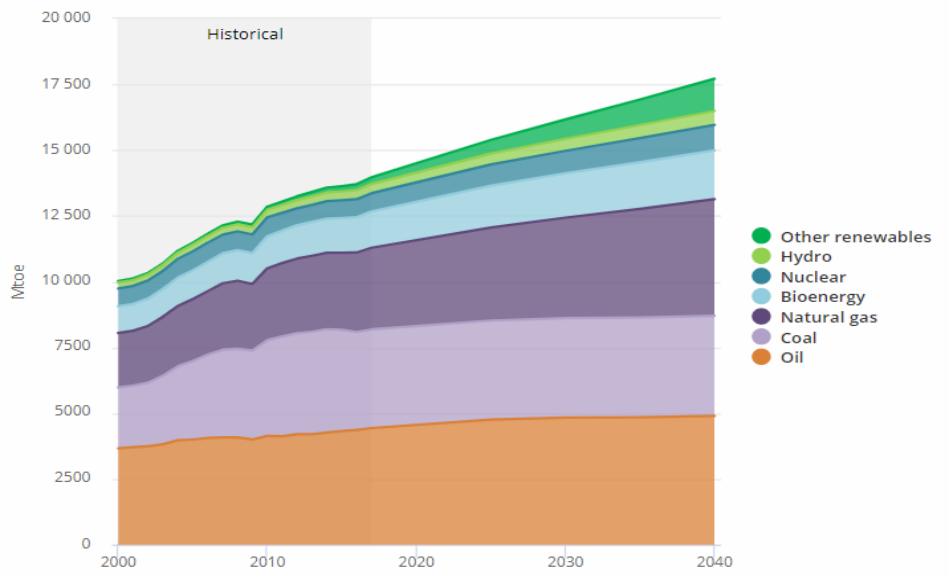

Figure 2.1. Share of different energy suppliers in global primary energy demand. ("Other renewables" includes wind, solar (photovoltaic and concentrating solar power), geothermal, and marine.) (Mtoe means million tons of oil equivalent) (International Energy Agency, 2019).

Hydrogen is one of the most promising energy carriers with the highest energy content of any known fuels by weight as 142 MJ/kg, nearly two times of natural gas (55 MJ/kg) and three times of gasoline (46 MJ/kg) (World Nuclear Association 2016). It is odorless and non-toxic and produces only water upon combustion. Although hydrogen is the most abundant element, molecular hydrogen is not found free in nature, unlike fossil fuels. It must be produced from a primary energy source and then it can be used as a fuel in an internal combustion engine or in a fuel cell. There are many processes for hydrogen production from both conventional and alternative energy resources. Currently, 48% of hydrogen is produced from natural gas, 30% from heavy oils and naphtha, 18% from coal and 4% from electrolysis (Kothari, Buddhi, and Sawhney 2008; Nikolaidis and Poullikkas 2017). As fossil fuels are consumed and environmental such as global warming are becoming important, renewable technologies have begun to attract greater attention and are proposed as alternatives to conventional technologies. Biological processes operating with ambient temperature and pressure have increased significantly over the last several years within the scope of sustainable development and waste minimization.

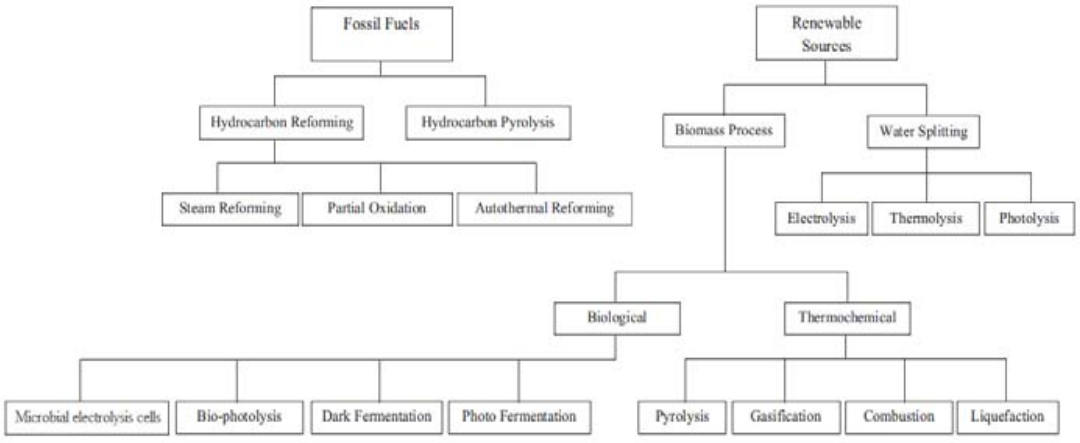

Figure 2.2. Hydrogen production methods (Kadier et al. 2018; Nikolaidis and Poullikkas 2017).

Bioenergy is one of the crucial sources of renewable energy and meets about 9% of world total primary energy demand. As seen in Figure 2.1, it meets the world final energy demand for all sectors more than five times when compared to wind and solar energy. In 2015, 13 EJ of bioenergy was used to supply heat, which is about 6% of world heat consumption. Moreover, about 500 TWh of electricity was supplied by biomass in 2016, representing 2% of world electricity generation (International Energy Agency, 2019). Recently, the usage of bioenergy for electricity and transport biofuels is growing fastest.

2.2. Commercial Hydrogen Production Techniques

2.2.1. Steam Reforming Method

Steam reforming is based on the catalytic conversion of hydrocarbons and steam to hydrogen and carbon oxides, including the main steps of reforming or synthesis gas generation, water-gas shift and methanation or gas purification. Raw materials may be methane, natural gas, methane-containing gases such as the various combination of light hydrocarbons that involve ethane, propane, butane, pentane, and light and heavy naphtha. Nickel is usually preferred as a catalyst to prevent poisoning from feedstock that contains organic sulfur compounds. Steam reforming is an endothermic process operating at a high temperature about 850-900 ^{o}C, pressures up to 3.5 MPa and 3.5 steam-to-carbon ratios to increase the hydrogen purity. The main chemical reactions are shown below (Kothari, Buddhi, and Sawhney 2008; Nikolaidis and Poullikkas 2017).

$$C_nH_m + nH_2O \rightarrow nCO + \left(n + \frac{m}{2}\right) H_2 \quad (2.1)$$

$$CO + H_2O \rightarrow CO_2 + H_2 \quad (2.2)$$

2.2.2. Partial Oxidation Method

Partial oxidation method depends on the conversion of steam, oxygen, and hydrocarbons to hydrogen and carbon oxides. The exothermic process operates at high temperature and pressure. The catalytic processes of methane and naphtha operate at about 950 ^{o}C and non-catalytic processes of hydrocarbons and heavy oil operate at 1150-1315 ^{o}C. The disadvantage of the method is its carbon monoxide emission along with carbon dioxide (Kothari, Buddhi, and Sawhney 2008; Nikolaidis and Poullikkas 2017).

$$C_nH_m + \frac{1}{2}nO_2 \rightarrow nCO + \frac{1}{2}mH_2 \qquad \text{catalytic} \tag{2.3}$$

$$C_nH_m + nH_2O \rightarrow nCO + \left(n + \frac{m}{2}\right)H_2 \qquad \text{noncatalytic} \tag{2.4}$$

Hydrogen can be obtained from coal with partial oxidation method. The process is named as coal gasification. Coal is reacted with steam at 800-900 ^{o}C and 450 psi, to produce CO, CO_2, and H_2 with a small amount of methane. Then, CO_2 is removed from the product by washing with monoethanolamine or potassium hydroxide or calcium carbonate. The basic reaction for gasification of coal is below (Kothari, Buddhi, and Sawhney 2008; Nikolaidis and Poullikkas 2017).

$$CH_{0.8} + 0.7O_2 + 0.6H_2O \rightarrow CO_2 + H_2 \tag{2.5}$$

2.2.3. Hydrocarbon Pyrolysis

Hydrocarbon pyrolysis is a well-known process. The hydrocarbon undergoes thermal decomposition. Carbon and hydrogen are the main products. The simple general reaction of decomposition is below (Nikolaidis and Poullikkas 2017).

$$C_nH_m \rightarrow nC + \frac{1}{2}mH_2 \tag{2.6}$$

2.2.4. Electrolysis

Electrolysis is one of the water-splitting techniques. The reaction is nonspontaneous and the required energy is supplied by electricity. When electrical current passes through the aqueous electrolyte, water splits to hydrogen and oxygen according to the following reaction (Nikolaidis and Poullikkas 2017).

$$2H_2O \rightarrow 2H_2 + O_2 \quad (2.7)$$

2.3. Biohydrogen Production Technologies

Biological hydrogen production has a potential to supply hydrogen for the sustainably, from renewable sources. Biological processes are less energy-intensive since most of them operate under ambient conditions. Moreover, they enable to utilize various waste as a feedstock, thus they contribute to waste recycling and minimization. Biophotolysis, photo and dark fermentations are used methods for hydrogen production.

2.3.1. Microbial Electrolysis Cells

Microbial electrolysis cells (MECs) is a new technology to produce biohydrogen. MECs system consists of anode and cathode (Cheng and Logan 2011). Organic substrates in wastewater are degraded by microorganisms at the anode to generate electron and protons; the electrons pass through the external circuit to the cathode when protons are diffused. Hydrogen is evolved at the cathode with the combination of protons and electrons at the cathode (Dong et al. 2017).

2.3.2. Biophotolysis

Photosynthetic microorganisms such as green algae and cyanobacteria can be used. Water and sunlight are the only requirements for hydrogen production. The biophotolysis is divided into direct and indirect processes.

In direct photolysis, solar energy is utilized to convert water to hydrogen and oxygen directly. The reaction of cell-free chloroplast-ferredoxin-hydrogenase system is:

$$2H_2O \rightarrow 2H_2 + O_2 \quad (2.8)$$

Some green algae could be used in a direct biophotolysis since they have the Fe-hydrogenase enzyme. The main drawback of the system is that the Fe-hydrogenase enzyme is very oxygen-sensitive. It is suggested that the partial pressure of O_2 needs to be below 0.1%, which equals to less than 1 μM O_2 in the liquid phase for simultaneous production of O_2 and H_2. To reduce oxygen concentration, sparging inert gases have been suggested. However, the product gas is diluted and substantial purification is needed to obtain hydrogen with acceptable purity. Therefore, though direct biophotolysis is attractive, it suffers from oxygen sensitivity and unfavorable economics (Hallenbeck and Benemann 2002).

Indirect biophotolysis offers a solution for the problem of sensitivity to oxygen by separating oxygen and hydrogen evolution. (Hallenbeck and Benemann 2002). Indirect biophotolysis consists of two steps. The general reaction for hydrogen production by cyanobacteria or blue-green algae utilizing water are (Nikolaidis and Poullikkas 2017):

$$12H_2O + 6CO_2 + \text{"light energy"} \rightarrow C_6H_{12}O_6 + 6O_2 \quad (2.9)$$

$$C_6H_{12}O_6 + 12H_2O + \text{"light energy"} \rightarrow 12H_2 + 6CO_2 \quad (2.10)$$

However, indirect biophotolysis systems are at the conceptual stage and need to be demonstrated even on an experimental level (Hallenbeck and Benemann 2002).

2.3.3. Dark Fermentation

Dark fermentation is one of the attractive methods of fermentation, enabling the utilization of waste materials, thus providing cost-effective energy generation. In dark fermentation, organic substrates are broken down to biohydrogen, volatile fatty acids, and carbon dioxide by fermentative bacteria under the anoxic condition without the presence of light. According to this metabolism, various volatile fatty acids (VFA) such as acetic acid, butyric acid, formic acid, lactic acid, and propionic acid are produced. Carbohydrates are usually used as carbon sources (Stepan Sarkissian and Fowler 1986).

The hydrogenase enzyme carries out biohydrogen produced in dark fermentation. There are three reaction paths that could be followed for biohydrogen production.

In the first reaction, the pyruvate is split into acetyl-CoA and formate by the pyruvate formate lyase (PFL) enzyme. Formate is converted to molecular hydrogen and carbon dioxide by the formate hydrogen lyase (FHL) (Hay et al. 2013).

$$\mathrm{Pyruvate + CoA \rightarrow Acetyl.\,CoA + Formate} \quad (2.11)$$

$$\mathrm{Formate + CoA \rightarrow H_2 + CO_2} \quad (2.12)$$

In the second reaction, the oxidation of pyruvate into acetyl CoA is reduced to ferredoxin (Fd) by pyruvate ferredoxin oxidoreductase (PFOR). Then, Fd oxides by Fd-dependent hydrogenase (HydA) and release electrons as molecular hydrogen when generating oxidized Fd (Hay et al. 2013).

$$\mathrm{Pyruvate + CoA + \ 2Fd.\,ox \leftrightarrow Acetyl.\,CoA + 2Fd.\,red + CO_2} \quad (2.13)$$

$$\mathrm{2H^+ + \ 2Fd(red) \rightarrow H_2 \ + 2Fd(ox)} \quad (2.14)$$

In the third reaction type, the formed oxidized Fd during the carbon metabolism is reduced by NADH. Electrons in reduced Fd have transferred protons with the help of HydA to produce molecular hydrogen(Hay et al. 2013).

$$\text{Glucose} + 2\text{NAD}^+ \rightarrow 2\ \text{Pyruvate} + 2\text{NADH} \quad (2.15)$$

$$2\text{NADH} + 4\text{Fd(ox)} \rightarrow 2\text{NAD}^+ + 4\text{Fd(red)} \quad (2.16)$$

$$4\text{Fd(red)} + 4\text{H}^+ \rightarrow 4\text{Fd(ox)} + 2\text{H}_2 \quad (2.17)$$

The maximum yield is accounted as 4 molH_2/mol glucose theoretically when acetic acid is the only VFA product and yield of 2 molH_2/mol glucose when butyric acid is the VFA product for the utilization of glucose as carbon source. The conversion of glucose to hydrogen with such two paths is given below (Hay et al. 2013).

$$\text{C}_6\text{H}_{12}\text{O}_6 + 2\text{H}_2\text{O} \rightarrow 4\text{H}_2 + 2\text{CH}_3\text{COOH} + 2\text{CO}_2 \quad (2.18)$$

$$\text{C}_6\text{H}_{12}\text{O}_6 + 2\text{H}_2\text{O} \rightarrow 2\text{H}_2 + \text{CH}_3\text{CH}_2\text{CH}_2\text{COOH} + 2\text{CO}_2 \quad (2.19)$$

Although high hydrogen production rates are possible, in real processes the yield is obtained lower than its theoretical value since carbohydrates are not fully metabolized and used to support and maintain microorganism growth in addition to hydrogen production (Brentner, Peccia, and Zimmerman 2010; Hay et al. 2013). Even under optimal conditions, about 67% of the original organic matter remains in the solution when a simple sugar is used for hydrogen production (Türker, Gümüs, and Tapan 2008).

Fermentative bacteria are sensitive to pH and temperature fluctuations and changes of these parameters could change the metabolic pathway and growth rate (Sinha and Pandey 2011; Türker, Gümüs, and Tapan 2008). Therefore, hydrogen production by dark fermentation process is strongly dependent on pH value, which should be kept between 5 and 6 for optimal production (Boodhun et al. 2017; Nikolaidis and Poullikkas 2017).

The major drawback of dark fermentation is low hydrogen purity, which makes usage of hydrogen in fuel cell difficult (Kayahan, Eroglu, and Koku 2017). The hydrogen in the effluent gas of the dark fermentation must be recovered by a gas separation technology to purified hydrogen (Brentner, Peccia, and Zimmerman 2010).

2.3.4. Integrated Systems

An integrated system is a sequential combination of dark fermentation (thermophilic) and photo fermentation processes. First, hydrogen, carbon dioxide, and organic acids are produced with the utilization of biomass by thermophilic microorganism in the dark fermentation. Then, produced organic acids are consumed by the photofermentative bacteria to produce more hydrogen in the photofermentation process.

Özgür et al. (2010) investigated sequential dark and photofermentation of sucrose-containing sugar beet molasses for hydrogen production in pH-controlled 2-l bioreactor and 55 ml glass bottle, respectively. The maximum hydrogen production reported as 1.37 mmol/lc.h (1.37 mol $H_2/(m^3.h)$) by *C. saccharolyticus* and hup-mutant strain of *R. capsulatus*. The hydrogen yield increased from 4.2 mol H_2/mol sucrose in dark fermentation to 13.7 mol H_2/mol sucrose by sequential dark and photo fermentation.

2.3.5. Photofermentation

Under limited nitrogen conditions, hydrogen can be produced using solar energy and organic acids. Due to the presence of nitrogenase enzyme, some photosynthetic bacteria enable to convert the organic acids into hydrogen and carbon dioxide according to the following reactions. When sucrose is fermented and only acetic acid is produced, 1 mol of sucrose makes it possible to obtain 24 mol of hydrogen. (Urbaniec and Grabarczyk 2014)

$$C_{12}H_{22}O_{11} + 5H_2O \rightarrow 4CH_3COOH + 8H_2 + 4CO_2 \quad (2.20)$$

$$4CH_3COOH + 8H_2O \rightarrow 16H_2 + 8CO_2 \quad (2.21)$$

With acetic, formic, lactic, propionic and butyric acid as the reactant, according to stoichiometric conversions of substrates into H_2 are presented below (Uyar, Eroglu, Yücel, and Gündüz 2009).

Acetate: $C_2H_4O_2 + 2H_2O \rightarrow 4H_2 + 2CO_2$ (2.22)

Lactate: $C_3H_6O_3 + 3H_2O \rightarrow 6H_2 + 3CO_2$ (2.23)

Formate: $CH_2O_2 \rightarrow H_2 + CO_2$ (2.24)

Propionate: $C_3H_6O_2 + 4H_2O \rightarrow 7H_2 + 3CO_2$ (2.25)

Butyrate: $C_4H_8O_2 + 6H_2O \rightarrow 10H_2 + 4CO_2$ (2.26)

Photosynthetic bacteria are promising organism due to the following reasons (Akkerman et al. 2002; Fascetti et al. 1998) :

- A high substrate to product conversion yield
- Lack of oxygen-evolving activity, which is desirable for biohydrogen production
- Ability to use a wide wavelength of light to operate under outdoor conditions
- Capability to use organic substrates (derived from wastes) for hydrogen generation that also helps in the bioremediation process.

Single-stage photofermentation process is a more cost-effective system to produce biohydrogen since increased reactor number and additional dark fermentation step such as optimization of dark fermenter effluent lead to high operational cost for two-stage systems (Keskin and Hallenbeck 2012).

Keskin et al. (2010) studied single-stage photofermentation with the utilization of sugar beet molasses by *Rhodobacter capsulatus* JP91 for hydrogen production in 125 ml serum bottle. The highest hydrogen production has been reported as 51 ml H_2/(l.h) (1.85 mol H_2/(m^3.h)) which is higher than sequential dark and photo fermentation process (Özgür, Mars, et al. 2010) and hydrogen yield was 10.5 mol H_2/mol sucrose.

2.4. General Characteristics of *Rhodobacter Capsulatus*

Purple non-sulfur bacteria (PNSB) are prokaryotic and photosynthetic microorganism which can grow as photoheterotrophs, photoautotrophs or chemoheterotrophs switching from one mode to another based on conditions such as degree of anaerobiosis, availability of carbon source and availability of a light source (Basak and Das 2007). When CO_2 is utilized as a carbon source, PNS bacteria grow autotrophically, utilization of organic compounds as a carbon source causes heterotrophic growth and existence of light lead to phototrophic growth. They can also live in dark conditions and tolerate oxygen at low levels (Biebl and Pfennig 1981) Since PNS bacteria do not use sulfide as an electron donor at high concentrations like sulfur bacteria, they called as non-sulfur bacteria. They grow at pH 6-9 and temperature range 25^{o}C-35^{o}C (Sasikala et al. 1993).

Rhodobacter capsulatus is a purple non-sulfur (PNS) bacteria that participate in biological hydrogen generation by photofermentation. It belongs to *Rhodospirillaceae* family and Rhodobacter genera. It is a rod-like shaped cell with a diameter of 0.5-1.2 x 2.0-2.5 μm (Imhoff, Trüper, and Pfennig 2005). The PNS bacteria is a yellowish-brown to greenish, however, color shifts from green to deep rose-red in the presence of oxygen because of the oxidation of the carotenoid. The maximum hydrogen production rate obtained at 27.5 ^{o}C and 287 W/m^2 (Androga et al. 2014). Bacteriochlorophyll *a* that is the photosynthetic pigment of the bacteria has characteristic absorption maxima values 376-378, 450-455, 478-480, 508-513, 590-592, 802-805 and 860-863 nm for living cells (Androga 2009).

Nitrogenase and hydrogenase are two key enzymes of the bacteria for the hydrogen production process. The nitrogenase enzyme reduces the protons to molecular hydrogen with the consumption of excess reducing equivalents generated by the oxidation of organic acids. However, hydrogenase enzyme function is reversible and it enables to consume hydrogen by producing ATP, protons and electrons. Therefore,

inactivation of uptake hydrogenase of *R. capsulatus* increased hydrogen production (Ozturk et al. 2006).

In this thesis, *Rhodobacter capsulatus* YO3 (hup^-) which is an uptake hydrogenase deleted (hup^-) mutant strain of *Rhodobacter capsulatus* by Dr. Yavuz Öztürk was used.

2.5. Photofermentation Metabolism of PNS Bacteria

Photosynthetic purple non-sulfur bacteria have just one photosystem, which is fixed in the intracellular membrane, to convert light energy to chemical energy (ATP). The primary aim of ATP synthesis is to supply biomass production. After a sufficient amount of ATP is utilized for growth, excess reducing power is used to maintain cellular redox has to be disposed to stabilize the cellular redox state. CO_2 fixation, H_2 production, and polyhydroxybutyrate (PHB) biosynthesis are three main metabolic pathways which compete for such electrons (Androga et al. 2012). Therefore, hydrogen production, which is the result of nitrogen fixation, starts when present ATP is passed over the needed amount of ATP for growth.

2.5.1. Hydrogen Production

In the PNSB photosystem, organic carbons are oxidized into CO_2 and electrons by citric acid (TCA) cycle, which itself is part of the integrated carbon network (Figure 2.3).

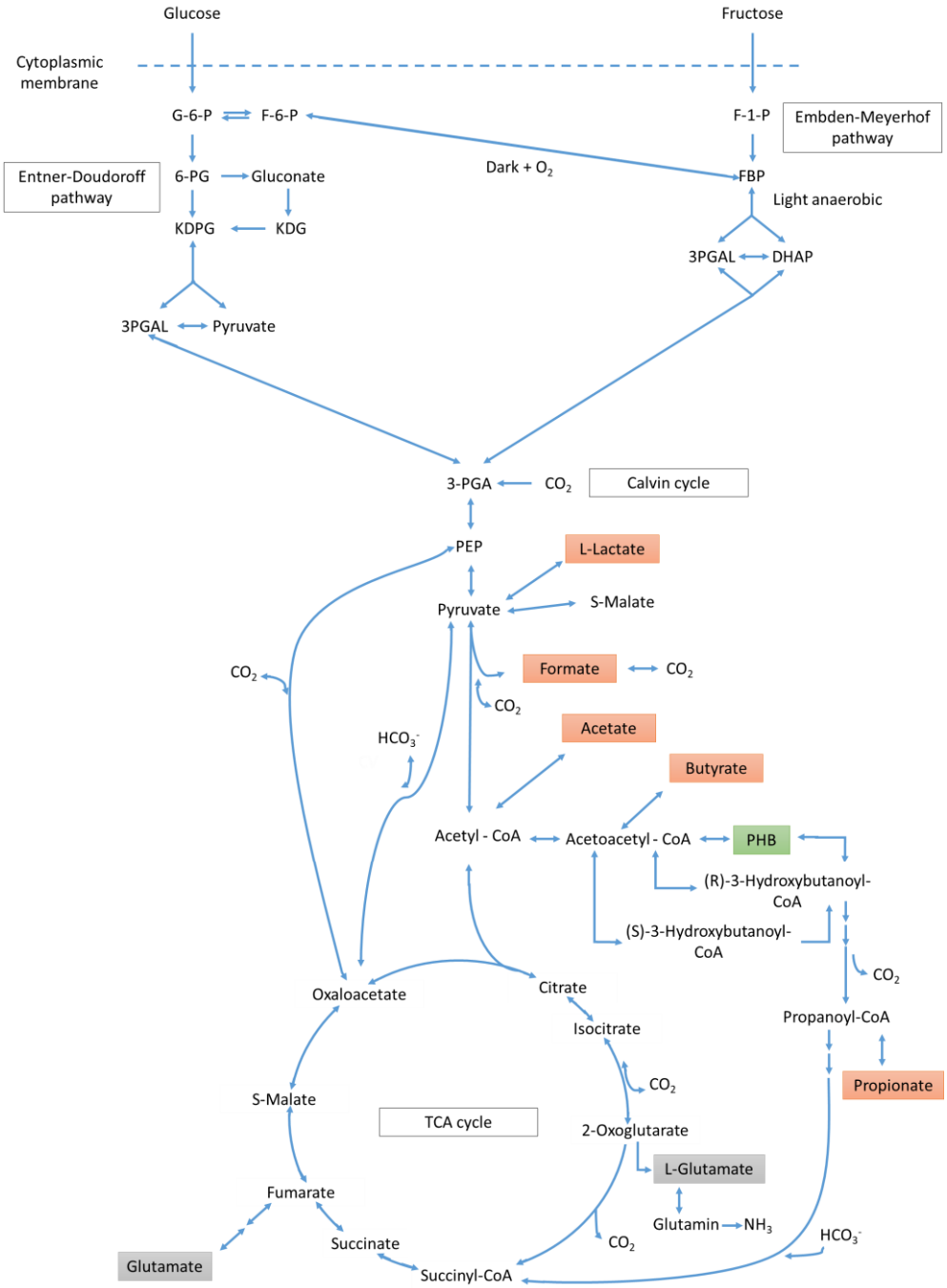

Figure 2.3. A sketch of the carbon metabolism in PNS bacteria *R. capsulatus*. G-6-P: glucose 6-phosphate, F-6-P: fructose 6-phosphate, 6-PG: 6-phosphogluconate, KDPG: 2-keto-3-deoxy-6-phosphogluconate, KDG: 2-keto-3-deoxygluconate, F-1-P: fructose-1-phosphate, DHAP: dihydroxyacetone phosphate, 3PGAL: glyceraldehyde 3-phosphate, 3-PGA: 3-phosphoglyceric acid, PHB: poly-β-hydroxybutyrate, PEP: phosphoenolpyruvate.

The photosynthetic part in PNSB is composed of photosystem (PS), a series of electron transport proteins (cytoplasmic cytochrome c, lipid-soluble quinones (Q/QH), cytochrome (Cyt) b/C1 complex, and) and a transmembrane ATP synthase protein as seen in Figure 2.4. The photosystem includes light-harvesting complex 1 (LH1) and 2 (LH2) and a reaction center which are protein-pigment complexes and contains various types of carotenoids and bacteriochlorophyll a. The LH systems take the light in the visible (450-590 nm) and near-infrared wavelength (800-875 nm) and transfer the energy to the reaction center which starts the cyclic electron transfer.

The released electron from TCA are delivered to cytochrome c and funneled through electron carrier proteins and delivered to ferredoxin. Simultaneously, protons are pumped to the membrane and cause the proton gradient. Forming a proton driving force provides ATP production by ATP synthase. Ferredoxin ensures to transfer of electrons to nitrogenase enzyme which catalyzes the reduction of protons to H_2 with the expense of ATP (Androga et al. 2012).

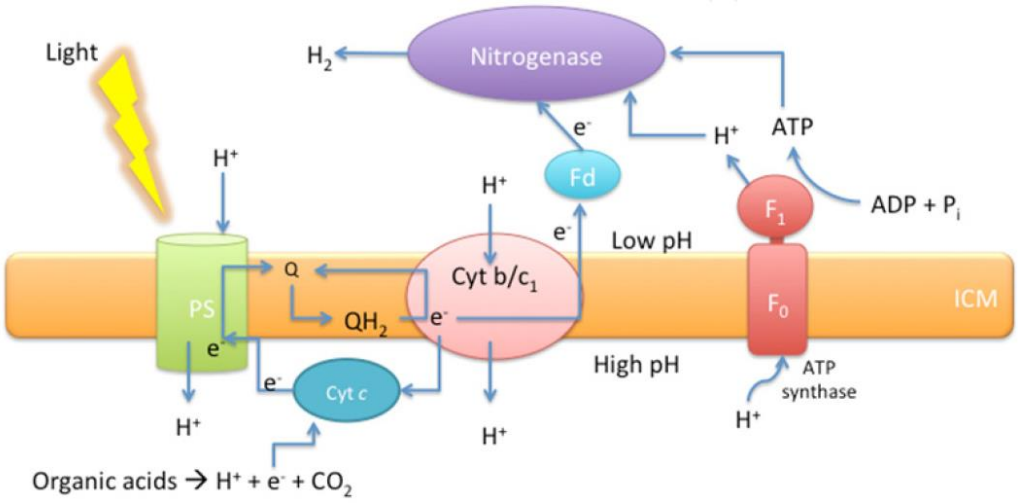

Figure 2.4. Hydrogen production pathway by photofermentation in PNSB. ICM: intracytoplasmic membrane, PS: photosystem, Fd: ferredoxin (Androga et al. 2012).

2.5.1.1. Nitrogenase

Nitrogenase is an enzyme responsible for hydrogen production. Nitrogenase activity was highest at between pH 6.5 and 7.0, and accumulation of NH_4^+ in the culture represses the nitrogenase activity (Peng et al. 1987). There are three different nitrogenases in PNSB, which have been classified based on their active center element. Nif is molybdenum centered (Mo-nitrogenase), Vnf is vanadium centered (V-nitrogenase) and Anf is iron centered (Fe-nitrogenase). *R. sphaeroides* has only Mo-nitrogenase, while *R. capsulatus* and *R. rubrum* have both Mo-nitrogenase and Fe-nitrogenase. In *R. palustris*, all three forms of nitrogenases are found (Androga et al. 2012).

Nitrogen (N_2) is used as an electron sink and converted to NH_3 by the nitrogenase enzyme. In N_2 fixation, nitrogenase enzyme produces 1 mole H_2 from 1 mole N_2 with consumption of 16 moles of ATP. When nitrogen is available, the formation of H_2 and ammonium from N_2 is shown in the following equation (Guwy et al. 2011):

$$N_2 + 16\,ATP + 8e^- + 8\,H+ \rightarrow 2NH_3 + 16\,ADP + 16Pi + H_2 \qquad (2.27)$$

However, when N_2 is not available, nitrogenase catalyzes proton reduction and produces 1 mole H_2 from 1 mole N_2 utilizing 4 ATP. The bulk of hydrogen production occurs when nitrogenase reduces protons to molecular hydrogen in the absence of nitrogen:

$$2H^+ + 2e^- + 4\,ATP \rightarrow H_2 + 4ADP + 4Pi \qquad (2.28)$$

In other words, nitrogenase produces hydrogen with 4 times higher efficiency, when N_2 is not present. Moreover, ammonium and cellular nitrogen existence regulate nitrogenase synthesis and activity. An abundance of nitrogen sources relative to the carbon content of the nutrient medium may also promote ammonia formation, which then suppresses the activity of nitrogenase. Therefore, the amount of nitrogen source is one the critical parameter for hydrogen production and production process should be carried out under nitrogen-limited environment.

2.5.1.2. Hydrogenase

Hydrogenase enzyme is another catalyst which participates in hydrogen metabolism. Hydrogenase catalyzes the oxidation of H_2 to produce protons and reducing equivalents, reversibly it catalyzes the reduction of protons to produce molecular hydrogen. Hydrogenases are classified according to the type of metal cofactor found in the active site as [FeFe]-hydrogenase, [NiFe]-hydrogenase, and [Fe]-hydrogenase. [NiFe]-hydrogenases usually are responsible for hydrogen consumption, and [FeFe]-hyrogenases tend to produce hydrogen. The direction of reaction depends on the redox status of the cell.

Hydrogen is produced and oxidized by the catalyst by the reversible reaction (Androga et al. 2012):

$$H_2 \leftrightarrow 2H^+ + 2e^- \tag{2.29}$$

2.5.2. CO_2 Fixation

PNSB can grow photoheterotrophically using light for energy and organic compounds for carbon and electrons. In photoheterotroph growth, utilizing carbon dioxide is used as an electron sink under to elude excess reducing equivalents and achieve redox homeostasis by PNSB (Dubbs and Tabita 2004).

PNSB can also grow photoautotrophically using light for energy, inorganic compounds, and water for electrons, and CO_2 for carbon. In the Calvin cycle, CO_2 is used to supply carbon for the cell by converting CO_2 into organic compounds for biosynthesis under autotrophic growth. Through this pathway, phosphoribulokinase (PRK) consumes ATP to form ribulose 1,5-bisphosphate (RuBP). RuBP is then combined with CO_2 via ribulose 1,5-bisphosphate carboxylase (RubisCO), resulting in two molecules of 3-phosphoglycerate (Gordon and McKinlay 2014).

2.5.3. Polyhydroxybutyrate (PHB) Biosynthesis

PNS bacteria are capable of producing large amounts of polyhydroxybutyrate (PHB) as reserve material, which affords an alternative pathway to hydrogen to discharge excess energy and reducing power under nitrogen limitation (Cetin et al. 2006; Hustade, Steinbüchel, and Schlegel 1993; Khatipov et al. 1998; Yigit et al. 1999). PHB is a biodegradable thermoplastic polymer, which has economical value. PHB is accumulated as an energy storage material under the limitation of nutritional elements such as N, S, P, O and Mg and excess carbon source conditions, similar to hydrogen production metabolism. The carbon source, nitrogen amount and pH are factors that affect its accumulation inside the cells.

Khatipov et al. demonstrated that acetate is the most advantageous carbon source for PHB production among lactate, pyruvate, and glucose and pH is a significant factor that affects the PHB accumulation. It has been reported that an increase in pH value increased PHB content markedly (Khatipov et al. 1998).

Hustede et al. used mutant cells defective in the synthesis of PHB in *R. sphaeroides* and showed that depletion of the PHB synthesis metabolism increased hydrogen production (Hustade, Steinbüchel, and Schlegel 1993).

Adessi et al. observed decreasing substrate-to-hydrogen conversion in response to increasing salinity, and pointed out the possibility of synthesis of additional carbon compounds such as PHB (Adessi et al. 2016).

Kim et al. used *R.sphaeroides* KD131 for photofermentation of acetate and glutamate to produce hydrogen by keeping pH to 7. When pH was controlled, cumulative hydrogen production volume increased 2.4 times nearly and PHB content decreased 2.4 times. Additionally, PHB synthase deleted-mutant was used for hydrogen production under pH-controlled environment and observed that hydrogen production volume increased 28 %. It was concluded that pH control had also an effect on soluble microbial products and secondary metabolites, that compete with hydrogen production to reduce power in addition to depressed PHB production (M. S. Kim et al. 2011).

2.5.4. Organic Acid Production

Organic acid production metabolism of the *R. capsulatus* is followed according to KEGG pathway. Lactate, formate, and acetate are evolved organic acids in pyruvate metabolism (Appendix A). Lactate is synthesized and produced from pyruvate by lactate dehydrogenase enzyme (1.1.1.27) with the following equation:

$$\text{Lactate} + NAD^+ \leftrightharpoons \text{pyruvate} + NADH + H^+ \quad (2.30)$$

Formate is an intermediate product for the acetyl-CoA synthesize from pyruvate by pyruvate formate-lyase (2.3.1.54).

$$\text{pyruvate} + \text{CoA} \leftrightharpoons \text{acetyl-CoA} + \text{formate} \quad (2.31)$$

Acetate provides an accessible path to synthesize acetyl-CoA. The highest biomass concentration, highest growth rate and the highest substrate conversion efficiency for PNS bacteria were reported on acetate among other organic acids (Uyar, Eroglu, Yücel, and Gündüz 2009; Wu, Liou, and Lee 2012). Acetate enters the TCA cycle at acetyl-CoA, which is catalyzed by the acetyl-CoA synthetase (6.2.1.1) enzyme according to equation 2.32.

$$\text{ATP} + \text{acetate} + \text{CoA} \leftrightharpoons \text{AMP} + \text{diphosphate} + \text{acetyl-CoA} \quad (2.32)$$

The pathway of propionate synthesis starts with the formation of acetyl-CoA from carbon substrates such as sugars, alcohols, organic acids or fatty acids and comprises glyoxylate, butanoate and propanoate metabolisms. Propionic acid is directly linked with propanoyl-CoA through a reversible reaction. Propanoyl-CoA is synthesized from crotonyl-CoA in glyoxylate. The main precursor for crotonyl-CoA synthesized butanoate metabolism is acetyl-CoA. PHB is an intermediate product which evolves in butanoate metabolism during crotonyl-CoA synthesis from acetyl-CoA. Propionate contributes to the TCA cycle also. It is converted to propanoyl-CoA and enters TCA cycle at a level of succinyl-CoA in propanoate metabolism.

Reaction system of crotonyl-CoA synthesis from acetyl-CoA in butanoate metabolism (Appendix B):

Acetoacetyl-CoA formation by acetyl-CoA C-acetyltransferase (2.3.1.9):

$$2 \text{ acetyl-CoA} \leftrightharpoons \text{CoA} + \text{acetoacetyl-CoA} \quad (2.33)$$

(S)-3-hydroxybutanoyl-CoA formation by 3-hydroxybutyryl-CoA dehydrogenase (1.1.1.157):

$$\text{(S)-3-hydroxybutanoyl-CoA} + NADP^+ \leftrightharpoons \text{3-acetoacetyl-CoA} + NADPH + H^+ \quad (2.34)$$

(R)-3-hydroxybutanoyl-CoA formation by acetoacetyl-CoA reductase (1.1.1.36):

$$\text{(R)-3-hydroxyacyl-CoA} + NADP^+ \leftrightharpoons \text{3-oxoacyl-CoA} + NADPH + H^+ \quad (2.35)$$

(3R)-3-hydroxybutanoyl-CoA formation by 3-hydroxybutyryl-CoA dehydratase (4.2.1.55):

$$\text{(3R)-3-hydroxybutanoyl-CoA} \leftrightharpoons \text{crotonyl-CoA} + H_2O \quad (2.36)$$

Reaction system for propanoyl-CoA synthesis from crotonyl-CoA in glyoxylate metabolism (Appendix C):

Crotonyl-CoA reductase (1.3.1.85) catalyzes crotonyl-CoA-dependent oxidation of NADPH in the presence of CO_2. When CO_2 is absent, the enzyme catalyzes the reduction of crotonyl-CoA to butanoyl-CoA, but with only 10% of maximal activity (relative to crotonyl-CoA carboxylation) in equation 2.37.

$$\text{crotonyl-CoA} + CO_2 + NADPH + H^+ = \text{(2S)-ethylmalonyl-CoA} + NADP^+ \quad (2.37)$$

(S)-methylmalonyl-CoA formation by methylmalonyl-CoA epimerase (5.1.99.1):

$$\text{(S)-methylmalonyl-CoA} = \text{(R)-methylmalonyl-CoA} \quad (2.38)$$

Ethylmalonyl-CoA mutase (5.4.99.63) is involved in the ethylmalonyl-CoA pathway for acetyl-CoA assimilation with coenzyme B12 for activity in equation 2.39.

$$\text{(2R)-ethylmalonyl-CoA} = \text{(2S)-methylsuccinyl-CoA} \quad (2.39)$$

(2S)-methylsuccinyl-CoA dehydrogenase (1.3.8.12) is involved in the ethylmalonyl-CoA pathway for acetyl-CoA assimilation. The enzyme contains FAD. Where etfp is electron-transfer flavoprotein in equation 2.40.

(2S)-methylsuccinyl-CoA + etfp = Mesaconyl-CoA + reduced-etfp (2.40)

Mesaconyl-CoA + H_2O formation by erythro-beta-methylmalonyl-CoA hydrolyse (4.2.1.48):

Mesaconyl-CoA + H_2O ⇋ L-erythro-3-Methylmalyl-CoA (2.41)

L-erythro-3-Methylmalyl-CoA formation by malyl-CoA lyase (4.1.3.24):

L-erythro-3-Methylmalyl-CoA ⇋ propanoyl-CoA + glyoxylate (2.42)

Reaction system for propionate synthesis and utilization via propanoyl-CoA in propanoate metabolism (Appendix D):

Propionate is synthesized from propanoyl-CoA by propionyl-CoA synthetase (6.2.1.17) based on the reversible equation.

ATP + propanoate + CoA ⇋ AMP + diphosphate + propanoyl-CoA (2.43)

Propionate is assimilated by converting propanoyl-CoA and enters the TCA cycle at the level of succinyl-CoA by common metabolic route methylmalonyl-CoA.

propionyl-CoA formation by (6.4.1.3)

ATP + propanoyl-CoA + HCO_3^- = ADP + phosphate + (S)-methylmalonyl-CoA (2.44)

methylmalonyl-CoA epimerase (5.1.99.1)

(S)-methylmalonyl-CoA ⇋ (R)-methylmalonyl-CoA (2.45)

Succinyl-CoA formation by methylmalonyl-CoA mutase (5.4.99.2)

(R)-methylmalonyl-CoA = succinyl-CoA (2.46)

In addition to isoleucine, methionine, and valine degradative metabolic pathway, propanoyl-CoA is also produced from degradation of odd-chain fatty acid (Voet, Voet, and Pratt 2001).

Wu et al. (2012) reported that *Rhodopseudomonas palustris* can utilize acetate, propionate, malate, and lactate for hydrogen production however, acetate and propionate are more favorable for PHB production. Pyruvate and oxaloacetate are the main metabolites of lactate and malate, thus acetyl-CoA may not be synthesized sufficiently to produce PHB. In contrast, acetate and propionate promote acetyl-CoA and produce PHB (Wu, Liou, and Lee 2012).

2.6. Factors Affecting Photofermentative Hydrogen Production

Hydrogen production by PNS bacteria depends on several physiological parameters such as temperature, pH, light intensity, bacterial strain, carbon and nitrogen sources, carbon to nitrogen ratio mode of operation and availability of different metals.

2.6.1. Effect of pH

The pH of the external cell is an important factor for the growth of microorganisms since it partially determines the cytoplasmic or intracellular pH which affects the enzyme activity and reaction rates, protein stability, structure of nucleic acids and other biological molecules (Slonczewski et al. 2009). The proton motive force (PMF) expressed in terms of mV depends on the difference between intracellular and extracellular pH and the transmembrane difference in electrical potential. The PMF is an alternative energy source for the cell to produce ATP and required for exchange of metabolites and ions, the localization of cell division and cytoskeletal proteins and regulation of autolysis (Glasser, Kern, and Newman 2014). Generally, the bacteria tend to keep their cytoplasmic pH value slightly higher than the exterior pH to drive the H^+ ions into the cell by generating negative PMF in the cell (Kashket 1985). An

inappropriate exterior pH leads to pH homeostasis in order to regulate PMF. The optimum pH for hydrogen production is 7.0 ± 0.2 for *R. capsulatus* being neutralophilic gram-negative bacteria (Merugu, Girisham, and Reddy 2010). To overcome low pH, different strategies are used by gram-negative neutrophilic bacteria such as sequestering the intracellular protons with biochemical reactions which consume protons or generate ammonia.

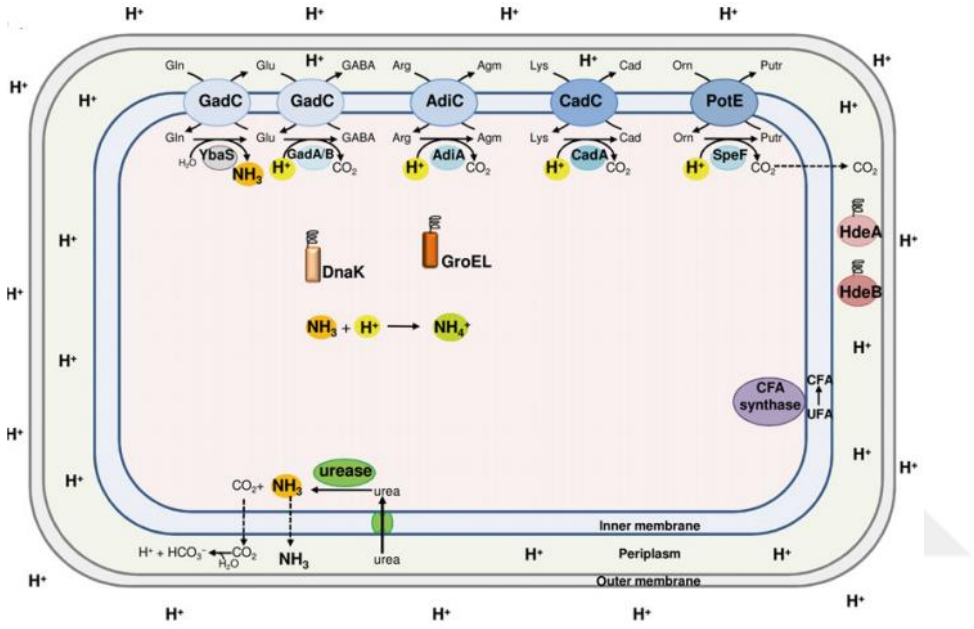

Figure 2.5. Schematic representation of all the mechanisms of protection against acid stress that can occur in gram-negative bacteria. The amino acid decarboxylase/antiporter systems (blue), dependent on glutamate (Glu; GadAB/GadC), arginine (Arg; AdiA/AdiC), lysine (Lys; CadA/CadC) and ornithine (Orn; SpeF/PotE) consume intracellular protons. The glutamine (Gln)-dependent system, consisting of glutaminase YbaS (grey) and glutamine/glutamate antiporter GadC. The cytoplasmic DnaK and GroEL (orange) and periplasmic HdeA and HdeB (dark red) are chaperones. CFA is cyclopropane fatty acids and UFA is unsaturated fatty acids. Agm: agmatine, GABA: γ-aminobutyric acid (Lund et al. 2014).

The amino acid-dependent decarboxylation is a proton-consuming biochemical reaction on some amino acids such as glutamate, lysine, arginine, and ornithine. Consumption of intracellular protons during decarboxylation keeps the internal pH suitable for cell survival. Each decarboxylase enzyme becomes active when the pH drops below 6. Decarboxylases are located in the cell membrane and provide entry of

amino acids and exit of the decarboxylation products. At acidic environment, proton moves into the cell and acidify the cytoplasm and glutamate decarboxylation starts. Glutamate is transported by GadC and converted to γ-aminobutyric acid (GABA) by GadA/B by consuming one proton and releasing CO_2. +1 charged GABA is transferred to periplasm or external environment with the concomitant glutamate uptake. Further, GABA may hold proton in the periplasm or out of the cell, in gram-negative bacteria (Richard and Foster 2004). Arginine-dependent system is also activated at low pH. +1 charged-arginine is converted into +2-charged agmatine with the consumption of one proton and the release of CO_2 by decarboxylase AdiA. Agmatine is transferred to the periplasm or out of the cell by AdiC. The translocation of arginine and agmatine contributes PMF across the membrane (Richard and Foster 2004). The Cad system is another conditional stress response which is induced only at low pH. The Cad system consists of CadA enzyme, transport protein CadB, and the regulatory protein CadC. Lysine is converted to cadaverine by the decarboxylase CadA with H^+ consumption. CadB allows importing of substrate lysine and export of the cadaverine. With the consumption of proton, intracellular H+ concentration is reduced (Mansouri, Nounou, and Nounou 2018). In acidic medium, the antiport protein potE catalyzes the exchange of putresine-putresine and ornithine-ornithine (Kashiwagi et al. 1992).

Urea is hydrolized by urease and converted to ammonia (NH_3) and CO_2. Ammonia production has a role in the protection of the cell from acid stress since NH_3 is used in a reaction which consumes proton. Deiminase and deaminase systems combine the ammonia with intracellular protons and produce the ammonium ion (NH_4^+) to increase pH in the cell (Lund et al. 2014). Cytoplasmic DnaK and GroEL and periplasmic HdeA and HdeB are the molecular chaperones evolve under acid stress (Lund et al. 2014). DnaK protein is increased in response to an acid shock to impair growth capacity in low-pH media (Xu et al. 2017). GroEL is quire resistance to heat shock, ethanol, and freezing but sensitive to oxidative, saline, and osmotic stresses, in contrast to GroEL, DnaK is unable to resist heat shock (Susin et al. 2006). Unsaturated

fatty acids (UFAs) is converted to CFAs with the addition of a methyl group from S-adenosyl-methionine to the double bond of UFA to decrease proton permeability under acid stress (Lund et al. 2014).

Protection mechanism against acid stress reduces the intracellular proton content and results in low hydrogen production (Wu, Liou, and Lee 2012). Furthermore, NH_4^+ which is the product of the deiminase-deaminase system represses the nitrogenase activity which is responsible for hydrogen production (Yakunin and Hallenbeck 2002).

Utilization of sugars as a carbon source by PNS bacteria causes volatile fatty acid accumulation which results in acidification during hydrogen production. Liu et al. (2014) reported that photofermentative hydrogen production on glucose increased by 45% when pH was kept at an optimum value for PNS bacteria.

An indirect effect of the pH is to reduce carbon dioxide for neutral pH value. In line with the theory of acid-base equilibria, the relative proportions of carbon dioxide, bicarbonate, and carbonate depend on the solution pH, subject to the following equilibria (Guo et al. 2008; Koku 2001; J. Li et al. 2007).

$$CO_2 + OH^- \rightarrow HCO_3^- \quad (2.47)$$

$$HCO_3^- + OH^- \rightarrow CO_3^{-2} \quad (2.48)$$

For pH values between 6 and 8, the forward reaction of the first equilibrium dominates so carbon dioxide was converted to primary bicarbonate during the run. A relatively high pH value thus traps the produced carbon dioxide, leading to high purity hydrogen (Koku 2001).

2.6.2. Effect of Temperature

Hydrogen production is an enzymatic reaction which highly affected by temperature. Low-temperature values slow down or stop the metabolism, however, high-temperature values can cause bacterial death. The optimum temperature for hydrogen production is 30-35 ^{o}C (Sasikala, Ramana, and Raghuveer Rao 1991) while optimum temperature has been reported as 30 ^{o}C for nitrogenase enzyme activity (Rainbird, Atkins, and Pate 1983). Özgür et al. (2010) reported that daily temperature fluctuations of 15-40 ^{o}C decreased hydrogen production by 50% (Özgür, Uyar, et al. 2010).

2.6.3. C/N Ratio

Hydrogen production in photosynthetic bacteria occurs under nitrogen-limited environment by nitrogenase enzyme thus carbon to nitrogen ratio is one of the crucial parameters for hydrogen production. C/N ratio has been frequently reported in the range between 45 and 46 in the literature (Androga, Ozgur, et al. 2011; Androga, Özgür, et al. 2011b; Boran et al. 2010) (Androga et al. 2014; Özgür, Uyar, et al. 2010; Sevinc et al. 2012). Low C/N ratio achieved by increasing the nitrogen source concentration was observed to accelerate growth and substantially reduce the lag period but also found to ultimately result in high cell densities which limited light transmission (Savasturk, Kayahan, and Koku 2018). On the other hand, high C/N ratios such as the frequently cited range of 45-56 in the literature are optimal for hydrogen production but result in a slow start.

2.6.4. Effect of Light

Light intensity and light-dark cycle are two key parameters that affect hydrogen production. Light has an important effect on hydrogen production since nitrogenase synthesis is stimulated by light and nitrogenase activity increases in *R. capsulatus* (Koku et al. 2002). The hydrogen productivity increased with increasing light intensity

until reached saturation at around 270W/m^2 (Uyar et al. 2007). The maximum hydrogen production rate obtained at 27.5 ^oC and 287 W/m^2 (Androga et al. 2014). Moreover, the lack of infrared light (750–950nm wavelength) decreases the photoproduction of hydrogen by 39% (Uyar et al. 2007).

Cyclic illumination period, light/dark cycle results in more stable nitrogenase activity (Meyer, Kelley, and Vignais 1978). It has been reported that short intermittent light/dark cycle (30 min light/30 min dark) increased hydrogen productivity (Wakayama et al. 2000).

2.7. Molasses as a Feedstock for Hydrogen Production

Biological hydrogen production is one of the most sustainable methods since it can be carried out under outdoor conditions because of the ability of PNS bacteria to use a wide spectrum of light at ambient temperature and utilize variety wastes as a carbon source. Various wastes such as olive mill effluent, sugar refinery wastewater, dairy industry wastewater, brewery wastewater, and glycerol have been used for photofermentative hydrogen production (Keskin and Hallenbeck 2012).

Molasses is an important by-product of the crystallization process of sugar beet or sugar cane refining industry for sugar production. Beet molasses are viscous and dark-colored syrups which were used as first sweeteners in human nutrition (Saric et al. 2016). Sugar beet molasses is used as a carbon source for dark, photofermentative and integrated systems for sustainable hydrogen produce since it has a high sucrose content around 50% by weight, various nitrogen sources (amino acids) and trace elements that promote nitrogenase activity such as iron and molybdenum.

In this thesis, sugar beet molasses was taken from a sugar factory in Ankara, Turkey (Ankara Şeker Fabrikası).

Sucrose containing molasses utilization by different species and fermentation process was tabulated (Table 2.1). The highest hydrogen production was reported by dark

fermentation of molasses in expanded granular sludge bed (EGSB) reactor which had a working volume of 3.35 l. For two-step sequential dark fermentation, the highest hydrogen production was 1.37 mol $H_2/(m^3.h)$ in 55 ml glass bottle, when rector volume increased to 4 l, productivity decreased to 0.67. Photofermentative process showed better productivity result when reactor volume increased for the utilization of molasses as 0.47 mol $H_2/(m^3.h)$. To our knowledge, pH control did not use for photofermentative hydrogen production with molasses utilization by PNSB bacteria.

Table 2.1. *Biological hydrogen production on sugar beet molasses by different processes*

Process	Operation mode	Reactor type	Reactor volume (l)	Microorganism	Maximum H_2 productivity (mol $H_2/(m^3.h)$)	Min. pH	References
Dark fermentation	Continuous	EGSB	3.350	Anaerobic mixed culture	25.70[a]	NA	(Guo et al. 2008)
	Batch	Bioreactor (pH-controlled)	1.500	*C. butyricum* W5	17.30	4.4	(Wang and Jin 2009)
Two-step dark and Photo fermentation	Batch	Glass bottle[b]	0.055	*Caldicellusiruptor saccharolyticus* + *R. capsulatus* YO3 (hup-)	1.37	6.4	(Özgür, Mars, et al. 2010)
	Continuous	Panel[b]	4.000	*C. saccharolyticus* + *R. capsulatus* YO3 (hup-)	0.67	NA	(Sevler Gokce Avcioglu et al. 2011)
Photo fermentation	Batch	Glass bottle	0.125	*R. capsulatus* JP91	0.29[a]	5.5	(Keskin and Hallenbeck 2012)
			0.055	*R. capsulatus* DSM 1710	0.20	6.4	(Sagir et al. 2017)
			0.055	*R. capsulatus* YO3 (hup-)	0.41	6.4	(Sagir et al. 2017)
			0.055	*Rhodobacter sphaeroides* O.U.001	0.10[a]	6.5	(Kars and Alparslan 2013)
	Continuous	Tubular	9.000	*R. capsulatus* YO3 (hup-)	0.31	5.8	(Kayahan et al. 2017)
			20.000	*R. capsulatus* YO3 (hup-)	0.47	6.5	(Savasturk et at. 2018)

NA data not available

[a] Values converted from the original data, [b] for photofermentation stage

2.8. Biological Hydrogen Production in the Middle East Technical University

Koku demonstrated that glutamate could be utilized as a carbon source in addition to a nitrogen source. It was found that night/dark cycle affected hydrogen production positively. Cell growth under the absence of carbon source was attributed to the utilization of produced PHB (Koku 2001).

Tabanoğlu investigated the performance of an 8 L panel solar bioreactor under outdoor conditions. Olive mill wastewater was used as a sole carbon source. The higher amount of PHB and carotenoid was obtained from outdoor conditions when compared to indoor conditions. This was interpreted as PHB being stored to supply energy for dark periods (Tabanoğlu 2002).

Ozturk studied the uptake hydrogenase of *R. capsulatus* strains and it was reported that the hydrogen production efficiency of *R. capsulatus* strains was increased by the chromosomal inactivation of uptake hydrogenase genes. *R. capsulatus* YO3 (hup^-), a mutant strain lacking the uptake hydrogenase was genetically modified (Öztürk 2005).

Uyar reported that glutamate was the best nitrogen source, adding iron increased the hydrogen production drastically, infrared light (750-950 nm) was very crucial, and temperature value should be below 40 ºC for growth. It was demonstrated that *R. capsulatus* YO3 (hup^-) has better productivity when compared to *R. capsulatus* wild type (Uyar 2008).

Androga showed that to reach stable biomass growth, glutamate concentration should be adjusted. In the study, panel photobioreactor (8 L) was operated at a single stage with *Rhodobacter capsulatus* YO_3 (hup^-). Acetate and glutamate were used for carbon and nitrogen source, and concentrations of them were optimized in the feed. The optimum C/N was reported as 25 in the feed and the highest productivity was obtained as 0.8 mmol H_2/Lc.h 0.8 mol $H_2/(m^3.h)$ (Androga 2009).

Avcıoglu scaled up solar panel photobioreactor to 20 L. Integrated system which is a combination of dark and photo fermentative process for hydrogen production with *R.*

capsulatus wild type (DSM 1710) and YO_3 hup$^-$ was used. Dark fermentor effluent of molasses containing acetate and lactate was used as a carbon source. The highest productivities were obtained as 0.69 and 0.08 mmol H_2/Lc.h (H_2/(m^3.h) while using 4 L and 20 L panel photobioreactors, respectively by *R. capsulatus* YO3 (hup$^-$). pH was controlled with sodium carbonate buffer (Sevler Gökçe Avcioglu 2010).

Boran aimed to implement solar pilot tubular reactor for hydrogen production. Integrated system hydrogen production with *R. capsulatus* wild type (DSM 1710) and YO3 hup$^-$ was used. The first time, solar tubular photobioreactor (90 L) made up of low-density polyethylene (LDPE) was developed as parallel with the ground. Cooling coil system was integrated. DFE of molasses was used as a carbon source of photofermentation. The highest productivity was reported as 0.12 mol H_2 /m^3.h for *R. capsulatus* YO3 (hup$^-$). The experiment lasted 15 days and pH was controlled with sodium carbonate buffer (Boran 2011).

Sağır investigated biological hydrogen production capacity for four different purple non-sulfur bacteria (*Rhodobacter capsulatus* (DSM 1710), *Rhodobacter capsulatus* YO3 (hup$^-$), *Rhodopseudomonas palustris* (DSM 127) and *Rhodobacter sphaeroides* O.U.001 (DSM 5864)). The type of carbon source used, sucrose or molasses, was the other parameter in addition to the bacteria strain. The experiment was carried out in 50 – 150 ml batch small scale glass bottle reactors under indoor conditions. The highest hydrogen productivity was found as 0.78 (mmol/Lc.h) for *R. palustris* on sucrose. According to highest hydrogen productivity on molasses, 0.55, 0.41, 0.5 and 0.02 (mmol/Lc.h) for *R. palustris*, *R. capsulatus* YO3 (hup$^-$), *R. sphaeroides* and *R. capsulatus* wild type, respectively. After *R. palustris*, *R. capsulatus* YO3 (hup$^-$) has the highest productivity (Sağır 2012).

Androga aimed to control temperature and design a U-tube tubular reactor made of glass. PVC cooling coils were inserted inside U-tubes parallel to each other. It was found that counter-current cooling was more effective for the tubular reactor to control

the temperature. The highest hydrogen production rate was obtained as 1.3 mol $H_2/(m^3.h)$ (Androga 2014).

Kayahan also designed a tubular photobioreactor (9-11 L). Glass U-tubes were used and put on top of each other and connected with 2 manifolds when compared to Androga work. The reactor was operated at single stage photofermentation. Molasses and acetic acid were used as a carbon source by *R. capsulatus* YO3 (hup^-) and compared. The highest hydrogen productivity was reported as 0.311and 0.114 mol $H_2/(m^3.h)$ for molasses and acetic acid, respectively. The experiments lasted 10-20 days. pH was tried to control using potassium phosphate buffer in the initial medium and adding feed having high pH value (Kayahan 2015).

Savasturk scaled up the tubular reactor designed by Kayahan from 9 L to 20 L. Molasses was used at single stage photofermentation by *R. capsulatus* YO3 (hup^-) and adding a high amount of glutamate, C/N ratio was lowered according to previous studies. The maximum productivity was obtained as 0.47 $H_2/(m^3.h)$. The hydrogen production lasted about 10 days and potassium phosphate buffer in the initial production medium was used to prevent pH decreasing (Savasturk, Kayahan, and Koku 2018).

In our laboratory, after parameters which affect hydrogen production were clarified and bacteria strain was selected, a different type of photobioreactors were designed. Firstly, the panel reactor was designed and tried under outdoor conditions. Then tubular photobioreactor was designed and operated under outdoor conditions to reach large volume and better mixing. Cooling systems were necessary for outdoor conditions so it was designed and cooling coils were integrated with tubular reactors. At the same time, various carbon sources were investigated, especially wastes were tried to utilize for sustainability and economical aspect. Molasses was decided as a carbon source at recent studies. Furthermore, different C/N ratio was used after

molasses was started to use. Lastly, a tubular photobioreactor reactor utilizing molasses was used with successful cooling system and scaled up.

When molasses was used, the pH value decreased due to the nature of sugar utilization. The decreasing pH limited the duration of production. In literature, several strategies have been tried, such as using a high initial pH and buffer concentrations, however, such methods are not robust solutions for sustained hydrogen production.

2.9. Developments of pH Control Strategy

The control of pH is a difficult control problem which has been extensively treated in the literature due to its highly non–linear and transient behavior. Models for the static and dynamic behavior of the pH processes and different pH control applications were developed in the literature with experimental acid-base reactions and searches still continue.

A general approach on modeling pH control process was developed by McAvoy et al. A mathematical model was built for the pH value of the continuously stirred tank reactor (CSTR) with the help of material balances, equilibrium relations, and electroneutrality condition. Weak acid and the strong base was studied. Acetic acid was neutralized by sodium hydroxide. A mathematical model was verified with a step input test performed experimentally (Mcavoy 1972).

Gustafsson and Waller used reaction invariant control method. The reaction was separated as variant and invariant parts. With the help of separation of the reaction, dynamic model of the pH process was expressed by the linear differential equation for the dynamic part and non-linear implicit algebraic equation was applied to the static part. Adaptive reaction invariant feedback pH control application has been reported (Gustafsson and Waller 1983).

Wright and Kravaris introduced a general mathematical model. A minimal-order model with the same input and output behavior model was derived. The strong acid equivalent was reformulated with an on-line estimation of the strong acid depending minimal-order which requires only nominal titration curve information. A linear controller based on strong acid equivalent was developed. The method of strong acid equivalent was implemented to laboratory-scale pH neutralization system. A proportional-integral (PI) controller was designed to control the neutralization process of strong acid equivalent in CSTR (Wright and Kravaris 1989).

Gustafson and Waller pointed out based on their researches that non-linear control is superior when the characteristic of the process are well known. However, linear feedback control may show the same performance with nonlinear control for not well-known system characteristic (Gustafsson and Waller 1992).

A new identification strategy was proposed by Sung for non-linearity and time-varying characteristic of the pH control process. The equivalent titration curve of the process stream was obtained to transform the measured pH value to the state variable which was a controlled variable for the PI controller. The study has reported a simple stability analysis to determine the PI controller parameters (Sung and Lee 1995).

Sung et al. developed an adaptive control strategy with the on-line recursive estimator to determine the total iron concentration and dissociation constant of a fictitious acid. A non–linear PI controller was designed according to obtained information from estimator to control the pH value. A good control performance and robustness established from the proposed controller under different modeling errors and measurement noise. However, it was assumed that the feed stream was composed of a single 1–protic weak acid. Thus, when new chemical species encountered in the system, the control performance might probably be poor due to changing the titration curve (Sung et al. 1998).

A fuzzy–self-tuning PI controller to control pH was studied by Babuska et al. on a small scale laboratory fermentation system. Proposed control system contained an

adaptive PI controller and a fuzzy self–tuning mechanism. Proportional gain and integral time of the PI controller were adjusted on–line by a single parameter updated using the output of the fuzzy inference system. The controller was tested and verified experimentally. It was shown that the fuzzy self–tuning PI controller was capable of controlling the pH value of a fermentation process accurately within the required range of pH (Babuska et al. 2002).

Kumar et al. studied neutralization of acetic acid with sodium hydroxide in a CSTR. The Wiener model containing a linear dynamic element and a static non–linear element was used. A non–linear PI controller was designed based on the Wiener model. The non–linear PI controller was tuned by pole placement method. It has been reported that the non–linear controller is superior when compared to local linear PI control according to the results of simulations and experiments (A. A. Kumar et al. 2004).

Vural et al. studied acetic acid and sodium hydroxide neutralization reaction to control pH in the tubular flow reactor. Experimental pH control in the nonlinear region was demonstrated for different control strategies of conventional PID, self-tuning PID, and fuzzy algorithms in spite of high dead-time of tubular flow reactor. Conventional PID parameters were obtained with the Cohen-Coon method. It has been reported that conventional PID control showed a better result than self-tuning PID control. Fuzzy controller, conventional PID was found satisfactory (Vural et al. 2015).

PID control has a linear nature and its tuned parameters are not changed during the operation. Therefore, PID control was not preferred for pH control in the literature generally. However, if the changes are small, PID can be accepted as satisfactory (Vural et al. 2015).

The control system was selected as PID control. PID control was more practical and advantageous because of its simplicity, industrial compatibility and satisfactory performance. Since acidification is a slow process, a conventional PID control system

may be feasible. Therefore, to control the pH of the biological process at 7.5 in the nonlinear region, conventional PID control was found suitable as a first step.

2.10. PID Control System

Proportional-integral-derivative (PID) control is an error-based feedback control which is commonly named as three-term control. PID control is one of the important and widely used industrial controllers due to past record success, wide availability and simplicity in use. The controller calculates the error value e(t) as a difference between the desired set point r(t) and the process output y(t) continuously and reduces the error signal to zero based on system proportional, integral and derivative parameters. The function of the feedback control system is to supply the desirable dynamic and steady-state response characteristic on closed-loop system by minimizing the effect of disturbance, eliminating the steady-state error and reducing the excessive control action (Calvo-Rolle et al. 2012; Johnson et al. 2005; Seborg et al. 2011).

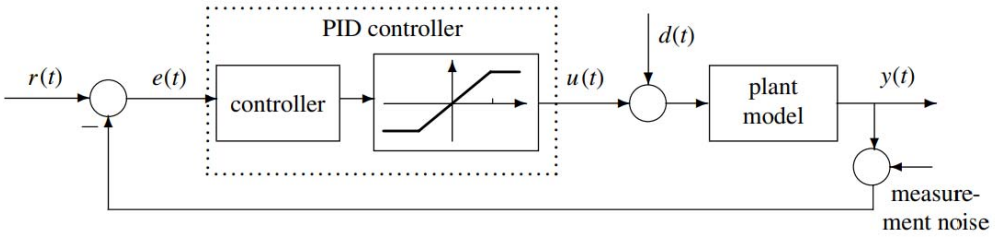

Figure 2.6. Typical PID control structure. y(t): process output, r(t): setpoint, u(t): controller output, d(t): disturbance signal, e(t): error signal

Proportional control is denoted by the P-term in the PID control. The controller gain (K_c) is adjusted to make the controller output close to set point. The proportional

control output is proportional to the error signal according to following equation (Seborg et al. 2011):

$$u(t) = \bar{u} + K_c e(t) \tag{2.47}$$

where u(t) is controller output, e(t) is error signal and $\bar{u}$ is bias (steady-state) value. When the error is zero, controller output is at nominal steady-state value. The main disadvantage of proportional-only control is steady-state error (offset).

Integral control is denoted by the I-term in the PID controller. τ_I is referred to as integral time or reset time which has units of time. For integral control, the adjustable parameter is τ_I to reduce the error in equation 2.48. Equation of integral control implies that u changes with time unless error value is equal to zero. Wen time integral is used, offset is zero. Since proportional control action is fast, integral control is generally used with proportional control. The disadvantage of using integral time is that it produces oscillatory responses of the controlled variable (Seborg et al. 2011).

$$u(t) = \bar{u} + \frac{1}{\tau_I}\int_0^t e(t)d(t) \tag{2.48}$$

The function of the derivative control action is to predict the future behavior of the error signal depending on its rate of change. Derivative control is expressed with the following equation, where τ_D is the derivative time in units of time. Derivative action is never used alone. Derivative control action contributes the improvement of dynamic response of the controlled variable by reducing settling time (Seborg et al. 2011).

$$u(t) = \bar{u} + \tau_D \frac{de(t)}{d(t)} \tag{2.49}$$

Combination of the proportional, integral and derivative control modes constitutes PID control system which is expressed in the equation.

$$u(t) = \bar{u} + K_c \left[e(t) + \frac{1}{\tau_I} \int_0^t e(t) d(t) + \tau_D \frac{de(t)}{d(t)} \right] \quad (2.50)$$

PI pH control system has been generally used in raceway and open photobioreactors to produce biomass from microalgae that can be used in feed, food, and cosmetics. CO_2 is used to control pH value during the photofermentation. These raceway reactors have 20 m^3 working volume (Carreño-Zagarra et al. 2019)

2.11. pH Control for Biological Hydrogen Production

The pH control system in biological hydrogen production process is generally used in small scale batch or continuous stirred tank reactor which have automatic titrator under controlled environment (Table 2.2). 1 l-tubular type reactor was used in photofermentation process to produce hydrogen by Palamae et al. (2018) with manual pH control. According to our knowledge, this study is the first time continuous pH control has been conducted for outdoor tubular photobioreactor with PNS bacteria.

Table 2.2. *pH-controlled biological hydrogen production by different processes*

Process	Mode of operation	Type of the bacteria	Reactor volume (L)	Reactor type	Carbon source	Manipulated variable	References
Dark fermentation	Batch	Anaerobic digester sludge	0.28	Serum bottle	Rice slurry	1 M HCl 1 M NaOH	(Fang, Li, and Zhang 2006)
		Anaerobic sludge	3.00	Fermenter	Sucrose	4 M NaOH 2 M HCl	(Mu, Wang, and Yu 2006)
		Enterobacter cloacae IIT-BT 08	0.05	Glass column fermenter	Sucrose	Not given	(N. Kumar and Das 2000)
		Mixed culture	3.00	Batch fermenter	Tequila vinasse wastewater	3.5 M H2SO4 10 N NaOH	(García-Depraect et al. 2019)
		Microbial consortium	1.5 0	STR	Cheese whey	1 M HCl 1 M NaOH	(Braz Romão et al. 2018)
		Clostridium	0.30	STR	Food waste	3M KOH	(Moon et al. 2015)
		Escherichia coli	1.00	STR	Cheese whey	2.5 M NaOH 2.5 HCl	(Rosales-Colunga et al. 2013)
		Mixed microflora	1.00	STR	Food waste	2.5 N NaOH	(Jun et al. 2008)
		Thermoanaerobacter thermohydrosulfuricus	1.00	STR	Glucose	2 M NaOH 2 M H2SO4	(Cook and Morgan 1994)
		Microbial consortium	2.00	STR	Xylose and lactose	5 N NaOH and 4 N HCl	(Calli et al. 2008)
	Fed-batch	Mixed culture	0.40	Fed-batch	Sugarcane vinass	0.1 NaOH	(Pouresmae et al. 2019)
	Continuous	Mixed culture	8.00	ASBR	Glucose	0.5 M NaOH 0.5 M HCl)	(Y. Li et al. 2010)
		Anaerobic sludge	3.00	STR	Glucose	6 M NaOH 4 M HCl	(Fang and Liu 2002)
		Mixed cultures	2.00	UASB	Sucrose	3 M NaOH/3 M HCl	(Zhao and Yu 2008)

Table 2.2. Continued

		Co-digestion	1.50	CSTR fermentor	Cypriot whey cheese)	6 M NaOH 6 M KOH 6 M HCl	(Stavropoulos et al. 2016)
Two-step dark and photofermentation	Fed-batch	*R. sphaeroides* O.U.001 and *C. acetobutylicum* DSM 792	0.12	Batch	Starch	1M NaOH 1M HCl	(Zagrodnik and Łaniecki 2017)
	Continuous	*Escherichia coli*	2.70	CSTR	Glucose	Electrodialysis	Redwood 2012
Photofermentation	Batch	*R.sphaeroides*	0.12	Batch	Glucose	NaOH	(Zagrodnik and Laniecki 2015)
		photoheterotrophic bacterial consortium	0.50	Glass bottle	Cassava wastewater	2 NaOH	(Lazaro et al. 2015)
		R.sphaeroides KD131	0.50	Bioreactor	Acetate and butyrate	2 M NaOH	(M. S. Kim et al. 2011)
	Continuous	*Rhodobacter sphaeroides*	1.00	Tubular	Oil palm	3 M NaOH 3 M HCl	(Palamae et al. 2018)

In this study, a pH control system was selected, constructed and integrated successfully to the last used tubular photobioreactor (20 L) operating under outdoor conditions. Moreover, the C/N ratio was investigated to obtain the optimal ratio for molasses utilization under indoor conditions. To observe only pH effect on hydrogen production rate, hydrogen purity, and carbon source utilization, several indoor experiments were carried out.

CHAPTER 3

MATERIALS AND METHODS

3.1. The Bacterial Strain

In all of the experiments, *Rhodobacter capsulatus* YO3 (hup^-) was used. This is a mutant strain obtained by Dr. Yavuz Öztürk (GMBE, TUBITAK MAM – Gebze) from the wild-type DSM 1710 by deleting the gene coding for the uptake hydrogenase enzyme (hup-).

3.2. Culture Media

3.2.1. Solid Media

Solid media included mineral–peptone–yeast extracts (MPYE) medium and agar (1.5% w/v) (Appendix E). After chemicals were prepared in distilled water, pH of media was adjusted to 7.5 by adding 0.5 M NaOH. For sterilization and dissolution of substances, media was autoclaved (NÜVE OT 90L) and cooled to around 40 ºC then, it was poured into the agar plates in laminar flow sterile cabin (NÜVE MN 090). When media solidified in plates, they could be stored at room temperature.

Stock bacteria, which were kept in an -80 ºC deep freezer, were activated on MPYE agar plates. The plates were wrapped with an aluminum foil to prevent light and kept in an incubator at 30 ºC. Within 4-6 day, bacteria colonies were visible. The plates were also used to detect contamination of any growth medium, stock bacteria or reactor sample during the experiment.

3.2.2. Growth Media

The Biebl and Pfennig (1981) medium contained 20 mM acetate as carbon source and 10 mM glutamate as nitrogen source was used for the growth of bacteria after activation on agar plate (Appendix E) (Biebl and Pfennig 1981). All substances were dissolved in distilled water, the pH of the media was adjusted to 6.4 by adding 5 M NaOH solution. The medium was sterilized by autoclave that worked at 121 ^{o}C for 20 minutes. The medium was cooled to about 30 ^{o}C and trace elements, iron citrate, and vitamin solutions were added to the medium in laminar flow sterile cabin.

3.2.3. Molasses Adaptation Media

Sucrose-containing molasses was used as a carbon source in the hydrogen production medium. Thus, Biebl and Pfennig medium was modified by adding molasses to supply that the bacteria can utilize sucrose in molasses effectively. Adaptation of bacteria to sucrose was performed in two steps (Appendix E).

a) First Adaptation Medium

The medium contained 20 mM acetate, 10 mM glutamate and 5 mM sucrose containing molasses. All chemicals of the Biebl and Pfennig recipe were dissolved in distilled water. pH was adjusted to 6.4 using NaOH. The medium was sterilized by autoclave. After the medium was cooled in laminar flow cabin, molasses was added to Biebl and Pfennig medium since molasses spoiled in the autoclave.

The bacteria were transferred to the first adaptation medium when its OD 1.0 – 1.5 at 660 nm.

b) Second Adaptation Medium

In the second adaptation medium, only molasses have been used in Biebl and Pfennig medium. The medium contained 10 mM glutamate and 5 mM sucrose as carbon sources. Molasses was added after autoclave thus; adaptation mediums were controlled with MPYE agar medium in case of contamination. Bacteria were transferred to the second adaptation medium before inoculation of hydrogen production medium.

3.2.4. Hydrogen Production Media

Molasses that was taken from Ankara sugar factory was used as a carbon source in the hydrogen production medium (Appendix F). In hydrogen production medium, sucrose concentration in molasses was 5 mM, 30 mM KH_2PO_4 solution was used as a buffer. Initial pH was adjusted to 7.5 with 5 M NaOH solution as parallel with previous studies (Kayahan, Eroglu, and Koku 2017; Sagir et al. 2017; Savasturk, Kayahan, and Koku 2018). Molasses solution contains, in addition to a high amount of sucrose (50% w/w), various nitrogen sources (amino acids) and trace elements that promote nitrogenase activity such as iron and molybdenum. The amount of glutamate was supplemented after the addition of molasses, according to the chosen C/N ratio. Fe and Mo were added to the molasses so that the final amount of Fe and Mo in the feedstock was 0.1 mM and 0.16 μM, respectively.

3.3. Implementation and Construction of pH Control System

3.3.1. pH Control System Selection

To obtain long-term photofermentative hydrogen production utilized waste, automated pH control is necessary. Tubular reactor was used since it is easier to scale up and it has a high surface-to-volume ratio for photofermentative hydrogen production.

In this thesis, the study copes with the pH control of a neutralization process between a weak acid and a strong base in a tubular reactor. The base flow rate was chosen as the manipulated variable.

Control of the pH has some difficulties because there are problems encountered in tubular reactor and neutralization process.

Mixing is one of the main problems in the tubular reactor. The flow was distributed through parallel tubes and reactor medium was mixed with the circulation by peristaltic pump continuously. Increase in mixing increases the mass transfer rate and

decrease the nutrient gradients in the reactor and eases the separation of the produced biogas from the reactor medium. However, there is an optimum flow rate value. According to a study, hydrogen productivities were obtained from the reactors mixed at 40, 80, 120 and 160 rpm and the reactor mixed 120 rpm had the highest productivity as 2.7 molH_2/(m^3.h) (Flickinger, 2013). High mixing power may cause cell damage because of shear stress. In this study, the volumetric flow rate was 80 L/h based on a previous study (Kayahan, 2015) and the reactor volume was 20 L so, hydraulic retention time (or residence time) was 25 minutes. It can be accepted as high lag time.

In addition to circulation of the medium, manifolds significantly contribute the mixing since they are conjugation point for medium flow. Reactor medium flow from tubes meets in the outlet manifold after recirculated flow was distributed by inlet manifold. Thus, flow distribution in the manifolds affects the mixing performance of this system.

The flow distribution in the manifolds depends on pressure changes derive from wall friction and fluid momentum (Acrivos, Babcock, & Pigford, 1959). In the U type horizontal manifolds, friction decreases the pressure in the reverse direction of the fluid however, fluid momentum increases the pressure along with the manifolds.

pH neutralization is accepted as a harder control process because of its high nonlinear characteristic, time-varying behavior and its high sensitivity to changes around the neutralization point (Elameen, Karsiti, and Ibrahim 2014). In the literature, adaptive pH control in continuously stirred tank reactor (CSTR) (Gustafsson & Waller, 1983), the nonlinear internal model controller (IMC) (Kulkarni et al. 1991), adaptive nonlinear control for CSTR (Henson & Seborg, 1994) was developed. Model predictive adaptive control system for CSTR was applied (Palancer et al. 1994).

PID control has a linear nature and its tuned parameters are not changed during the operation. Therefore, PID control was not preferred for pH control in the literature. However, when the changes are small, PID can show good performance (Vural et al. 2015).

In this study, a pH controller was installed to the pilot-scale (20 L) glass stacked U-tube photobioreactor, tuned and operated to maintain the pH close to optimum during continuous operation. Since acidification is a slow process, a conventional PID control system was selected.

The control system was selected as PID control. PID control was practical and advantageous because of its simplicity, industrial compatibility, and satisfactory performance. Thus, to control the pH of the biological process at 7.5 in the nonlinear region, it was found suitable as a first step.

3.3.2. Implementation to the Reactor

Measurement and base feeding points were determined. Since manifolds contribute the mixing, the exit of the outlet manifold was chosen as the pH measurement point. Base feeding point was determined as the entrance of the inlet manifold according to the flow direction of the liquid (Figure 3.1).

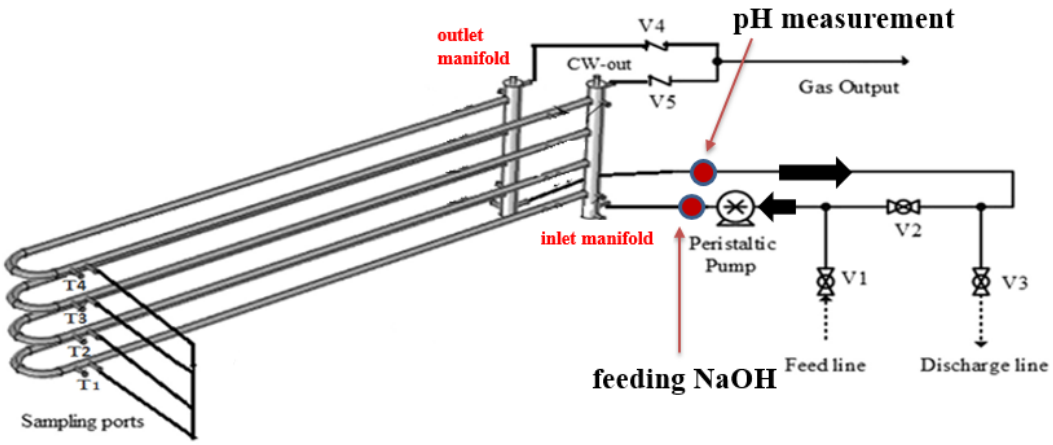

Figure 3.1. Stacked U-tube photobioreactor.

The sensor should remain in liquid at a certain level in order to make an accurate measurement. To observe the level of the reactor liquid in pH probe port, transparent glass septum was constructed in RUN290817. Between the probe and the septum, rubber O-rings and silicone-based glue were used. For the circulation pipe connection, metal screw clamps were used only. During the experiments, pressure changed depends on biogas production so, the liquid level in septum changed.

To keep the pressure high in order to increase the liquid level, the pH probe was placed near the bottom side of the outlet manifold. In the port connection, the pressure was increased by momentum effect in the same flow direction and gravitational force, thus the liquid level was kept high.

High pressure in pH probe may cause biogas leakage to the atmosphere, at the same time low pressure in base feeding port may cause air leakage to the reactor. It was observed that glass septum (Figure 3.2) was not enough and observed both liquid and gas leakage. Very tight port construction is necessary. A new port was constructed in RUN160818 (Figure 3.3). Threaded connection fitted to screw of the probe was placed in the septum. The new port was tested which was mentioned and there was no leakage.

Base feed port was placed near the top of the manifold to ease the base flow by keeping the liquid level low. High reactor medium liquid level could block the base flow and rise inside the base feeding line. Therefore, the pressure was decreased due to friction and gravitational force. However, low pressure could cause air leakage to the reactor.

Base feeding port was made of glass in RUN290817 to adjust the changing liquid level in the port (Figure 3.4). To tight the connections and prevent liquid and gas leakage, metal T-fitting was constructed and made it fit to feeding pipe and circulation line of the reactor. Before usage, it was tested in case of leakage as mentioned and used in RUN160818 (Figure 3.5).

Figure 3.2. The picture of pH port in RUN290817.

Figure 3.3. The picture of pH port in RUN160818.

Figure 3.4. The picture of the base port in RUN290817.

Figure 3.5. The picture of the base port in RUN160818.

3.3.3. Tuning Parameters

The response to an input effect is delayed in many processes, and the photobioreactor system in this study is a typical case. Because the reactor is tubular, with a high surface-area-to-volume ratio, mixing takes time and the change in pH in response to input of base solution is gradual, especially when the feed and measurement points are at opposing ends of the tubular geometry (Vural et al. 2015).

An empirical method is used instead of the theoretical method since it may not be practical for a process that requires a large number of equations and unknown parameters. In bioprocess system, 5 different organic acids: acetic acid, lactic acid, propionic acid, butyric acid, and formic acid are produced. The production of weak acids is a very slow and complex process since acid productions may change based on carbon source, environmental conditions such as light intensity, temperature and pH and ion stress. Therefore, the empirical model should be more feasible for system identification.

Each system has its own specifications such as volume, solution characteristic, temperature conditions. Thus, real experimental setup should be developed directly from experimental data for each system, specifically. Step test is used fitting first-order-model. A plot of the output response of a process to a step-change in the input is processed reaction curve. After step input is sent, the reaction curve reaches steady-state. However, step input may cause base accumulation for a batch system.

In the test run using the emulated hydrogen production medium and pilot-scale (20 L) stacked tubular reactor was used. 30 mM KH_2PO_4 was added to 20 L distilled water. Acetic acid which is mostly produced by the purple nonsulphur bacteria was chosen to simulate the hydrogen production experiment. Acetic acid was added to the reactor medium until the pH of the reactor was 6.7. First, the 2 M NaOH was fed to the reactor at a constant maximum flow rate (5.5 ml/min) of the controller pump to observe the time that the system pH starts to change (Figure 3.6). Then, at the desired value base feeding was stopped to observe deviation because of the overloading of the base. Since

there was a time delay, when pH control read the desired value at the outlet of the reactor, an excess amount of base was fed to the reactor.

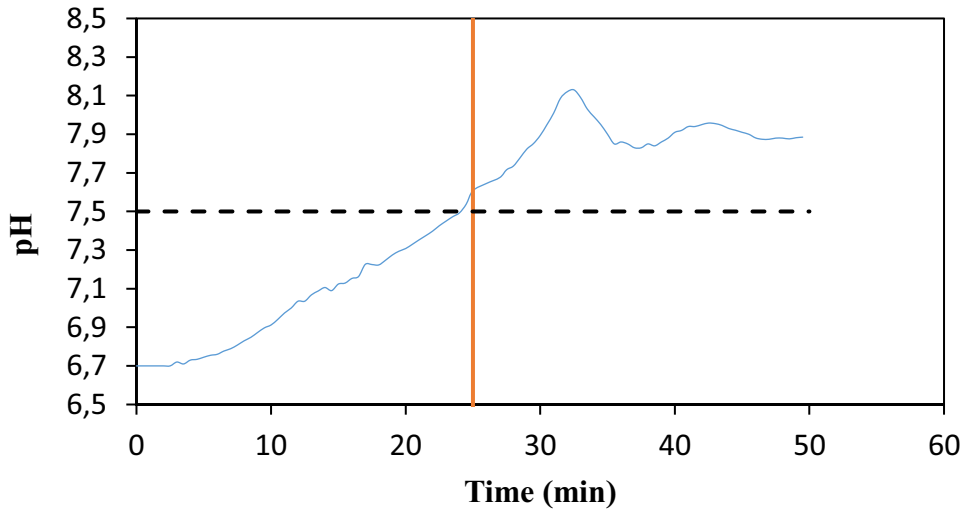

Figure 3.6. Response curve of pH in hydrogen production medium (HPM) without bacteria, under constant base flow rate. The dashed line indicates the desired pH value and the solid line indicates switching of the base pump on or off.

In Figure 3.6, after 5th minutes, system pH started to increase. In other words, pH control perceives the base feeding after 5 minutes. The time delay was taken around 5 minutes, graphically. When the pump was shut down at 25th minutes when controller read pH as 7.5, the system stabilized only after 10-15 minutes and at a value 7.9 pH. The offset was because of the excess base loading and the delay due to slow mixing. Since the acidification process is slow as well, conservative control parameters were selected to deal with the large lag time. According to the graph, time constant (τ) was determined as 7.5 minutes.

To tune parameters, Cohen Coon tuning rules were applied. Where K is process gain, τ is time constant, θ is time delay, K_c is controller gain, τ_I is integral time, τ_D is derivative time.

$$K_C = \frac{1}{K}.\frac{\theta}{\tau}.\left(\frac{4}{3}+\frac{\theta}{4.\tau}\right) \qquad (3.1)$$

$$\tau_I = \theta \frac{32 + 6\frac{\theta}{\tau}}{13 + 8\frac{\theta}{\tau}} \tag{3.2}$$

$$\tau_D = \theta \frac{4}{11 + 2\frac{\theta}{\tau}} \tag{3.3}$$

$$\tau_I = 5 \frac{32 + 6\frac{5}{7.5}}{13 + 8\frac{5}{7.5}} = 10 \tag{3.4}$$

$$\tau_D = 5 \frac{4}{11 + 2\frac{5}{7.5}} = 2 \tag{3.5}$$

The procedure depicted in Figure 3.6, was repeated with PID control and a set point of 7.5, using several parameter sets and the combination that resulted in the least offset was selected. The gain was determined experimentally. To observe the effect of parameters, different τ_I and τ_D values were tried tabulated in Table 3.1.

Table 3.1. *Parameters of PID controller.*

RUN	**Kc**	**τ_I**	**τ_D**
RUN1	10	0.1	0
RUN2	1	10	2
RUN3	0.1	10	2

3.4. Experimental Set-up of Outdoor Experiments

3.4.1. Pilot Scale Tubular Photobioreactor

The reactor consists of 4 glass U-tubes as shown schematically in Figure 3.7, and in the photographs in Figures 3.8 and 3.9. The glass tubes have 3 sections connected via rubber bellows. The diameter and length of each U-tubes are 4 cm 3.8 m, respectively, and the wall thickness of the tubes is 2 mm**.** The vertical distance between the tubes is 6.5 cm. The U-tubes are tilted 30 °C with respect to the horizontal axis to facilitate collection of the produced gas. The tubes are connected with 2vertical manifolds, one for inlet and the other for the outlet of fluid, both of which have 6 cm diameter. The height of the inlet manifold is 52 cm and that of the outlet manifold is 60 cm. The produced gas in U-tubes is carried out by medium flow and pressure differences in the tubes on the headspace of manifolds and transferred to the gas collection unit via one-way check valves. Thus, headspace pressures are kept constant by one-way check valves (HAMLET) at 1/3 psi. Since each tube connected with the outlet, the manifold is elevated at an angle of 30 ° above the inlet manifold, and because the flow direction is through the outlet, most of the produced gas is collected in the headspace of the outlet manifold. The total liquid working volume of the PBR is 20 L.

Polyurethane pipes having 5.5 mm inlet diameter and 8 mm outlet diameter were used as the connection lines between the gas outlet of the manifolds and the gas collection unit. The gas collection unit, made of glass, has a volume of about 10 L. The water displacement method was used to collect produced gas in the gas collection unit.

Each U-tube has 2 sample ports. Of the 8 ports on the tubes of the PBR, 4 were used for sampling and the others were used to insert thermocouples to measure temperature.

A peristaltic pump (Masterflex 6424-36) was used to mix the reactor medium. The liquid reactor medium was circulated continuously by a circulation pump at a rate of 60 L/h.

In order to keep the reactor temperature below 40 °C during the day, a cooling system was used. The cooling system consists of a thermocouple which continuously measures temperature of reactor, a process water cooler (PNÖSO PSS 6 D) and pump (PEDROLLO PKm 60) and a temperature control unit. The cool process water enters the PBR via both manifolds and flows into the spiral glass coils inserted in manifolds, counter-current to the culture medium. The process water that has warmed due to radiative and convective heat transfer from the surroundings, leaves the PBR from the exit ports of the manifolds, and is cooled and returned to the reactor by the cooling system. The circulation rate is regulated by the cooling system according to the reactor temperature measured by the thermocouple.

3.4.2. Process Flow Diagram

The process flow diagram is presented below (Figure 3.7). The liquid including hydrogen production medium and bacteria was circulated by a peristaltic pump. Circulated reactor medium entered from the bottom of the inlet manifold and distributed to the tubes by manifold. The liquid flowed through tubes and mixed in outlet manifold. The mixed liquid was taken from the bottom of the outlet manifold and recirculated by a peristaltic pump. Produced gas accumulated in the headspaces of manifolds and collected in the gas collection unit through check valves (V4 and V5). The check valves opened when the gauge pressure in headspaces exceeded 1/3 psi. The check valves were one way so, produced gas could not come back to headspace. Cooling water entered from the bottom of both manifolds as shown as CW in and exited from the top of the manifolds as shown as CW out. 8 ports were placed on the reactor. 4 ports T1 - T4 were temperature ports. 4 ports were used for sampling.

Feeding was fed to reactor in two ways. Firstly, 1 L feed was given to the reactor and equal volume of reactor liquid was simultaneously taken to maintain constant reactor volume and avoid pressure increasing. V2 was closed to stop circulation and feeding line (V1) and discharge line (V3) was opened. Secondly, an equal volume of feeding was fed to the reactor from 4 sample ports to distribute the feed homogeneously.

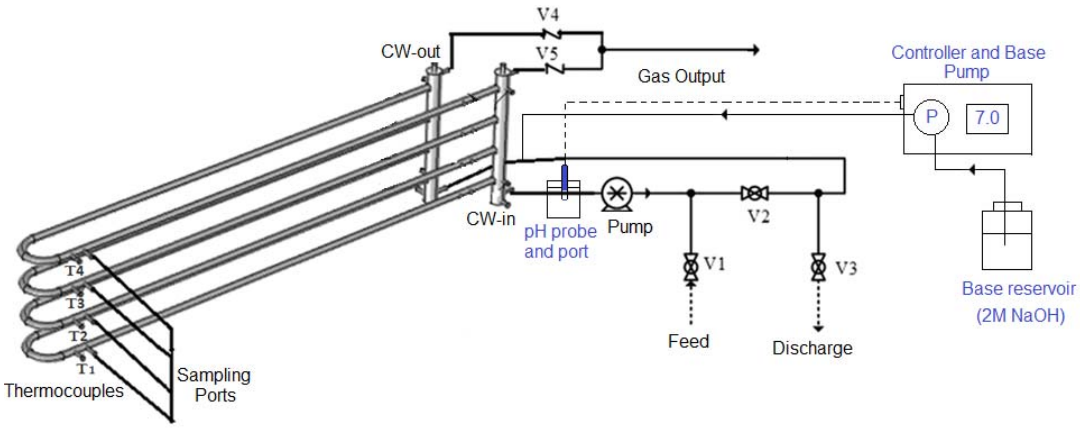

Figure 3.7. Schematic diagram of the U-tube reactor with the pH control system for anaerobic photofermentative hydrogen production. CW: Cold Water streams, T1-T4: thermocouple ports, V1-V3: feeding/discharge valves, V4-V5: Gas check valves.

3.4.3. Operation

3.4.3.1. Leakage Test

The reactor connections of tubes were tightened manually. Soap bubbles were applied to all connections on U-tubes and pressurized air was given to an empty reactor by a compressor to detect leakage. For circulation pipe connections including valves, pipe tees and were placed in a water tank and compressed air was applied to detect any bubble on water. pH probe and base feeding ports (constructed in RUN160818) were tested in a water tank with compressed air after probe and feeding line were connected tightly.

3.4.3.2. Sterilization

The reactor was filled with 3 % hydrogen peroxide (H_2O_2) solution and circulated for 24 hours. After the reactor was emptied, filled with distilled water only and circulated for 12 hours. To remove all hydrogen peroxide, the reactor was circulated with distilled water 2 times for 1 hour before startup of the experiment.

3.4.3.3. Inoculation and Start-Up Procedure

The reactor was opened to the atmosphere and only circulation pipe was connected with the reactor. The bacteria were inoculated into hydrogen production medium in 20 L plastic bottle. The reactor was filled with the liquid medium in the bottle via feeding line as soon as possible after sterilization until air was left headspace of manifolds. Since the volume of headspaces is small, argon flush was not needed. pH probe was inserted in septum and connected with pH controller. 2 M NaOH solution was prepared in 1 L bottle and connected with the pump of pH controller. The base was pumped through base feeding line to empty air in the line and linked with the reactor. Gas collection unit was filled with tap water, completely. Check valves were connected with manifolds and gas collection unit. Feeding and discharge line (V1 & V3) were closed and V2 was opened. Circulation pump was opened to start mixing.

3.4.3.4. Continuous Feeding

In RUN290817, the feed was given when sucrose concentration decreased below 2 mM in the reactor to ensure the bacteria to consume molasses completely. Each morning, sucrose concentration in the reactor was analyzed by HPLC, before feeding. If the sucrose concentration was below 2 mM, it was completed to 5 mM by adding molasses. The molasses was given in 1 L feed to the reactor while 1 L medium in the reactor was taken out. The feed included 2 mM sodium glutamate, vitamins, trace elements, Fe-citrate and buffer.

The concentrations of vitamin, trace element, Fe-citrate and buffer solutions were adjusted for 1 L hydrogen production medium. The feeding started on 4th day of the experiment when all sucrose consumed suddenly and the bacteria concentration decreased.

In RUN160818, feeding strategy was to keep sucrose concentration at 5 mM. The sample was taken from the reactor and analyzed by HPLC each morning. The sucrose concentration in the feed was adjusted and completed to 5 mM. The feed contained molasses and distilled water only. Molasses was diluted in 200 mL distilled water and it was fed to the reactor from sample ports of 4 U-tubes at equal volume.

The reason for the changed feeding strategy and methods was discussed in the 'Results and Discussion' part.

Figure 3.8. The picture of the experimental setup in RUN160818 with pH control.

Figure 3.9. The picture of the experimental setup in RUN290817 with base feeding port.

Figure 3.10. The picture of the experimental setup in RUN290817 with pH probe septum.

3.4.3.5. Sampling

In RUN290817 and RUN160818**,** samples were taken two times a day. For reactor medium analyses, 2nd and 4th tubes (counted from the bottom) were used.

In the morning, 2 samples were taken from the reactor medium and analyzed in HPLC for sucrose and organic acid concentrations, UV Spectrophotometer for OD and pH. The gas volume produced in the previous day was read from gas collection and one sample was taken from the top of it in order to analyze in GC. Then, the gas collection unit was refilled with water. In the evening, 2 samples were taken from the reactor medium and analyzed in HPLC, UV Spectrophotometer, and pH. pH value was measured from all four different tubes in some days to observe homogeneity of pH.

3.5. Experimental Set-up of Indoor Experiments

Indoor experiments were performed in 55 ml glass bottles which were used as photobioreactors. To carried out parallel experiments based on various parameters that affect hydrogen productivity, small scale photobioreactors were useful. The reactors were filled with 45 ml hydrogen production medium, 5 ml bacteria and the remaining 5 ml of the reactor volume was used as headspace to enable gas analyses. Black rubber stoppers which are generally used for blood collection were used as the reactor cap. Before usage, all reactors were washed with 70 % Ethanol solution. To remove alcohol from reactors, they were washed with tap water and distilled water. Then, the reactors and rubber stoppers were autoclaved at 121 ^{0}C for 20 minutes.

After growing on molasses adaptation medium, bacteria were inoculated (10 % v/v) into the reactors which were filled with the 45 ml hydrogen production medium in sterile laminar flow cabin. The reactors were sealed with rubber stoppers. Argon gas was flushed through the reactors in 3 minutes to make the environment fully anaerobic. The reactors were placed in the incubator to keep the temperature at the desired value (Figure 3.11). The illumination was supplied by 100 W tungsten lamps.

The light intensity of the reactors was adjusted by luxmeter (EXTECH HD450). Gas collection units were 250 ml cylindrical glass tubes and filled with distilled water. The produced gas which was collected in headspaces of reactors was transferred to gas collection units via thin plastic line. Water shift method was used to measure the volume of produced gas and gas analyses were taken from the top of the reactors.

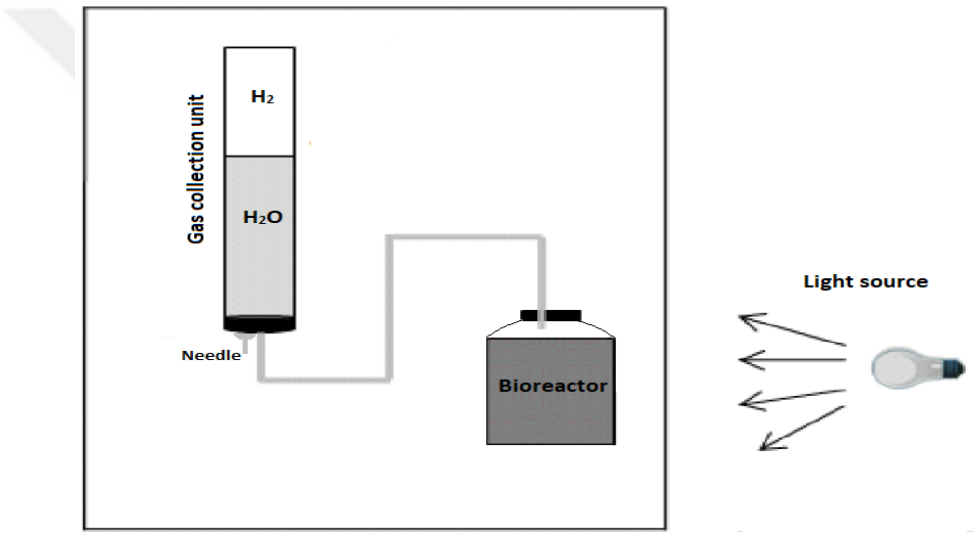

Figure 3.11. Schematic illustration of the indoor experimental setup.

Figure 3.12. The picture of the experimental setup operated under the indoor condition for hydrogen production.

3.5.1. Sampling

The samples were taken from glass batch reactors once a day. A gas sample was taken from the top of the reactors and analyzed in GC, firstly. The 2.5 ml sample was taken from each reactor medium. 1.5 ml sample was analyzed in pH meter and UV Spectrophotometer for OD, respectively. 1 ml sample was analyzed in HPLC for sucrose and organic acid concentrations.

When 2.5 ml sample was taken, same volume autoclaved distilled water was given to the reactor to keep the volume constant and prevent pressure drop in the reactor.

3.6. Experimental Procedure

3.6.1. Preparation of Inoculum

All liquid to liquid inoculation was performed when bacterial OD reached to 1.0 – 1.5 at 660 nm with 10% v/v inoculation ratio, and bacterial growth in tubes was carried out in an incubator (NÜVE cooled incubator ES250) at 30 ºC and illumination of 2000-2500 lux by tungsten lamps.

A single colony of bacteria was removed from solid MPYE agar plate and inoculated into 1.5 ml Eppendorf tube including growth media. Eppendorf tubes were waited (about 2 days) at the incubator. 1.5 ml bacteria were inoculated to 15 ml growth media. Then, bacteria were transferred to 50 ml of 1st adaptation. After about 36 hours at the incubator, they were inoculated to 50 ml 2nd adaptation media with the same inoculum ratio. Adapted bacteria were inoculated with various inoculation ratio to hydrogen production medium to reach the desired initial bacterial concentration.

3.6.2. Storage of the Bacteria

Glycerol was diluted with distilled water (30 % v/v) and autoclaved. When bacteria from growth medium was inoculated (2/3 v/v) into 1.5 – 2 ml cryogenic vials including glycerol solution. For long term storage of the bacteria, vials were kept at -80 ºC.

3.6.3. Base Media

2 M NaOH which was used in the pH control system solution was prepared with distilled water. For sterilization, the NaOH solution was autoclaved at 121 ºC for 20 minutes.

3.7. Analyses

3.7.1. Molasses Analyses

Molasses was obtained from Ankara Sugar Factory, Turkey (Appendix F). The sugar content, density and the concentration of some elements (Na, K, Ca, Mg, Fe, Mn, and Zn) were reported by the Ankara Sugar Factory. The total amino acids and minerals (Fe, Mo, S, K) were analyzed by Düzen Norwest Laboratory, Ankara, Turkey. Sucrose forms 52% w/w of molasses. Glutamic acid was taken into account as the nitrogen source in molasses when glutamate was added to reach the desired C/N ratio. Since the molasses needed to be diluted to adjust the sucrose content, Fe and Mo were also needed to be added to obtain the desired amounts necessary for bacterial growth.

3.7.2. Sugar and Organic Acid Analysis

Sucrose and organic acid concentrations from the reactor were analyzed by a High-Performance Liquid Chromatography (HPLC) system (Shimadzu 20A). The samples were filtered with 22 μm filters before analysis. HPLC had two detectors: Refractive index (RI) to measure sucrose concentration and UV detectors to measure organic acid concentrations that worked in series and equipped with an ion-exchange organic acid column (Alltech IOA-1000, 300 mm x 7.8 mm) (Appendix I & H). The mobile phase was 8.5 mM H_2SO_4 at 0.4 mL/min flow rate and the column temperature was 66 °C. Injection volume was 20 μL and filtered samples were injected to the system with the help of an autosampler (Shimadzu SIL-10AC). Sample time was 55 minutes.

The sucrose concentration was analyzed by RI detector and organic acids concentrations were determined by UV detector, simultaneously.

The retention times and peak areas were given by computer-based HPLC. Calibration was done with standard solutions.

3.7.3. pH Analyses

The pH of the sample for indoor experiments was measured by a pH meter (Mettler Toledo MP220). The instrument was calibrated once per day, before usage. Two-point calibrations were made with Mettler Toledo pH buffer solutions as 4.01 and 7.00.

For outdoor experiments, pH was measured by the PID control system, continuously. The control system was custom-built by pairing a Mettler Toledo M300 measurement equipped with control device with a Watson-Marlow Sci q400 peristaltic pump (maximum flow rate of 0.3 L/h) and the pH probe (Mettler Toledo InPro 3250/PT100).

3.7.4. Cell Concentration

The bacterial concentration was measured by a UV Spectrophotometer (Shimadzu UV–1800) at 660 nm. Distilled water was used as a blank solution. An optical density (OD) of 1.0 corresponds to 0.46 g/L bacterial cell concentration for *R. capsulatus* YO3 (hup^-) (Sagir et al. 2017).

3.7.5. Light Intensity

Indoor experiments and bacterial growth at the incubator was illuminated by 100 W tungsten lamps. Light intensity was measured by luxmeter (EXTECH HD450).

For outdoor experiments, solar light intensity was measured and recorded online by a weather station (Davis Vantage Pro2 Weather Station equipped with a solar radiation sensor) connected to a computer.

3.7.6. Temperature Measurements

The reactor temperature was recorded by Fe-constantan (J-type) thermocouples with an online data logger (Ordel UDL100).
The ambient air temperature was recorded online by a weather station (Davis Vantage Pro2 Weather Station) connected to a computer.

3.7.7. Gas Analysis

The produced gas composition was determined using a Gas Chromatograph (Agilent Technologies 6890 N) equipped with a thermal conductivity detector (TCD) and a Supelco Carboxen 1010 column (Appendix G). The injection was made with a 100 µL sample volume by a syringe (Hamilton 22 GA 500 µL gas-tight syringe). Argon was used as a carrier gas. The flow rate of Argon gas was 26 mL/min. The oven, injector and detector temperatures were 140, 160 and 170 ºC, respectively.

3.7.8. Sodium Analysis

A Jenway PFP7 Flame Photometer was used to determine the daily variation of sodium concentration. The sample was filtered with 0.22 µm filters before analysis. Fuel was natural gas. The calibration curve was prepared with NaCl solution. Three-point calibration was done after every 5 samples.

3.7.9. Ammonium Analysis

Ammonia analyses were carried out by a Hach-Lange Spectrophotometer with NH_4-N kits (HACH LANGE AmVer High Range Ammonia Reagent Set 26069-45).

CHAPTER 4

RESULTS AND DISCUSSION

Indoor experiments were carried out in small glass bioreactors (50 ml) with *R. capsulatus* YO3 (hup$^-$) utilized molasses. In RUN150718, molasses concentration and C/N ratio were optimized under indoor conditions. In RUN121118, C/N ratio was optimized under simulated outdoor condition (light-dark cycle and temperature fluctuation). In RUN030419, pH was kept constant manually and the effect of constant pH on molasses utilization was observed.

Two outdoor experiments for hydrogen production with *R. capsulatus* YO3 (hup$^-$) utilized molasses were performed on U-tube tubular photobioreactor (20L). RUN290817, the feasibility of connection points for pH measurement and base feeding was observed and liquid level on constructed glass ports was adjusted. Homogeneity of pH value on the parallel stacked tubes was followed and the feeding method was adjusted according to result. In RUN160818, PID pH control was applied to the reactor and worked for 48 days. When pH was kept constant, the effects of pH value on the hydrogen production and the bacteria were observed.

4.1. Indoor Experiments

Photofermentative hydrogen production on molasses as a sole carbon source by *R. capsulatus* YO3 (hup$^-$) was studied. Glutamate was nitrogen source. Since carbon to nitrogen ratio is one of the most important parameters that affect the hydrogen production and stability of cell growth, optimization of it was necessary. Although there was much research about C/N ratio in the previous studies, there was no optimum C/N value when molasses was utilized as a carbon source.

Moreover, needed molasses and glutamate amount could differ under indoor and outdoor conditions because of changing temperature and light-dark cycle. In the present study, the C/N ratio was optimized for molasses utilization. Indoor conditions were supplied under constant temperature and continuous illumination and outdoor conditions were simulated with changing temperature (day and night) and light-dark cycle. pH is the other most important factor for hydrogen production. The concentration of molasses was also studied previously and determined as 5 mM with initial pH regulation (Keskin and Hallenbeck 2012; Sagir et al. 2017). However, molasses utilization in a controlled pH environment has not been studied in detail in the literature. For this reason, various molasses concentrations effect on hydrogen productivity with pH control was studied after determination of the C/N ratio.

The optimizations of the C/N ratio for various molasses and glutamate concentrations under indoor and outdoor conditions were presented separately in section 4.1.1 and 4.1.2 respectively. Finally, the results of hydrogen productivity on molasses under pH control were given in section 4.1.3.

4.1.1. RUN150718, Optimization of C/N for Indoor Conditions

The PNS bacteria, which were grown on acetate containing growth medium, were adapted to molasses containing sucrose. When the bacteria OD was 2.018 at 660 nm (0.94 g/L), they were inoculated into the hydrogen production medium. Sucrose concentrations were changed as 2, 5 and 10 mM in hydrogen production medium. C/N ratios were regulated as 15,30 and 45 for each molasses concentrations by adding glutamate. The initial pH was 7.5 and 30 mM KH_2PO_4 was used. Inoculation ratio was 10%. The glass bottle reactor volume was 50 ml. All reactors were flushed with argon in 3 minutes at the startup. The experiment was carried out under continuous illumination 2000 – 2200 lux and constant temperature at 30^{o}C.

Table 4.1. *Changing molasses and C/N ratios in hydrogen production medium.*

Molasses (mM)	C/N	Glutamate (mM)
2	15	2.40
2	30	0.96
2	45	0.60
5	15	6.00
5	30	2.40
5	45	1.50
10	15	12.00
10	30	4.80
10	45	3.00

4.1.1.1. Cell growth, Sucrose Utilization, and Hydrogen Production

The bacteria dry cell weights were between 0.22 and 0.26 g/L at the startup. The exponential phase lasted 30 – 45 hours. The cell concentration reached maximum value the hydrogen production medium(HPM) including 5 mM sucrose containing molasses with 15 C/N ratio and 10 mM sucrose containing molasses with 45 C/N ratio as 0.84 and 0.81 g/L, respectively. On the other hand, 2 mM sucrose containing molasses with 30 and 45 C/N ratio showed the lowest cell concentration as 0.48 and 0.44 g/L. However, when the C/N ratio was decreased to 15 by adding more nitrogen source for 2 mM sucrose containing molasses medium, the cell concentration increased dramatically. Since the bacteria need carbon and nitrogen source for growth, 2 mM sucrose containing molasses could not be enough and they could utilize glutamate for both carbon and nitrogen source. Interestingly, the bacterial cell concentration increased dramatically at exponential phase, then It decreased significantly when C/N was 15. In other words, bacteria went directly to the death phase after exponential phase without reaching to stabilization for low C/N ratio.

The cell concentration was stabilized at hydrogen production mediums containing 5 mM sucrose - 30 and 45 C/N ratio and 2 mM sucrose – 30 C/N (Figure 4.1).

Stable and optimized biomass concentration is necessary for continuous hydrogen production (Androga, Özgür, et al. 2011a). The highest amounts of hydrogen in volume were obtained from HPM containing 5 mM sucrose - 30 and 45 C/N ratio and 2 mM sucrose – 30 C/N, in parallel with mediums showing cell stabilization. The lowest hydrogen amount in volume was obtained from HPM having 15 C/N ratio for all sucrose concentrations. The hydrogen production started and reached to its highest value in about 30 hours, then production stopped suddenly for 15 C/N ratio. At the lowest C/N ratio, bacteria did not go stationary phase, since they directly entered to death phase as mentioned, hydrogen production stopped.

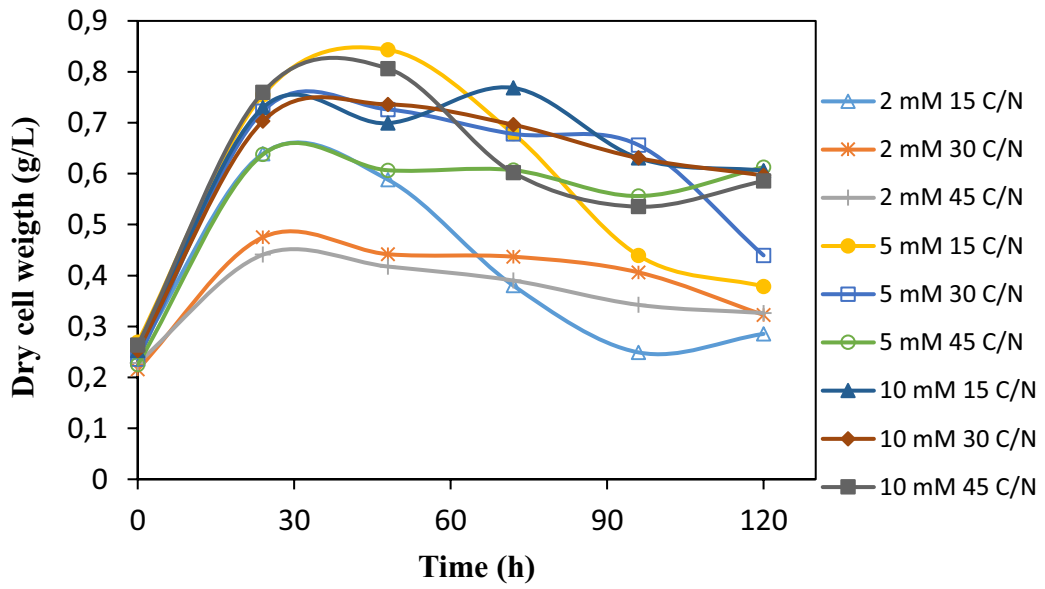

Figure 4.1. The growth *R. capsulatus* YO3 (hup$^-$) on 2 mM, 5 mM and 10 mM sucrose containing HPM with 15, 30 and 45 C/N ratio.

Sucrose utilization for 2 and 5 mM sucrose concentrations had nearly the same trend as independent from the C/N ratio. However, sucrose consumption increased with decreasing C/N ratio for 10 mM sucrose medium (Figure 4.2).

Sucrose concentration could decrease from 5 mM to about 1.8 mM for hydrogen production medium containing 5 Mm. Interestingly, when sucrose concentration increased to 10 mM, it also decreased to 1.8 mM at the same time interval.

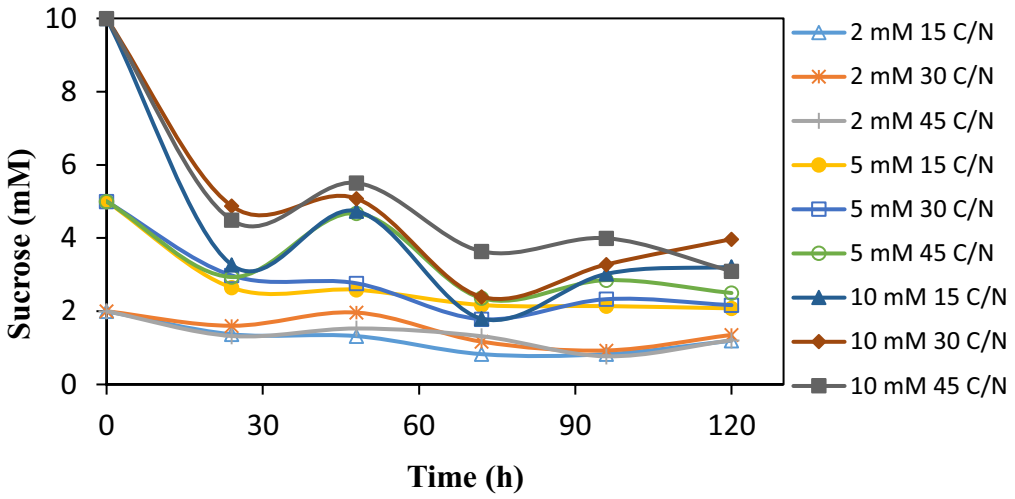

Figure 4.2. Sucrose utilization on 2 mM, 5 mM and 10 mM sucrose containing HPM with 15, 30 and 45 C/N ratio.

Under continuous illumination and constant temperature, the maximum productivity was 0.60 mol $H_2/(m^3.h)$ for 5 mM sucrose containing molasses and 45 C/N ratio when the cell concentration was 0.64 g/L (Figure 4.4). The lowest productivity was 0.23 mol $H_2/(m^3.h)$ for 2 mM sucrose – 15 C/N. 5 Mm sucrose showed better hydrogen productivity for all changing C/N ratios when compared to 2 and 10 mM. C/N=45 was obtained as an optimum value for 5 mM sucrose. Based on hydrogen productions, adding a high amount of glutamate removed the stationary phase and decreased hydrogen production duration.

The hydrogen was produced only in the exponential phase for low C/N ratio. Although, it has been reported that 25 was the optimum C/N ratio for *R. capsulatus* YO3 (hup$^-$) when acetate was utilized as carbon source under indoor conditions (continuous illumination and 30 ^oC) (Androga, Özgür, et al. 2011a), in this study, C/N=45 was found as optimum ratio for molasses utilization. Molasses contains various amino acids and trace elements promoting hydrogen production activity such as iron and molybdenum (Sagir et al. 2018) in addition to sucrose. Thus, molasses was needed a lower amount of glutamate when compared to the defined medium. On the other hand, when no glutamate was added and molasses was sole carbon source, the cell concentration was very low (0.5 g/L) to produce hydrogen effectively (Kayahan, Eroglu, and Koku 2017). It can be concluded that when the type of carbon source was changed, the C/N ratio should be optimized again.

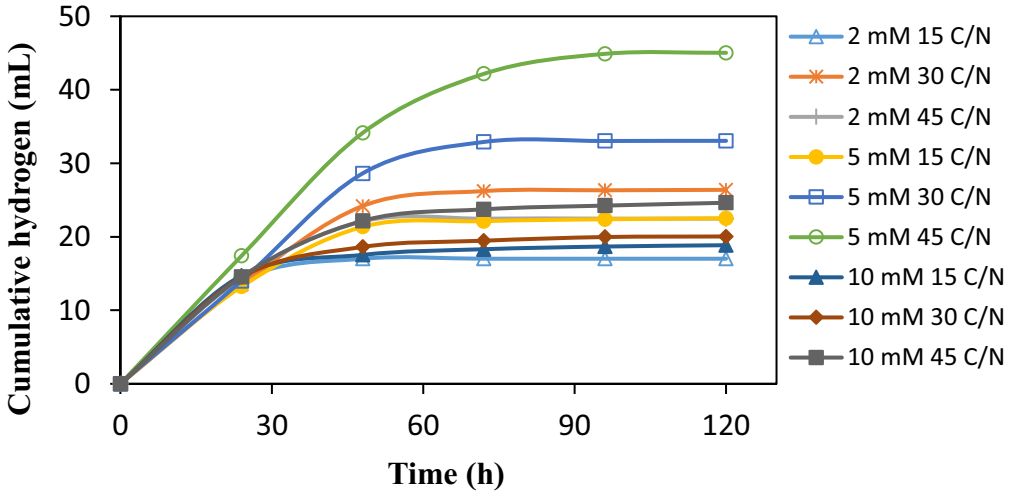

Figure 4.3. The cumulative hydrogen production on 2 mM, 5 mM and 10 mM sucrose with 15,30 and 45 C/N ratio HPM.

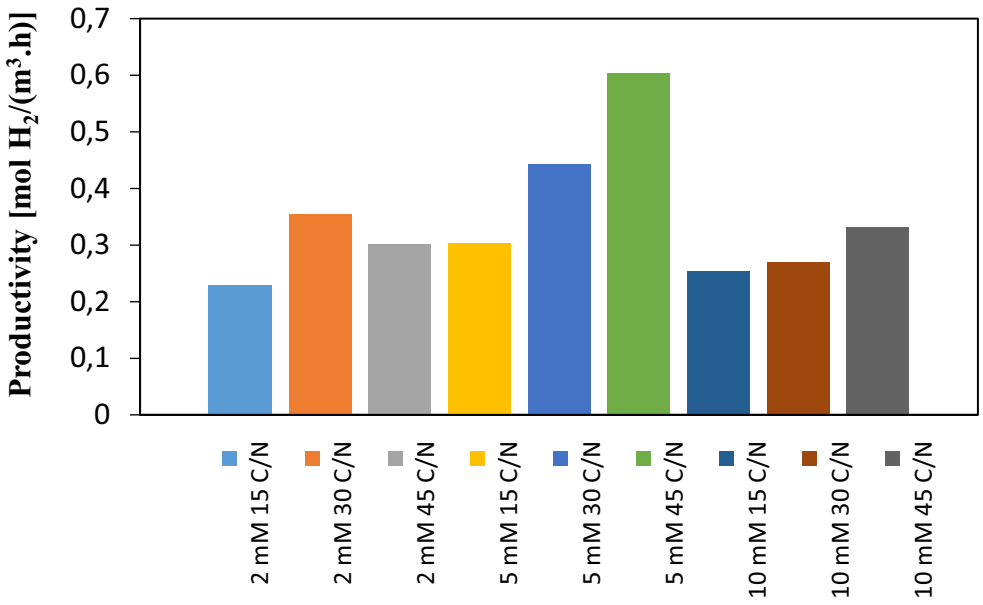

Figure 4.4. Hydrogen productivity on 2 mM, 5 mM and 10 mM sucrose containing HPM with 15, 30 and 45 C/N ratio.

4.1.1.2. pH and Hydrogen Percentage

pH value was around 7, 6.5 and 5.8 for 2, 5 and 10 mM sucrose containing molasses respectively. pH value decreased with the increasing molasses concentration because of the accumulation of organic acids as expected and it can be concluded that C/N ratio did not affect the pH value (Figure 4.5).

Unlike pH value, hydrogen percentage was affected by the C/N ratio in addition to molasses concentration. Hydrogen purity decreased with increasing molasses concentration in parallel with decreasing pH value (Figure 4.6). The amino acid-dependent decarboxylation (glutamate, lysine, arginine, and ornithine) is a protection mechanism for acid stress. Decarboxylation reaction consumes a proton biochemical by releasing CO_2 to keep the internal pH suitable for cell survival.

Decomposition of urea to ammonia and CO_2 also occurs under acid stress (Lund et al. 2014). Additionally, high glutamate resulted in ammonium formation that repress the

nitrogenase activity. Probably, increase in molasses decreases the pH value and caused high CO_2 production. Thus, hydrogen purity was low for high molasses amount.

When the C/N ratio increased from 15 to 45, the hydrogen percentage was also increased for 5 and 10 mM sucrose concentrations. However, C/N=30 gave the highest hydrogen percentage for 2 mM sucrose, this can be attributed to higher hydrogen production as seen in cumulative hydrogen production trend (Figure 4.3). The highest hydrogen percentages were 85 %, 79 % and 60 % for HPM containing 2 mM-30 C/N, 5 mM-45 C/N and 10 mM-45 C/N, respectively. Probably, high glutamate concentration provided ammonia formation that represses the nitrogenase activity resulted in low hydrogen production and purity.

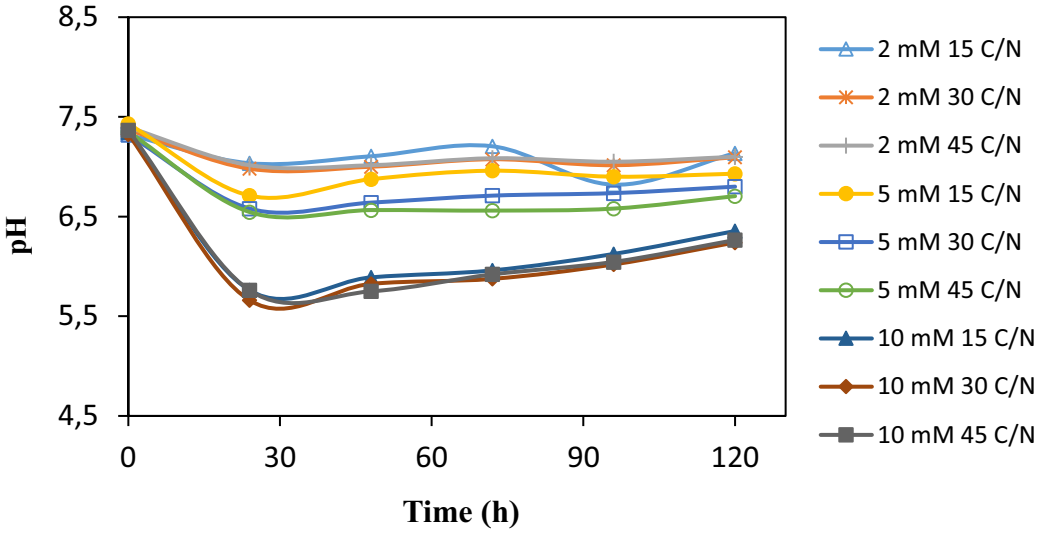

Figure 4.5. pH change on 2 mM, 5 mM and 10 mM sucrose containing HPM with 15, 30 and 45 C/N ratio.

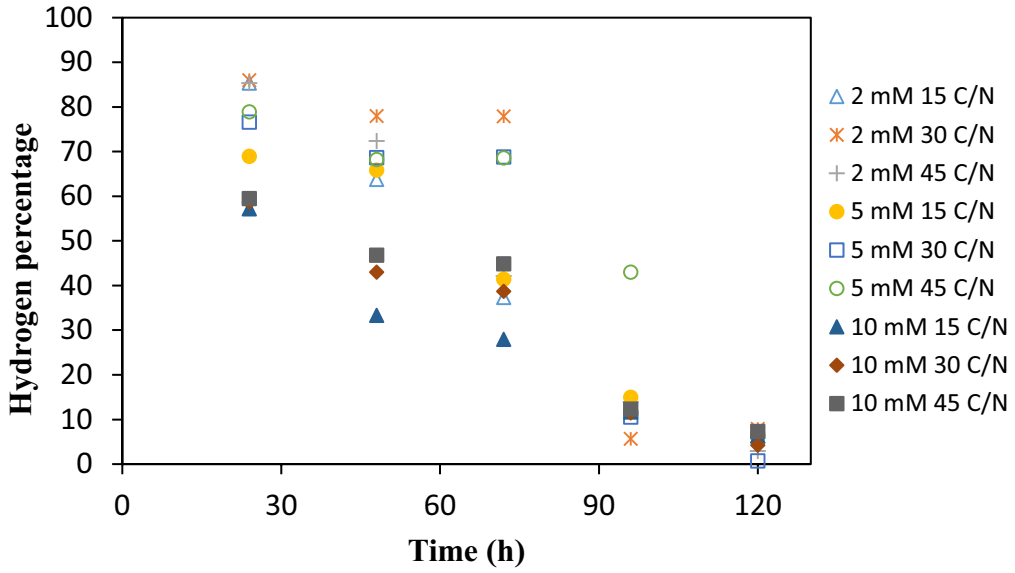

Figure 4.6. Hydrogen percentage on 2 mM, 5 mM and 10 mM sucrose containing HPM with 15, 30 and 45 C/N ratio. Rest of the gas is carbon dioxide.

4.1.1.3. Organic Acids

Lactic acid concentration reached to about 2.5 mM for HP medium containing 10 mM sucrose as maximum (Figure 4.7). Lactic acid production increased with increasing sucrose concentration. C/N=30 for 5 and 10 mM sucrose had higher lactic acid concentration when compared to 45 and 15 C/N ratios. There was no lactic acid production for 2 mM sucrose.

Formic acid production could not depend on sucrose concentration. The highest formic acid concentration was 6.5 mM for 5 mM sucrose and 45 C/N (Figure 4.8).

Acetic acid had reached 2.3 mM as maximum with HP medium containing 10 mM sucrose. There was no acetic acid production when 2 and 5 mM sucrose concentrations were used (Figure 4.9).

Propionic acid production was the same for 2 and 5 mM sucrose concentrations and its concentration changed around 2.5. However, propionic acid concentration increased nearly 5 times when 10 mM sucrose was used (Figure 4.10).Butyric acid

was only produced when high sucrose concentration and low glutamate concentration was used in hydrogen production medium. The highest butyric acid concentration was 15 mM that was produced by HP medium included 10 mM sucrose – 30 C/N (Figure 4.11).

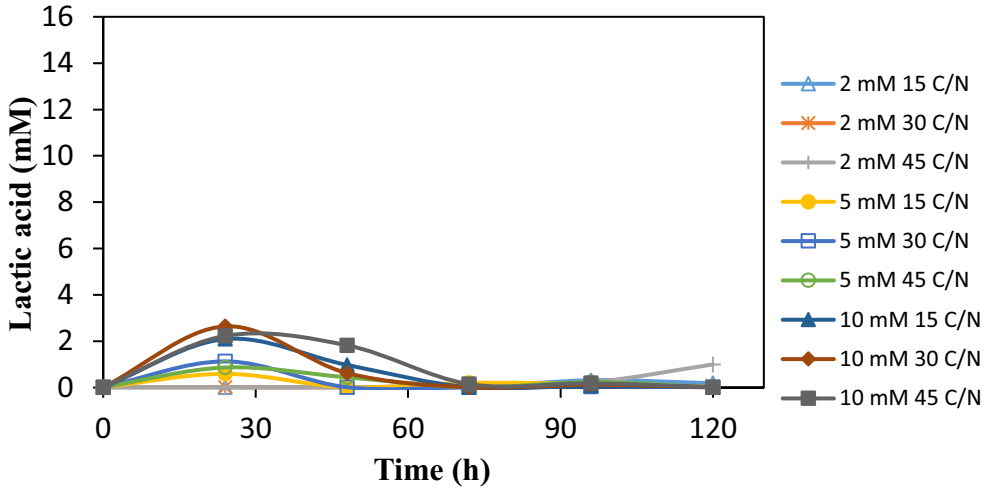

Figure 4.7. Lactic acid production on 2 mM, 5 mM and 10 mM sucrose containing HPM with 15, 30 and 45 C/N ratio.

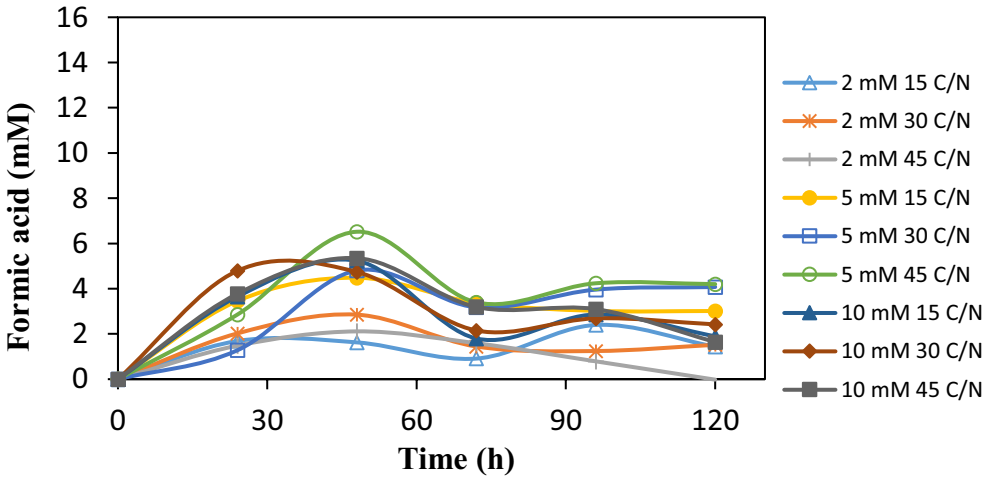

Figure 4.8. Formic acid production on 2 mM, 5 mM and 10 mM sucrose HPM with 15, 30 and 45 C/N ratio.

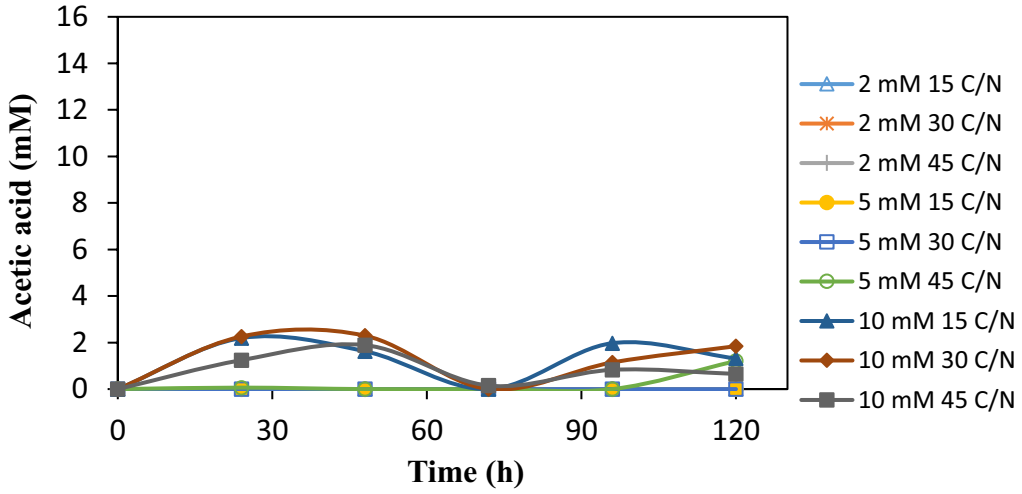

Figure 4.9. Acetic acid production on 2 mM, 5 mM and 10 mM sucrose containing HPM with 15, 30 and 45 C/N ratio.

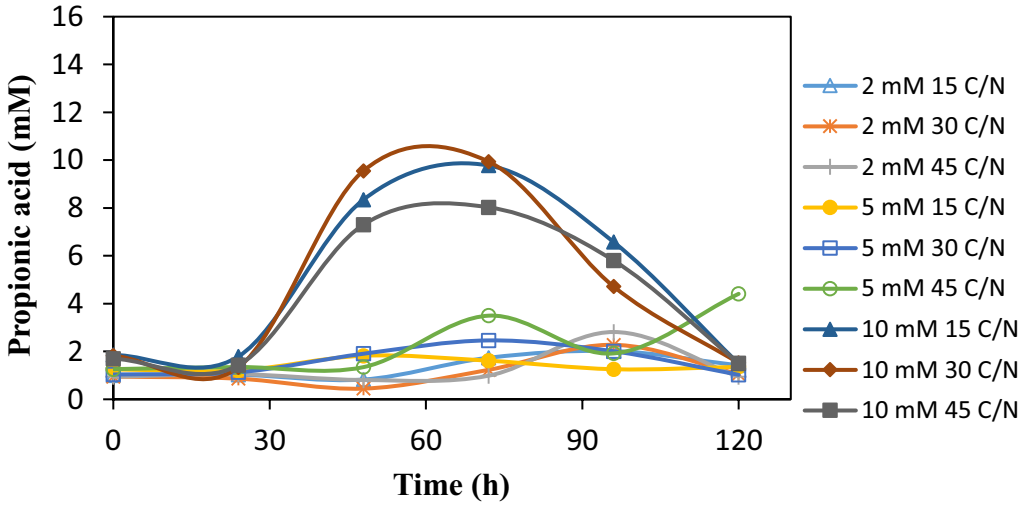

Figure 4.10. Propionic acid production on 2 mM, 5 mM and 10 mM sucrose containing HPM with 15, 30 and 45 C/N ratio.

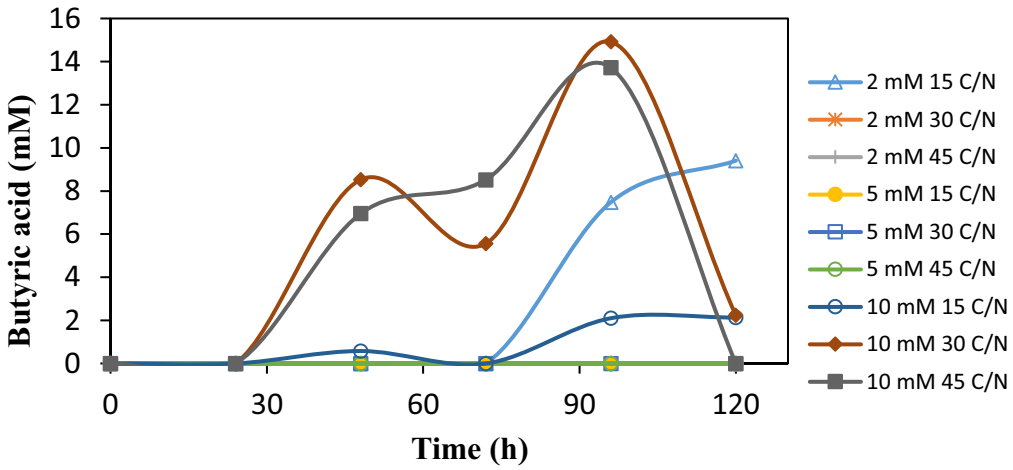

Figure 4.11. Butyric acid production on 2 mM, 5 mM and 10 mM sucrose containing HPM with 15, 30 and 45 C/N ratio.

4.1.2. RUN121118, Optimization C/N for Simulated Outdoor Conditions

The effect of changes in daily temperature and light/dark cycle on optimization of C/N ratio for *R. capsulatus* YO3 (hup^-) was investigated.

The PNS bacteria were adapted to molasses containing sucrose. When the bacteria OD was about 2 at 660 nm, they were inoculated into hydrogen production medium. In RUN150718, 5 mM sucrose containing molasses had the highest hydrogen productivity. Thus, sucrose concentration was regulated as 5 mM in hydrogen production medium. C/N ratios were regulated as 15,30 and 45 by adding glutamate. The initial pH was 7.5 and 30 mM KH_2PO_4 was used. Inoculation ratio was 10%. The glass bottle reactor volume was 50 ml. All reactors were flushed with argon in 3 minutes at the startup. In order to simulate outdoor conditions, an indoor experiment was designed in which temperature was changed daily between 7 ^oC and 30 ^oC depending on temperatures of the outdoor experiment that was carried out in September in Ankara (RUN290817). For day and night simulation, the experiment was also exposed to daily light/dark cycle (10 h light/14 h dark) based on the sunshine duration of RUN290817.

Table 4.2. *Changing C/N ratios for 5 mM in hydrogen production medium.*

Molasses (mM)	C/N	Glutamate	D/N Cycle
5	15	6	√
5	30	2.4	√
5	45	1.5	√
5	15	6	x
5	30	2.4	x
5	45	1.5	x

4.1.2.1. Cell growth, Sucrose Utilization, and Hydrogen Production

The bacteria dry cell weight was 0.26 g/L at the startup. The exponential phase lasted about 45 hours for experiments that were performed at constant temperature under continuous illumination (indoor conditions) (Figure 4.12). The exponential phase was about 100 hours for reactors that were exposed to day and night conditions (D/N). The highest cell concentration was 0.98 g/L for indoor and 0.92 g/L for D/N conditions. The main difference for cell growth was cell concentration decreased sharply after the stationary phase under indoor conditions, however, it decreased smoothly under D/N cycle to nearly the same value. This sharp decreasing could not be attributed to sucrose consumption because consumed sucrose trend was nearly the same for all reactors. Moreover, even if indoor experiments showed a sharp decrease in growth curve after 100 hours, they continued to consume sucrose.

According to Figure 4.13, it could be deduced that sucrose consumption by *R. capsulatus* YO3 (hup^-) was not affected by changing temperature and light. Additionally, glutamate amount did not affect sucrose consumption and it reached to about 1.5 mM for all reactors.

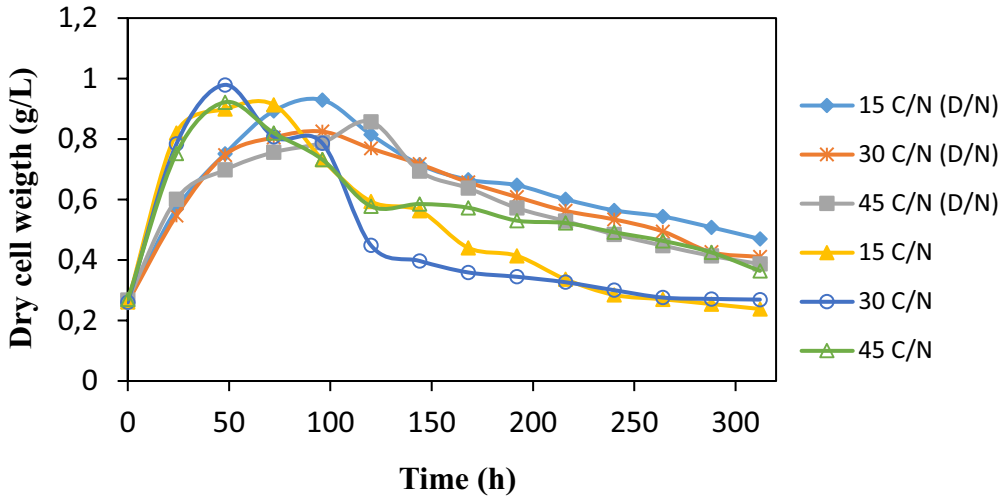

Figure 4.12. The growth of *R. capsulatus* YO3 (hup$^-$) on 5 mM sucrose HPM with 15, 30 and 45 C/N ratio under constant temperature – continuous illumination and simulated outdoor conditions.

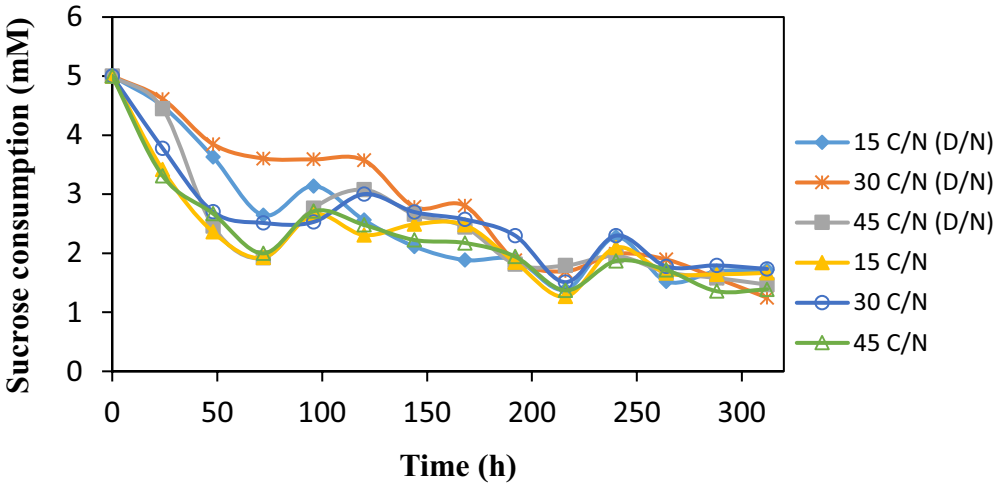

Figure 4.13. Sucrose consumption on 5 mM sucrose containing HPM with 15, 30 and 45 C/N ratio under constant temperature – continuous illumination and simulated outdoor conditions.

Under continuous illumination and constant temperature, hydrogen was produced during the exponential phase and early stationary phase and highest hydrogen volume produced by HP medium having 45 C/N ratio. On the other hand, hydrogen production continued until death phase and higher hydrogen volume was obtained from HP medium with C/N=45 for day and night cycle.

The highest hydrogen productivity was 0.69 $H_2/(m^3.h)$ for D/N cycle and 0.38 $H_2/(m^3.h)$ for the indoor experiment (Figure 4.15). As expected, C/N was very affective on hydrogen production. Adding glutamate decreased the hydrogen production for both experiment conditions, gradually. Ozgur et al. (2010) investigated hydrogen production by *R. capsulatus* in constant temperature 30 °C - continuous illumination, changing temperature (15 °C – 40 °C) – continuous illumination and changing temperature (15 °C – 40 °C) – light/dark cycle (16h/8h). Hydrogen production medium included 40mM of acetate, 7.5mM of lactate and 2mM of glutamate and the highest hydrogen production was obtained from constant temperature and continuous illumination conditions. It has been reported that the lowest hydrogen production observed under temperature cycle and light cycles. In this study, productivity results were the opposite. It can be attributed to the difference of carbon source and molasses could give better hydrogen productivity under outdoor conditions for *R. capsulatus*.

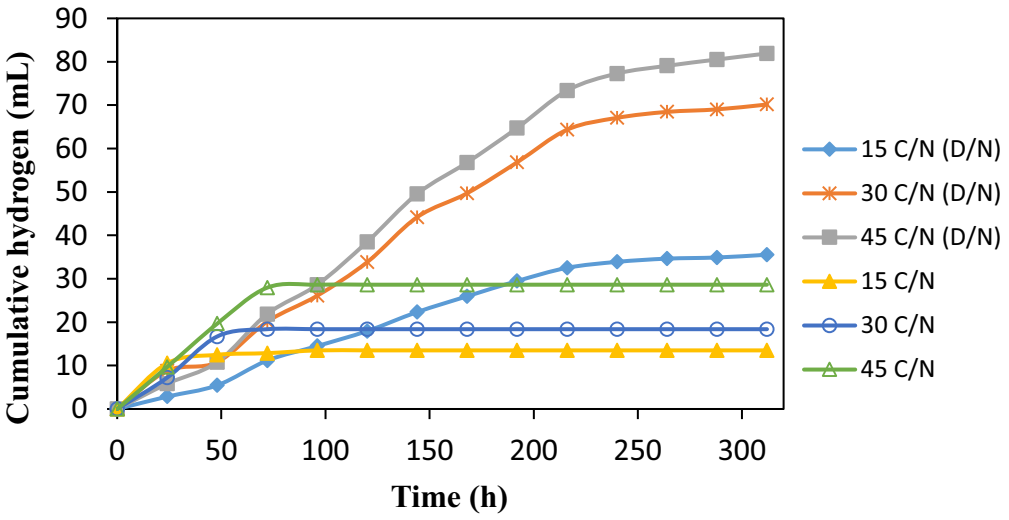

Figure 4.14. Cumulative hydrogen production on 5 mM sucrose containing HPM with 15, 30 and 45 C/N ratio under constant temperature – continuous illumination and simulated outdoor conditions.

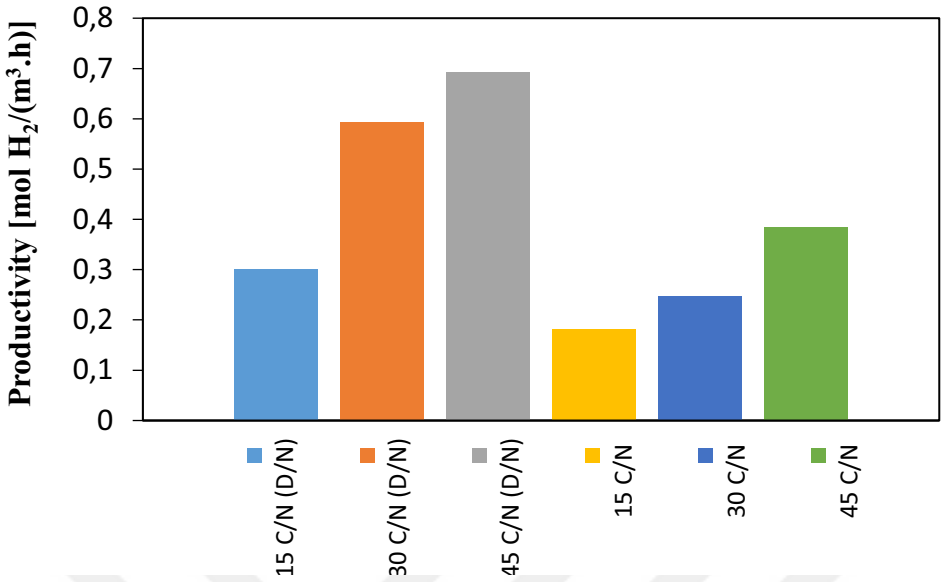

Figure 4.15. Hydrogen productivity on 5 mM sucrose containing HPM with 15, 30 and 45 C/N ratio under constant temperature – continuous illumination and simulated outdoor conditions

4.1.2.2. pH and Hydrogen Percentage

pH value decreased to around 6.4 for all reactors (Figure 4.16). It can be concluded that pH was not affected by the C/N ratio and changing temperature and light conditions. In the first 100 h, pH was higher for reactors that were exposed to temperature and light cycle. Parallel with pH, hydrogen percentages higher under day and night cycle (Figure 4.17). After 120 h, hydrogen percentages were very close to each other.

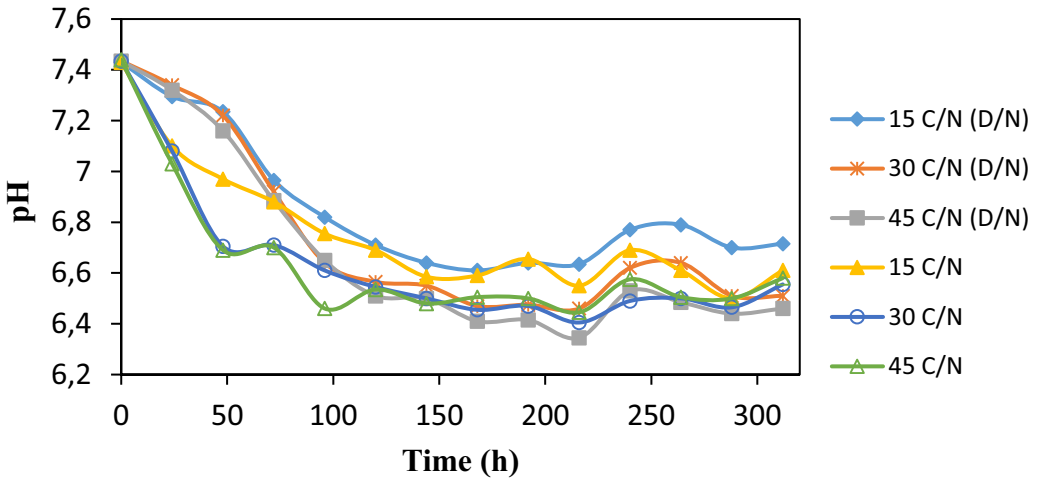

Figure 4.16. pH change on 5 mM sucrose containing HPM with 15, 30 and 45 C/N ratio under constant temperature – continuous illumination and simulated outdoor conditions.

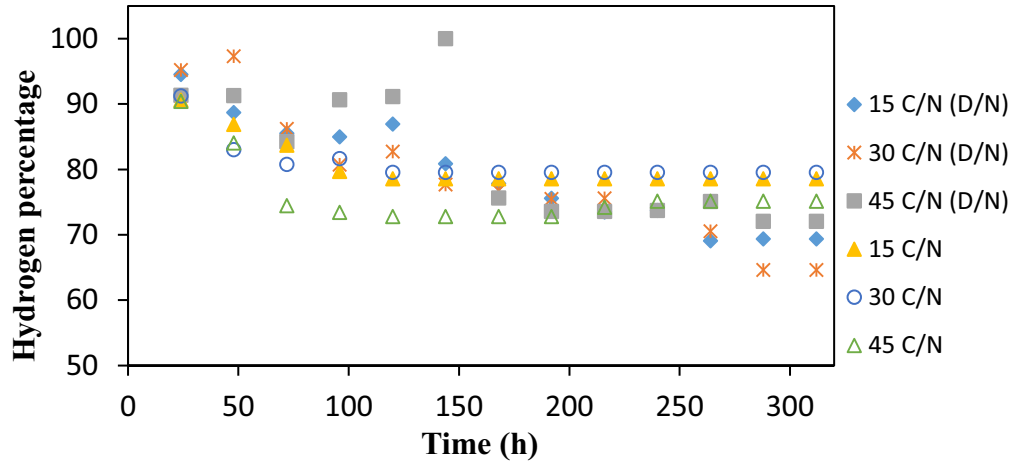

Figure 4.17. Hydrogen percentage on 5 mM sucrose containing HPM with 15, 30 and 45 C/N ratio under constant temperature – continuous illumination and simulated outdoor conditions. Rest of the gas is carbon dioxide.

4.1.2.3. Organic Acids

Lactic and formic acids were produced by all reactors at low concentrations, disorderly (Figure 4.18 and 4.19). However, propionic acid production was provided by glutamate independently from temperature and light cycle (Figure 4.20) in the first 120 h. Additionally, butyric acid was no observed.

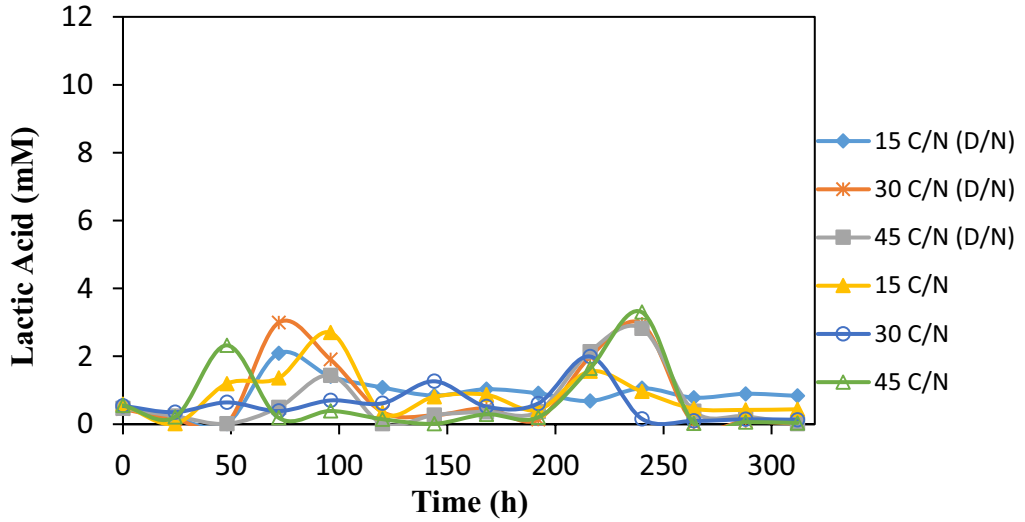

Figure 4.18. Lactic acid production on 5 mM sucrose containing HPM with 15, 30 and 45 C/N ratio under constant temperature – continuous illumination and simulated outdoor conditions.

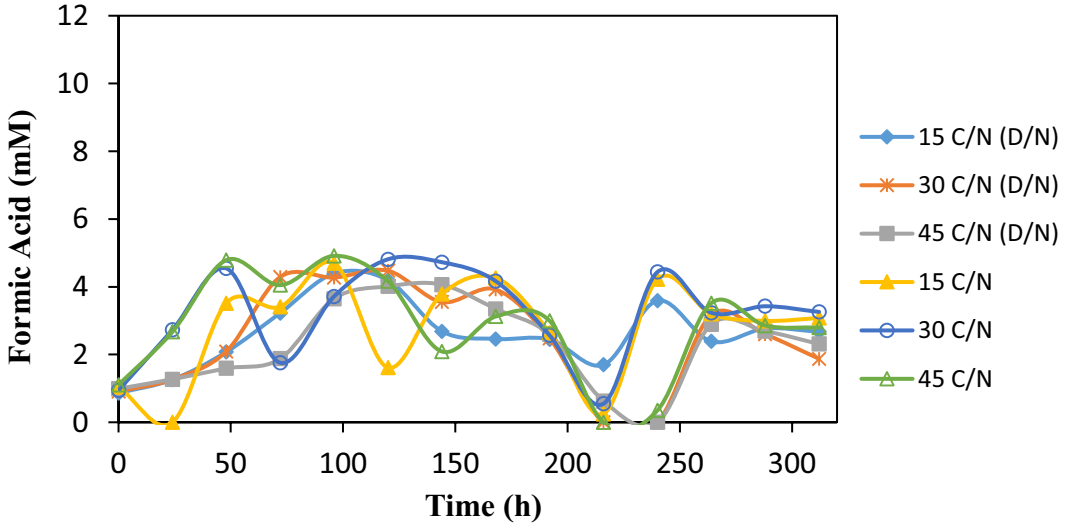

Figure 4.19. Formic acid production on 5 mM sucrose containing HPM with 15, 30 and 45 C/N ratio under constant temperature – continuous illumination and simulated outdoor conditions.

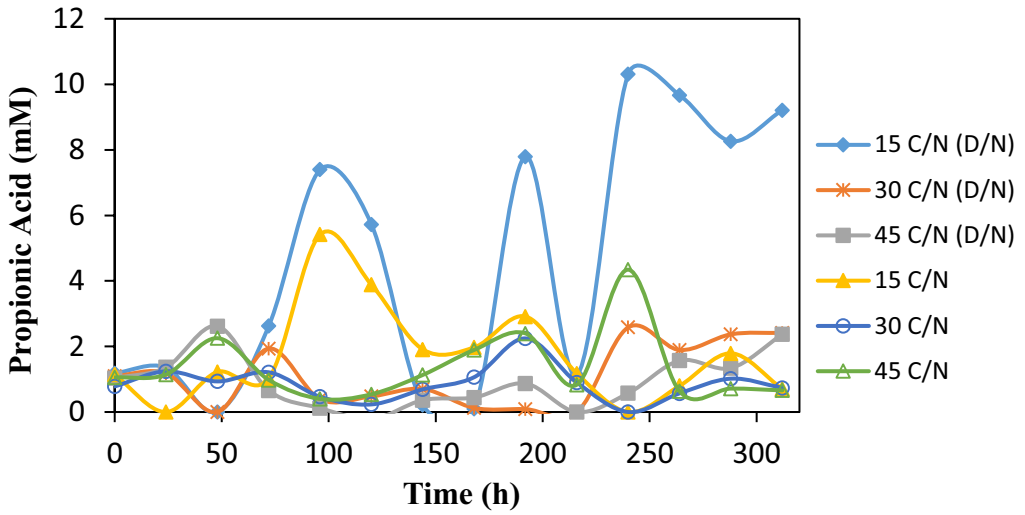

Figure 4.20. Propionic acid production on 5 mM sucrose containing HPM with 15, 30 and 45 C/N ratio under constant temperature – continuous illumination and simulated outdoor conditions.

4.1.3. RUN030419, Optimization of Molasses Concentration Under pH Control

The effect of pH on different molasses concentrations for *R. capsulatus* YO3 (hup^-) was investigated.

The PNS bacteria were adapted to molasses containing sucrose. When the bacteria OD was about 2 at 660 nm, they were inoculated into hydrogen production medium. In RUN121118, when C/N was regulated to 45, the highest hydrogen productivity was obtained. Thus, sucrose concentration was regulated as 5 mM in hydrogen production medium. C/N ratios were regulated as 45 by adding glutamate. The initial pH was 7.5 and 30 mM KH_2PO_4 was used. Inoculation ratio was 10%. The glass bottle reactor volume was 50 ml. All reactors were flushed with argon. In order to keep the pH constant at 7.0, 0.5 mM NaOH was used.

In this run, in addition to the selection of different initial sucrose concentrations, the effect of pH control was investigated. Therefore, two sets of initial sucrose concentrations were prepared, one with pH control and the other without, as shown in

Table 4.4. It should be noted that the runs, without pH control, are not the prior runs of Table 4.2, but were prepared to run simultaneously with controlled pH reactors.

Table 4.3. *Changing molasses concentrations and constant C/N ratio in hydrogen production medium.*

Molasses (mM)	C/N	Glutamate (mM)	pH control
5	45	1.5	x
10	45	3	x
15	45	4.5	x
5	45	1.5	√
10	45	3	√
15	45	4.5	√

4.1.3.1. Cell growth, Sucrose Utilization, and Hydrogen Production

The bacteria dry cell weight was between 0.1 and 0.2 g/L at the startup. The exponential phase lasted about 45 hours for experiments that were performed at a constant temperature under continuous illumination. The highest cell concentration was 0.61 g/L when the pH was not controlled (Figure 4.21). The highest cell concentration was obtained as 0.82 g/L when pH was controlled. The main difference for cell growth was cell concentration decreased to about 0.4 g/L after the stationary phase, however, bacterial cell concentration decreased to around 0.7 g/L. The stationary phase lasted 168 hours under pH control it was equal to two times of the experiments under no pH control.

According to Figure 4.22, it could be deduced that sucrose consumption by *R. capsulatus* YO3 (hup^-) was not affected by changing molasses concentrations or existence of pH control.

The highest hydrogen productivity was 0.5 molH_2/(m^3.h) for HPM 15 mM sucrose containing molasses (Figure 4.24). Interestingly, an increase in molasses concentration increased to hydrogen productivity. Although it has been reported that high concentration (above 5mM) of molasses may be harmful (Keskin and Hallenbeck 2012), pH may modify the enzyme activity, the diversity of the side products and the toxicity of harmful substances (Akhlaghi et al. 2017; Braz Romão et al. 2018; Fang and Liu 2002; Hwang et al. 2004; Khanal et al. 2004; I. S. Kim et al. 2004; B. F. Liu et al. 2010; Shi and Yu 2005; Xie et al. 2010). In this experiment, it was demonstrated that molasses concentration can be increased when the pH was controlled (Figure 4.25).

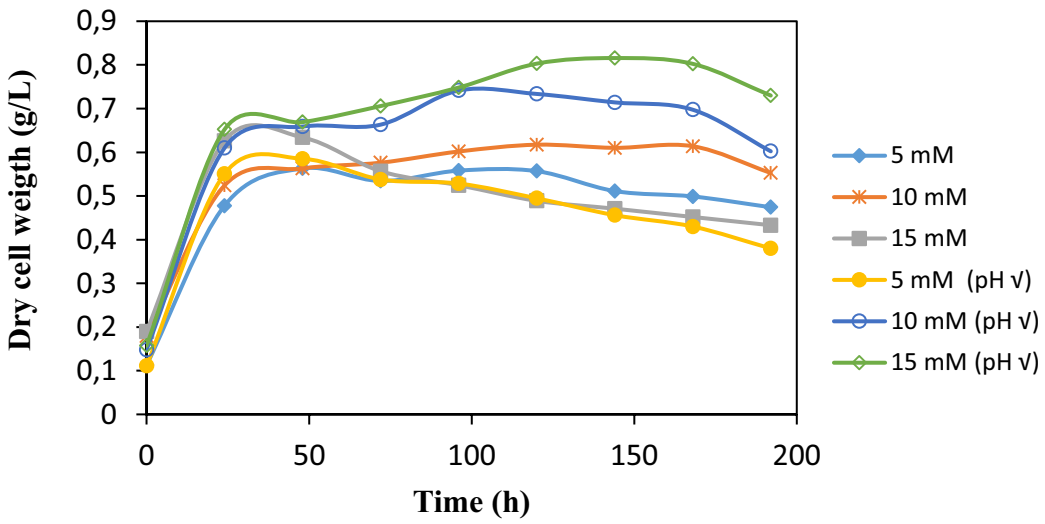

Figure 4.21. The growth of by *R. capsulatus* YO3 (hup$^-$) on 5, 10 and 15 mM sucrose containing HPM with 45 C/N ratio under constant temperature – continuous illumination with and without pH control.

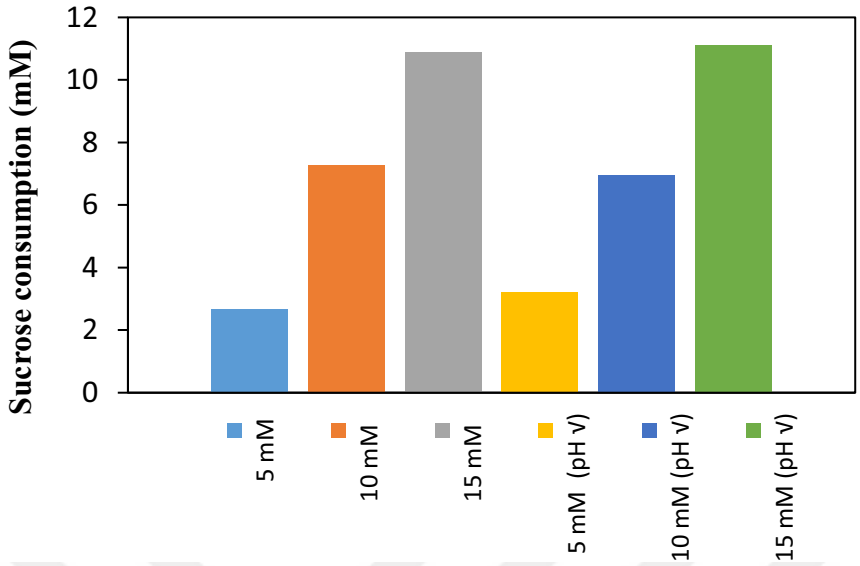

Figure 4.22. Sucrose utilization on 5, 10 and 15 mM sucrose containing HPM with 45 C/N ratio under constant temperature – continuous illumination with and without pH control.

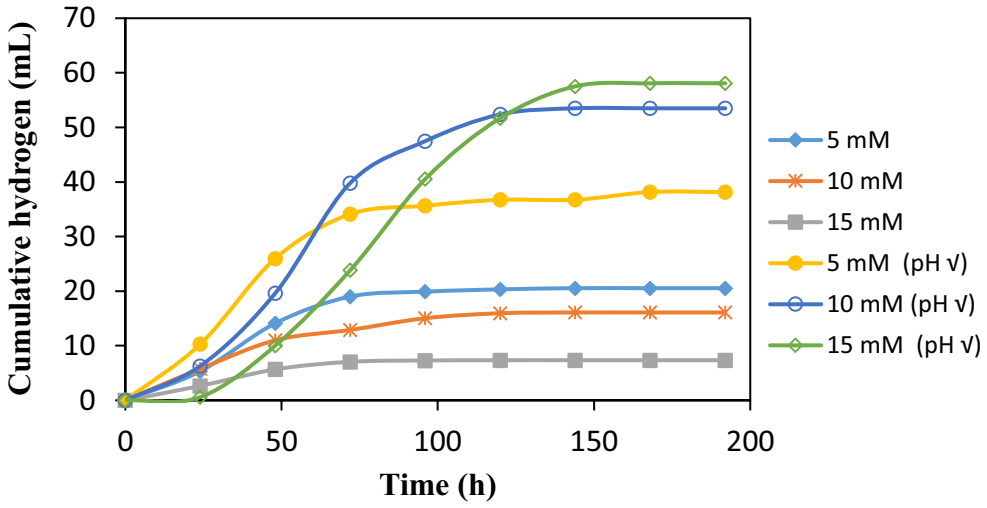

Figure 4.23. Cumulative hydrogen production on 5, 10 and 15 mM sucrose containing HPM with 45 C/N ratio under constant temperature – continuous illumination with and without pH control.

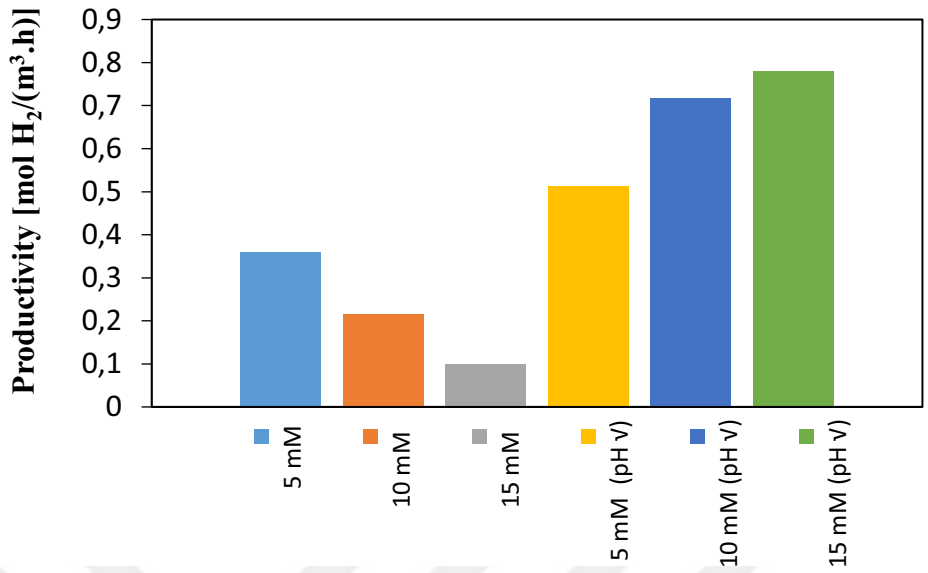

Figure 4.24. The hydrogen productivity on 5, 10 and 15 mM sucrose containing HPM with 45 C/N ratio under constant temperature – continuous illumination with and without pH control.

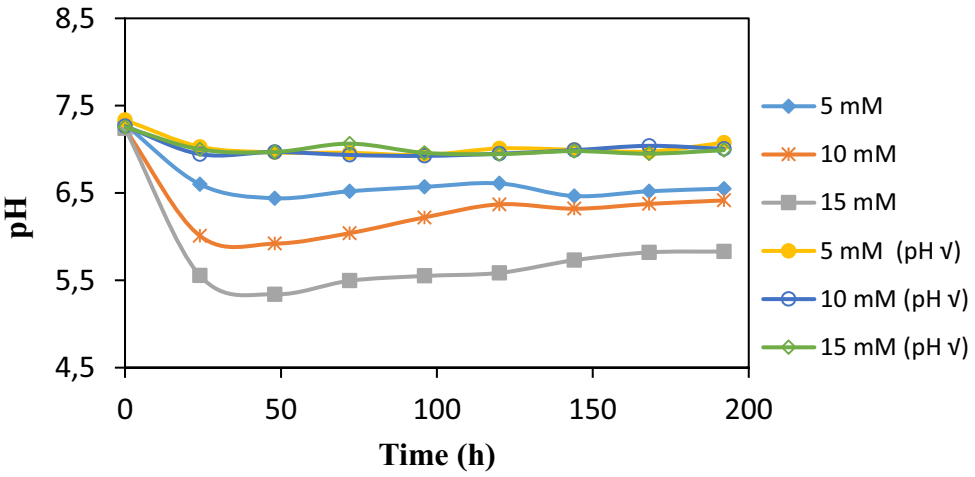

Figure 4.25. The pH change on 5, 10 and 15 mM sucrose containing HPM with 45 C/N ratio under constant temperature – continuous illumination with and without pH control.

4.1.3.2. Hydrogen Percentage

Hydrogen percentage was around 75% for HPM containing 5, 10 and 15 mM molasses under pH control (Figure 4.26). However, the hydrogen percentage was around 25% for 15 mM sucrose. The experiment showed that pH control affects the hydrogen purity significantly and allows the use of higher molasses concentration.

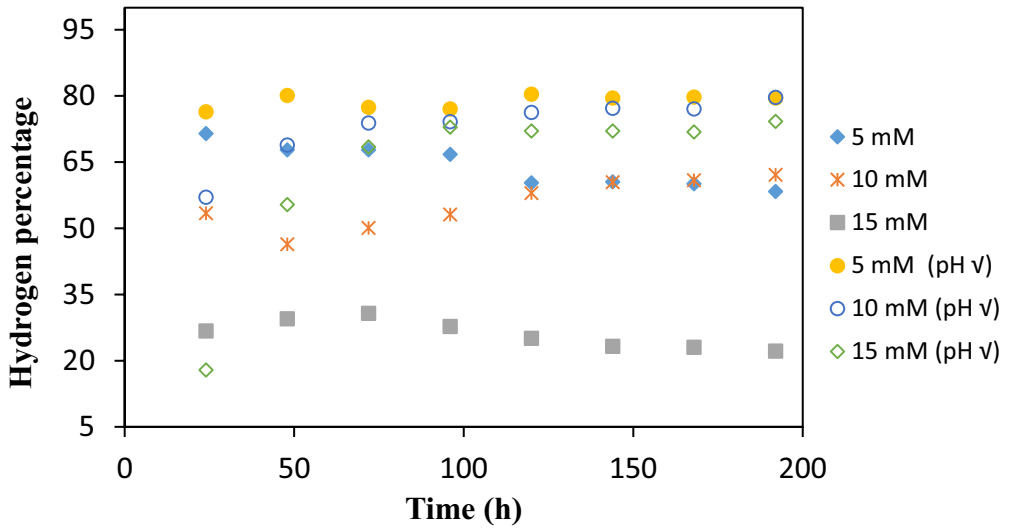

Figure 4.26. The hydrogen percentage on 5, 10 and 15 mM sucrose containing HPM with 45 C/N ratio under constant temperature – continuous illumination with and without pH control. Rest of the gas is carbon dioxide.

4.1.3.3. Organic acids and Ammonium

In Figure 4.27, lactic acid was produced slightly higher with the increasing glutamate. Although formic production was low for all reactors, it can be deduced that production of formic acid promoted by pH control (Figure 4.28). Although acetic acid production did not distribute regularly, it seemed that acetic acid production decreased with pH control (Figure 4.29). Propionic and butyric acid productions were negligible. The ammonium ion is also produced under the acid stress by gram-negative neutrophilic bacteria to reduce proton in the cell in addition to glutamate decomposition (Lund et al. 2014). Thus, it was observed that NH_4^+ concentration was very high when pH

decreased (Figure 4.31). Furthermore, ammonium ion represses the nitrogenase activity that conducts hydrogen production. Increasing hydrogen productivity can be attributed to ammonium concentration that is strongly affected by pH control since sucrose consumption did not change for same sucrose-containing molasses. Although increasing glutamate concentration increased the ammonium ion concentration, pH control could reduce its production. It can be concluded that pH effect is high on ammonia production when compared to glutamate decomposition. Additionally, CO_2 was released under acid stress due to decomposition of the urea and proton-consuming decarboxylation reaction. It may be another reason for low productivity of uncontrolled pH reactors.

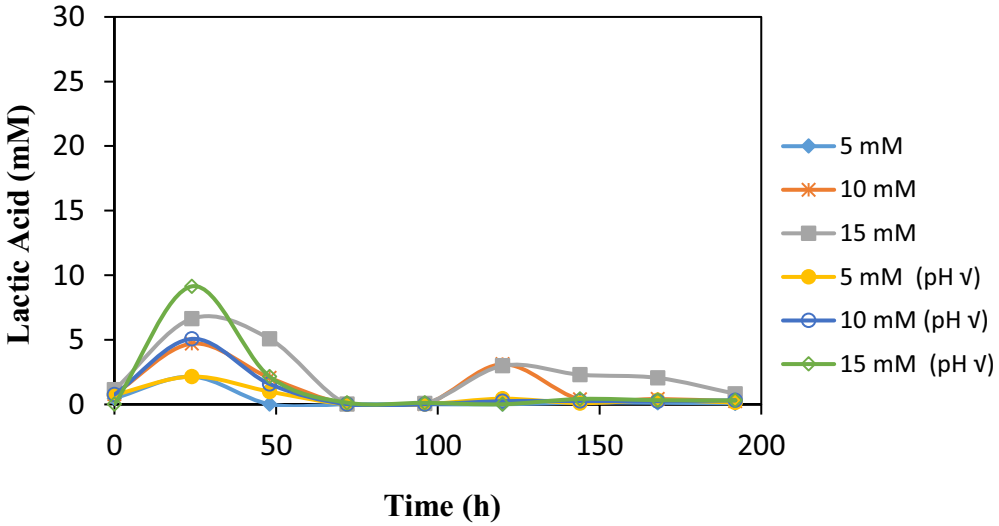

Figure 4.27. Lactic acid production on 5, 10 and 15 mM sucrose containing HPM with 45 C/N ratio under constant temperature – continuous illumination with and without pH control.

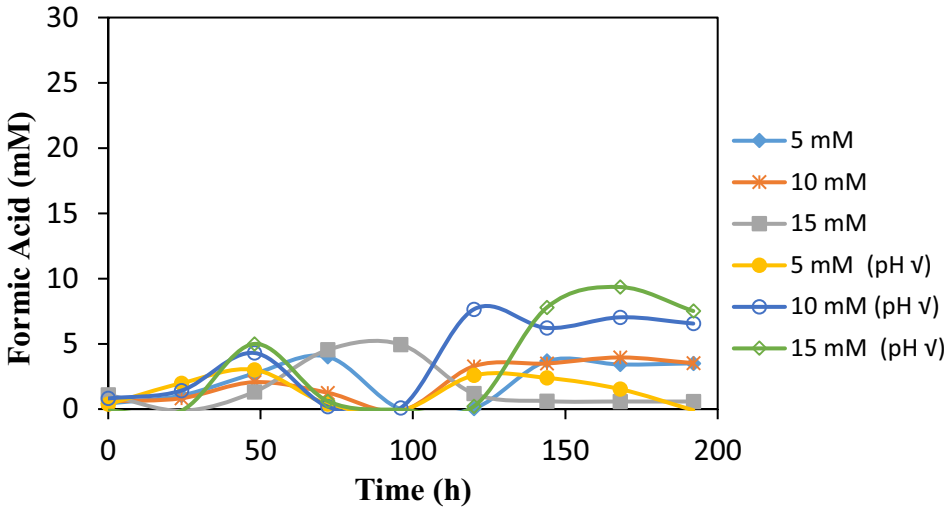

Figure 4.28. Formic acid production on 5, 10 and 15 mM sucrose containing HPM with 45 C/N ratio under constant temperature – continuous illumination with and without pH control.

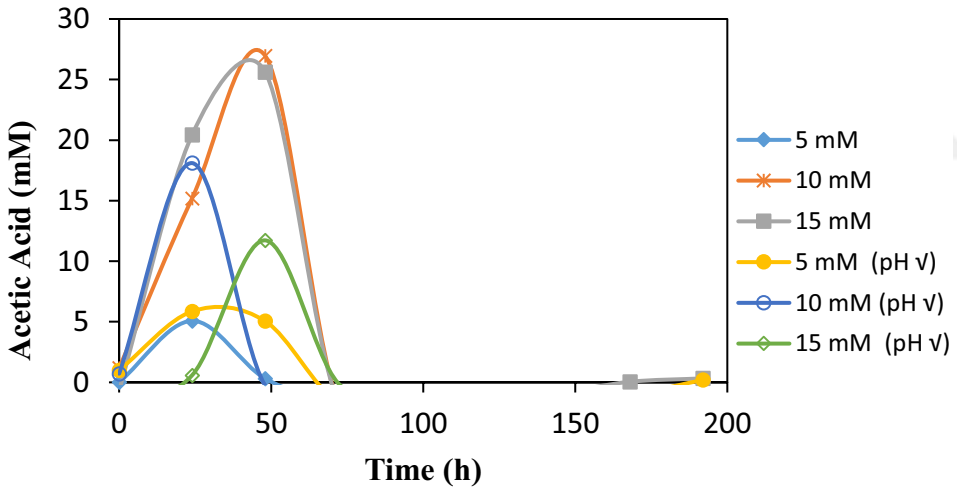

Figure 4.29. Acetic acid production on 5, 10 and 15 mM sucrose containing HPM with 45 C/N ratio under constant temperature – continuous illumination with and without pH control.

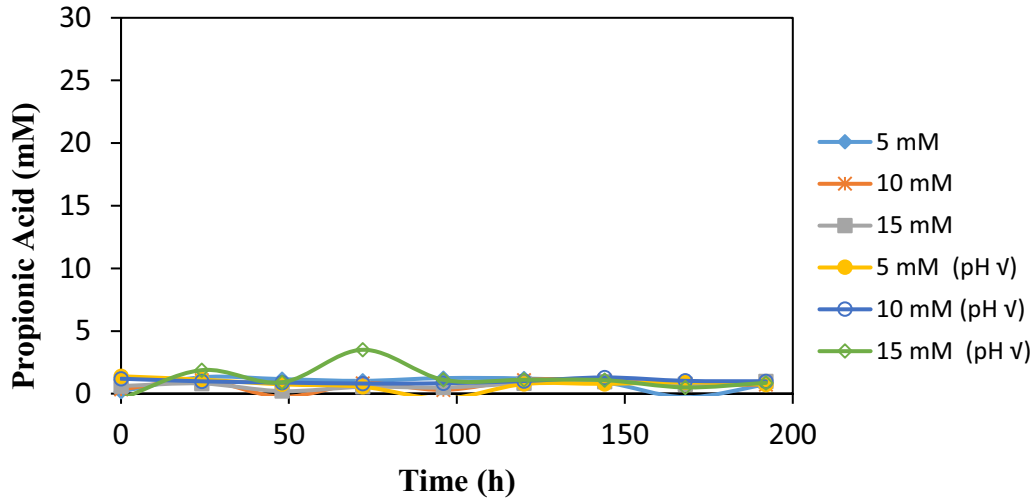

Figure 4.30. Propionic acid production on 5, 10 and 15 mM sucrose containing HPM with 45 C/N ratio under constant temperature – continuous illumination with and without pH control.

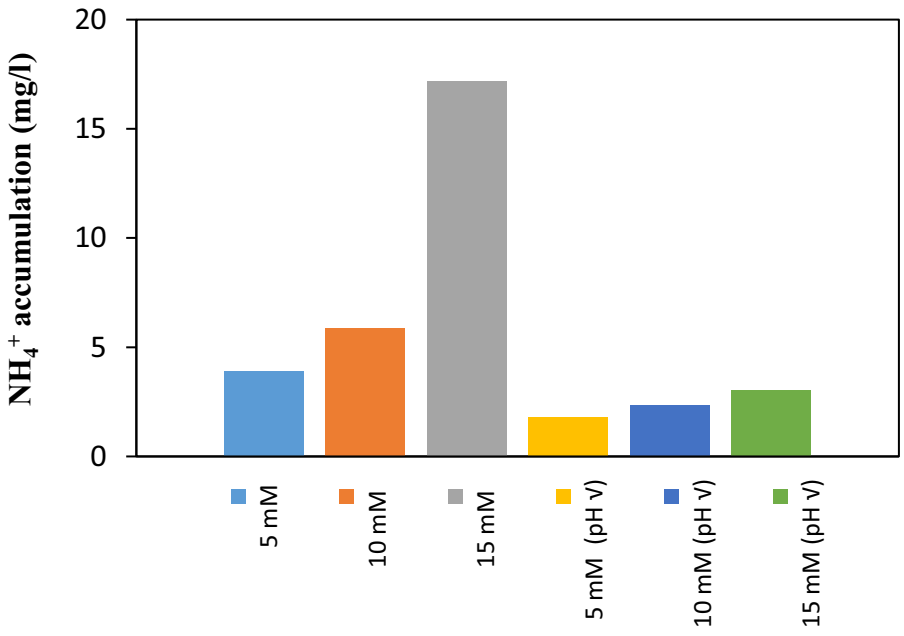

Figure 4.31. Ammonium ion production on 5, 10 and 15 mM sucrose containing HPM with 45 C/N ratio under constant temperature – continuous illumination with and without pH control.

4.2. Outdoor Experiments

4.2.1. PID Control Tuning

The test was performed with an emulated hydrogen production medium without bacteria using pilot-scale (20 L) stacked tubular reactor. Parameters are calculated and optimized by Cohen Coon running rules.

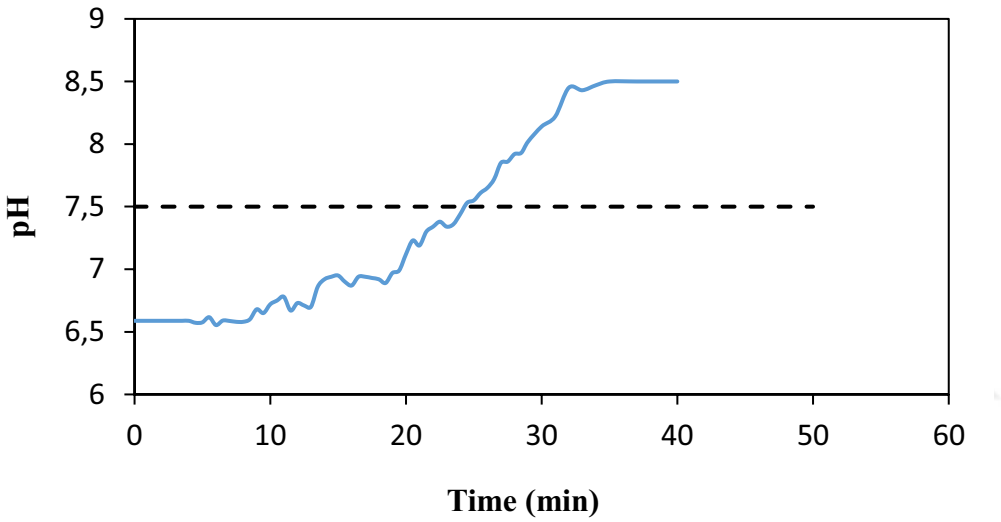

Figure 4.32. Response of the system for RUN1. Kc = 10, τI = 0.1 and τD = 0. The dashed line indicates the desired pH value

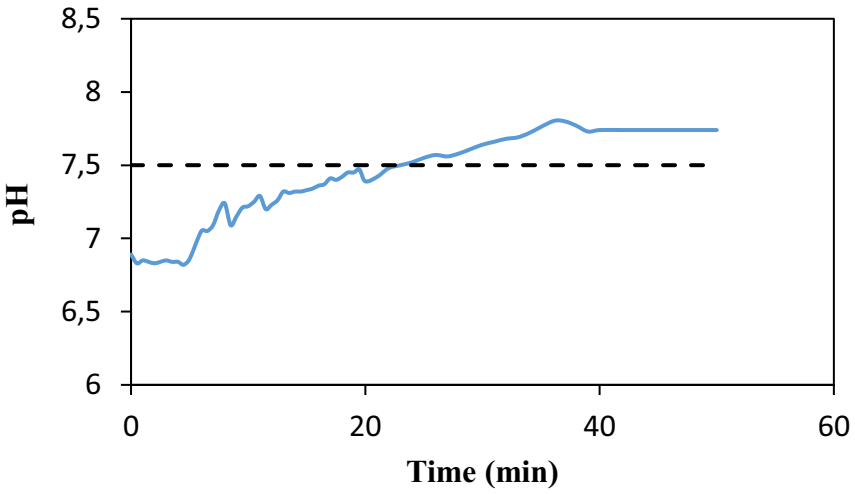

Figure 4.33. Response of the system for RUN2. Kc = 1, τI = 10 and τD = 2. The dashed line indicates the desired pH value

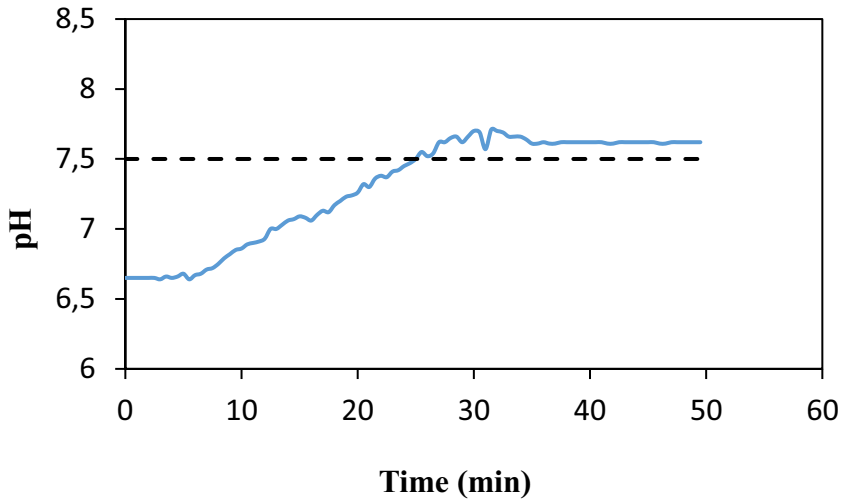

Figure 4.34. Response of the system for RUN3. Kc = 0.1, τI = 10 and τD = 2. The dashed line indicates the desired pH value

RUN1 was the aggressive controller and it was tried to understand of aggressive controller effect on the system (Figure 4.32). There was an oscillation. Additionally, the pH of RUN1 stabilized at 8.5 and it was high offset value.

Based on calculation time integral and time derivative was applied in RUN2 and RUN3. To obtain a more conservative controller for the sluggish system, the gain should be decreased. For RUN2 it was decreased 10 times when compared to RUN1. However, there was still an offset of around 0.2 (Figure 4.33).

In RUN3, the gain was decreased to 0.1 and Figure 4.34 showed better result. There was no base accumulation and controller was kept the pH at 7.5.

The finalized PID values were Kc = 0.1 (gain), τ_D = 2 min (derivative time) and τ_I = 10 min (integral time). The response graph with these parameter values is given, which shows that the medium was maintained much more effectively around the given set point.

4.2.2. RUN290817, August 29 - September 9, 2017, with *Rhodobacter Capsulatus* YO3 (hup$^-$) on Molasses

The experiment with *R. capsulatus* YO3 (hup$^-$) was performed between August 29 and September 9, 2017. The reactor was U-tube tubular photobioreactor made up the glass. The volume of the reactor was 20 L. Temperature was kept below 40 °C successfully during the experiment by the cooling system. Molasses was used as the carbon sources and sucrose concentration was analyzed daily. Startup concentration was 5 mM in the reactor. Feeding and dilution strategies were applied during the experiment. Samples were taken from the 2nd and 4th tubes for sucrose, cell concentration, and pH and reported. 1st and 3rd tubes also were observed for pH. The reactor was circulated continuously at an 80.4 L/h recirculation flowrate and the Reynolds number was 296. This experiment was the first trial of pH control integration to the tubular reactor.

PID control system was operated at first 2 days with 2 mM NaOH. Then, pH was tried to be controlled manually.

4.2.2.1. Solar Irradiation and Temperatures

The inoculation was made on August 29 and the experiment was conducted for 11 days. The temperature of the reactor, air temperature, and solar irradiance are shown in Figure 4.35.

The reactor temperature was maintained in the 30 – 35 °C range during day time. However, the temperatures for the night felt to around 7 °C. Since the experiment was performed during September, the higher temperature difference was observed for the day and night cycle.

At Ankara, sunshine duration was taken as 06.32 a.m. and 06.50 p.m. for September. The average solar radiation was obtained as 400 – 500 W/m^2 during the day time. At the 8th day of the experiments, the average radiation felt to about 200 W/m^2 due to cloudy and rainy periods.

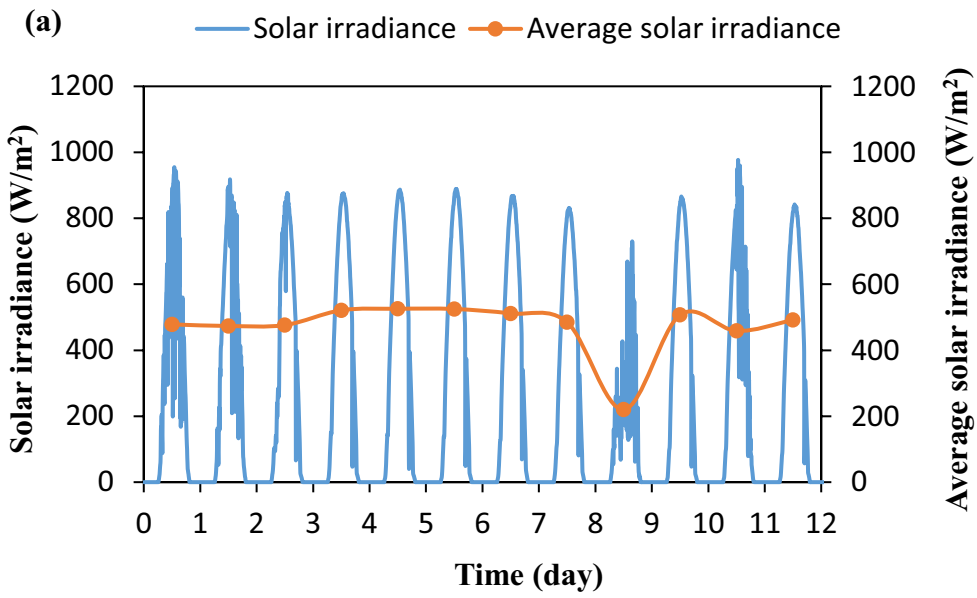

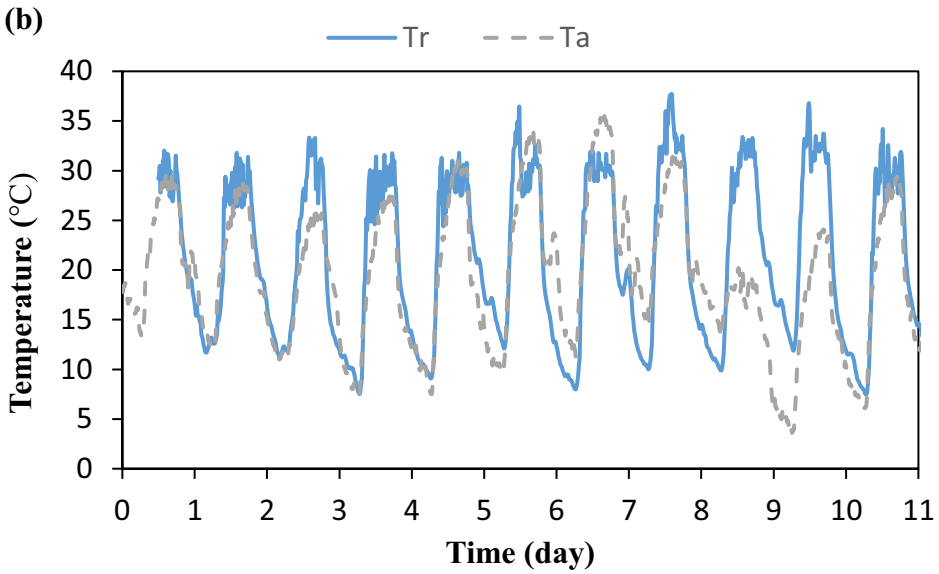

Figure 4.35. (a) The change in daily and average solar irradiance and (b) the temperature variation in the reactor, ambient air. Tr represents the temperature of the reactor measured from the second tube counted from the ground. Ta is the ambient temperature. The experiment started on 29 August 2017.

4.2.2.2. pH Value

pH was kept between 7.0 and 7.5 adding by 2 M NaOH, manually.

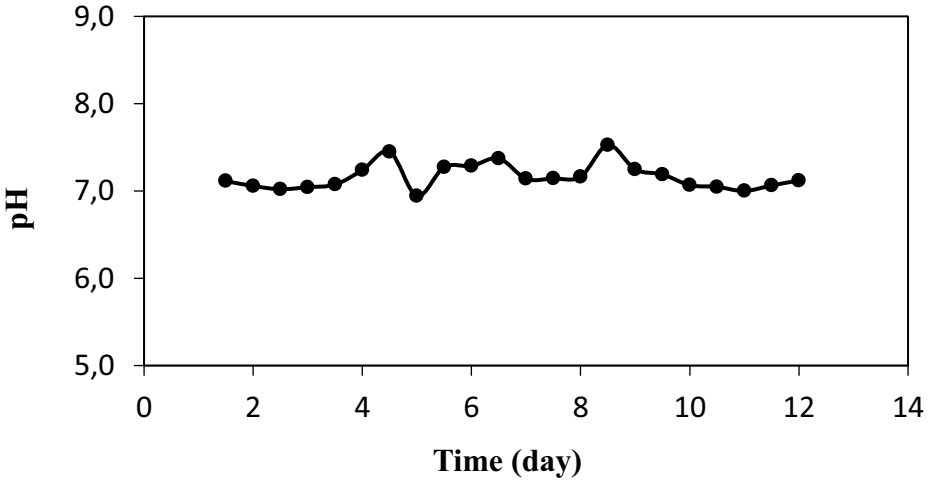

Figure 4.36. Daily variation in total organic acid concentration and pH

Previously, it has been reported that after feeding, pH decreased even more (Kayahan, Eroglu, and Koku 2017). In this study, pH also decreased after feeding and it was tried to be manipulated to set it around 7 again manually. However, there was a problem with mixing. 1 L molasses was fed to the inlet manifold which distributes the feeding through parallel tubes via the feeding line (Figure 3.7, V1) and 1 L reactor medium was taken. During first feeding on the 4th day, molasses tended to settle in the lower regions of the manifold and accumulated in the 1st tube (Figure 4.38), when Reynolds number was 296 (80 L/h). This can be attributed to the high density of molasses. Moreover, mixing was not enough to distribute the molasses through the other tubes. Thus, inside the bottom tube, a higher amount of molasses was utilized and pH profile was not homogeneous as seen in Figure 4.37, pH was recovered by adding base from the sample port. For the second feeding on the 5th day, Reynolds number increased to 496 (180 l/h which is the maximum flow rate of the pump) to enhance the mixing of molasses in the manifold. However, molasses accumulated in the bottom tube again and pH was decreased inside the tube on the 7th day. Hydrogen production can completely stop around a pH of 5.0 (Sasikala et al., 1991). Moreover, Jianzheng et al. have reported that a decrease in pH may not recoverable for the microorganism (J. Li et al. 2007). Therefore, a quarter of the bacteria might be inhibited when they have exposed the low pH. In addition to this, the bacteria in other tubes might not be supplied with sucrose for growth and hydrogen production.

Accumulation of molasses in the bottom tube also made pH control harder. In the bottom tube because of the excess sucrose, pH was decreasing sharply. This case caused excess base loading and an increase in pH value to above 8.0 for the other tubes. Without homogeneous pH distribution, applying pH control was not viable.

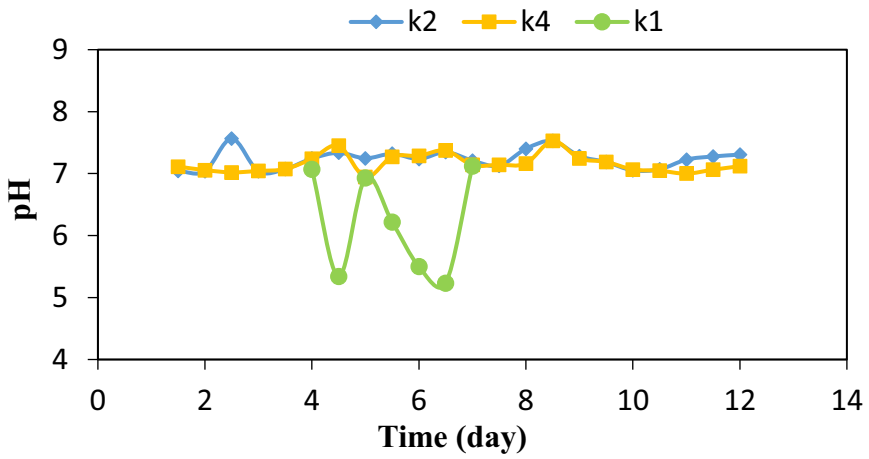

Figure 4.37. Daily variation in pH for 1st (k1), 2nd (k2) and 4th (k4) tubes.

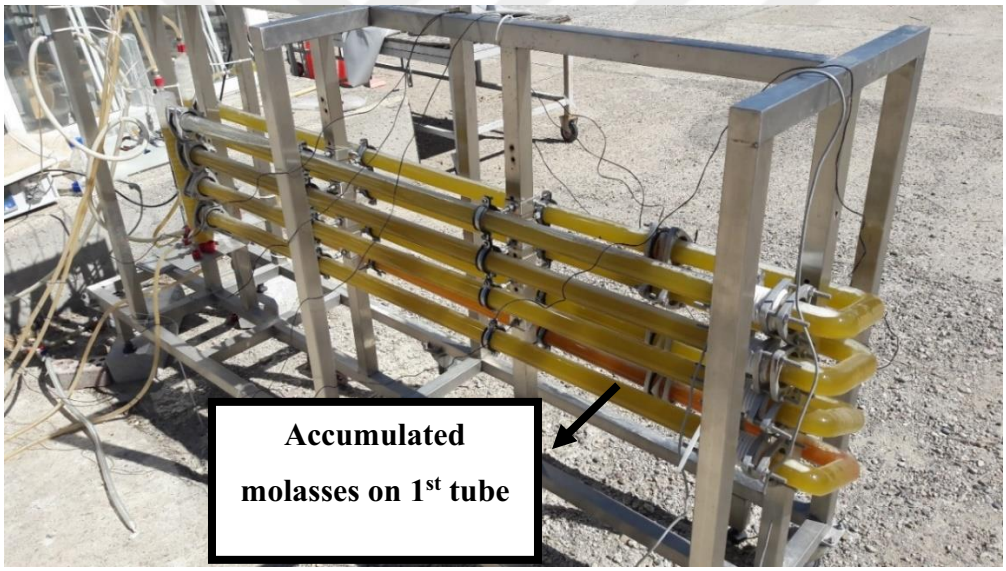

Figure 4.38. A photograph of stacked U-tube photobioreactor inlet manifold performed with *R. capsulatus* YO3 (hup^-) on molasses

Diameter and length ratio of the manifold can be the reason of the maldistribution (Ahn, Lee, and Shin 1998) in addition to the high density of molasses. To solve the problem, an equal volume of the feed was injected to tubes directly from sample ports for the next outdoor experiment (RUN290817, instead of from the feeding line and manifolds.

4.2.2.3. Cell growth, Sucrose Utilization, and Hydrogen Production

The reactor was started with 5 mM sucrose that was obtained diluting molasses. All sucrose was consumed at the 4th day of the experiment thus, molasses was fed to the reactor to keep the sucrose amount at 5 Mm (Figure 4.39). To keep a continuous feeding strategy, second feeding was given on the 5th day of the experiment. However, after that day no more feed was given since sucrose was not consumed completely.

C/N ratio was determined as 29 (5 mM sucrose and 2.5 mM Na-glutamate). Generally, the C/N ratio was determined as 45 in recent years (Androga, Özgür, et al. 2011b) in order to reduce lag time C/N ratio was lowered to 13 (Savasturk, Kayahan, and Koku 2018), however low C/N ratio caused to reduce the duration of the production. In this study, to reduce lag time concentration was started slightly high as 0.3 and C/N ratio was increased to 29. According to cell growth (Figure 4.40), the lag time was around 2 days and at the 3rd day, bacterial growth reached early exponential phase.

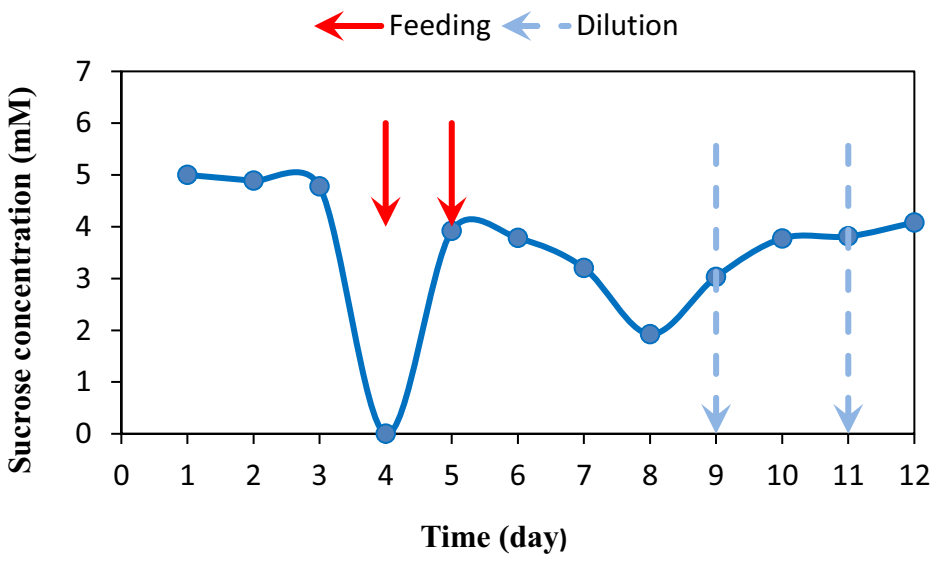

Figure 4.39. Daily sucrose concentration change (mM).

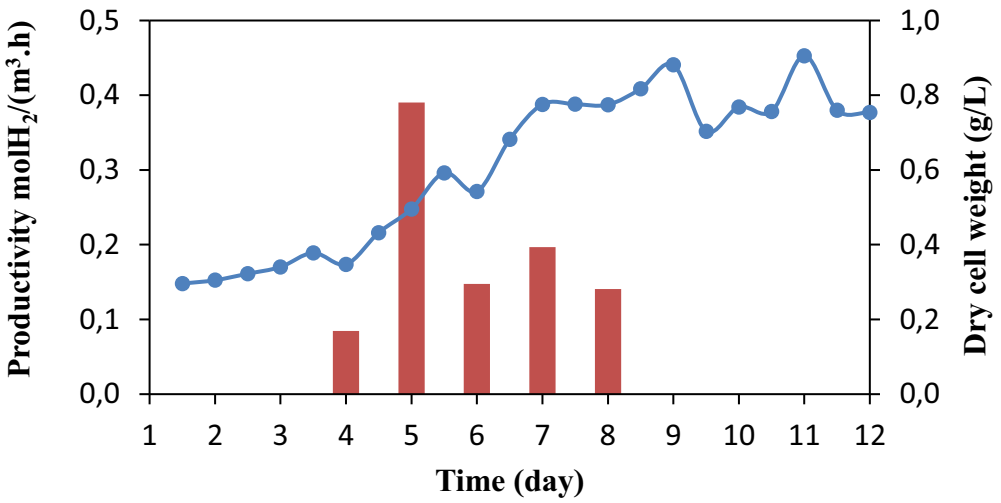

Figure 4.40. Daily dry cell weight change and hydrogen productivity.

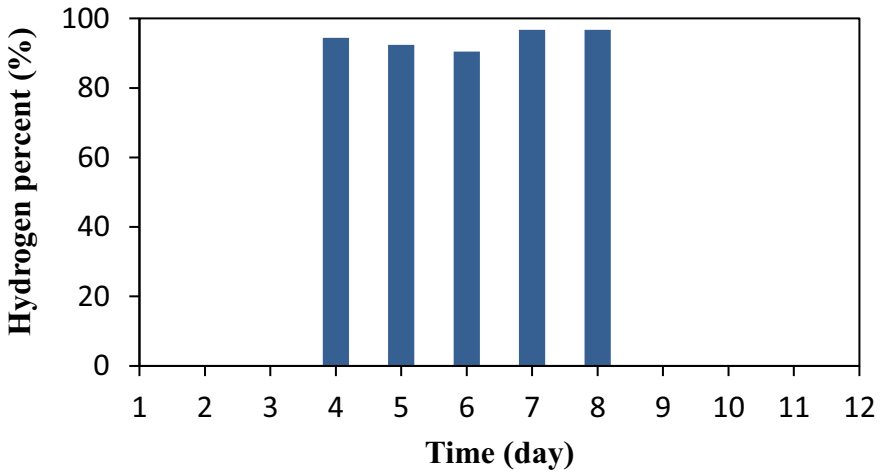

Figure 4.41. Daily hydrogen percentage change. Rest of the gas is carbon dioxide.

Hydrogen production started on the 4th day of the experiment in the early exponential phase. The maximum productivity was 0.4 mol H_2/(m^3.h) when the bacteria concentration was 0.5 g/L. Hydrogen production continued during the exponential phase and stopped when the bacterial growth reached to 0.9 g/L.

When cell concentration reached to 0.9 g/L to enable light penetration to promote hydrogen production, the reactor was diluted 50%. After just one day, cell concentration reached again 0.9 g/L. The reactor was diluted 50% second time at the 11th day of the experiment however it did not promote hydrogen production. It can be concluded that bacterial growth was stabilized at 0.9 g/L. At the stabilization, point dilution could not be a solution to decrease cell concentration since it could be reached the same value in one day.

The highest and average hydrogen percentage was 97% and 94%, respectively (Figure 4.41).

4.2.2.4. Organic Acid Production and Utilization

Lactic acid, formic acid, acetic acid, propionic acid, and butyric acid concentrations were followed for this experiment (Figure 4.42). Lactic acid was mostly insignificant. Formic acid was produced in the late exponential growth phase. Acetic acid was produced and consumed continuously. The highest acetic acid concentration was 30 mM on the 9th day of the experiment.

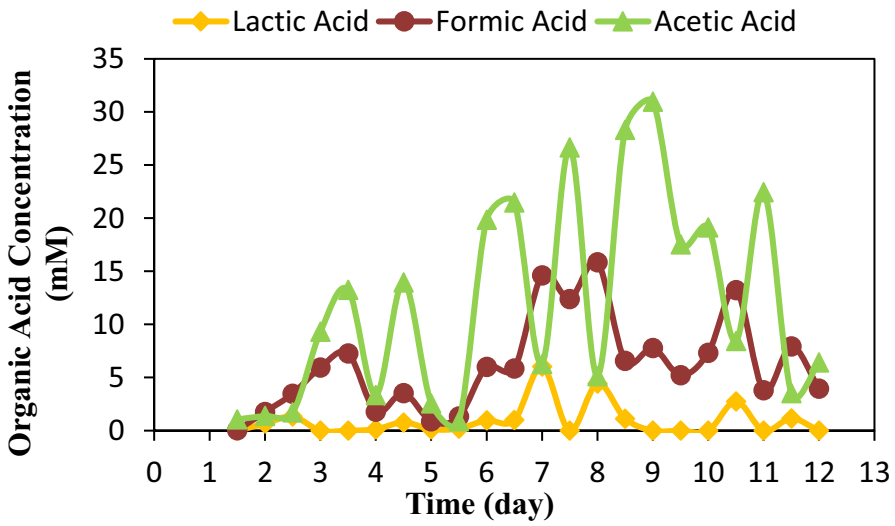

Figure 4.42. Daily lactic, formic and acetic acid concentrations change.

To summarize the main findings and conclusions from this run, a number of connections had to be increased with NaOH feeding port, pH meter septum. Glass ports caused leakage problem, however, they enabled to observe changing liquid level in ports. Leakage problem probably affected the bacteria metabolism such as inhibition of nitrogenase enzyme that reduces hydrogen productivity. At the same time, since during the experiment leakage problem could not be solved completely, hydrogen could not be collected properly. Therefore, hydrogen productivity could be obtained only for 3rd, 4th, 5th, 6th and 7th days, partially.

4.2.3. RUN290817, August 16 – October 2, 2017, with *Rhodobacter Capsulatus* YO3 (hup$^-$) on Molasses

Based on previous run, base feeding port and pH probe septum were improved to prevent leakage. To provide homogeneous molasses distribution, feeding process was changed. C/N ratio was used as 45 according to optimization results of small scale indoor experiments. In this run, automated PID pH control was use during the experiment.

4.2.3.1. Solar Irradiation and Temperature

The PBR operation started on August 16th and was operated for 48 days until October 2nd. During this period, daylight time decreased from 13.7 hours on day 1 to 12.3 hours on day 48. Average solar irradiance was between 400 – 500 W/m^2 for the first half of the experiment, and 300 – 400 W/m^2 for the rest (Figure 4.43). Significant dips were observed on rainy and cloudy days, especially on day 43.

The temperature of the 2nd port from the bottom is plotted, which displays the instantaneous temperature in 5-minute intervals, as well as the daytime and night-time averages. The reactor medium was cooled during the day by water at 15 ^{o}C to keep it below 30 ^{o}C. Only for a few days, the medium temperature was close to 40 ^{o}C. During

the first half of the experiment, the reactor temperature was around 30 ºC. With decreasing light irradiance in the subsequent days, the reactor average temperature decreased to around 19 ºC, reaching night-time temperatures as low as 11 ºC (Figure 4.44) after the 40th day. This probably slowed down the bacterial metabolism and might be one of the reasons for the slow growth of the bacteria after the last dilution and ammonium supplement. It should be mentioned that the period of night-time illumination might have benefited the sustenance of the bacteria directly by providing ATP via absorbed light and indirectly by the thermal energy absorbed by the medium.

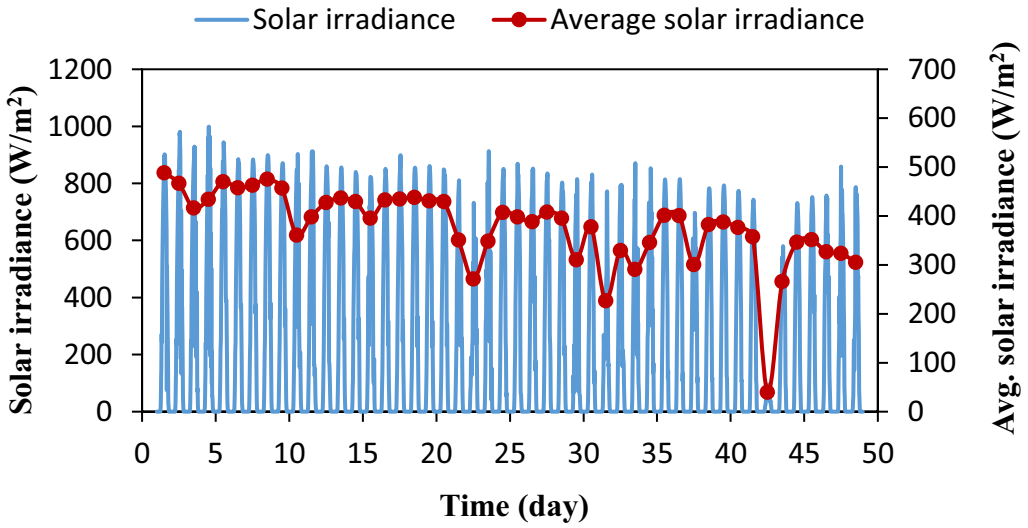

Figure 4.43. The hourly variation of solar radiation daily and average solar irradiance. The experiment started on August 16th, 2018 (Day 1 in the graph).

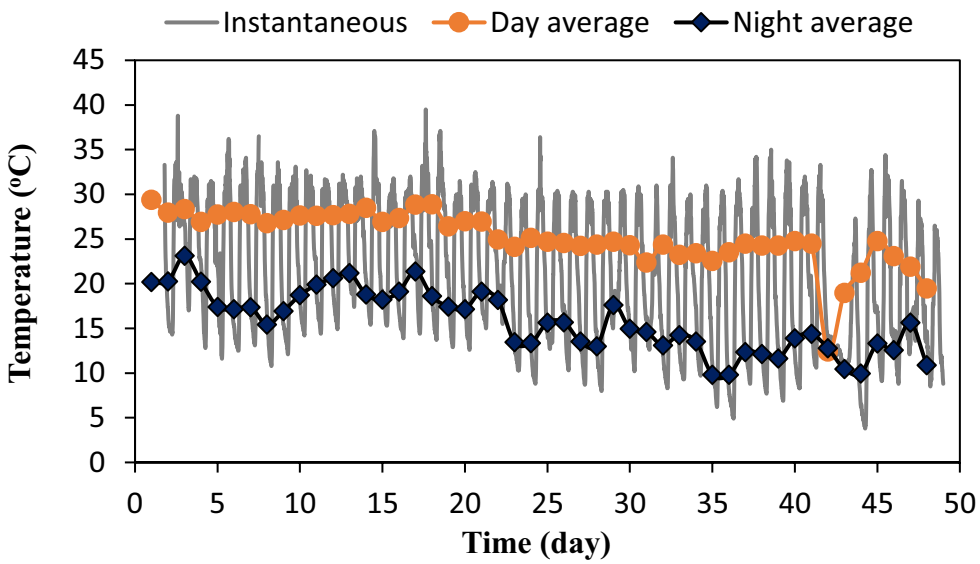

Figure 4.44. The instantaneous, day average and night average temperatures in the reactor.

4.2.3.2. Results of pH Control During Continuous Photofermentation

Figure 4.45 illustrates the daily variation of pH and total organic acid during continuous photobiological hydrogen production run. pH was successfully maintained around the set point of 7.0 except for a few days where power failures occurred. It should be emphasized that high amounts of organic acid were produced during the operation however with pH control, the hydrogen production continued for 48 days. Operation is very much improved compared to previous studies using molasses with the same bacteria and reactor type, in which the duration was 12 and 16 days (Kayahan, Eroglu, and Koku 2016, 2017; Savasturk, Kayahan, and Koku 2018). The limited duration of these studies correlated with the continuous decrease in pH. A stable pH value was maintained in the present work, leading to much longer operation time and enabled continuous feeding of the culture with molasses.

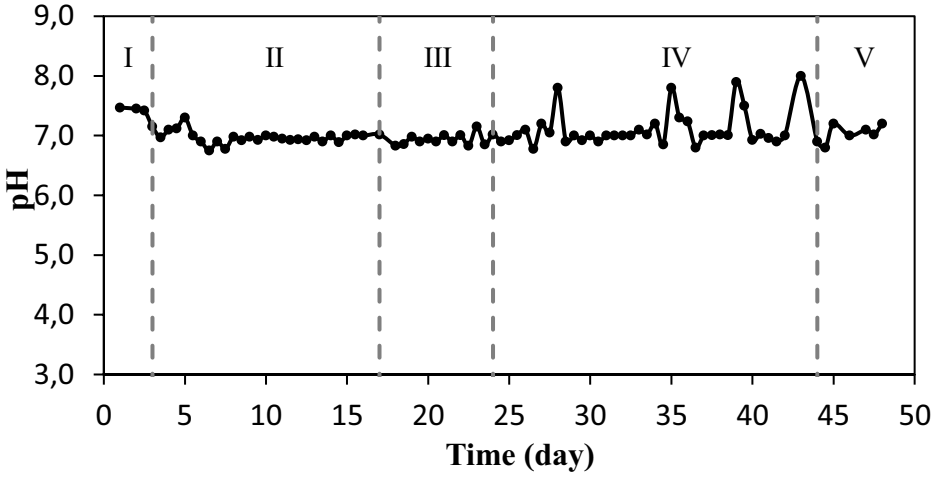

Figure 4.45. Daily variation of pH and total organic acid during continuous photobiological hydrogen production run.

An indirect benefit of the pH control was that the hydrogen purity remained at high values throughout the entire experiment. This is presumably due to the relation between the pH and dissolved carbonate species. In line with the theory of acid-base equilibria, the relative proportions of carbon dioxide, bicarbonate, and carbonate depend on the solution pH, subject to the following equilibria (Guo et al. 2008; Koku 2001; J. Li et al. 2007).

$CO_2 + OH^- \rightarrow HCO_3^-$

$HCO_3^- + OH^- \rightarrow CO_3^{-2}$

For pH values between 6 and 8, the forward reaction of the first equilibrium dominates so carbon dioxide was converted to primary bicarbonate during the run. A relatively high pH value thus traps the produced carbon dioxide, leading to high purity hydrogen (Koku 2001). In this study, the highest and average hydrogen percentages were obtained as 100% and 90%, respectively, since pH was controlled around 7.

4.2.3.3. Operation and Feeding Strategy

Table 4.4. *Operation and feeding strategy during the experiment. The experiment started on August 16th, 2018 and ended on October 2nd 2018 (48 days total).*

Phases	**Operation/Feed strategy**	**Days**
Phase I	Batch mode. No feeding.	1 - 3
Phase II	Carbon feed: Daily replenished the consumed sucrose to 5 mM. Glutamate fed on days 3, 5 and 14. Iron and molybdenum feed on days 13 and 17. Illumination with natural daylight only.	3 - 17
1st Dilution on day 17		
Phase III	Carbon feed: Same as Phase II. Illumination with natural daylight only.	17 - 24
2nd Dilution on day 24		
Phase IV	Carbon feed: Fed 5 mM sucrose-containing molasses, every other day. Glutamate fed on day 39. Trace elements, iron and vitamins fed on days 36 and 43 days. Illumination by natural daylight with artificial illumination at night.	24 - 44
3rd Dilution on day 32		
4th Dilution on day 39		
Phase V	Carbon feed: Same as Phase IV. Illumination by natural daylight only.	44 - 48

4.2.3.4. Cell growth, Sucrose Utilization, and Hydrogen Production

The growth curve for the bacteria (Figure 4.47) displays an initial lag during Phase I, which is an adaptation period that depends on several factors such as the age and volume of the inoculum, temperature and the (initial) C/N ratio. Of these, the C/N ratio is a manipulated variable that is critical for hydrogen production as well as growth and should be optimized for a chosen combination of carbon and nitrogen sources. A low C/N ratio has been observed to accelerate growth and substantially reduce the lag period, but was also found to ultimately result in high cell densities which limited light transmission (Androga, Özgür, et al. 2011a; Savasturk, Kayahan, and Koku 2018) and a relatively quick termination of hydrogen production. On the other hand, high C/N ratios such as those within the frequently cited range of 45-56 in the literature (Androga et al. 2014; Androga, Ozgur, et al. 2011; Androga, Özgür, et al. 2011b; Boran et al. 2010; Özgür, Uyar, et al. 2010; Sevinc et al. 2012) are optimal for hydrogen production but result in a slow start. Therefore, the strategy in this experiment was to start with a high C/N ratio (45) and monitor the bacterial concentration to reach and maintain a value of around 1.0 g/L. Thus, upon observing a rather pronounced lag during the first 3 days, 1 mM Na-glutamate was fed to promote growth in the 3rd and 5th days of the experiment. The cell concentration rose rapidly thereafter and was successfully maintained between 0.8-1.0 g/L for the majority of the run. This range coincides with the optimum cell concentrations suggested as 0.8 to 1.5 g/L (Androga, Ozgur, et al. 2011; Sevler Gökçe Avcioglu et al. 2011) in the literature.

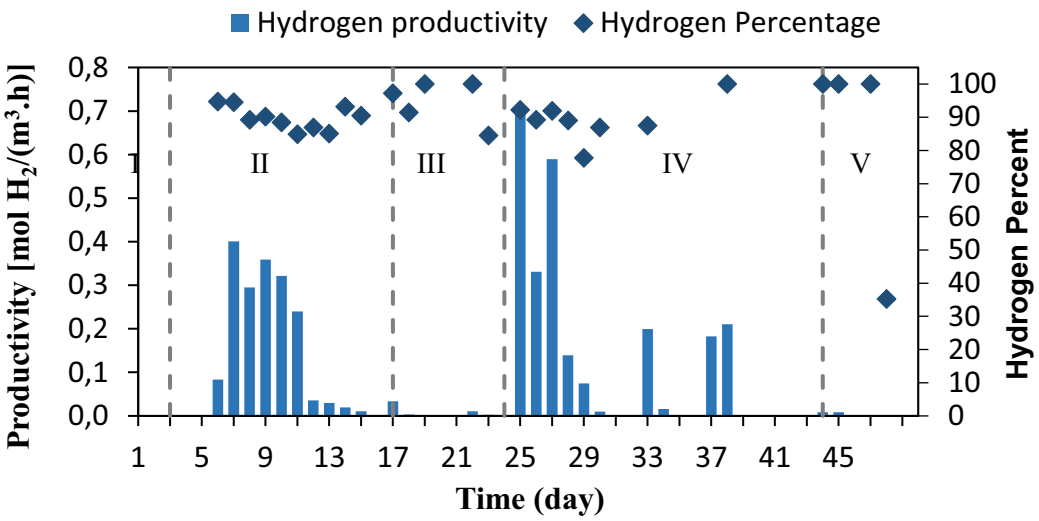

Figure 4.46. Composition of the produced gas and hydrogen productivity. The experiment started on August 16th, 2018 (Day 1 in the graph). Rest of the gas is carbon dioxide.

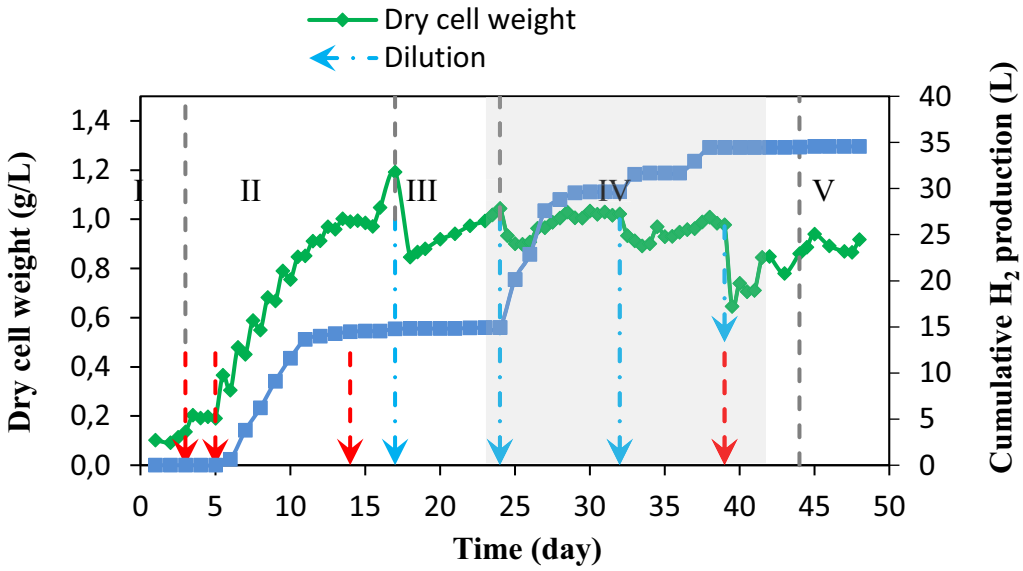

Figure 4.47. Daily variation of cell concentration and cumulative hydrogen production. The shaded region corresponds to continuous illumination period. Solid blue lines indicate a change in feed strategy, whereas green bars display hydrogen productivity.

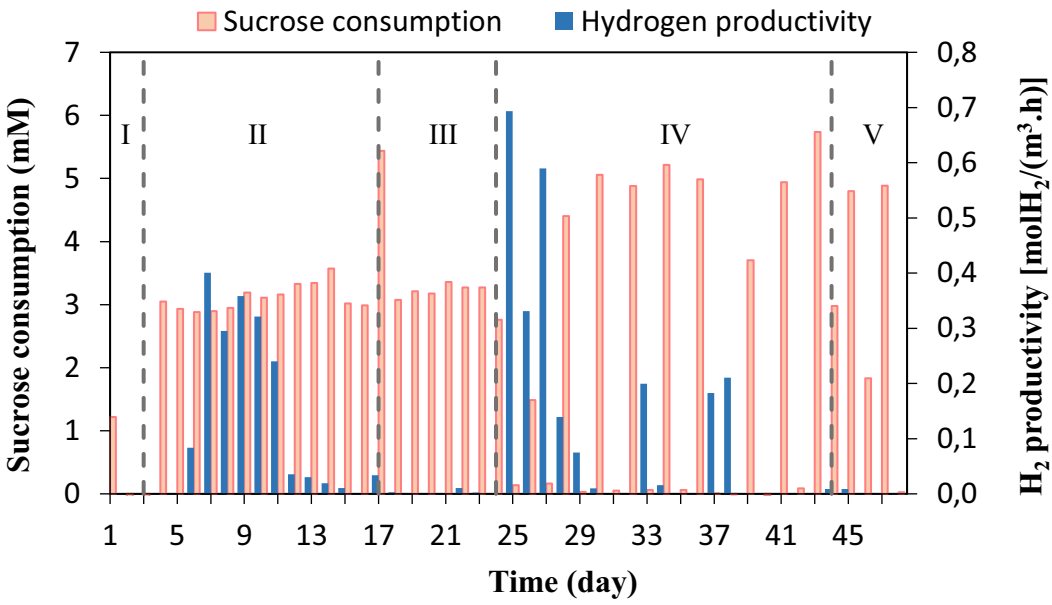

Figure 4.48. Daily variation of sucrose consumption and hydrogen productivity. The grey dashed lines correspond to the transitions between the phases summarized in Table 4.4.

The sucrose consumption and the hydrogen production graphs are displayed in Figure 4.48. At the early exponential phase, molasses feeding was started at a rate of 0.2 L/day and sucrose concentration was kept at 5 mM (Phase II). Most of the sucrose was consumed rapidly by the bacteria, such that when measured every day before feeding, the sucrose concentration had reached its lower limit of about 1 mM. During the entire run, 2.64 moles of sucrose were fed and of this amount, 2.57 moles were used, resulting in an overall conversion of 97%. This result is consistent with reports of improved sucrose utilization under controlled pH (Jun et al. 2008; T. Liu et al. 2014); in prior studies with the pilot-scale PBR with no pH control, sucrose could not be utilized by the bacteria at concentrations below 3 mM (Savasturk, Kayahan, and Koku 2018).

Hydrogen production started in the mid-exponential phase when the cell concentration reached 0.36 g/L. During Phase II, the highest productivity and molar yields were at the 7th day of the experiment as 0.40 molH_2/(m^3.h).

When growth reached the stationary phase, hydrogen production decreased sharply. Adding iron and molybdenum did not promote productivity. To recover hydrogen production, the reactor was diluted 50% with distilled water on the 17th day. Feeding was continued after the dilution and sucrose were consumed steadily, but hydrogen production was still extremely low (Phase III). Presumably, the continuous feeding of sodium ions by the controller base pump induced a metabolic shift to pathways alternative to hydrogen production. Kim et al. proposed that a sudden increase of the exterior sodium concentration changed the metabolic pathway (D. Kim, Kim, and Shin 2009), which possibly was the adaptation of bacteria to chronic sodium toxicity.

The fact that sucrose consumption continued on days 17-24, with no hydrogen production (Figure 4.48), suggests an endogenous metabolic activity. A material balance on the carbon-containing species within the liquid medium and the headspace gas for this period shows that when the sum of carbon from the organic acids produced, from the CO_2 that has been retained by the medium and from the collected biogas is estimated, approximately 55 % of the carbon from the consumed sucrose remains unaccounted for (Appendix N). PNSB is capable of producing large amounts of polyhydroxybutyrate (PHB) as reserve material, which affords an alternative pathway to hydrogen to discharge excess energy and reducing power under nitrogen limitation (Cetin et al. 2006; Hustade, Steinbüchel, and Schlegel 1993; Khatipov et al. 1998; Yigit et al. 1999), so it can be surmised that the 'lost' carbon was stored endogenously. Similar findings and arguments have been presented by Adessi et al., who observed decreasing substrate-to-hydrogen conversion in response to increasing salinity, and pointed out the possibility of synthesis of additional carbon compounds such as PHB (Adessi et al. 2016).

To decrease the sodium stress, a second dilution was then applied and additionally, artificial illumination of 600 W (3x200W tungsten lamps) was applied during the night at Phase IV. Furthermore, the feed strategy was modified. In Phase II, it was noticed that hydrogen production slowed down visibly after molasses feeding. It is not clear whether this reversible slowdown was caused by the temporary loss of the medium

transmittance (due to the opaque nature of the molasses) or by a metabolic shift. Regardless of the cause, for Phase IV, the feeding strategy was changed to feeding 5 mM sucrose every other day (5 mM sucrose) to avoid interfering with ongoing production.

The combined influence of these changes restarted the hydrogen production, and on the 25th day of the experiment, the highest hydrogen productivity of the entire experiment was obtained as 0.69 molH_2/(m^3·h) with a cell concentration of 0.9 g/L. Interestingly, no sucrose consumption occurred on this day so hydrogen production cannot be attributed to sucrose, or the consumption of organic acids, as the amounts of the latter were found to increase during the 25th day. This was also the case on the 27th, 29th and 38th days of the experiment, when there was no feed and no sucrose consumption, but hydrogen was produced nevertheless.

Hydrogen production without sucrose consumption during phase IV might be explained by the utilization of endogenous substrates synthesized during phase III described above (Koku et al. 2003; Uyar, Eroglu, Yücel, and Gunduz 2009). Thus, the accumulated endogenous reserves of PHB were probably used as the substrate for hydrogen production. Restricting the carbon feed to alternate days, dilution of the medium, nighttime illumination and keeping the pH around 7.0 may altogether have stimulated PHB utilization.

In phase IV, cumulative hydrogen production gradually increased after each dilution cycle (Figure 4.48). After the addition of trace elements, iron and vitamins on the 36th day, hydrogen productivity increased a bit further. Towards the end of phase IV, to increase the bacterial concentration and to improve its resistance to worsening weather conditions, glutamate was added after the 4th dilution (day 39). However, the low ambient temperatures and the increase in ammonium concentration after the addition of glutamate appear to have adversely affected hydrogen production. The hydrogen production gradually came to a complete stop at the end of Phase V and the experiment was terminated.

4.2.3.5. Production and Consumption of Organic Acids

Organic acids (acetic, lactic, formic, butyric and propionic acids) from the PBR medium were analyzed every day and night. All species were observed to be both generated and consumed, which is expected, as these are natural metabolites of the overall carbon flow. On the 25th and 27th days, when the hydrogen productivities were 0.69 and 0.59 mol $H_2/(m^3 \cdot h)$, respectively the corresponding total organic acid concentrations were 300 and 210 mM.

All acids were produced in significant amounts and reached concentrations of 75 mM or higher, except butyrate, which remained below 25 mM (Figure 4.49). Butyrate concentrations higher than 25 mM have been reported to result in inhibition of hydrogen production (Guwy et al. 2011), so the observed range in this study is low enough to rule out such an inhibition. In previous studies without pH control lactic and propionic acid formation from molasses utilization by *R. capsulatus* was observed to be low (Sevler Gökçe Avcioglu et al. 2011; Kayahan, Eroglu, and Koku 2017), but in the present study, starting from Phase II acetic acid and propionic acid and lactic acid started to accumulate. A similar increase in the concentrations of the same organic acids was also observed by Kim et al. during hydrogen production under a high-sodium environment (D. Kim, Kim, and Shin 2009). This difference might also be indicative of the metabolic shift to non-hydrogen pathways as mentioned previously.

It has been reported that propionic and acetic acid provides the PHB formation due to their relation with acetyl-CoA instead of pyruvate (Wu, Liou, and Lee 2012). PHB is an intermediate product between acetyl-CoA and propanoate. When highest hydrogen production was obtained, sucrose consumption was not observed. PHB might decompose to propionic acid by contributing the hydrogen production. Therefore, high propionic acid concentration may be proof of PHB production. Additionally, propionic acid production can be derived from odd-chain fatty acid degradation (Voet, Voet, and Pratt 2001).

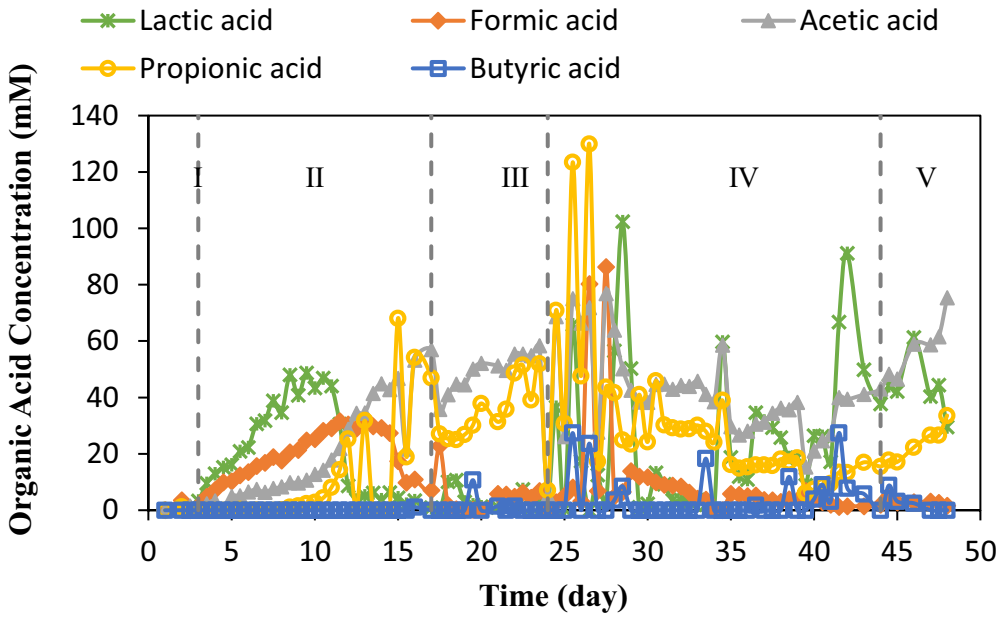

Figure 4.49. Variation in organic acid concentrations with time.

4.2.3.6. Ammonium and Sodium Analyses

Ammonium can be produced during photofermentation by the metabolic breakdown of the glutamate or from nitrogenous compounds within molasses. It has an inhibitory effect on the nitrogenase enzyme, the main catalyst for hydrogen production. Thus, limiting or the removal of ammonium is necessary for photofermentative hydrogen production (Budiman and Wu 2018).

Ammonium was apparently utilized as a nitrogen source during most of the experiment. However, after the 4th dilution, in the final phase (Phase V), the ammonium concentration spiked up, possibly as a result of the glutamate addition that was meant to strengthen the bacteria, and remained high (55 – 65 mg/L) during the last 10 days of the experiment where hydrogen productivity was very low (0.01 H_2 mol/(m^3·h)) (Figure 4.50). High concentrations of ammonia (>2-3 mM) for photofermentation of Rhodobacter species have been reported to be inhibitory for hydrogen production (Argun, Kargi, and Kapdan 2009; Özgür, Mars, et al. 2010).

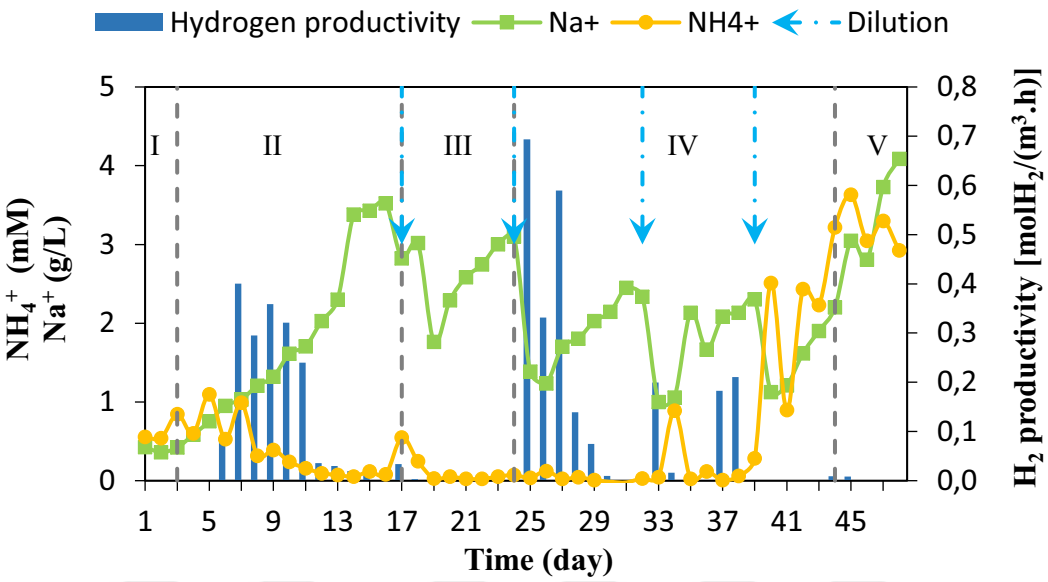

Figure 4.50. Daily variation of sodium and ammonium concentration and hydrogen productivity. The grey dashed lines correspond to the transitions between the phases summarized in Table 4.1.

The addition of sodium hydroxide for pH control resulted in the accumulation of sodium ions, and the sharp decrease of hydrogen production in Phase II can be at least partially attributed to the increased sodium concentration, reaching a maximum of 3.5 g/L (Figure 4.50). At high concentrations, sodium can be inhibitory or even toxic. It has been reported that although PNSB species can be natively or adapted to be salt-tolerant, both growth and photofermentative hydrogen production decrease and eventually stop at increasing levels of salt (Adessi et al. 2016; D. Kim, Kim, and Shin 2009; Uygur and Kargı 2004). Kim et al. reported a decrease in hydrogen production by 50% at 3.0 g/L sodium (D. Kim, Kim, and Shin 2009). The decline in hydrogen production is probably linked to the inhibition of nitrogenase in response to salt stress, which has previously been reported in strains of *R. capsulatus* (Adessi et al. 2016; Igeno et al. 1995). Therefore, one intended effect of the dilutions was to decrease the sodium concentration.

After the first dilution, hydrogen production was not observed, even though sodium concentration decreased to around 1.8 g/L. It was only after the second dilution was applied together with artificial illumination that hydrogen productivity was recovered, as discussed above. But even under continuous illumination, hydrogen production decreased with increasing sodium concentration during phase IV.

CHAPTER 5

CONCLUSION

A pH control implementation to U-tube tubular reactor was proposed in this study with the goal of long-term hydrogen production. Feedback PID control system was used to control pH of the PBR. The base was chosen as 2 M NaOH and the flow rate of the base was manipulated variable. pH measurement and base feeding points were determined on the reactor and ports were constructed. Then, based on system identification with high time delay, PID control parameters were tunned. Controller gain, integral time and derivative time were tunned as 0.1, 10 and 2, respectively. Because of the nonlinear nature of the pH neutralization, PID control system was not commonly used. The PID pH control system was successfully implemented by accounting for and compensating the large mixing-time due to the high surface-to-volume ratio using a proper choice of control parameters. To our knowledge, this is the first time continuous pH adjustment has been employed for a pilot-scale, outdoor tubular PBR with PNSB.

Optimization of molasses concentration and carbon to nitrogen ratio under indoor, outdoor and pH controlled conditions was also proposed as minor goals.

Indoor experiments were carried out with *Rhodobacter capsulatus* YO3 (hup^-) on glass batch photobioreactors utilizing sucrose-containing molasses as the carbon source. Indoor experiments aimed to use molasses effectively and increase the utilization of molasses at its high concentrations.

RUN150718 was performed under continuous illumination and constant temperature. C/N ratio was changed between 15 and 45 and molasses concentration was changed between 2 and 10 mM in hydrogen production medium. The highest productivity was 0.6 mol $H_2/(m^3.h)$ for HPM containing 5 mM sucrose containing molasses when C/N

was 45. Increase in sucrose concentration increased propionic and butyric acid production significantly. The pH of the HPM containing 10 mM sucrose concentration molasses decreased to 5.5. The cell stabilization was not observed on HPM with 15 C/N, the death phase followed the exponential phase. Hydrogen purity was affected strongly from C/N ratio and sucrose concentration. The lowest hydrogen purity was obtained from HPM containing 10 mM sucrose when C/N was 15.

RUN121118 aimed to optimized C/N ratio under outdoor conditions. To simulate day/night cycle of outdoor conditions, an indoor experiment was designed in which temperature was changed daily and light/dark cycle (10 h/14 h) was applied. C/N ratio was between 15 and 45 and sucrose-containing molasses concentration was 5 mM in HPM. The highest productivity was 0.7 mol $H_2/(m^3.h)$ for HPM containing 5 mM sucrose containing molasses when C/N was 45. Sucrose consumption was not affected by changing temperature and light. In the experiment, it was concluded that the day/night cycle improved hydrogen production significantly.

RUN030419 aimed to investigate the effect of pH on changing molasses concentrations for *R. capsulatus* YO3 (hup^-) under controlled indoor conditions by keeping the pH constant, manually. C/N ratio was 45 and sucrose-containing molasses concentration was between 5 and 15 mM in HPM. The highest hydrogen productivity was 0.8 mol $H_2/(m^3.h)$ for HPM containing 15 mM sucrose containing molasses under constant pH. In the experiment, it was observed that the ammonium ion production was reduced by pH control. Contrary to RUN150718 and RUN121118, increase in molasses concentration increased the hydrogen productivity, significantly.

The outdoor experiments were run with *Rhodobacter capsulatus* YO3 (hup^-) on a pilot scale (20 L) stacked U-tube photobioreactor utilizing sucrose-containing molasses as the carbon source. RUN290817 was carried out between August 29 – September 9, 2017. pH distribution on tubes and the implementation of the control system were monitored. From the results of this run, it has been concluded that molasses feeding method should be changed for the homogeneous distribution of pH. Implementation

points of the ports should be adjusted. These findings lead to succeeding pH control implementation and hydrogen production experiments for RUN160818.

RUN160818 was carried out on August 16 – October 2, 2018, using sucrose-containing molasses as the carbon source with *Rhodobacter capsulatus* YO3 (hup^-) on a pilot scale (20 L) stacked U-tube photobioreactor under outdoor conditions. The pH of the reactor medium was kept around 7.0 by PID control system. Compared to prior studies with the same strain, same nutrient, and same PBR type, the application of pH control resulted in a steady pH, stable bacterial concentration and prolonged gas production at high purities of hydrogen. The hydrogen production duration was increased to 48 days from about 12 days. The highest hydrogen productivity was 0.69 mol $H_2/(m^3.h)$. The highest and average hydrogen percentages were 100% and 90%. The highest light conversion efficiency was 0.121% on the 25^{th} day of the experiment. However, continuous feeding of the base to counter the natural acidification resulted in the accumulation of sodium ions, which correlated with the cessation of hydrogen production. Production resumed after dilution combined with night-time artificial illumination. PNSB could be adapted to sodium stress and hydrogen production was observed when Na^+ was 3 g/L. Propionic and lactic acid concentrations were high among other organic acids and total organic acid concentration reached 300 mM on the 25^{th} day of the experiment. During the experiment, hydrogen production was observed without sucrose consumption. Continuous consumption of the molasses sucrose during both outcomes suggests a reversible shift from the hydrogen production metabolism to another carbon-consuming pathway, possibly PHB production.

When compared to other studies which utilized molasses with *R. capsulatus* YO3 (hup^-) and same reactor type, maximum hydrogen productivity and amount of hydrogen volume were obtained in this study (Table 5.1). Operation time increased to 48 days. The highest average hydrogen purity was obtained due to the pH control system.

Table 5.1. *Summary of results and comparison with previous outdoor studies using the same strain and molasses as the feed.*

	This study (RUN160818)	(Savasturk, Kayahan, and Koku 2018)	Kayahan *et al.*, 2017
Reactor type	U-tube photobioreactor	U-tube photobioreactor	U-tube photobioreactor
Volume of the reactor (L)	20	20	9
Amount of hydrogen produced (L)	34.6	15.9	4.56
Maximum hydrogen productivity [H_2mol/(m^3.h)]	0.69	0.47	0.31
Average hydrogen productivity [mol/(m^3.h)]	0.11	0.070	0.11
Maximum hydrogen % of produced gas	100	94.1	84.7
Average hydrogen % of produced gas	90	83	33
Operation time (day)	48	17	12
Minimum pH	6.8	6.5	5.8
Maximum bacterial concentration (g/L)	1.2	1.1	0.6
Lag time to start hydrogen production (h)	120	18	96

REFERENCES

Adessi, A., Concato, M., Sanchini, A., Rossi, F., & De Philippis, R. (2016). Hydrogen production under salt stress conditions by a freshwater *Rhodopseudomonas palustris strain. Applied Microbiology and Biotechnology*, *100*(6), 2917–2926. https://doi.org/10.1007/s00253-016-7291-4

Ahn, H., Lee, S., & Shin, S. (1998). Flow distribution in manifolds for low reynolds number flow. *KSME International Journal*, *12*(1), 87–95. https://doi.org/10.1007/BF02946537

Akhlaghi, M., Boni, M. R., De Gioannis, G., Muntoni, A., Polettini, A., Pomi, R., … Spiga, D. (2017). A parametric response surface study of fermentative hydrogen production from cheese whey. *Bioresource Technology*, *244*(June), 473–483. https://doi.org/10.1016/j.biortech.2017.07.158

Akkerman, I., Janssen, M., Rocha, J., & Wijffels, R. H. (2002). Photobiological hydrogen production: photochemical efficiency and bioreactor design. *International Journal of Hydrogen Energy*, (27), 1195–1208.

Androga, D. D. (2009). *Biological Hydrogen Production on Acetate in Continuous Panel Photobioreactors Using Rhodobacter Capsulatus*. Middle East Technical University. https://doi.org/10.1038/132817a0

Androga, D. D. (2014). *Modeling and simulation of photobioreactors for biological hydrogen production*. Middle East Technical University.

Androga, D. D., Özgür, E., Eroglu, I., Gündüz, U., & Yücel, M. (2011a). Significance of carbon to nitrogen ratio on the long-term stability of continuous photofermentative hydrogen production. *International Journal of Hydrogen Energy*, *36*(24), 15583–15594. https://doi.org/10.1016/j.ijhydene.2011.09.043

Androga, D. D., Özgür, E., Eroglu, I., Gündüz, U., & Yücel, M. (2011b). Significance

of carbon to nitrogen ratio on the long-term stability of continuous photofermentative hydrogen production. *International Journal of Hydrogen Energy*, *36*(24), 15583–15594. https://doi.org/10.1016/j.ijhydene.2011.09.043

Androga, D. D., Özgür, E., Eroglu, I., Gündüz, U., & Yücel, M. (2012). Photofermentative Hydrogen Production in Outdoor Conditions. In D. Minic (Ed.), *Hydrogen Energy - Challenges and Perspectives* (pp. 77–120). Intech. https://doi.org/http://dx.doi.org/10.5772/57353

Androga, D. D., Ozgur, E., Gunduz, U., Yucel, M., & Eroglu, I. (2011). Factors affecting the longterm stability of biomass and hydrogen productivity in outdoor photofermentation. *International Journal of Hydrogen Energy*, *36*(17), 11369–11378. https://doi.org/10.1016/j.ijhydene.2010.12.054

Androga, D. D., Sevinc, P., Koku, H., Yücel, M., Gündüz, U., & Eroğlu, I. (2014). Optimization of temperature and light intensity for improved photofermentative hydrogen production using *Rhodobacter capsulatus* DSM 1710. *International Journal of Hydrogen Energy*, *39*, 2472–2480. https://doi.org/10.1016/j.ijhydene.2013.11.114

Argun, H., Kargi, F., & Kapdan, I. K. (2009). Effects of the substrate and cell concentration on bio-hydrogen production from ground wheat by combined dark and photo-fermentation. *International Journal of Hydrogen Energy*, *34*(15), 6181–6188. https://doi.org/10.1016/j.ijhydene.2009.05.130

Arooj, M. F., Han, S. K., Kim, S. H., Kim, D. H., & Shin, H. S. (2008). Continuous biohydrogen production in a CSTR using starch as a substrate. *International Journal of Hydrogen Energy*, *33*(13), 3289–3294. https://doi.org/10.1016/j.ijhydene.2008.04.022

Avcioglu, Sevler Gökçe. (2010). *Scale up of panel photobioreactors for hydrogen production by PNS Bacteria*. Middle East Technical University.

Avcioglu, Sevler Gokce, Ozgur, E., Eroglu, I., Yucel, M., & Gunduz, U. (2011).

Biohydrogen production in an outdoor panel photobioreactor on dark fermentation effluent of molasses. *International Journal of Hydrogen Energy*, *36*(17), 11360–11368. https://doi.org/10.1016/j.ijhydene.2010.12.046

Avcioglu, Sevler Gökçe, Ozgur, E., Eroglu, I., Yucel, M., & Gunduz, U. (2011). Biohydrogen production in an outdoor panel photobioreactor on dark fermentation effluent of molasses. *International Journal of Hydrogen Energy*, *36*(17), 11360–11368. https://doi.org/10.1016/j.ijhydene.2010.12.046

Babuska, R., Oosterhoff, J., Oudshoorn, A., & Bruijn, P. M. (2002). Fuzzy self-tuning PI control of pH in fermentation. *Engineering Applications of Artificial Intelligence*, *15*(1), 3–15. https://doi.org/10.1016/S0952-1976(02)00003-9

Basak, N., & Das, D. (2007). The prospect of purple non-sulfur (PNS) photosynthetic bacteria for hydrogen production : the present state of the art, *23*, 31–42. https://doi.org/10.1007/s11274-006-9190-9

Biebl, H., & Pfennig, N. (1981). Isolation of Members of the Family *Rhodospirillaceae*. In M. P. Starr, H. Stolp, H. Truper, A. Balows, & H. Schlegel (Eds.), *The Prokaryotes* (pp. 267–273). Springer-Verlag Berlin Heidelberg.

Boodhun, B. S. F., Mudhoo, A., Kumar, G., Kim, S. H., & Lin, C. Y. (2017). Research perspectives on constraints, prospects and opportunities in biohydrogen production. *International Journal of Hydrogen Energy*, *42*(45), 27471–27481. https://doi.org/10.1016/j.ijhydene.2017.04.077

Boran, E. (2011). *Process Development for Continuous Photofermentative Hydrogen Production*. Middle East Technical University.

Boran, E., Özgür, E., Burg, J. Van Der, Yücel, M., Gündüz, U., & Eroglu, I. (2010). Biological hydrogen production by *Rhodobacter capsulatus* in solar tubular photo bioreactor. *Journal of Cleaner Production*, *18*, S29–S35. https://doi.org/10.1016/j.jclepro.2010.03.018

Braz Romão, B., Moreira Silva, F. T., Coutinho de Barcelos Costa, H., Santos

Moreira, F., de Souza Ferreira, J., Regina Xavier Batista, F., & Luiz Cardoso, V. (2018). Influence of heat pre-treated inoculum and pH control on the hydrogen production by microbial consortium. *Environmental Progress and Sustainable Energy*, *37*(1), 505–512. https://doi.org/10.1002/ep.12672

Brentner, L. B., Peccia, J., & Zimmerman, J. B. (2010). Challenges in Developing Biohydrogen as a Sustainable Energy Source : Implications for a Research Agenda. *Environmental Science and Technology*, *44*(7), 2243–2254.

Budiman, P. M., & Wu, T. Y. (2018). Role of chemicals addition in affecting biohydrogen production through photofermentation. *Energy Conversion and Management*, *165*, 509–527. https://doi.org/10.1016/j.enconman.2018.01.058

Calli, B., Schoenmaekers, K., Vanbroekhoven, K., & Diels, L. (2008). Dark fermentative H_2 production from xylose and lactose-effects of on-line pH control. *International Journal of Hydrogen Energy*, *33*(2), 522–530. https://doi.org/10.1016/j.ijhydene.2007.10.012

Calvo-Rolle, J. L., Quintian-Pardo, H., Casanova, A. C., & Alaiz-Moreton, H. (2012). *PID Controller Design Approaches - Theory, Tuning and Application to Frontier Areas*. (M. Vagia, Ed.). InTech. https://doi.org/10.5772/2628

Carreño-Zagarra, J. J., Guzmán, J. L., Moreno, J. C., & Villamizar, R. (2019). Linear active disturbance rejection control for a raceway photobioreactor. *Control Engineering Practice*, *85*(December 2018), 271–279. https://doi.org/10.1016/j.conengprac.2019.02.007

Cetin, D., Gündüz, U., Eroglu, İ., Yucel, M., & Turker, L. (2006). Poly-beta-hydroxybutyrate accumulation and releasing by hydrogen producing bacteria, *Rhodobacter sphaeroides* OU001. A transmission electron microscopic study. *African Journal of Biotechnology*, *5*(22), 2069–2072. https://doi.org/10.4314/ajb.v5i22.55960

Chen, C., Yeh, K., Lo, Y., Wang, H., & Chang, J. (2010). Engineering strategies for

the enhanced photo-H_2 production using effluents of dark fermentation processes as substrate. *International Journal of Hydrogen Energy*, *35*(24), 13356–13364. https://doi.org/10.1016/j.ijhydene.2009.11.070

Cheng, S., & Logan, B. E. (2011). High hydrogen production rate of microbial electrolysis cell (MEC) with reduced electrode spacing. *Bioresource Technology*, *102*, 3571–3574. https://doi.org/10.1016/j.biortech.2010.10.025

Cook, G. M., & Morgan, H. W. (1994). Hyperbolic growth of *Thermoanaerobacter thermohydrosulfuricus* (*Clostridium thermohydrosulfuricum*) increases ethanol production in pH-controlled batch culture. *Applied Microbiology and Biotechnology*, *41*(1), 84–89. https://doi.org/10.1007/BF00166086

Das, D., & Veziroğlu, T. N. (2001). Hydrogen production by biological processes : a survey of literature. *International Journal of Hydrogen Energy*, *26*, 13–28.

Dong, Z.-S., Zhao, Y., Fan, L., Wang, Y.-X., Wang, J.-W., & Zhang, K. (2017). Simultaneous Sulfide Removal and Hydrogen Production in a Microbial Electrolysis Cell. *Int. J. Electrochem. Sci*, *12*, 10553–10566. https://doi.org/10.20964/2017.11.53

Dubbs, J. M., & Tabita, F. R. (2004). Regulators of nonsulfur purple phototrophic bacteria and the interactive control of CO_2 assimilation , nitrogen fixation, hydrogen metabolism and energy generation, *28*, 353–376. https://doi.org/10.1016/j.femsre.2004.01.002

Elameen, M. H. E., Karsiti, M. N., & Ibrahim, R. (2014). Nonlinear model feedback linearization control strategy of a pH neutralization process. *2014 5th International Conference on Intelligent and Advanced Systems: Technological Convergence for Sustainable Future, ICIAS 2014 - Proceedings*. https://doi.org/10.1109/ICIAS.2014.6869488

Eroglu, I., Aslan, K., Gündüz, U., Yücel, M., & Türker, L. (1999). Substrate consumption rates for hydrogen production by *Rhodobacter sphaeroides* in a

column photobioreactor. *Journal of Biotechnology*, *70*(1–3), 103–113. https://doi.org/10.1016/S0079-6352(99)80104-0

Fang, H. H. P., Li, C., & Zhang, T. (2006). Acidophilic biohydrogen production from rice slurry. *International Journal of Hydrogen Energy*, *31*(6), 683–692. https://doi.org/10.1016/j.ijhydene.2005.07.005

Fang, H. H. P., & Liu, H. (2002). Effect of pH on hydrogen production from glucose by a mixed culture. *Bioresource Technology*, *82*(1), 87–93. https://doi.org/10.1016/S0960-8524(01)00110-9

Fang, H. H. P., Liu, H., & Zhang, T. (2005). Phototrophic hydrogen production from acetate and butyrate in wastewater. *International Journal of Hydrogen Energy*, *30*, 785–793. https://doi.org/10.1016/j.ijhydene.2004.12.010

Fascetti, E., D'addario, E., Todini, O., & Robertiello, A. (1998). Photosynthetic hydrogen evolution with volatile organic acids derived from the fermentation of source selected municipal solid wastes. *International Journal of Hydrogen Energy*, *23*(9), 753–760. https://doi.org/10.1016/s0360-3199(97)00123-7

García-Depraect, O., Rene, E. R., Gómez-Romero, J., López-López, A., & León-Becerril, E. (2019). Enhanced biohydrogen production from the dark co-fermentation of tequila vinasse and nixtamalization wastewater: Novel insights into ecological regulation by pH. *Fuel*, *253*(May), 159–166. https://doi.org/10.1016/j.fuel.2019.04.147

Glasser, N. R., Kern, S. E., & Newman, D. K. (2014). Phenazine redox cycling enhances anaerobic survival in *Pseudomonas aeruginosa* by facilitating generation of ATP and a proton-motive force. *Molecular Microbiology*, *92*(2), 399–412. https://doi.org/10.1111/mmi.12566

Gordon, G. C., & McKinlay, J. B. (2014). Calvin cycle mutants of photoheterotrophic purple nonsulfur bacteria fail to grow due to an electron imbalance rather than toxic metabolite accumulation. *Journal of Bacteriology*, *196*(6), 1231–1237.

https://doi.org/10.1128/JB.01299-13

Guo, W.-Q., Ren, N.-Q., Wang, X.-J., Xiang, W.-S., Meng, Z.-H., Ding, J., … Zhang, L.-S. (2008). Biohydrogen production from ethanol-type fermentation of molasses in an expanded granular sludge bed (EGSB) reactor. *International Journal of Hydrogen Energy*, *33*(19), 4981–4988. https://doi.org/10.1016/j.ijhydene.2008.05.033

Gustafsson, T. K., & Waller, K. V. (1983). Dynamic modeling and reaction invariant control of pH. *Chemical Engineering Science*, *38*(3), 389–398. https://doi.org/10.1016/0009-2509(83)80157-2

Gustafsson, T. K., & Waller, K. V. (1992). Nonlinear and Adaptive Control of pH. *Industrial and Engineering Chemistry Research*, *31*(12), 2681–2693. https://doi.org/10.1021/ie00012a009

Guwy, A. J., Dinsdale, R. M., Kim, J. R., Massanet-Nicolau, J., & Premier, G. (2011). Fermentative biohydrogen production systems integration. *Bioresource Technology*, *102*(18), 8534–8542. https://doi.org/10.1016/j.biortech.2011.04.051

Hallenbeck, P. C., & Benemann, J. R. (2002). Biological hydrogen production; Fundamentals and limiting processes. *International Journal of Hydrogen Energy*, *27*(11–12), 1185–1193. https://doi.org/10.1016/S0360-3199(02)00131-3

Hay, J. X. W., Wu, T. Y., Juan, J. C., & Jahim, J. (2013). Biohydrogen production through photo fermentation or dark fermentation using waste as a substrate: Overview, economics, and future prospects of hydrogen usage. *Biofuels, Bioproducts and Biorefining*, *7*, 334–352. https://doi.org/10.1002/bbb

Hustade, E., Steinbüchel, A., & Schlegel, H. G. (1993). Relationship between the photoproduction of hydrogen and the accumulation of PHB in non-sulphur purple bacteria. *Applied Microbiology and Biotechnology*, *39*(87), 93.

Hwang, M. H., Jang, N. J., Hyun, S. H., & Kim, I. S. (2004). Anaerobic bio-hydrogen

production from ethanol fermentation: The role of pH. *Journal of Biotechnology*, *111*(3), 297–309. https://doi.org/10.1016/j.jbiotec.2004.04.024

Igeno, M. I., Del Moral, C. G., Castillo, F., & Caballero, F. J. (1995). Halotolerance of the phototrophic bacterium *Rhodobacter capsulatus* E1F1 is dependent on the nitrogen source. *Applied and Environmental Microbiology*, *61*(8), 2970–2975.

Imhoff, Trüper, & Pfennig. (2005). *Bergey's Manual® of Systematic Bacteriology*. (G. Garrity, D. J. Brenner, N. R. Krieg, & J. R. Staley, Eds.) (Second). Springer.

Jianzheng, L., Nanqi, R., Ming, L., & Yong, W. (2002). Hydrogen bio-production by anaerobic fermentation of organic wastewater in pilot-scale. *Acta Energiae Solaris Sin*, *23*(2), 252–256.

Johnson, M. A., Moradi, M. H., Crowe, J., Tan, K. K., Lee, T. H., Ferdous, R., … Greenwood, D. R. (2005). *PID control: New identification and design methods*. *PID Control: New Identification and Design Methods*. Springer London. https://doi.org/10.1007/1-84628-148-2

Jun, Y.-S., Yu, S.-H., Ryu, K., & Lee, T.-J. (2008). Kinetic Study of pH Effects on Biological Hydrogen Production by a Mixed Culture. *Journal of Microbiology and Biotechnology*, *18*(6), 1130–1135.

Kadier, A., Jiang, Y., Lai, B., Rai, P. K., Chandrasekhar, K., Mohamed, A., & Kalil, M. S. (2018). Biohydrogen production in microbial electrolysis cells from renewable resources. In *Bioenergy and Biofuels* (pp. 331–356). CRC Press. https://doi.org/10.1201/9781351228138-12

Kalamaras, C. M., & Efstathiou, A. M. (2013). Hydrogen Production Technologies: Current State and Future Developments. *Conference Papers in Energy*, *2013*, 1–9. https://doi.org/10.1155/2013/690627

Kars, G., & Alparslan, Ü. (2013). Valorization of sugar beet molasses for the production of biohydrogen and 5-aminolevulinic acid by *Rhodobacter sphaeroides* O.U.001 in a biorefinery concept. *International Journal of*

Hydrogen Energy, *38*(34), 14488–14494. https://doi.org/10.1016/j.ijhydene.2013.09.050

Kashiwagi, K., Miyamoto, S., Suzuki, F., Kobayashi, H., Igarashi, K., & Maas, W. K. (1992). *Excretion of putrescine by the putrescine ornithine antiporter encoded by the potE gene of Eschelichia coli (polyamine transport/potE protein)*. *Biochemistry* (Vol. 89).

Kashket, E. (1985). The Proton Motive Force in Bacteria: A Critical Assessment of Methods. *Annual Review of Microbiology*, *39*(1), 219–242. https://doi.org/10.1146/annurev.micro.39.1.219

Kayahan, E. (2015). *Design and Analysis of Tubular Photobioreactors for Biohydrogen Production*. Middle East Technical University.

Kayahan, E., Eroglu, I., & Koku, H. (2016). Design of an outdoor stacked e tubular reactor for biological hydrogen production. *International Journal of Hydrogen Energy*, *41*(42), 19357–19366. https://doi.org/10.1016/j.ijhydene.2016.04.086

Kayahan, E., Eroglu, I., & Koku, H. (2017). A compact tubular photobioreactor for outdoor hydrogen production from molasses. *International Journal of Hydrogen Energy*, *42*(4), 2575–2582. https://doi.org/10.1016/j.ijhydene.2016.08.014

Keskin, T., & Hallenbeck, P. C. (2012). Hydrogen production from sugar industry wastes using single-stage photofermentation. *Bioresource Technology*, *112*, 131–136. https://doi.org/10.1016/j.biortech.2012.02.077

Khanal, S. K., Chen, W. H., Li, L., & Sung, S. (2004). Biological hydrogen production: Effects of pH and intermediate products. *International Journal of Hydrogen Energy*, *29*(11), 1123–1131. https://doi.org/10.1016/j.ijhydene.2003.11.002

Khatipov, E., Miyake, M., Miyake, J., & Asada, Y. (1998). Accumulation of poly-B-hydroxybutyrate by Rhodobacter sphaeroides on various carbon and nitrogen substrates. *FEMS Microbiology Letters*, *162*, 39–45.

Kim, D., Kim, S., & Shin, H. (2009). Sodium inhibition of fermentative hydrogen production. *International Journal of Hydrogen Energy*, *34*(8), 3295–3304. https://doi.org/10.1016/j.ijhydene.2009.02.051

Kim, I. S., Hwang, M. H., Jang, N. J., Hyun, S. H., & Lee, S. T. (2004). Effect of low pH on the activity of hydrogen utilizing methanogen in bio-hydrogen process. *International Journal of Hydrogen Energy*, *29*(11), 1133–1140. https://doi.org/10.1016/j.ijhydene.2003.08.017

Kim, M. S., Kim, D. H., Son, H. N., Ten, L. N., & Lee, J. K. (2011). Enhancing photo-fermentative hydrogen production by Rhodobacter sphaeroides KD131 and its PHB synthase deleted-mutant from acetate and butyrate. *International Journal of Hydrogen Energy*, *36*(21), 13964–13971. https://doi.org/10.1016/j.ijhydene.2011.03.099

Koku, H. (2001). *Hydrogen Metabolism and Factors Affecting Hydrogen Production in Rhodobacter Sphaeroides*. Middle East Technical University.

Koku, H., Eroğlu, I., Gündüz, U., Yücel, M., & Türker, L. (2002). Aspects of the metabolism of hydrogen production by Rhodobacter sphaeroides. *International Journal of Hydrogen Energy*, *27*, 1315–1329. https://doi.org/10.1016/S0360-3199(02)00127-1

Koku, H., Eroğlu, I., Gündüz, U., Yücel, M., & Türker, L. (2003). Kinetics of biological hydrogen production by the photosynthetic bacterium *Rhodobacter sphaeroides* O.U. 001. *International Journal of Hydrogen Energy*, *28*(4), 381–388. https://doi.org/10.1016/S0360-3199(02)00080-0

Kothari, R., Buddhi, D., & Sawhney, R. L. (2008). Comparison of environmental and economic aspects of various hydrogen production methods. *Renewable and Sustainable Energy Reviews*, *12*(2), 553–563. https://doi.org/10.1016/j.rser.2006.07.012

Kumar, A. A., Chidambaram, M., Rao, V. S. R., & Pickhardt, R. (2004). Nonlinear PI

Controller for pH process. https://doi.org/10.1080/00986440490261872

Kumar, N., & Das, D. (2000). Enhancement of hydrogen production by Enterobacter cloacae IIT-BT 08. *Process Biochemistry*, *35*(6), 589–593. https://doi.org/10.1016/S0032-9592(99)00109-0

Lazaro, C. Z., Bosio, M., Ferreira, J. dos S., Varesche, M. B. A., & Silva, E. L. (2015). The Biological Hydrogen Production Potential of Agroindustrial Residues. *Waste and Biomass Valorization*, *6*(3), 273–280. https://doi.org/10.1007/s12649-015-9353-8

Li, J., Li, B., Zhu, G., Ren, N., Bo, L., & He, J. (2007). Hydrogen production from diluted molasses by anaerobic hydrogen producing bacteria in an anaerobic baffled reactor (ABR). *International Journal of Hydrogen Energy*, *32*, 3274–3283. https://doi.org/10.1016/j.ijhydene.2007.04.023

Li, Y., Zhu, J., Wu, X., Miller, C., & Wang, L. (2010). The effect of pH on continuous biohydrogen production from swine wastewater supplemented with glucose. *Applied Biochemistry and Biotechnology*, *162*(5), 1286–1296. https://doi.org/10.1007/s12010-010-8914-3

Liu, B. F., Ren, N. Q., Tang, J., Ding, J., Liu, W. Z., Xu, J. F., … Xie, G. J. (2010). Bio-hydrogen production by mixed culture of photo- and dark-fermentation bacteria. *International Journal of Hydrogen Energy*, *35*(7), 2858–2862. https://doi.org/10.1016/j.ijhydene.2009.05.005

Liu, T., Zhu, L., Wei, W., & Zhou, Z. (2014). Function of glucose catabolic pathways in hydrogen production from glucose in *Rhodobacter sphaeroides* 6016. *International Journal of Hydrogen Energy*, *39*(9), 4215–4221. https://doi.org/10.1016/j.ijhydene.2013.12.188

Lund, P., Tramonti, A., De Biase, D., Pasteur-Fondazione, I., & Bolognetti, C. (2014). Coping with low pH: molecular strategies in neutralophilic bacteria. https://doi.org/10.1111/1574-6976.12076

Mansouri, M., Nounou, H., & Nounou, M. (2018). State Estimation and Process Monitoring of Nonlinear Biological Phenomena Modeled by S-systems. In K.-C. Wong (Ed.), *Computational Biology and Bioinformatics: gene regulation.* (pp. 318–320). CRC Press.

Mcavoy, T. J. (1972). Hybrid simulation of a pH stirred tank control system. *Simulation*, *18*(3), 114–120. https://doi.org/10.1177/003754977201800305

Merugu, R., Girisham, S., & Reddy, S. M. (2010). Bioproduction of hydrogen by *Rhodobacter capsulatus* KU002 isolated from leather industry effluents. *International Journal of Hydrogen Energy*, *35*(18), 9591–9597. https://doi.org/10.1016/j.ijhydene.2010.06.057

Meyer, J., Kelley, B. C., & Vignais, P. M. (1978). Effect of light nitrogenase function and synthesis in *Rhodopseudomonas capsulata*. *Journal of Bacteriology*, *136*(1), 201–208. Retrieved from http://www.ncbi.nlm.nih.gov/pubmed/711666

Moon, C., Jang, S., Yun, Y. M., Lee, M. K., Kim, D. H., Kang, W. S., … Kim, M. S. (2015). Effect of the accuracy of pH control on hydrogen fermentation. *Bioresource Technology*, *179*, 595–601. https://doi.org/10.1016/j.biortech.2014.10.128

Mu, Y., Wang, G., & Yu, H. Q. (2006). Response surface methodological analysis on biohydrogen production by enriched anaerobic cultures. *Enzyme and Microbial Technology*, *38*(7), 905–913. https://doi.org/10.1016/j.enzmictec.2005.08.016

Nath, K., & Das, D. (2004, October). Improvement of fermentative hydrogen production: Various approaches. *Applied Microbiology and Biotechnology*. https://doi.org/10.1007/s00253-004-1644-0

Nikolaidis, P., & Poullikkas, A. (2017). A comparative overview of hydrogen production processes. *Renewable and Sustainable Energy Reviews*, *67*(January), 597–611. https://doi.org/10.1016/j.rser.2016.09.044

Özgür, E., Mars, A. E., Peksel, B., Louwerse, A., Yücel, M., Gündüz, U., … Eroğlu,

I. (2010). Biohydrogen production from beet molasses by sequential dark and photofermentation. *International Journal of Hydrogen Energy*, *35*(2), 511–517. https://doi.org/10.1016/j.ijhydene.2009.10.094

Özgür, E., Uyar, B., Öztürk, Y., Yücel, M., Gündüz, U., & Eroglu, İ. (2010). Biohydrogen production by *Rhodobacter capsulatus* on acetate at fluctuating temperatures. *Resources, Conservation and Recycling*, *54*, 310–314. https://doi.org/10.1016/j.resconrec.2009.06.002

Öztürk, Y. (2005). *Characterization of the Genetically Modified Cytochrome Systems and Their Application to Biohydrogen Production in Rhodobacter Capsulatus*. Middle East Technical University.

Ozturk, Y., Yucel, M., Daldal, F., Mandacı, S., Gunduz, U., Turker, L., & Eroglu, I. (2006). Hydrogen production by using *Rhodobacter capsulatus* mutants with genetically modified electron transfer chains. *International Journal of Hydrogen Energy*, *31*, 1545–1552. https://doi.org/10.1016/j.ijhydene.2006.06.042

Palamae, S., Choorit, W., Dechatiwongse, P., Zhang, D., Antonio, E., & Chisti, Y. (2018). Production of renewable biohydrogen by *Rhodobacter sphaeroides* S10 : A comparison of photobioreactors. *Journal of Cleaner Production*, *181*, 318–328. https://doi.org/10.1016/j.jclepro.2018.01.238

Peng, Y., Stevens, P., De Vos, P., & De Ley, J. (1987). Relation between pH, Hydrogenase and Nitrogenase Activity, NH_4^+ Concentration and Hydrogen Production in Cultures of *Rhodobacter Sulfidophilus*. *Journal of General Microbiology*, *133*(5), 1243–1247. https://doi.org/10.1099/00221287-133-5-1243

Pham, D. N., & Burgess, B. K. (1993). Nitrogenase Reactivity: Effects of pH on Substrate Reduction and CO Inhibition. *Biochemistry*, *32*(49), 13725–13731. https://doi.org/10.1021/bi00212a043

Pouresmaeil, S., Nosrati, M., & Ebrahimi, S. (2019). Operating control for enrichment

of hydrogen-producing bacteria from anaerobic sludge and kinetic analysis for vinasse inhibition. *Journal of Environmental Chemical Engineering*, *7*(3), 103090. https://doi.org/10.1016/j.jece.2019.103090

Rainbird, R. M., Atkins, C. A., & Pate, J. S. (1983). Effect of temperature on nitrogenase functioning in cowpea nodules. *Plant Physiology*, *73*(2), 392–394. https://doi.org/10.1104/pp.73.2.392

Ramachandran, R., & Menon, R. K. (1998). An overview of industrial uses of hydrogen. *International Journal of Hydrogen Energy*, *23*(7), 593–598.

Ren, N., Li, J., Li, B., Wang, Y., & Liu, S. (2006). Biohydrogen production from molasses by anaerobic fermentation with a pilot-scale bioreactor system. *International Journal of Hydrogen Energy*, *31*, 2147–2157. https://doi.org/10.1016/j.ijhydene.2006.02.011

Richard, H., & Foster, J. W. (2004). *Escherichia coli* glutamate- and arginine-dependent acid resistance systems increase internal pH and reverse transmembrane potential. *Journal of Bacteriology*, *186*(18), 6032–6041. https://doi.org/10.1128/JB.186.18.6032-6041.2004

Rosales-Colunga, L. M., Alvarado-Cuevas, Z. D., Razo-Flores, E., & De León Rodríguez, A. (2013). Maximizing hydrogen production and substrate consumption by *Escherichia coli* WDHL in cheese whey fermentation. *Applied Biochemistry and Biotechnology*, *171*(3), 704–715. https://doi.org/10.1007/s12010-013-0394-9

Sagir, E., Alipour, S., Elkahlout, K., Koku, H., Gunduz, U., Eroglu, I., & Yucel, M. (2018). Biological hydrogen production from sugar beet molasses by agar immobilized *R. capsulatus* in a panel photobioreactor. *International Journal of Hydrogen Energy*, *43*(32), 14987–14995. https://doi.org/10.1016/j.ijhydene.2018.06.052

Sagir, E., Ozgur, E., Gunduz, U., Eroglu, I., & Yucel, M. (2017). Single-stage

photofermentative biohydrogen production from sugar beet molasses by different purple non-sulfur bacteria. *Bioprocess and Biosystems Engineering*, *40*(11), 1589–1601. https://doi.org/10.1007/s00449-017-1815-x

Sağır, E. (2012). *Photobiological Hydrogen Production From Sugar Beet Molasses*. Middle East Technical University. https://doi.org/10.1016/j.nbt.2012.08.109

Saric, L., Filipcev, B., Simurina, O., Plavsic, D. V, Saric, B., Lazarevic, J. M., & Milovanovic, I. (2016). Sugar Beet Molasses : Properties and Applications in Osmotic Dehydration of Fruits and Vegetables. *Food and Feed Research*, *43*(2), 135–144. https://doi.org/10.5937/FFR1602

Sasikala, K., Ramana, C. V., & Raghuveer Rao, P. (1991). Environmental regulation for optimal biomass yield and photoproduction of hydrogen by *Rhodobacter sphaeroides* O.U. 001. *International Journal of Hydrogen Energy*, *16*(9), 597–601. https://doi.org/10.1016/0360-3199(91)90082-T

Sasikala, K., Ramana, C. V., Rao, P. R., & Kovacs, K. L. (1993). Anoxygenic Phototrophic Bacteria: Physiology and Advances in Hydrogen Production Technology. *Advances in Applied Microbiology*, *38*(C), 211–295. https://doi.org/10.1016/S0065-2164(08)70217-X

Savasturk, D., Kayahan, E., & Koku, H. (2018). Photofermentative hydrogen production from molasses: Scale-up and outdoor operation at low carbon-to-nitrogen ratio. *International Journal of Hydrogen Energy*, *43*(26), 11676–11687. https://doi.org/10.1016/j.ijhydene.2018.01.014

Seborg, D. E., Mellichamp, D. A., Edgar, T. F., & Doyle, F. J. (2011). *Process dynamics and control* (3rd ed.). John Wiley & Sons.

Sevinc, P., Gündüz, U., Eroğlu, I., & Yücel, M. (2012). Kinetic analysis of photosynthetic growth , hydrogen production and dual substrate utilization by *Rhodobacter capsulatus*. *International Journal of Hydrogen Energy*, *37*, 16430–16436. https://doi.org/10.1016/j.ijhydene.2012.02.176

Shi, X. Y., & Yu, H. Q. (2005). Optimization of glutamate concentration and pH for H_2 production from volatile fatty acids by *Rhodopseudomonas capsulata*. *Letters in Applied Microbiology*, *40*(6), 401–406. https://doi.org/10.1111/j.1472-765X.2005.01700.x

Sinha, P., & Pandey, A. (2011). An evaluative report and challenges for fermentative biohydrogen production. *International Journal of Hydrogen Energy*, *36*(13), 7460–7478. https://doi.org/10.1016/j.ijhydene.2011.03.077

Slonczewski, J. L., Fujisawa, M., Dopson, M., & Krulwich, T. A. (2009). Cytoplasmic pH Measurement and Homeostasis in Bacteria and Archaea. *Advances in Microbial Physiology*, *55*. https://doi.org/10.1016/S0065-2911(09)05501-5

Staffell, I., Scamman, D., Velazquez Abad, A., Balcombe, P., Dodds, P. E., Ekins, P., … Ward, K. R. (2019, February 1). The role of hydrogen and fuel cells in the global energy system. *Energy and Environmental Science*. Royal Society of Chemistry. https://doi.org/10.1039/c8ee01157e

Stavropoulos, K. P., Kopsahelis, A., Zafiri, C., & Kornaros, M. (2016). Effect of pH on Continuous Biohydrogen Production from End-of-Life Dairy Products (EoL-DPs) via Dark Fermentation. *Waste and Biomass Valorization*, *7*(4), 753–764. https://doi.org/10.1007/s12649-016-9548-7

Stepan Sarkissian, G., & Fowler, M. W. (1986). The Metabolism and Utilization of Carbohydrates by Suspension Cultures of Plant Cells. In *Carbohydrate Metabolism in Cultured Cells* (pp. 151–181). Springer US. https://doi.org/10.1007/978-1-4684-7679-8_5

Sung, S. W., & Lee, I. B. (1995). pH Control Using a Simple Set Point Change. *Industrial and Engineering Chemistry Research*, *34*(5), 1730–1734. https://doi.org/10.1021/ie00044a024

Sung, S. W., Lee, I. B., Choi, J. Y., & Lee, J. (1998). Adaptive control for pH systems. *Chemical Engineering Science*, *53*(10), 1941–1953.

https://doi.org/10.1016/S0009-2509(98)00050-5

Susin, M. F., Baldini, R. L., Gueiros-Filho, F., & Gomes, S. L. (2006). GroES/GroEL and DnaK/DnaJ Have Distinct Roles in Stress Responses and During Cell Cycle Progression in *Caulobacter crescentus*. *Journal of Bacteriology*, *188*(23), 8044–8053. https://doi.org/10.1128/JB.00824-06

Tabanoğlu, A. (2002). *Hydrogen production by rhodobacter sphaeroides O.U.001 in a solar bioreactor*. Middle East Technical University.

Tosun, I. (2012). *The Thermodynamics of Phase and Reaction Equilibria*. *The Thermodynamics of Phase and Reaction Equilibria*. Elsevier B.V. https://doi.org/10.1016/C2011-0-09077-4

Türker, L., Gümüs, S., & Tapan, A. (2008). Biohydrogen production: Molecular aspects. *Journal of Scientific and Industrial Research*, *67*(11), 994–1016.

Urbaniec, K., & Grabarczyk, R. (2014). Hydrogen production from sugar beet molasses - A techno-economic study. *Journal of Cleaner Production*, *65*, 324–329. https://doi.org/10.1016/j.jclepro.2013.08.027

Uyar, B. (2008). *Hydrogen production by microorganisms in solar bioreactor*. Middle East Technical University.

Uyar, B., Eroglu, I., Yücel, M., & Gunduz, U. (2009). Photofermentative hydrogen production from volatile fatty acids present in dark fermentation effluents. *International Journal of Hydrogen Energy*, *34*, 4517–4523. https://doi.org/10.1016/j.ijhydene.2008.07.057

Uyar, B., Eroglu, I., Yücel, M., & Gündüz, U. (2009). Photofermentative hydrogen production from volatile fatty acids present in dark fermentation effluents. *International Journal of Hydrogen Energy*, *34*(10), 4517–4523. https://doi.org/10.1016/j.ijhydene.2008.07.057

Uyar, B., Eroglu, I., Yücel, M., Gündüz, U., & Türker, L. (2007). Effect of light

intensity, wavelength and illumination protocol on hydrogen production in photobioreactors. *International Journal of Hydrogen Energy*, *32*(18), 4670–4677. https://doi.org/10.1016/j.ijhydene.2007.07.002

Uygur, A., & Kargı, F. (2004). Salt inhibition on biological nutrient removal from saline wastewater in a sequencing batch reactor, *34*, 313–318. https://doi.org/10.1016/j.enzmictec.2003.11.010

Voet, D., Voet, J. G., & Pratt, C. W. (2001). *Fundamentals of Biochemistry (Upgrade Edition)*. Wiley.

Vural, I. H., Altinten, A., Hapoglu, H., Erdogan, S., & Alpbaz, M. (2015). Application of pH control to a tubular flow reactor. *Chinese Journal of Chemical Engineering*, *23*(1), 154–161. https://doi.org/10.1016/j.cjche.2014.10.002

Wakayama, T., Nakada, E., Asada, Y., & Miyake, J. (2000). Effect of light/dark cycle on bacterial hydrogen production by *Rhodobacter sphaeroides* RV. From hour to second range. *Applied Biochemistry and Biotechnology*, *84–86*, 431–440.

Wang, X., & Jin, B. (2009). Process optimization of biological hydrogen production from molasses by a newly isolated Clostridium butyricum W5. *Journal of Bioscience and Bioengineering*, *107*(2), 138–144. https://doi.org/10.1016/j.jbiosc.2008.10.012

Wietschel, M., & Ball, M. (2009). The hydrogen economy: Opportunities and challenges. In *The Hydrogen Economy: Opportunities and Challenges* (Vol. 9780521882, pp. 38–40). https://doi.org/10.1017/CBO9780511635359

World Nuclear Association. (2016). *Heat values of various fuels*. *Information Library / Facts and Figures*. Retrieved from http://www.world-nuclear.org/information-library/facts-and-figures/heat-values-of-various-fuels.aspx

Wright, R. A., & Kravaris, C. (1989). Nonlinear pH Control in a CSTR. In *1989 American Control Conference* (pp. 1540–1544). IEEE. https://doi.org/10.23919/ACC.1989.4790431

Wu, S. C., Liou, S. Z., & Lee, C. M. (2012). Correlation between bio-hydrogen production and polyhydroxybutyrate (PHB) synthesis by *Rhodopseudomonas palustris* WP3-5. *Bioresource Technology*, *113*, 44–50. https://doi.org/10.1016/j.biortech.2012.01.090

Xie, G. J., Feng, L. B., Ren, N. Q., Ding, J., Liu, C., Xing, D. F., … Ren, H. Y. (2010). Control strategies for hydrogen production through co-culture of Ethanoligenens harbinense B49 and immobilized *Rhodopseudomonas faecalis* RLD-53. *International Journal of Hydrogen Energy*, *35*, 1929–1935. https://doi.org/10.1016/j.ijhydene.2009.12.138

Xu, X., Jiao, L., Feng, X., Ran, J., Liang, X., & Zhao, R. (2017). Heterogeneous expression of DnaK gene from *Alicyclobacillus acidoterrestris* improves the resistance of *Escherichia coli* against heat and acid stress. *AMB Express*, *7*(1). https://doi.org/10.1186/s13568-017-0337-x

Yakunin, A. F., & Hallenbeck, P. C. (2002). AmtB is necessary for NH_4^+ -induced nitrogenase switch-off and ADP-ribosylation in *Rhodobacter capsulatus*. *Journal of Bacteriology*, *184*(15), 4081–4088. https://doi.org/10.1128/JB.184.15.4081-4088.2002

Yigit, D. Ö., Gündüz, U., Türker, L., Yücel, M., & Eroglu, I. (1999). Identification of by-products in hydrogen producing bacteria; *Rhodobacter sphaeroides* O.U. 001 grown in the waste water of a sugar refinery. *Progress in Industrial Microbiology*, *35*, 125–131. https://doi.org/10.1016/S0079-6352(99)80106-4

Zagrodnik, R., & Laniecki, M. (2015). The role of pH control on biohydrogen production by single stage hybrid dark- and photo-fermentation. *Bioresource Technology*, *194*, 187–195. https://doi.org/10.1016/j.biortech.2015.07.028

Zagrodnik, R., & Łaniecki, M. (2017). Hydrogen production from starch by co-culture of Clostridium acetobutylicum and *Rhodobacter sphaeroides* in one step hybrid dark- and photofermentation in repeated fed-batch reactor. *Bioresource*

Technology, *224*, 298–306. https://doi.org/10.1016/j.biortech.2016.10.060

Zhao, Q. B., & Yu, H. Q. (2008). Fermentative H_2 production in an upflow anaerobic sludge blanket reactor at various pH values. *Bioresource Technology*, *99*(5), 1353–1358. https://doi.org/10.1016/j.biortech.2007.02.005

APPENDICES

A. Pyruvate Metabolism of *R. capsulatus*

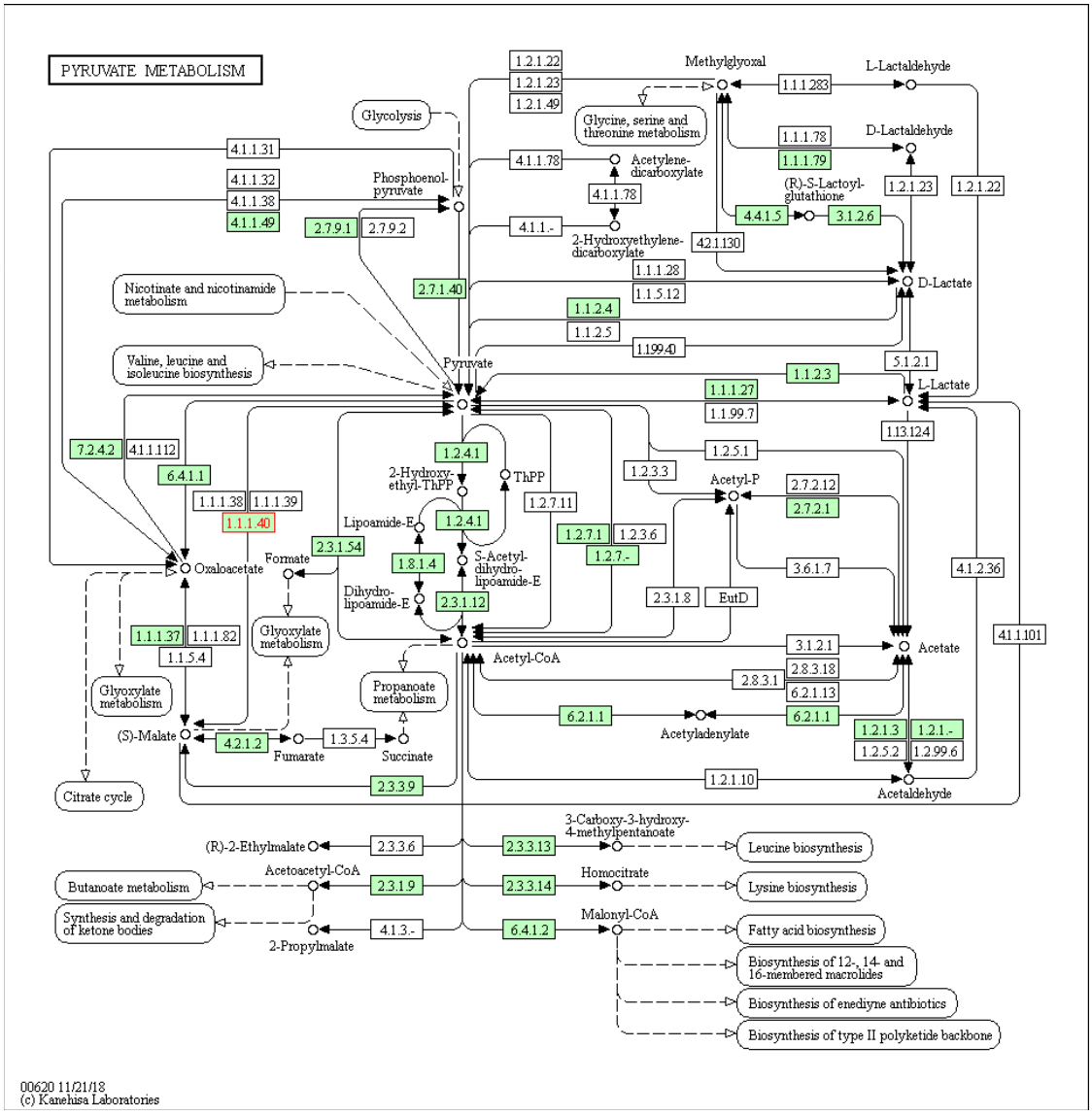

Figure 0.1. Pathway map of pyruvate metabolism in *R. capsulatus* (Kanehisa, 2018)

B. Butanoate Metabolism of *R. capsulatus*

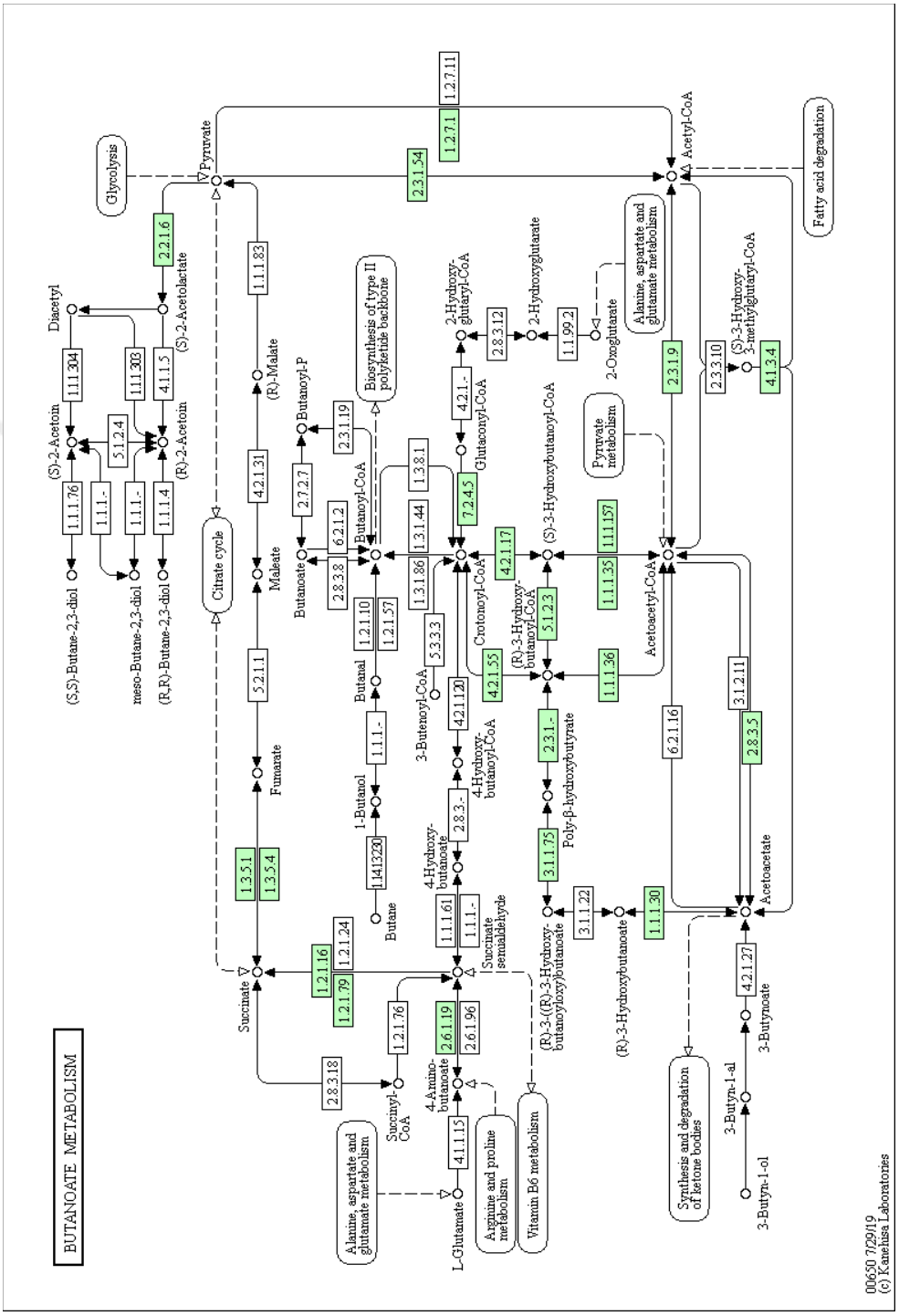

Figure 0.2. Pathway map of pyruvate metabolism in *R. capsulatus* (Kanehisa, 2019)

C. Glyoxylate Metabolism of *R. capsulatus*

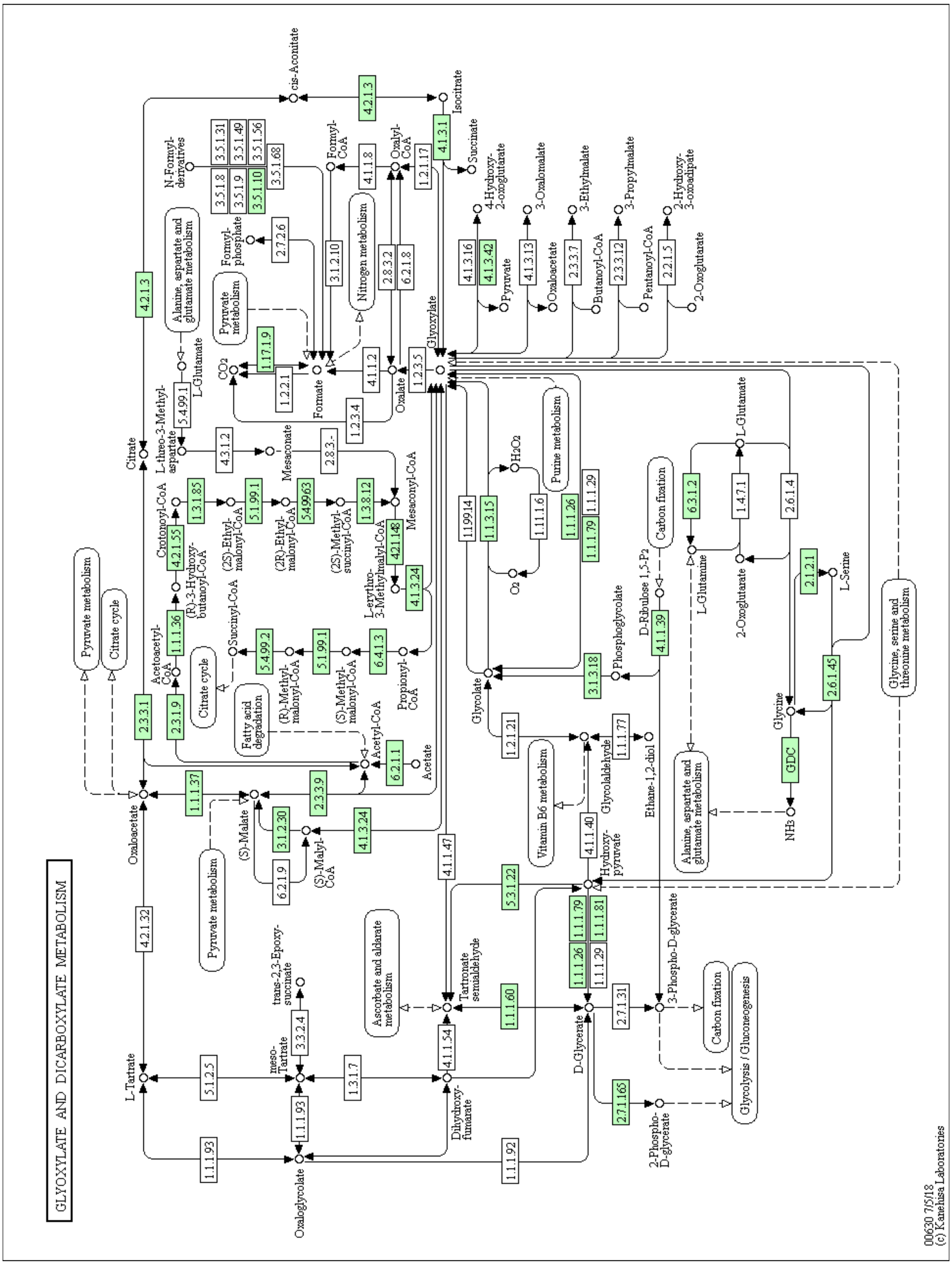

Figure 0.3. Pathway map of glyoxylate metabolism in *R. capsulatus* (Kanehisa, 2018)

D. Propanoate Metabolism of *R. capsulatus*

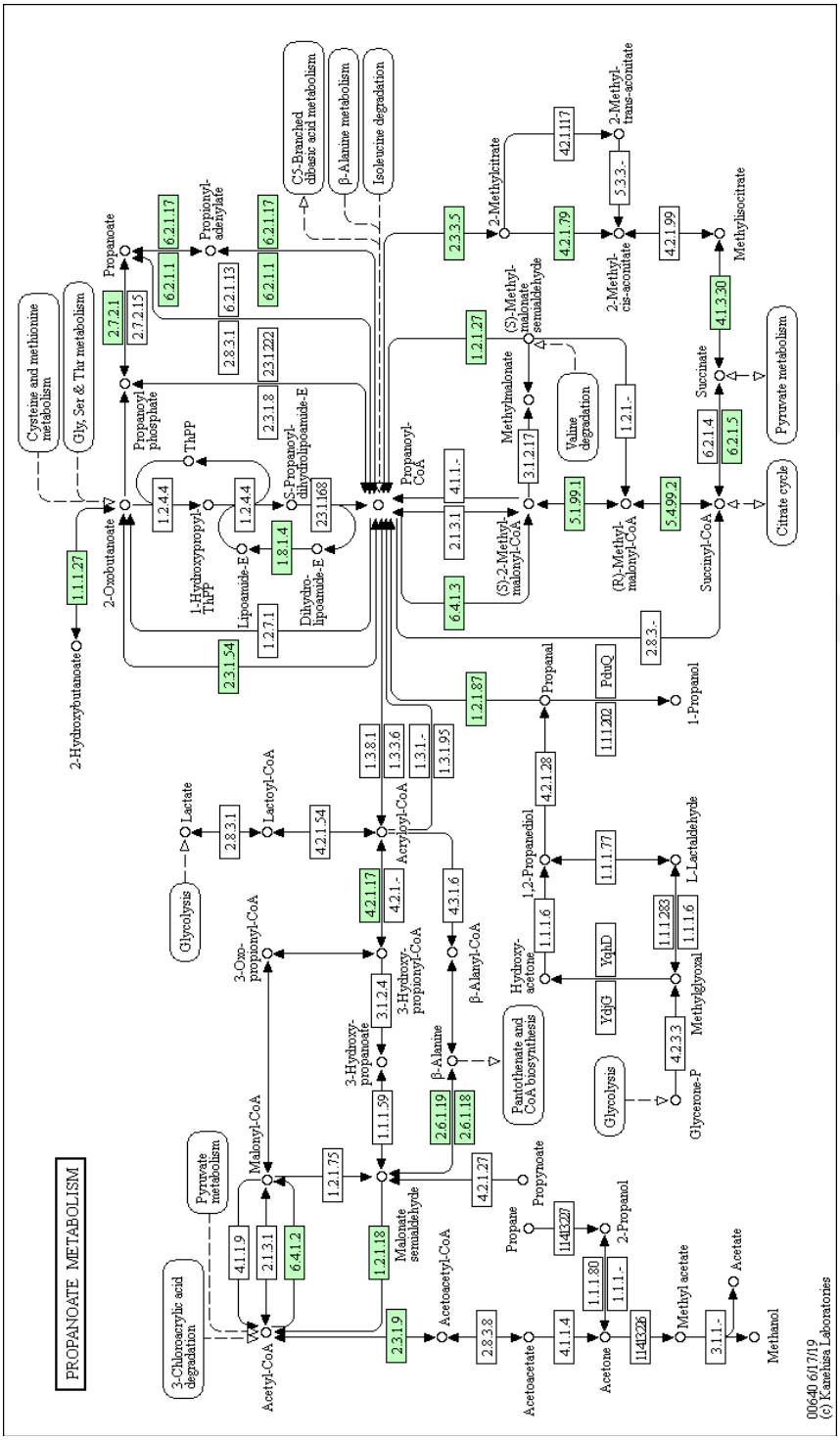

Figure 0.4. Pathway map of propanoate metabolism in *R. capsulatus* (Kanehisa, 2019)

E. Composition of the Growth Media

Table 0.1. *Solid MPYE media*

Component	**Amount**
Bacto Peptone	3 g/l
Yeast extract	3 g/l
$MgCl_2$	0.32 g/l
$CaCl_2$	0.14 g/l
Agar - Agar	15 g/l

pH of the medium was adjusted to 7.0 by adding 0.5 M NaOH solution and aoutoclaved at 121 ºC 20 minutes.

Table 0.2. *Growth media*

Component	**Amount**
KH_2PO_4	3 g/l
$MgSO_4.7H_2O$	0.5 g/l
$CaCl_2.2H_2O$	0.05 g/l
Acetic acid	1.15 µl
Na - Glutamate	1.85 g/l
*Vitamin Solution (10X stock solution)	0.1 ml/l
*Trace Element Solution (10X stock solution)	0.1 ml/l
*Iron Citrate Solution (50X stock solution)	0.5 ml/l

pH of the medium was adjusted to 6.4 by adding to 5 M NaOH. *Vitamin, trace element and iron citrate solutions were added after autoclave.

Table 0.3. *Vitamin Solutions (10X)*

Component	**Amount**
Thiamin Chloride Hydrochloride	0.5 g
Niacin (Nicotinic Acid)	0.5 g
D+ Biotin	15 mg

The substances of vitamin solution were dissolved in 100 ml distilled water and filtered by 0.2 μm filter. Prepared solution was stored in glass tube coated with aluminum foil and kept at 4 ºC.

Table 0.4. *Trace Element Solution (10X)*

Component	**Amount**
HCl (25% v/v)	1 ml/l
$ZnCl_2$	70 mg/l
$MnCl_2.4H_2O$	100 mg/l
H_3BO_3	60 mg/l
$CoCl_2.6H_2O$	200 mg/l
$CuCl_2.2H_2O$	20 mg/l
$NiCl_2.6H_2O$	20 mg/l
$NaMoO_4.2H_2O$	40 mg/l

The components of trace element solutions were dissolved in 100 ml distilled water and autoclaved. Trace element solution was stored at 4 ºC and dark conditions.

Table 0.5. *Iron Citrate Solution (50X)*

Component	**Amount**
Fe – Citrate	5 g

Ferric citrate was dissolved in 100 ml distilled water and autoclaved. After filtration, it was stored at 4 ^{o}C and dark conditions.

Table 0.6. *First Adaptation Media*

Component	**Amount**
KH_2PO_4	3 g/l
$MgSO_4.7H_2O$	0.5 g/l
$CaCl_2.2H_2O$	0.05 g/l
Na - Glutamate	1.85 g/l
Acetic acid	1.15 µl
*Molasses	3.3 g/l
*Vitamin Solution (10X stock solution)	0.1 ml/l
*Trace Element Solution (10X stock solution)	0.1 ml/l
*Iron Citrate Solution (50X stock solution)	0.5 ml/l

The components of the first adaptation medium was dissolved in distilled water. pH of the medium was adjusted to 6.4 by adding 5 M NaOH. *Molasses, vitamin, trace element and iron citrate solutions were added after autoclave.

Table 0.7.*Second Adaptation Media*

Component	**Amount**
KH_2PO_4	3 g/l
$MgSO_4.7H_2O$	0.5 g/l
$CaCl_2.2H_2O$	0.05 g/l
Na - Glutamate	1.85 g/l
*Molasses	3.3 g/l
*Vitamin Solution (10X stock solution)	0.1 ml/l
*Trace Element Solution (10X stock solution)	0.1 ml/l
*Iron Citrate Solution (50X stock solution)	0.5 ml/l

The components of the second adaptation medium was dissolved in distilled water. pH of the medium was adjusted to 6.4 by adding 5 M NaOH. *Molasses, vitamin, trace element and iron citrate solutions were added after autoclave.

F. Molasses Analyses

Table 0.8. *Content of molasses produced in Ankara Sugar Factory in 2013. Molasses was analyzed by Ankara Sugar Factory.*

Parameter	**Method**	**Results**
Refractometric dry matter	ICUMSA Method GC 4-13	82.36
Polar sugar (%)	British Sugar Method (CCS Handbook, 213, 2956)	51.52
pH	ICUMSA method GS 1/2/3/4/7(8-23	62.55
Invert sugar [1] (%)	Berlin Institude Method (ICUMSA Sugar Analysis, 55, 1979)	8.62
Invert sugar [1] (g/100 Pol)		0.229
Sucrose (w/w %)	ICUMSA method GS 4/3-7) x 0.95	51.85
Total nitrogen (%)	British sugar method (CCS Handbook, 213, 2956)	1.7
Total nitrogen (g/100Bx)		2.06
Density (g/cm3)	Density without air	1.272
Na (mg/kg)	Inductively coupled plasma-optical emission spectrometry method	6810
K (mg/kg)		34100
Ca (mg/kg)		2750
Mg (mg/kg)		7
Fe (mg/kg)		15
Mn (mg/kg)		16
Zn (mg/kg)		9

[1] Invert sugar is the mixture of glucose and fructose.

Table 0.9. *Amino acids in molasses which were analzed by Düzen Norwest Laboratory in Ankara.*

Amino acids	**Units**	**Results**
Aspartic Acid	g/100g	0.358
Glutamic Acid	g/100g	2.541
Asparagine	g/100g	< 0.10 [2]
Serine	g/100g	0.229
Histidine	g/100g	< 0.25 [2]
Glycine	g/100g	0.192
Theronine	g/100g	0.066
Citrulline	g/100g	< 0.07 [2]
Arginine	g/100g	0.08
Alanine	g/100g	0.252
Tyrosine	g/100g	0.191
Cystine	g/100g	< 0.30 [2]
Valine	g/100g	0.139
Methionine	g/100g	< 0.12 [2]
Tryptophan	g/100g	< 0.28 [2]
Isoleucine	g/100g	0.202
Omithine	g/100g	< 0.29 [2]
Lysine	g/100g	0.172
Hydrocproline	g/100g	< 0.27 [2]
Sarcosine	g/100g	< 0.09 [2]
Phenylaline	g/100g	< 0.23 [2]
Prolin	g/100g	0.234
Total Aminoacid	g/100g	4.7

[2] Method detection limit

Table 0.10. *Elements which could be identified by Düzen Norwest Laboratory in Ankara, in molasses.*

Elements	**Units**	**Results**
Iron (Fe)	mg/kg	14.1
Molybdenum (Mo)	mg/kg	0.22
Sulphur (S)	g/kg	1.03
Potassium (K)	g/kg	35.6

G. Calibration Curve of the Dry Cell Weight

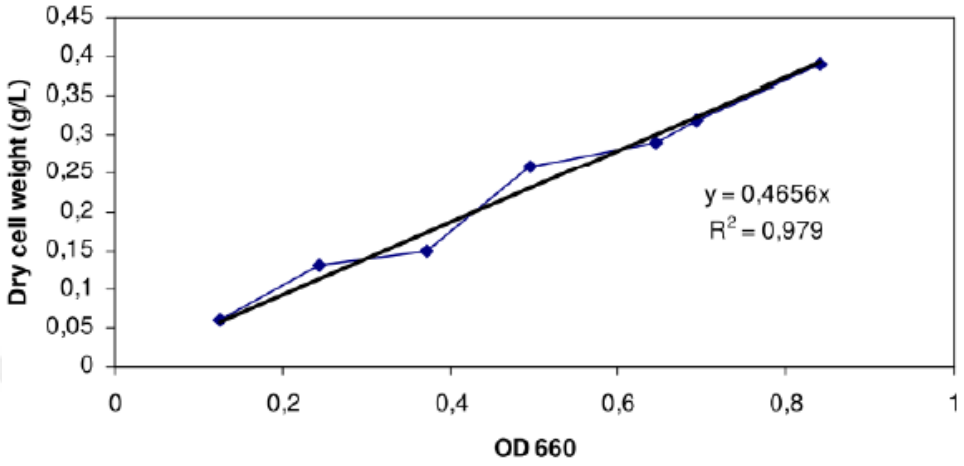

Figure 0.5. Calibration curve for the dry cell weight versus OD660 of the *Rhodobacter capsulatus* YO3 (hup-) (Öztürk, 2005). Optical density of 1.0 at 660 nm corresponds to 0.4656 gdcw/Lc.

H. Sample Gas Chromatogram for Gas Anaylsis

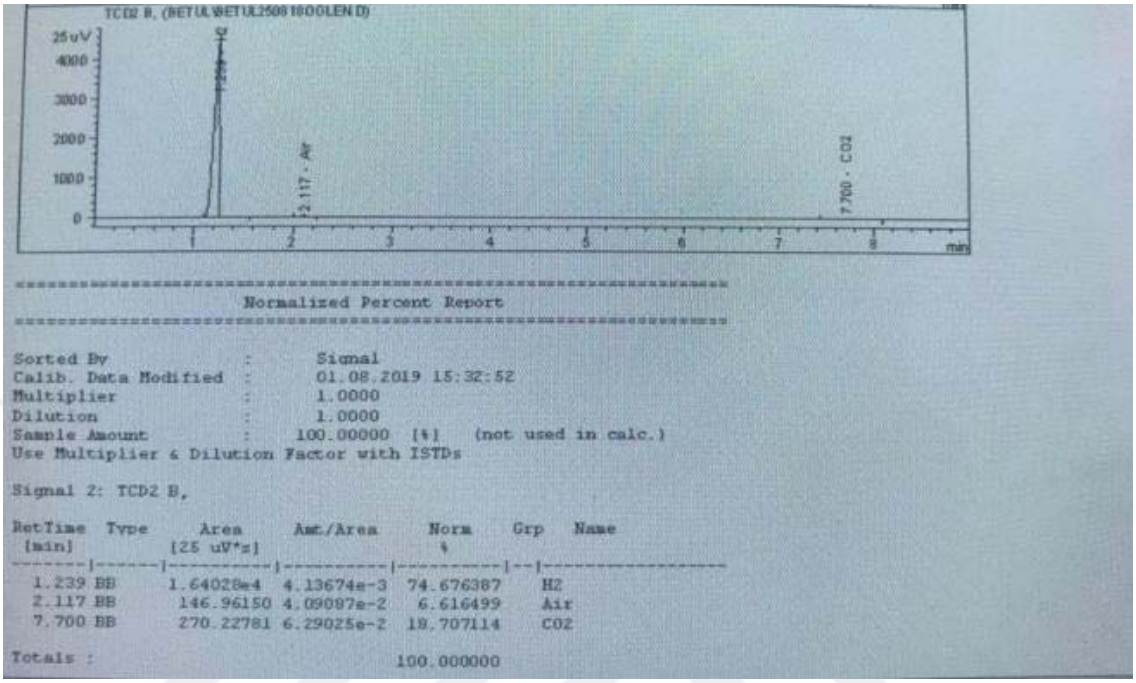

Normalized Percent Report

Sorted By : Signal
Calib. Data Modified : 01.08.2019 15:32:52
Multiplier : 1.0000
Dilution : 1.0000
Sample Amount : 100.00000 [%] (not used in calc.)
Use Multiplier & Dilution Factor with ISTDs

Signal 2: TCD2 B,

RetTime [min]	Type	Area [25 uV*s]	Amt./Area	Norm %	Grp	Name
1.239	BB	1.64028e4	4.13674e-3	74.676387		H2
2.117	BB	146.96150	4.09097e-2	6.616499		Air
7.700	BB	270.22781	6.29025e-2	18.707114		CO2
Totals :				100.000000		

Figure 0.6. Sample gas chromatogram

İ. HPLC Calibration Curves of Organic Acids

Retention Time Determination

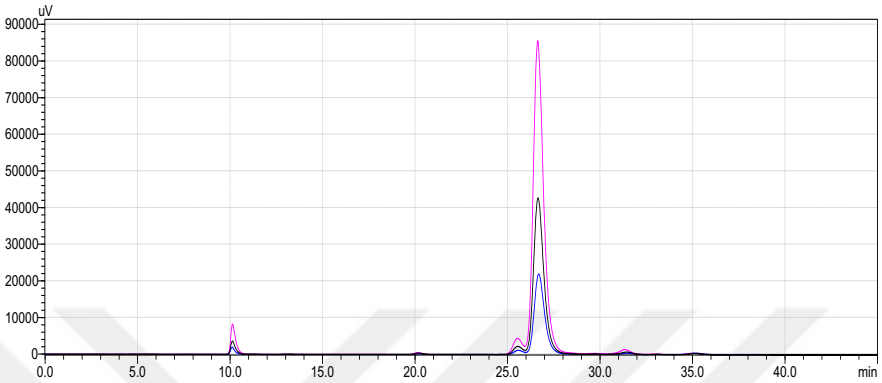

Figure 0.7. HPLC chromatogram of lactic acid. Concentrations of lactic acid are 5, 10 and 15 mM. Retention time of lactic acid is 26.5 minutes.

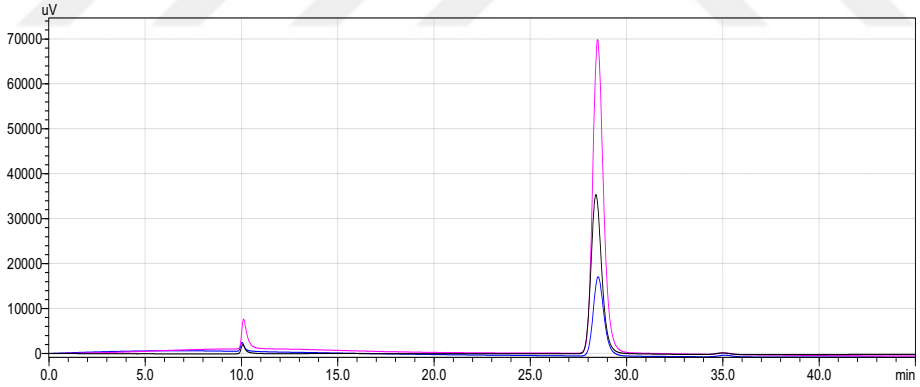

Figure 0.8. HPLC chromatogram of formic acid. Concentrations of formic acid are 5, 10 and 15 mM. Retention time of formic acid is 28.5 minutes.

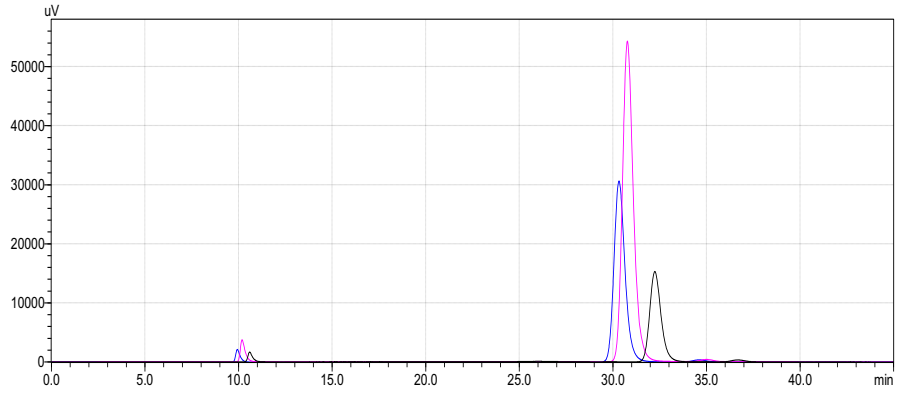

Figure 0.9. HPLC chromatogram of acetic acid. Concentrations of acetic acid are 5, 10 and 15 mM. Retention time of acetic acid is between 30.5 and 32.5 minutes

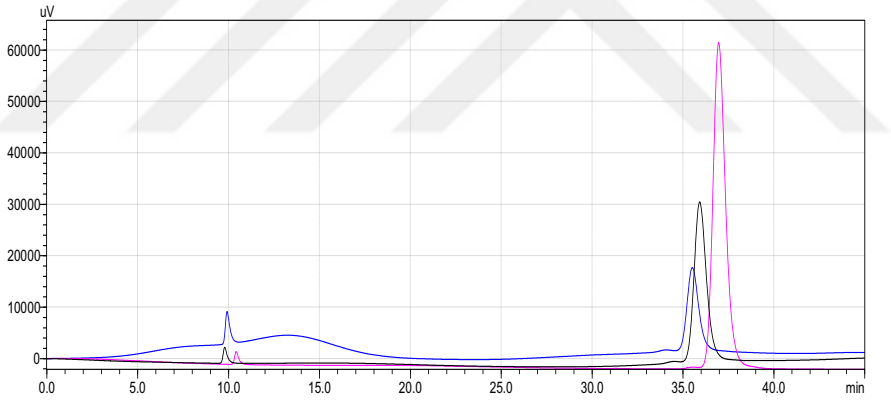

Figure 0.10. HPLC chromatogram of propionic acid. Concentrations of propionic acid are 5, 10 and 15 mM. Retention time of propionic acid is between 35.5 and 37 minutes.

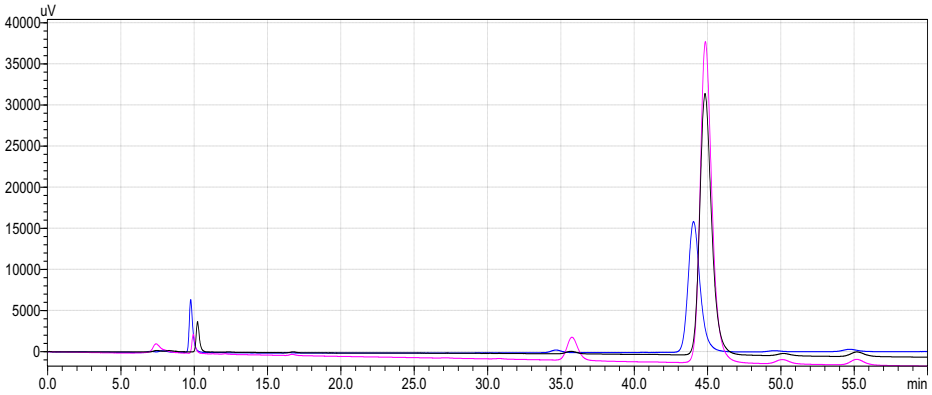

Figure 0.11. HPLC chromatogram of butyric acid. Concentrations of butyric acid are 5, 10 and 15 mM. Retention time of butyric acid is between 44 and 45 minutes.

Calibration Curves

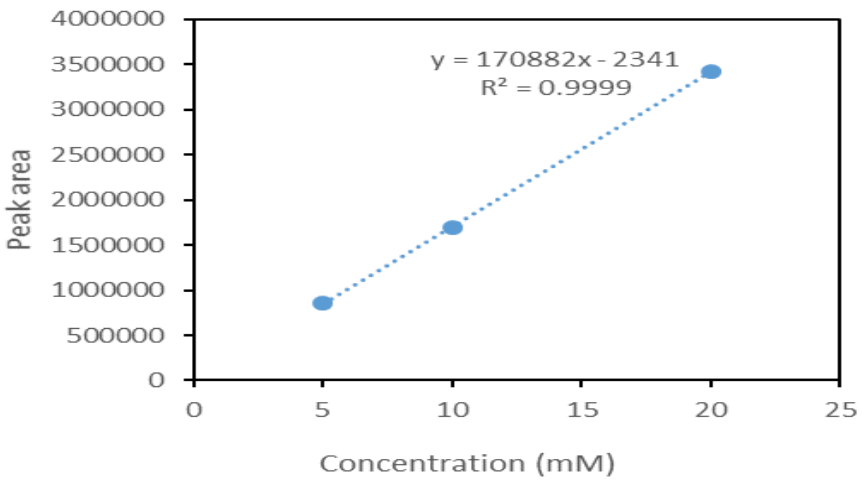

Figure 0.12. HPLC calibration for lactic acid.

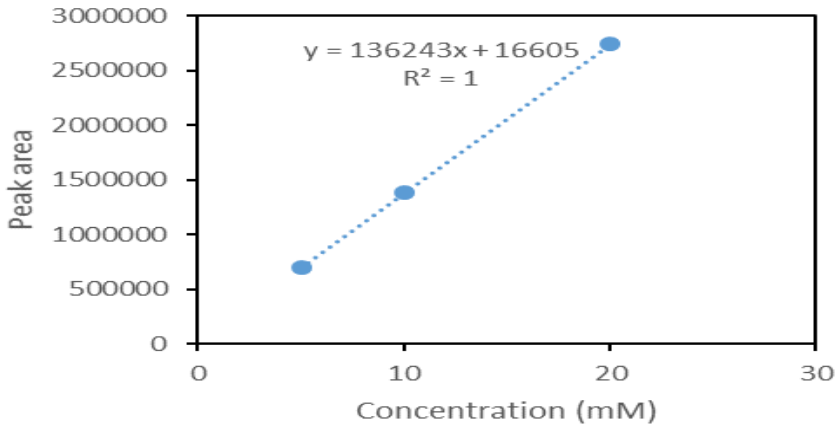

Figure 0.13. HPLC calibration for formic acid.

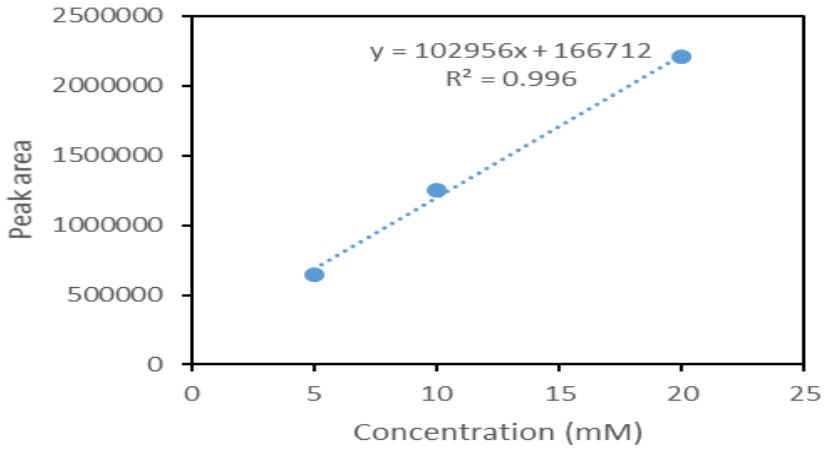

Figure 0.14. HPLC calibration for acetic acid.

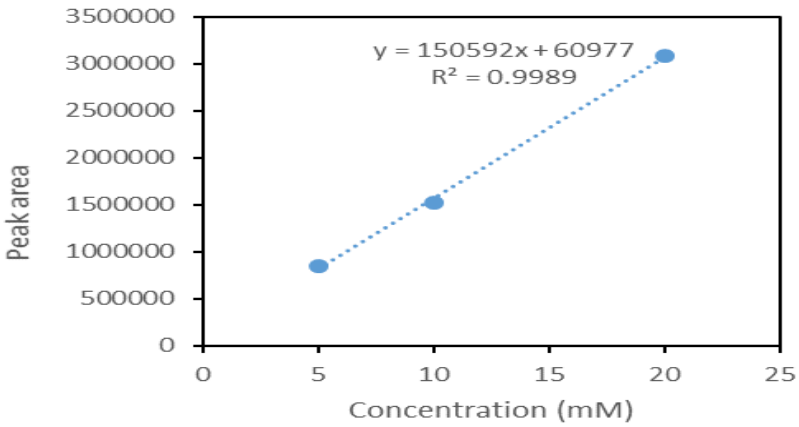

Figure 0.15. HPLC calibration for propionic acid.

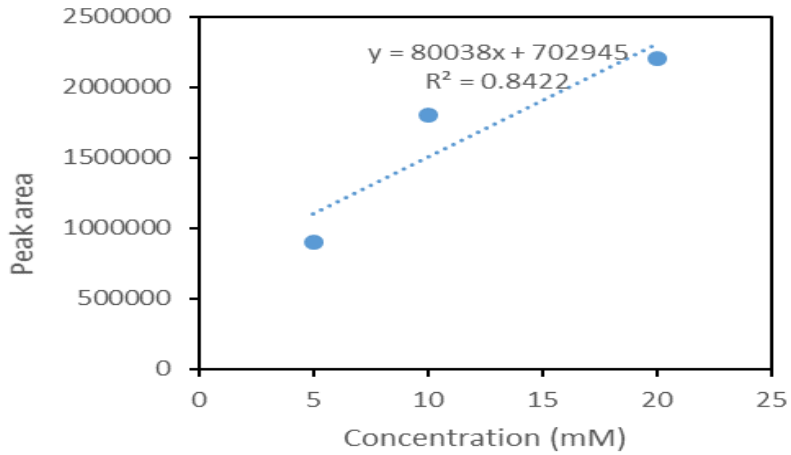

Figure 0.16. HPLC calibration for butyric acid.

J. Circulation Pump Calibration Curve

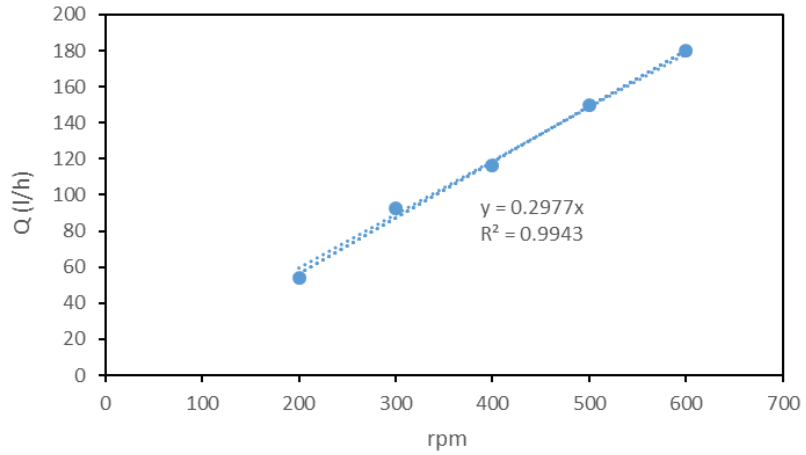

Figure 0.17. Volumetric flow rate of circulation peristaltic pump for revolutions per minute (rpm)

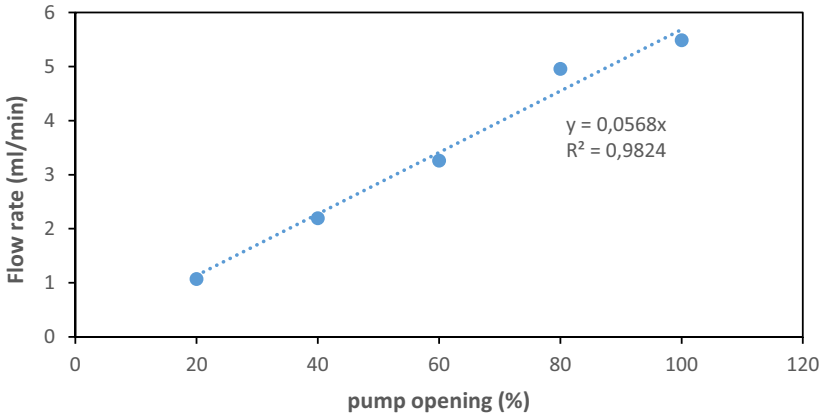

Figure 0.18. Volumetric flow rate of pH peristaltic pump for pump opening.

Sample Gas Chromatogram for Gas Anaylsis

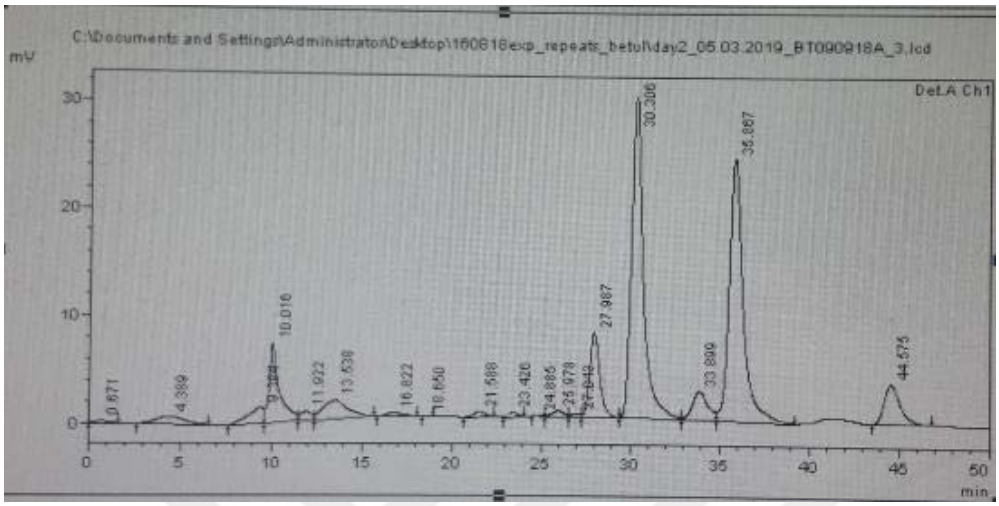

Figure 0.19. HPLC-UV detector result for August 9, 2018.

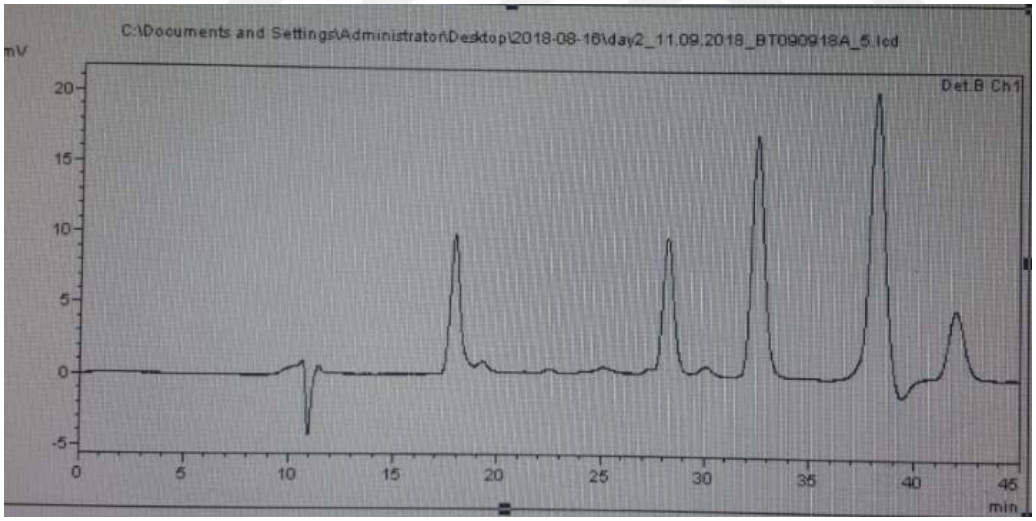

Figure 0.20. HPLC-RID detector result for August 9, 2018.

K. Outdoor Experimental Data

Table 0.11. *Daily variation in cell concentration of RUN160818. The experiment was started on August 16, 2018. OD1, OD2, OD3 and OD4 show tube numbers counted from bottom.*

Date	Hour	Day	OD1	OD2	OD3	OD4	ODavg.	Avg. Cell Conc. (gdcw/Lc)
16.08.18	16:30	1.0	0.220	0.215	0.218	0.218	0.218	0.101
17.08.18	08:30	2.0	0.205	0.205	0.194	0.179	0.196	0.091
	18:30	2.5	0.250	0.250	0.218	0.250	0.242	0.113
18.08.18	08:30	3.0	0.281	0.285	0.297	0.295	0.290	0.135
	18:45	3.5	0.356	0.350	0.663	0.375	0.436	0.203
19.08.18	08:45	4.0	0.416	0.419	0.406	0.402	0.411	0.191
	19:30	4.5	0.424	0.424	0.415	0.422	0.421	0.196
20.08.18	09:00	5.0	0.389	0.409	0.386	0.450	0.409	0.190
	18:30	5.5	0.596	0.603	0.776	1.162	0.784	0.365
21.08.18	09:30	6.0	0.633	0.620	0.664	0.695	0.653	0.304
	19:00	6.5	0.966	1.080	0.979	1.084	1.027	0.478
22.08.18	09:15	7.0	0.929	0.950	0.940	1.051	0.968	0.450
	19:00	7.5	1.230	1.238	1.320	1.264	1.263	0.588
23.08.18	08:15	8.0	1.141	1.191	1.202	1.188	1.181	0.550
	18:30	8.5	1.440	1.493	1.464	1.458	1.464	0.682
24.08.18	09:05	9.0	1.410	1.451	1.455	1.420	1.434	0.668
	19:15	9.5	1.692	1.644	1.693	1.755	1.696	0.790
25.08.18	09:10	10.0	1.629	1.631	1.608	1.609	1.619	0.754
	18:30	10.5	1.811	1.805	1.838	1.823	1.819	0.847
26.08.18	08:30	11.0	1.810	1.824	1.829	1.851	1.829	0.851
	18:25	11.5	1.953	1.949	1.976	1.942	1.955	0.910
27.08.18	09:10	12.0	2.074	1.898	1.927	1.937	1.959	0.912
	18:30	12.5	2.064	2.098	2.074	2.090	2.082	0.969

28.08.18	08:30	13.0	2.075	2.056	2.031	2.076	2.060	0.959
	18:30	13.5	2.237	2.129	2.134	2.106	2.152	1.002
29.08.18	08:30	14.0	2.093	2.120	2.115	2.174	2.126	0.990
	18:40	14.5	2.116	2.138	2.138	2.146	2.135	0.994
30.08.18	09:30	15.0	2.126	2.125	2.093	2.117	2.115	0.985
	18:30	15.5	2.119	2.107	1.918	2.198	2.086	0.971
31.08.18	12:00	16.0	2.223	2.320	2.107	2.342	2.248	1.047
01.09.18	12:00	17.0	2.540	2.583	2.551	2.560	2.559	1.191
02.09.18	08:50	18.0	1.756	1.720	1.730	2.060	1.817	0.846
	18:50	18.5	1.860	1.870	1.866	1.853	1.862	0.867
03.09.18	08:40	19.0	1.873	1.869	1.868	1.941	1.888	0.879
04.09.18	08:50	20.0	2.031	1.970	1.911	1.973	1.971	0.918
05.09.18	9:00	21.0	2.059	2.041	1.998	1.988	2.022	0.941
06.09.18	10:00	22.0	2.112	2.082	2.077	2.090	2.090	0.973
07.09.18	09:15	23.0	2.149	2.153	2.110	2.116	2.132	0.993
	17:25	23.5		2.182		2.188	2.185	1.017
08.09.18	09:00	24.0	2.267	2.240	2.210	2.252	2.242	1.044
	19:30	24.5	1.845	2.313	1.857	2.000	2.004	0.933
09.09.18	09:00	25.0	1.980	2.313	1.755	1.691	1.935	0.901
	18:00	25.5	1.781	2.254	1.811	1.869	1.929	0.898
10.09.18	09:00	26.0	1.937	2.151	1.817	1.883	1.947	0.907
	18:30	26.5	1.956	2.342	1.958	2.010	2.067	0.962
11.09.18	09:00	27.0	2.022	2.353	1.969	1.954	2.075	0.966
	18:00	27.5	2.091	2.341	1.997	2.049	2.120	0.987
12.09.18	09:00	28.0	2.125	2.401	2.039	2.066	2.158	1.005
	18:00	28.5	2.147	2.395	2.117	2.180	2.210	1.029
13.09.18	09:00	29.0	2.125	2.346	2.085	2.080	2.159	1.005
	18:00	29.5	2.113	2.277	2.119	2.115	2.156	1.004
14.09.18	09:00	30.0	2.172	2.382	2.147	2.173	2.219	1.033

	17:40	30.5	2.190	2.209	2.191	2.174	2.191	1.020
15.09.18	09:00	31.0	2.264	2.286	2.136	2.160	2.212	1.030
	18:25	31.5	2.204	2.207	2.150	2.173	2.184	1.017
16.09.18	09:18	32.0	2.198	2.226	2.170	2.178	2.193	1.021
	18:30	32.5	1.864	2.238	1.798	2.116	2.004	0.933
17.09.18	09:30	33.0	1.851	2.252	1.788	1.941	1.958	0.912
	18:30	33.5	1.888	2.221	1.780	1.765	1.914	0.891
18.09.18	09:00	34.0	1.855	2.355	1.776	1.751	1.934	0.901
	18:00	34.5	1.984	2.320	1.882	2.143	2.082	0.969
19.09.18	09:00	35.0	1.923	2.047	1.901	2.114	1.996	0.929
	18:00	35.5	1.982	1.958	1.943	2.111	1.999	0.931
20.09.18	10:00	36.0	2.101	1.976	1.975	2.079	2.033	0.946
	18:00	36.5	1.992	2.080	2.056	2.097	2.056	0.957
21.09.18	09:20	37.0	2.090	2.030	2.071	2.067	2.065	0.961
	18:30	37.5	2.122	2.121	2.128	2.124	2.124	0.989
22.09.18	09:30	38.0	2.182	2.204	2.145	2.126	2.164	1.008
	18:00	38.5	2.135	2.099	2.107	2.113	2.114	0.984
23.09.18	09:00	39.0	2.101	2.092	2.111	2.093	2.099	0.977
	18:00	39.5	1.369	1.242	1.258	1.677	1.387	0.646
24.09.18	10:00	40.0	1.563	1.444	1.528	1.818	1.588	0.739
	18:30	40.5	1.532	1.506	1.523	1.495	1.514	0.705
25.09.18	09:30	41.0	1.532	1.546	1.526	1.504	1.527	0.711
	18:30	41.5	1.760	1.953	1.763	1.773	1.812	0.844
26.09.18	09:30	42.0	1.772	2.078	1.709	1.730	1.822	0.848
27.09.18	15:30	43.0	1.591	1.827	1.652	1.623	1.673	0.779
28.09.18	09:30	44.0	1.844	1.887	1.867	1.791	1.847	0.860
	19:00	44.5	1.870	1.870	1.839	2.033	1.903	0.886
29.09.18	10:00	45.0	2.254	1.909	1.810	2.101	2.019	0.940
30.09.18	13:00	46.0	1.921	1.966	1.892	1.882	1.915	0.892

01.10.18	09:30	47.0	1.939	1.848	1.807	1.873	1.867	0.869
	18:00	47.5	1.808	1.785	2.001	1.843	1.859	0.866
02.10.18	10:00	48.0	1.909	2.049	1.865	2.061	1.971	0.918

Table 0.12. *Daily variation in pH of RUN160818. The experiment was started on August 16, 2018.*

Date	**Hour**	**Day**	**pH1**	**pH2**	**pH3**	**pH4**	**Reactor pH**
16.08.18	16:30	1.0	7.42	7.43	7.44	7.44	7.47
17.08.18	08:30	2.0	7.42	7.44	7.44	7.44	7.45
	18:30	2.5	7.39	7.41	7.43	7.42	7.42
18.08.18	08:30	3.0	7.13	7.13	7.13	7.13	7.15
	18:45	3.5	6.90	6.94	6.92	6.92	6.97
19.08.18	08:45	4.0	7.07	7.08	7.09	7.08	7.10
	19:30	4.5	7.20	7.20	7.12	7.10	7.12
20.08.18	09:00	5.0	7.30	7.32	7.28	7.20	7.30
	18:30	5.5	7.00	7.01	7.00	6.67	7.00
21.08.18	09:30	6.0	6.84	6.85	6.86	6.81	6.90
	19:00	6.5	6.66	6.66	6.67	6.48	6.75
22.08.18	09:15	7.0	6.85	6.84	6.88	6.60	6.90
	19:00	7.5	6.64	6.69	6.71	6.37	6.78
23.08.18	08:15	8.0	6.88	6.95	6.93	6.92	6.98
	18:30	8.5	6.82	6.65	6.84	6.83	6.92
24.08.18	09:05	9.0	6.93	6.93	6.94	6.92	6.98
	19:15	9.5	6.90	6.85	6.93	6.65	6.93
25.08.18	09:10	10.0	6.96	6.95	6.96	6.96	7.00
	18:30	10.5	6.93	6.92	6.92	6.80	6.98
26.08.18	08:30	11.0	6.91	6.84	6.96	6.87	6.95
	18:25	11.5	6.88	6.89	6.89	6.86	6.93

27.08.18	09:10	12.0	6.91	6.92	6.91	6.92	6.94
	18:30	12.5	6.91	6.93	6.87	6.90	6.92
28.08.18	08:30	13.0	6.95	6.93	6.94	6.93	6.98
	18:30	13.5	6.86	6.87	6.83	6.86	6.90
29.08.18	08:30	14.0	6.96	6.92	6.92	6.99	7.00
	18:40	14.5	6.85	6.84	6.85	6.81	6.89
30.08.18	09:30	15.0	6.96	7.00	6.99	6.99	7.00
	18:30	15.5	7.00	7.01	7.00	7.00	7.02
31.08.18	12:00	16.0	6.99	7.01	7.00	7.00	7.00
01.09.18	12:00	17.0	7.00	6.98	7.01	7.02	7.02
02.09.18	08:50	18.0					6.83
	18:50	18.5					6.86
03.09.18	08:40	19.0					6.98
04.09.18	08:50	20.0					6.90
05.09.18	9:00	21.0					6.95
06.09.18	10:00	22.0					6.90
07.09.18	09:15	23.0					7.01
	17:25	23.5					6.90
08.09.18	09:00	24.0					7.01
	19:30	24.5					6.83
09.09.18	09:00	25.0					7.15
	18:00	25.5					6.85
10.09.18	09:00	26.0					7.02
	18:30	26.5					6.90
11.09.18	09:00	27.0					6.92
	18:00	27.5					7.01
12.09.18	09:00	28.0	7.02	6.51	7.14	7.15	7.10
	18:00	28.5	6.70	5.92	6.73	6.65	6.78
13.09.18	09:00	29.0	7.52	5.55	7.70	7.70	7.20

	18:00	29.5	7.30	5.82	7.19	7.34	7.05
14.09.18	09:00	30.0	7.72	5.95	7.89	7.96	7.80
	17:40	30.5	6.85	6.03	7.00	6.79	6.90
15.09.18	09:00	31.0	6.99	6.96	7.02	7.00	7.00
	18:25	31.5	7.00	6.96	7.01	7.00	6.92
16.09.18	09:18	32.0	6.98	6.99	7.02	7.04	7.00
	18:30	32.5	6.89	6.90	6.90	6.84	6.90
17.09.18	09:30	33.0	6.91	6.95	7.00	7.00	7.00
	18:30	33.5	7.00	7.00	7.03	7.01	7.00
18.09.18	09:00	34.0	7.01	7.06	7.08	7.04	7.00
	18:00	34.5	6.97	7.00	7.10	7.03	7.00
19.09.18	09:00	35.0	7.23	7.03	7.25	6.87	7.10
	18:00	35.5	7.13	7.00	7.12	7.14	7.02
20.09.18	10:00	36.0	7.27	7.00	7.18	7.10	7.20
	18:00	36.5	6.81	6.88	6.90	6.82	6.85
21.09.18	09:20	37.0					7.80
	18:30	37.5	7.29	7.31	7.33	7.31	7.30
22.09.18	09:30	38.0	7.32	7.23	7.21	7.33	7.24
	18:00	38.5	6.94	6.45	6.88	6.60	6.80
23.09.18	09:00	39.0	6.96	7.11	7.11	7.03	7.00
	18:00	39.5	7.02	7.03	7.05	7.05	7.01
24.09.18	10:00	40.0	6.98	7.04	7.09	7.07	7.02
	18:30	40.5	6.96	7.06	7.03	7.00	7.01
25.09.18	09:30	41.0					7.90
	18:30	41.5	7.52	7.55	7.03		7.50
26.09.18	09:30	42.0	6.98	6.86	6.94	6.92	6.93
27.09.18	15:30	43.0	7.01	7.09	7.09	7.07	7.03
28.09.18	09:30	44.0	6.99	7.00	6.99	7.01	6.96
	19:00	44.5	6.94	6.50	6.95	6.91	6.90

29.09.18	10:00	45.0					7.00
30.09.18	13:00	46.0					8.00
01.10.18	09:30	47.0	6.83	6.92	6.86	6.92	6.90
	18:00	47.5	6.77	6.84	6.86	6.67	6.80
02.10.18	10:00	48.0					7.20

Table 0.13. *Daily variation in organic acids and sucrose concentrations of RUN160818. The experiment was started on August 16, 2018.*

Date	Day	Lactic acid (mM)	Formic acid (mM)	Acetic acid (mM)	Propionic acid (mM)	Butyric acid (mM)	Total acid (g/L)	Sucrose (mM)
16.08.18	1.0	0.01	0.00	0.00	0.00	0.00	0.00	5.00
17.08.18	2.0	0.01	3.58	0.00	1.15	0.00	0.45	3.78
	2.5	1.30	0.00	1.44	0.00	0.00	0.20	3.96
18.08.18	3.0	3.32	1.47	0.42	0.00	0.00	0.47	2.73
	3.5	9.50	4.81	2.25	0.00	0.00	1.48	3.01
19.08.18	4.0	12.98	7.11	3.31	0.00	0.00	2.08	2.54
	4.5	15.22	9.87	0.00	0.00	0.00	2.37	1.99
20.08.18	5.0	16.10	10.19	4.88	0.00	0.00	2.77	2.00
	5.5	20.93	12.42	5.15	0.28	0.00	3.47	2.07
21.08.18	6.0	22.29	13.53	6.47	0.00	0.00	3.76	1.73
	6.5	30.71	15.66	7.36	0.10	0.00	4.79	2.20
22.08.18	7.0	31.73	16.81	6.35	0.00	0.00	4.93	2.03
	7.5	38.87	18.90	7.68	0.00	0.00	5.87	2.13
23.08.18	8.0	34.67	17.61	8.26	0.23	0.00	5.41	1.74
	8.5	47.97	20.60	9.81	1.14	0.00	7.07	2.09
24.08.18	9.0	40.78	21.34	9.71	1.52	0.00	6.52	2.02
	9.5	48.68	24.73	10.63	2.32	0.00	7.69	1.83
25.08.18	10.0	43.39	25.22	12.70	2.76	0.00	7.42	1.78

	10.5	46.94	28.16	14.16	4.33	0.00	8.24	1.87
26.08.18	11.0	44.04	29.08	17.87	8.10	0.00	8.57	2.42
	11.5	30.52	31.59	21.92	14.37	0.00	8.31	1.86
27.08.18	12.0	8.64	30.45	28.70	25.21	0.00	7.44	1.75
	12.5	3.61	28.91	34.38	0.00	0.00	5.30	1.72
28.08.18	13.0	5.07	32.62	34.48	31.79	0.00	8.17	1.75
	13.5	6.14	29.78	41.44	0.00	0.00	6.04	1.70
29.08.18	14.0	3.80	29.20	44.81	0.00	0.00	5.98	1.60
	14.5	6.22	27.38	42.75	0.00	0.00	5.89	1.43
30.08.18	15.0	4.46	17.34	46.74	68.06	0.00	10.00	1.49
	15.5	2.18	9.77	21.68	18.96	0.00	3.89	1.47
31.08.18	16.0	3.42	10.90	53.29	54.25	1.04	8.72	1.38
01.09.18	17.0	0.86	7.00	56.94	46.99	0.00	7.68	1.39
	17.5	0.01	22.77	35.76	27.09	0.00	6.45	0.95
02.09.18	18.0	10.14	1.83	40.93	25.41	0.00	5.44	0.90
	18.5	10.66	0.37	44.77	25.04	0.00	5.54	0.82
03.09.18	19.0	3.01	0.00	44.49	26.80	0.00	4.93	0.85
	19.5	1.91	0.13	50.09	30.12	10.68	6.37	0.84
04.09.18	20.0	1.28	0.00	52.11	37.86	0.00	6.05	0.81
05.09.18	21.0	1.02	5.76	51.23	31.35	1.42	6.20	0.82
	21.5	3.92	5.55	49.61	35.85	0.00	6.55	0.76
06.09.18	22.0	1.94	4.76	55.44	48.62	1.41	7.71	0.80
	22.5	7.39	6.21	55.34	51.43	0.00	8.42	0.72
07.09.18	23.0	1.08	4.42	54.81	39.08	0.00	6.73	0.80
	23.5	4.49	6.79	58.32	51.89	0.00	8.43	0.72
08.09.18	24.0	0.28	0.42	5.08	7.14	0.00	0.90	0.72
	24.5	36.53	2.85	68.64	70.87	0.00	12.95	1.06
09.09.18	25.0	0.39	5.05	26.07	30.84	0.00	4.39	0.30
	25.5	65.80	8.05	75.03	123.38	27.38	22.80	0.16

10.09.18	26.0	17.40	3.20	66.36	47.58	0.00	9.40	0.48
	26.5	0.01	80.20	71.89	129.88	23.64	24.11	3.99
11.09.18	27.0	12.55	6.87	27.71	17.30	0.00	4.77	0.29
	27.5	2.79	86.22	76.85	43.60	0.00	16.79	0.13
12.09.18	28.0	56.50	4.84	63.93	41.70	3.56	12.82	0.62
	28.5	102.38	6.45	50.19	24.94	8.48	15.48	1.22
13.09.18	29.0	50.25	13.84	42.53	23.43	0.00	10.21	0.33
	29.5	0.98	11.87	38.43	41.00	0.00	6.63	0.30
14.09.18	30.0	2.26	11.67	38.28	24.22	0.00	5.47	0.33
	30.5	13.30	9.91	44.66	45.91	0.00	8.28	0.27
15.09.18	31.0	9.15	8.95	44.74	30.27	0.00	6.66	0.34
	31.5	3.51	8.77	42.88	29.28	0.00	5.94	0.29
16.09.18	32.0	3.61	8.46	44.31	28.77	0.00	5.97	0.19
	32.5	3.01	6.23	43.94	28.88	0.00	5.68	0.31
17.09.18	33.0	3.61	4.10	45.80	30.11	0.00	5.72	0.31
	33.5	1.98	3.72	41.12	27.97	18.30	6.71	0.24
18.09.18	34.0	0.01	0.00	38.53	24.08	0.00	4.10	0.28
	34.5	59.66	0.00	58.57	38.95	0.00	11.78	0.06
19.09.18	35.0	18.71	5.75	29.61	16.19	0.00	5.24	0.17
	35.5	11.93	5.44	26.69	14.97	0.00	4.33	0.11
20.09.18	36.0	10.91	5.05	28.04	15.38	0.00	4.32	0.11
	36.5	34.59	5.21	30.49	16.05	1.79	6.82	0.12
21.09.18	37.0	31.69	3.60	31.23	16.08	0.00	6.28	0.10
	37.5	29.26	3.58	34.42	15.85	0.00	6.24	0.09
22.09.18	38.0	25.75	2.97	36.20	18.14	0.00	6.14	0.10
	38.5	18.72	3.83	35.60	17.10	11.84	6.52	0.11
23.09.18	39.0	18.65	3.41	38.22	18.61	0.00	5.70	0.08
	39.5	8.90	6.84	15.29	6.03	0.00	2.86	1.38
24.09.18	40.0	26.47	3.85	21.00	7.41	3.88	4.92	0.07

	40.5	26.27	2.87	24.69	8.62	9.08	5.58	0.11
25.09.18	41.0	17.11	1.89	26.77	9.51	3.18	4.32	0.05
	41.5	66.78	1.12	39.97	13.41	27.41	11.94	0.11
26.09.18	42.0	91.12	1.41	39.37	13.31	7.84	12.39	0.03
27.09.18	43.0	49.78	1.40	41.06	17.00	5.78	8.86	0.58
28.09.18	44.0	37.70	1.88	43.00	15.55	0.00	7.32	4.84
	44.5	44.14	5.09	48.26	17.78	8.76	9.48	1.86
29.09.18	45.0	42.11	2.78	46.59	17.13	3.15	8.42	2.06
30.09.18	46.0	61.29	2.85	58.96	22.29	2.48	11.22	0.23
01.10.18	47.0	40.25	3.03	58.73	26.64	0.00	9.43	0.17
	47.5	44.35	2.61	61.54	26.59	0.00	9.92	0.29
02.10.18	48.0	29.52	1.59	75.40	33.60	0.00	9.84	0.26

Table 0.14. *Daily variation in ammonium and sodium ion concentrations of RUN160818. The experiment was started on August 16, 2018.*

Date	**Day**	**NH_4^+ (mg/l)**	**NH_4^+ (mM)**	**Na^+ (g/l)**	**Na^+ (mM)**
16.08.18	1	10.0	0.6	0.4	18.5
17.08.18	2	9.8	0.5	0.4	15.8
18.08.18	3	15.2	0.8	0.4	18.3
19.08.18	4	10.8	0.6	0.6	25.4
20.08.18	5	19.8	1.1	0.8	32.8
21.08.18	6	9.5	0.5	1.0	41.4
22.08.18	7	17.8	1.0	1.0	44.9
23.08.18	8	5.7	0.3	1.2	52.5
24.08.18	9	7.0	0.4	1.3	57.5
25.08.18	10	4.3	0.2	1.6	70.2

26.08.18	11	2.9	0.2	1.7	74.2
27.08.18	12	1.7	0.1	2.0	88.2
28.08.18	13	1.3	0.1	2.3	100.1
29.08.18	14	0.9	0.1	3.4	147.0
30.08.18	15	2.1	0.1	3.4	149.1
31.08.18	16	1.4	0.1	3.5	153.1
01.09.18	17	9.9	0.5	2.8	122.8
02.09.18	18	4.4	0.2	3.0	131.3
03.09.18	19	0.5	0.0	1.8	76.7
04.09.18	20	0.9	0.1	2.3	99.6
05.09.18	21	0.4	0.0	2.6	112.5
06.09.18	22	0.4	0.0	2.7	119.4
07.09.18	23	0.9	0.1	3.0	130.7
08.09.18	24	1.3	0.1	3.1	134.8
09.09.18	25	0.7	0.0	1.4	60.2
10.09.18	26	2.2	0.1	1.2	53.8
11.09.18	27	0.4	0.0	1.7	74.0
12.09.18	28	0.8	0.0	1.8	78.4
13.09.18	29	0.1	0.0	2.0	88.2
14.09.18	30	-0.2	0.0	2.1	93.2
15.09.18	31	-0.4	0.0	2.5	106.6
16.09.18	32	0.5	0.0	2.3	101.5
17.09.18	33	0.8	0.0	1.0	43.5
18.09.18	34	16.0	0.9	1.1	46.0
19.09.18	35	0.4	0.0	2.1	92.7
20.09.18	36	2.1	0.1	1.7	72.5
21.09.18	37	0.1	0.0	2.1	90.7
22.09.18	38	1.1	0.1	2.1	92.7
23.09.18	39	5.1	0.3	2.3	100.2

24.09.18	40	45.3	2.5	1.1	49.0
25.09.18	41	16.2	0.9	1.2	52.7
26.09.18	42	43.9	2.4	1.6	70.3
27.09.18	43	40.2	2.2	1.9	82.8
28.09.18	44	58.1	3.2	2.2	95.7
29.09.18	45	65.5	3.6	3.0	132.5
30.09.18	46	54.9	3.0	2.8	122.0
01.10.18	47	59.5	3.3	3.7	162.3
02.10.18	48	52.7	2.9	4.1	177.7

Table 0.15. *Daily biogas production and solar radiation of RUN160818. The experiment was started on August 16, 2018.*

Date	**Day**	**Biogas Content**		**Daily produced biogas (ml)**	**H_2 produced (mol)**	**H_2 productivity (mol $H_2/m^3.h$)**	**Daily solar radiation (W/m^2)**
		H_2 %	**CO_2 %**				
16.08.18	1	0.0	0.0	0	0.000	0.000	488.565
17.08.18	2	0.0	0.0	0	0.000	0.000	466.671
18.08.18	3	0.0	0.0	0	0.000	0.000	416.271
19.08.18	4	0.0	0.0	0	0.000	0.000	433.975
20.08.18	5	0.0	0.0	0	0.000	0.000	469.931
21.08.18	6	94.7	5.3	618	0.021	0.083	457.690
22.08.18	7	94.6	5.4	2973	0.102	0.401	463.069
23.08.18	8	89.2	10.8	2322	0.075	0.295	475.138
24.08.18	9	90.2	9.8	2790	0.091	0.359	456.621
25.08.18	10	88.5	11.5	2547	0.082	0.321	360.897
26.08.18	11	84.9	15.1	1984	0.061	0.240	398.207

27.08.18	12	87.0	13.0	287	0.009	0.036	427.517
28.08.18	13	85.1	14.9	249	0.008	0.030	436.414
29.08.18	14	93.2	6.8	147	0.005	0.019	429.207
30.08.18	15	90.5	9.5	84	0.003	0.011	395.552
31.08.18	16	0.0	0.0	0	0.000	0.000	432.483
01.09.18	17	97.2	2.8	244	0.009	0.034	434.586
02.09.18	18	91.4	8.6	24	0.001	0.003	437.897
03.09.18	19	100.0	0.0	6	0.000	0.001	430.966
04.09.18	20	100.0	0.0	0	0.000	0.000	429.241
05.09.18	21	100.0	0.0	0	0.000	0.000	351.207
06.09.18	22	100.0	0.0	75	0.003	0.011	270.862
07.09.18	23	84.6	15.4	19	0.001	0.002	348.069
08.09.18	24	0.0	0.0	0	0.000	0.000	407.448
09.09.18	25	92.2	7.8	5278	0.176	0.693	397.759
10.09.18	26	89.2	10.8	2604	0.084	0.331	388.379
11.09.18	27	91.9	8.1	4501	0.150	0.590	407.759
12.09.18	28	89.0	11.0	1098	0.035	0.139	395.207
13.09.18	29	77.8	22.2	675	0.019	0.075	310.586
14.09.18	30	87.0	13.0	81	0.003	0.010	377.724
15.09.18	31	0.0	0.0	0	0.000	0.000	226.862
16.09.18	32	0.0	0.0	0	0.000	0.000	329.069
17.09.18	33	87.5	12.5	1600	0.051	0.200	290.655
18.09.18	34	100	0.0	128	0.004	0.016	346.000
19.09.18	35	0.0	0.0	0	0.000	0.000	401.345
20.09.18	36	0.0	0.0	0	0.000	0.000	400.828
21.09.18	37	0.0	0.0	1281	0.046	0.183	300.276
22.09.18	38	100.0	0.0	1478	0.053	0.211	382.586
23.09.18	39	0.0	0.0	0	0.000	0.000	387.379
24.09.18	40	0.0	0.0	0	0.000	0.000	376.759

25.09.18	41	0.0	0.0	0	0.000	0.000	357.586
26.09.18	42	0.0	0.0	0	0.000	0.000	39.759
27.09.18	43	0.0	0.0	0	0.000	0.000	265.931
28.09.18	44	100.0	0.0	62	0.002	0.009	346.207
29.09.18	45	100.0	0.0	60	0.002	0.009	351.793
30.09.18	46	0.0	0.0	0	0.000	0.000	326.759
01.10.18	47	100.0	0.0	7	0.000	0.001	323.690
02.10.18	48	35.2	64.8	13	0.000	0.001	305.103

Table 0.16. *Weather station data of RUN160818 for August 20, September 2 and October 1, 2018 . The experiment was started on August 16, 2018.*

Date	**Time**	**Air temperature (°C)**	**Humidity**	**Dew point (°C)**	**Wind speed (m/s)**	**Heat Index**	**Pressure (bar)**	**Solar Radiation (W/m²)**
20.08.18	0	21.7	37.0	6.4	3.2	20.3	755.1	0.0
20.08.18	0:30	21.5	35.0	5.4	4.8	19.9	755.3	0.0
20.08.18	1:00	20.9	37.0	5.7	3.2	19.3	755.4	0.0
20.08.18	1:30	20.3	39.0	5.9	1.6	18.9	755.3	0.0
20.08.18	2:00	16.9	47.0	5.5	0.0	15.8	755.3	0.0
20.08.18	2:30	14.7	56.0	6.0	0.0	13.8	755.4	0.0
20.08.18	3:00	13.6	60.0	6.0	0.0	12.9	755.3	0.0
20.08.18	3:30	13.1	62.0	6.0	0.0	12.4	755.4	0.0
20.08.18	4:00	13.2	64.0	6.5	0.0	12.6	755.3	0.0
20.08.18	4:30	13.2	64.0	6.6	0.0	12.6	755.3	0.0
20.08.18	5:00	12.5	67.0	6.5	0.0	12.0	755.3	0.0
20.08.18	5:30	12.0	70.0	6.7	0.0	11.6	755.3	0.0
20.08.18	6:00	11.9	70.0	6.6	0.0	11.6	755.4	0.0

20.08.18	6:30	11.9	73.0	7.3	0.0	11.6	755.5	12.0
20.08.18	7:00	14.9	65.0	8.4	0.0	14.4	755.6	53.0
20.08.18	7:30	18.6	51.0	8.3	0.0	17.7	755.7	125.0
20.08.18	8:00	19.9	46.0	8.0	1.6	19.0	755.7	224.0
20.08.18	8:30	21.0	44.0	8.3	1.6	19.8	755.6	251.0
20.08.18	9:00	22.2	39.0	7.6	1.6	21.1	755.6	425.0
20.08.18	9:30	22.2	40.0	8.0	3.2	21.2	755.6	532.0
20.08.18	10:00	24.2	35.0	7.7	1.6	23.5	755.6	623.0
20.08.18	10:30	24.2	34.0	7.3	3.2	23.4	755.6	713.0
20.08.18	11:00	25.1	31.0	6.7	1.6	24.4	755.4	715.0
20.08.18	11:30	25.5	27.0	5.1	3.2	24.6	755.4	843.0
20.08.18	12:00	26.8	26.0	5.7	3.2	25.4	755.3	877.0
20.08.18	12:30	27.3	25.0	5.5	1.6	25.8	755.2	699.0
20.08.18	13:00	26.7	22.0	3.2	3.2	25.1	755.0	944.0
20.08.18	13:30	28.6	19.0	2.7	1.6	26.9	755.0	922.0
20.08.18	14:00	29.2	21.0	4.6	3.2	27.5	754.8	885.0
20.08.18	14:30	28.9	21.0	4.4	3.2	27.3	754.8	849.0
20.08.18	15:00	29.7	20.0	4.4	3.2	27.9	754.6	799.0
20.08.18	15:30	28.8	20.0	3.6	3.2	27.1	754.5	730.0
20.08.18	16:00	29.6	20.0	4.3	3.2	27.8	754.3	665.0
20.08.18	16:30	28.7	21.0	4.2	1.6	27.1	754.2	417.0
20.08.18	17:00	29.2	20.0	3.9	1.6	27.5	754.0	387.0
20.08.18	17:30	29.3	21.0	4.7	1.6	27.6	754.0	391.0
20.08.18	18:00	28.8	21.0	4.3	1.6	27.2	753.9	291.0
20.08.18	18:30	29.3	21.0	4.7	0.0	27.6	753.9	183.0
20.08.18	19:00	27.3	24.0	4.9	0.0	25.8	753.9	55.0
20.08.18	19:30	22.6	32.0	5.1	0.0	21.3	754.1	17.0
20.08.18	20:00	19.9	35.0	4.0	0.0	18.3	754.4	1.0
20.08.18	20:30	19.8	36.0	4.3	0.0	18.2	754.5	0.0

20.08.18	21:00	19.5	36.0	4.0	1.6	17.8	754.7	0.0
20.08.18	21:30	18.4	39.0	4.2	0.0	16.9	755.0	0.0
20.08.18	22:00	16.7	47.0	5.3	0.0	15.6	755.1	0.0
20.08.18	22:30	16.4	50.0	5.9	0.0	15.3	755.3	0.0
20.08.18	23:00	16.3	52.0	6.4	0.0	15.3	755.4	0.0
20.08.18	23:30	16.1	53.0	6.5	0.0	15.1	755.5	0.0
02.09.18	0:00	19.6	50.0	8.9	0.0	18.8	757.4	0.0
02.09.18	0:30	18.6	54.0	9.1	0.0	17.9	757.3	0.0
02.09.18	1:00	17.9	57.0	9.3	0.0	17.3	757.3	0.0
02.09.18	1:30	18.4	56.0	9.5	1.6	17.8	757.2	0.0
02.09.18	2:00	18.2	57.0	9.6	0.0	17.6	757.1	0.0
02.09.18	2:30	17.0	61.0	9.4	0.0	16.4	757.1	0.0
02.09.18	3:00	16.3	62.0	9.0	0.0	15.8	757.1	0.0
02.09.18	3:30	15.9	66.0	9.5	0.0	15.4	757.4	0.0
02.09.18	4:00	16.0	65.0	9.4	0.0	15.6	757.3	0.0
02.09.18	4:30	16.2	67.0	10.1	0.0	15.8	757.5	0.0
02.09.18	5:00	16.1	68.0	10.1	0.0	15.7	757.6	0.0
02.09.18	5:30	16.1	69.0	10.4	0.0	15.8	757.6	0.0
02.09.18	6:00	15.1	73.0	10.3	0.0	14.8	757.6	0.0
02.09.18	6:30	15.3	73.0	10.5	0.0	15.0	757.8	3.0
02.09.18	7:00	16.1	73.0	11.3	0.0	15.9	757.9	30.0
02.09.18	7:30	18.7	66.0	12.2	0.0	18.6	757.9	95.0
02.09.18	8:00	22.4	52.0	12.1	0.0	22.1	757.9	153.0
02.09.18	8:30	23.2	49.0	11.9	1.6	22.9	757.7	281.0
02.09.18	9:00	24.7	46.0	12.3	1.6	24.5	757.6	391.0
02.09.18	9:30	25.5	44.0	12.3	1.6	25.2	757.6	486.0
02.09.18	10:00	26.7	41.0	12.4	1.6	26.2	757.6	579.0
02.09.18	10:30	28.0	37.0	12.0	1.6	27.4	757.6	645.0
02.09.18	11:00	28.7	34.0	11.3	1.6	28.1	757.5	716.0

02.09.18	11:30	29.8	30.0	10.3	1.6	28.8	757.3	775.0
02.09.18	12:00	30.8	19.0	4.5	3.2	28.8	757.1	819.0
02.09.18	12:30	30.9	21.0	6.1	3.2	29.1	756.9	848.0
02.09.18	13:00	32.0	20.0	6.2	3.2	30.0	756.7	855.0
02.09.18	13:30	32.0	20.0	6.2	3.2	30.0	756.5	854.0
02.09.18	14:00	32.8	18.0	5.3	3.2	30.8	756.3	839.0
02.09.18	14:30	32.9	17.0	4.7	4.8	30.9	756.2	804.0
02.09.18	15:00	33.4	14.0	2.3	3.2	31.2	755.9	755.0
02.09.18	15:30	33.3	14.0	2.2	3.2	31.1	755.7	693.0
02.09.18	16:00	33.4	14.0	2.3	4.8	31.2	755.7	618.0
02.09.18	16:30	33.3	15.0	3.2	3.2	31.2	755.7	529.0
02.09.18	17:00	32.6	16.0	3.5	3.2	30.5	755.7	227.0
02.09.18	17:30	32.4	17.0	4.2	4.8	30.4	755.6	333.0
02.09.18	18:00	31.8	19.0	5.3	1.6	29.7	755.5	229.0
02.09.18	18:30	30.8	20.0	5.2	1.6	28.9	755.5	109.0
02.09.18	19:00	28.9	24.0	6.3	0.0	27.5	755.5	27.0
02.09.18	19:30	26.2	27.0	5.7	0.0	25.1	755.7	6.0
02.09.18	20:00	23.1	33.0	6.0	0.0	22.2	756.0	0.0
02.09.18	20:30	24.0	36.0	8.0	0.0	23.4	756.4	0.0
02.09.18	21:00	24.2	39.0	9.4	1.6	23.7	756.6	0.0
02.09.18	21:30	21.5	46.0	9.4	0.0	20.4	756.7	0.0
02.09.18	22:00	22.1	49.0	10.8	0.0	21.4	756.7	0.0
02.09.18	22:30	21.4	52.0	11.1	0.0	20.6	756.5	0.0
02.09.18	23:00	23.2	52.0	12.8	0.0	23.2	756.6	0.0
02.09.18	23:30	23.7	51.0	13.0	1.6	23.8	756.6	0.0
01.10.18	0:00	14.6	81.0	11.3	0.0	14.4	757.4	0.0
01.10.18	0:30	17.4	62.0	10.0	3.2	16.9	757.3	0.0
01.10.18	1:00	18.0	59.0	9.9	4.8	17.5	757.3	0.0
01.10.18	1:30	18.1	57.0	9.5	4.8	17.5	757.4	0.0

01.10.18	2:00	17.7	60.0	9.9	4.8	17.2	757.4	0.0
01.10.18	2:30	17.2	62.0	9.8	4.8	16.7	757.4	0.0
01.10.18	3:00	17.9	59.0	9.8	4.8	17.3	757.4	0.0
01.10.18	3:30	17.7	61.0	10.1	3.2	17.3	757.4	0.0
01.10.18	4:00	17.5	61.0	9.9	3.2	17.0	757.1	0.0
01.10.18	4:30	18.1	58.0	9.7	4.8	17.6	757.0	0.0
01.10.18	5:00	17.9	60.0	10.1	9.7	17.4	756.9	0.0
01.10.18	5:30	17.2	66.0	10.8	9.7	16.9	757.1	0.0
01.10.18	6:00	16.1	74.0	11.4	6.4	15.8	757.3	0.0
01.10.18	6:30	15.8	78.0	12.0	6.4	15.7	757.5	0.0
01.10.18	7:00	15.0	84.0	12.3	4.8	15.0	757.6	0.0
01.10.18	7:30	14.2	88.0	12.2	6.4	14.2	757.8	28.0
01.10.18	8:00	14.8	88.0	12.9	1.6	14.9	757.9	154.0
01.10.18	8:30	15.2	86.0	12.9	0.0	15.3	758.0	206.0
01.10.18	9:00	16.4	81.0	13.2	0.0	16.5	757.8	289.0
01.10.18	9:30	17.8	75.0	13.3	1.6	17.8	757.9	404.0
01.10.18	10:00	18.3	75.0	13.8	1.6	18.4	757.8	308.0
01.10.18	10:30	18.7	71.0	13.3	3.2	18.8	757.7	470.0
01.10.18	11:00	19.8	66.0	13.3	3.2	19.9	757.6	588.0
01.10.18	11:30	21.1	56.0	11.9	4.8	20.4	757.5	625.0
01.10.18	12:00	22.2	51.0	11.5	4.8	21.7	757.3	859.0
01.10.18	12:30	20.9	56.0	11.8	4.8	20.3	757.3	196.0
01.10.18	13:00	22.7	49.0	11.4	4.8	22.3	757.0	528.0
01.10.18	13:30	23.3	45.0	10.7	6.4	23.0	756.8	778.0
01.10.18	14:00	23.2	43.0	9.9	8.0	22.7	756.5	704.0
01.10.18	14:30	23.9	43.0	10.5	6.4	23.6	756.4	689.0
01.10.18	15:00	24.2	40.0	9.7	6.4	23.7	756.2	647.0
01.10.18	15:30	24.6	37.0	8.9	6.4	24.0	756.1	575.0
01.10.18	16:00	24.8	37.0	9.1	4.8	24.2	756.0	530.0

01.10.18	16:30	24.2	38.0	9.0	4.8	23.7	756.0	373.0
01.10.18	17:00	24.6	38.0	9.3	3.2	24.0	755.9	286.0
01.10.18	17:30	23.3	41.0	9.3	1.6	22.9	755.9	89.0
01.10.18	18:00	22.8	43.0	9.5	1.6	22.2	755.8	54.0
01.10.18	18:30	19.8	54.0	10.3	0.0	19.3	755.7	7.0
01.10.18	19:00	17.9	63.0	10.8	1.6	17.6	755.9	0.0
01.10.18	19:30	16.8	66.0	10.4	0.0	16.5	756.1	0.0
01.10.18	20:00	17.0	74.0	12.3	1.6	16.9	756.5	0.0
01.10.18	20:30	17.7	61.0	10.1	6.4	17.3	756.7	0.0
01.10.18	21:00	18.3	54.0	8.8	9.7	17.6	756.9	0.0
01.10.18	21:30	15.2	77.0	11.2	8.0	14.9	757.2	0.0
01.10.18	22:00	14.4	83.0	11.6	0.0	14.4	757.8	0.0
01.10.18	22:30	14.1	84.0	11.4	0.0	14.0	758.2	0.0
01.10.18	23:00	15.5	71.0	10.3	3.2	15.2	758.3	0.0
01.10.18	23:30	15.5	70.0	10.0	1.6	15.2	758.5	0.0

Table 0.17. *Detected rainy days by weather station of RUN160818. The experiment was started on August 16, 2018.*

Date	**Time**	**Rain**	**Rain rate**
29.08.18	19:30	1.8	12.4
29.08.18	20:00	1.8	15.7
29.08.18	20:30	0.3	1.3
29.08.18	21:00	0.0	0.0
29.08.18	21:30	0.8	4.6
30.08.18	4:00	0.3	0.0
05.09.18	23:30	0.3	0.0
13.09.18	15:30	0.3	0.0

29.09.18	19:30	0.5	10.9
29.09.18	20:00	1.3	4.8
29.09.18	20:30	1.5	39.4
30.09.18	19:30	4.6	52.6
01.10.18	7:00	1.0	40.4
01.10.18	7:30	1.5	27.9
01.10.18	10:30	0.3	0.0
01.10.18	20:00	0.3	0.0
01.10.18	21:30	0.8	19.0

Table 0.18. *Temperature (ºC) data of RUN160818 for August 20, September 2 and October 1, 2018. T2, T3 and T4 show number of tubes counted from bottom.*

Date	**20.08.18**			**02.09.18**			**01.10.18**		
Time	**T2**	**T3**	**T4**	**T2**	**T3**	**T4**	**T2**	**T3**	**T4**
0:09	21.3	22.0	24.5	20.6	20.2	20.2	23.0	23.1	23.7
0:19	21.2	21.9	24.3	20.3	19.9	19.7	23.1	23.3	24.1
0:29	21.2	22.0	24.3	19.9	19.4	19.1	23.2	23.2	23.9
0:39	21.0	21.7	24.2	19.4	18.9	18.8	23.1	23.2	23.9
0:49	21.0	21.5	24.2	18.9	18.4	18.6	23.2	23.3	24.0
0:59	20.8	21.3	24.1	18.7	18.1	18.5	23.1	23.2	23.7
1:09	20.5	21.1	24.0	18.3	17.7	18.3	23.2	23.2	23.9
1:19	20.4	20.9	23.8	18.1	17.4	18.2	22.9	23.1	23.5
1:29	20.2	20.7	23.8	17.8	17.2	18.6	22.9	23.0	23.5
1:39	20.0	20.6	23.3	17.8	17.2	18.9	22.8	22.9	23.4
1:49	19.6	20.1	22.8	17.7	17.1	18.7	22.7	22.8	23.6
1:59	19.0	19.5	22.3	17.7	17.0	18.8	22.6	22.7	23.2
2:09	18.3	18.5	21.4	17.8	17.1	18.1	22.5	22.5	23.1

2:19	17.5	17.8	21.4	17.6	16.9	18.3	22.4	22.5	22.7
2:29	16.7	17.3	20.9	17.5	16.8	17.6	22.0	22.2	21.8
2:39	16.2	16.4	20.8	17.1	16.5	17.1	21.5	21.6	20.7
2:49	15.6	15.9	20.5	17.0	16.3	17.0	20.8	20.9	19.8
2:59	15.1	15.5	20.3	16.7	16.0	17.0	20.2	20.3	19.1
3:09	14.7	15.1	20.2	16.5	15.8	16.7	19.6	19.7	18.9
3:19	14.4	15.4	20.2	16.3	15.7	16.6	19.1	19.2	18.1
3:29	14.1	16.9	20.2	16.1	15.4	16.2	18.4	18.5	18.1
3:39	13.9	15.8	20.0	15.8	15.2	16.3	18.0	18.2	17.7
3:49	13.7	15.6	19.7	15.7	15.1	16.2	17.6	17.7	17.2
3:59	13.6	23.4	19.8	15.6	15.0	16.2	17.1	17.2	16.9
4:09	13.4	14.4	19.8	15.6	14.8	16.6	16.8	16.9	16.5
4:19	13.2	14.9	19.5	15.5	14.9	16.3	16.6	16.7	17.0
4:29	13.2	15.2	19.7	15.5	14.8	16.5	16.3	16.5	16.4
4:39	13.2	15.3	19.3	15.4	14.7	16.4	16.0	16.1	16.2
4:49	13.1	15.2	19.1	15.3	14.7	16.3	15.8	15.9	15.9
4:59	13.0	15.0	19.2	15.3	14.7	16.2	15.6	15.6	15.8
5:09	12.8	15.1	19.0	15.2	14.5	16.2	15.3	15.4	15.8
5:19	12.6	14.7	18.8	15.0	14.4	16.0	15.1	15.2	15.5
5:29	12.4	14.7	18.6	15.0	14.5	16.1	15.0	15.1	15.4
5:39	12.3	12.1	18.7	15.0	14.4	16.0	14.8	14.9	15.1
5:49	12.2	12.1	18.6	14.9	14.3	15.7	14.7	14.7	15.2
5:59	12.1	12.0	18.7	14.9	14.3	15.8	14.6	14.7	15.1
6:09	12.0	11.9	18.3	14.7	14.1	15.4	14.4	14.5	15.6
6:19	12.0	11.8	18.2	14.5	13.9	15.0	14.3	14.5	15.1
6:29	11.9	11.7	18.3	14.5	13.8	15.1	14.3	14.5	15.1
6:39	11.8	11.6	18.6	14.4	13.7	15.4	14.3	14.4	15.6
6:49	11.9	11.8	20.4	14.5	13.8	15.4	14.5	14.5	16.3
6:59	12.2	12.1	21.7	14.6	13.8	16.3	14.7	14.8	16.7

7:09	12.6	12.6	22.1	14.8	14.1	16.9	15.0	15.1	17.6
7:19	13.0	13.0	22.8	15.2	14.8	18.0	15.4	15.6	18.3
7:29	13.9	14.1	23.2	15.8	15.4	19.5	16.1	16.3	19.8
7:39	15.4	15.3	23.8	16.7	16.1	20.2	16.9	17.1	21.0
7:49	17.1	17.0	24.6	17.7	17.7	21.3	18.0	18.2	22.0
7:59	18.7	18.7	24.7	19.2	20.7	22.5	19.4	19.6	23.3
8:09	20.0	20.1	24.4	21.3	22.9	23.2	21.6	21.8	23.0
8:19	21.8	21.6	24.7	23.6	25.2	24.6	23.7	23.9	24.5
8:29	22.8	22.6	24.9	25.0	26.7	24.6	25.4	25.8	25.2
8:39	24.1	23.8	25.6	26.2	27.8	25.5	26.6	27.0	26.5
8:49	24.5	24.4	27.3	27.3	28.9	26.8	27.8	28.3	26.8
8:59	25.8	25.5	27.2	28.6	30.0	28.8	28.8	29.2	27.6
9:09	26.7	26.6	26.4	29.4	30.3	29.1	29.6	30.0	27.7
9:19	27.3	27.3	27.7	27.7	31.3	27.9	30.5	30.8	28.1
9:29	27.8	28.2	28.2	28.7	31.9	29.4	30.9	31.2	27.8
9:39	28.1	28.2	28.0	27.5	31.3	28.4	31.7	31.7	28.3
9:49	28.5	28.4	27.9	28.8	30.6	28.5	32.0	31.8	28.4
9:59	28.8	28.6	31.2	28.2	31.1	28.6	33.0	32.7	27.5
10:09	29.5	29.3	31.8	28.4	32.2	30.5	33.7	33.2	29.7
10:19	29.9	29.8	27.8	28.0	32.3	30.9	30.7	31.5	30.3
10:29	30.3	30.3	28.2	27.9	33.5	31.8	27.8	29.8	31.3
10:39	29.6	30.1	30.5	29.2	34.0	31.7	29.3	30.0	30.6
10:49	29.3	29.7	30.0	29.5	35.6	34.0	29.5	29.9	30.6
10:59	27.2	29.0	28.3	29.5	36.6	33.8	29.4	30.0	31.2
11:09	28.3	28.0	29.9	29.1	36.6	33.9	28.5	29.2	30.4
11:19	28.5	28.6	29.5	28.8	36.0	31.7	28.0	28.7	33.0
11:29	28.4	28.5	30.0	29.6	36.8	34.3	28.0	28.8	31.3
11:39	29.1	29.7	31.5	29.2	36.2	34.3	27.0	28.6	31.5
11:49	29.7	31.1	32.3	29.2	35.8	32.5	26.2	28.2	31.5

11:59	29.7	31.0	33.9	28.4	36.1	33.7	27.7	29.0	31.9
12:09	29.8	32.0	32.2	27.0	36.5	34.1	29.6	30.3	34.7
12:19	30.1	31.0	32.0	26.9	37.1	35.0	29.5	30.2	34.6
12:29	29.1	30.1	33.1	27.2	36.5	34.3	29.3	29.5	35.0
12:39	30.6	31.4	32.2	28.3	36.2	35.5	29.7	29.7	32.9
12:49	30.6	29.3	32.5	28.9	34.1	36.2	28.9	29.3	34.1
12:59	29.1	28.4	32.8	29.3	34.1	36.2	28.5	28.6	33.7
13:09	31.6	31.4	32.4	30.0	34.7	36.1	28.1	28.8	34.5
13:19	30.7	30.7	31.5	30.3	34.2	35.8	27.9	28.9	33.7
13:29	30.6	31.3	31.3	30.3	32.5	34.1	28.7	29.6	36.7
13:39	30.3	31.4	32.3	30.3	31.0	35.6	29.6	30.7	35.9
13:49	29.6	30.8	30.7	31.8	31.7	37.0	30.6	31.9	36.5
13:59	31.6	32.6	30.6	31.7	31.2	37.7	30.0	31.5	36.5
14:09	30.1	32.1	31.3	30.9	31.2	37.6	31.0	30.3	36.5
14:19	29.3	31.6	30.8	30.8	31.3	35.9	30.4	34.1	36.3
14:29	29.5	32.6	31.5	31.3	31.3	35.9	33.3	35.7	36.1
14:39	28.4	34.6	32.0	30.5	31.6	37.0	28.7	30.0	35.9
14:49	30.4	34.5	33.0	30.2	32.3	37.9	31.8	35.5	35.3
14:59	31.8	33.7	32.2	29.3	32.9	35.6	34.5	38.0	35.1
15:09	30.9	33.5	31.8	29.8	30.8	37.9	33.2	39.5	35.3
15:19	28.1	32.1	33.2	30.3	30.3	36.2	33.4	39.0	37.0
15:29	26.0	33.2	35.0	32.3	31.3	36.6	33.3	36.7	36.1
15:39	28.5	33.9	35.6	29.7	31.1	37.5	32.0	35.2	36.9
15:49	29.4	33.2	37.8	28.8	29.9	38.4	31.3	34.7	37.3
15:59	29.2	33.4	38.2	30.9	30.4	38.7	30.7	34.8	35.3
16:09	27.6	35.3	37.8	28.9	30.5	37.5	31.2	34.2	36.3
16:19	27.9	36.2	37.8	29.0	29.8	37.4	31.5	33.3	35.9
16:29	29.9	36.2	34.0	31.5	30.7	37.4	31.6	33.5	36.3
16:39	29.3	34.0	34.5	31.3	30.5	36.0	31.5	34.1	37.5

16:49	28.4	35.4	33.8	31.3	30.3	37.8	31.6	33.9	37.6
16:59	30.8	36.0	35.7	31.5	30.2	38.0	31.6	33.6	35.4
17:09	30.2	33.8	40.0	31.5	30.0	37.5	31.0	33.0	36.1
17:19	29.6	33.2	38.9	30.7	29.3	35.8	30.8	32.6	34.4
17:29	30.5	33.1	38.0	29.7	28.9	36.4	30.4	32.2	36.2
17:39	30.9	34.0	38.2	29.4	28.8	35.8	30.4	31.9	35.3
17:49	29.7	31.5	37.8	28.9	28.3	36.0	29.7	32.0	35.8
17:59	30.4	31.6	37.2	28.8	28.8	35.3	29.3	31.8	34.7
18:09	30.8	31.2	34.0	28.5	28.8	35.1	29.8	31.8	33.5
18:19	29.1	30.8	34.1	28.1	28.7	33.8	28.7	31.8	33.7
18:29	29.0	30.4	34.7	29.1	28.7	32.7	29.8	32.3	32.7
18:39	29.3	30.0	31.2	29.5	28.8	32.6	29.6	32.3	32.3
18:49	29.3	29.7	31.5	29.0	28.5	30.8	28.7	31.7	30.8
18:59	28.9	29.2	29.8	29.3	28.4	30.7	28.5	31.0	28.6
19:09	28.0	28.1	29.0	29.1	28.3	30.0	27.8	29.9	28.1
19:19	26.9	26.7	28.2	28.7	28.1	28.5	27.1	28.7	26.3
19:29	26.1	25.4	27.5	28.5	28.0	27.3	26.5	27.6	25.4
19:39	24.9	24.2	26.9	27.6	27.2	25.0	25.9	26.5	25.1
19:49	23.9	23.0	26.0	26.6	26.2	24.8	25.5	25.7	25.4
19:59	23.0	22.0	25.6	25.8	25.3	23.5	25.2	25.2	24.9
20:09	22.0	21.2	25.2	25.0	24.5	23.0	24.8	24.7	24.5
20:19	21.4	20.4	25.0	24.2	23.7	22.5	24.7	24.4	24.8
20:29	20.7	19.8	24.8	23.8	23.2	24.7	24.5	24.1	25.3
20:39	20.3	19.4	24.5	23.7	23.3	23.7	24.8	24.3	25.4
20:49	20.0	19.2	24.3	23.5	23.1	24.7	24.8	24.4	25.7
20:59	19.7	18.9	24.1	23.6	23.2	24.1	24.8	24.4	25.8
21:09	19.4	18.7	23.8	23.5	23.2	23.8	25.0	24.6	25.9
21:19	19.1	18.4	23.3	23.1	22.9	22.2	24.9	24.5	25.5
21:29	18.8	18.2	23.5	22.5	22.3	21.7	25.1	24.7	25.9

21:39	18.7	18.1	23.1	22.1	21.7	21.6	25.2	24.8	25.5
21:49	18.2	17.6	22.9	21.8	21.2	21.5	25.1	24.7	25.4
21:59	17.8	17.2	22.6	21.3	20.8	21.3	25.1	24.7	25.9
22:09	17.4	16.8	22.7	21.5	21.0	22.6	25.2	24.8	26.1
22:19	17.0	16.5	22.4	21.6	21.2	22.3	25.2	24.8	25.9
22:29	16.7	16.2	22.2	21.6	21.2	21.8	25.2	24.8	25.8
22:39	16.4	16.0	22.0	21.3	20.9	21.4	25.2	24.8	25.3
22:49	16.3	15.9	21.7	21.1	20.7	21.6	25.0	24.5	25.2
22:59	16.1	15.8	21.7	21.2	20.8	22.6	24.8	24.5	24.8
23:09	16.1	15.7	21.5	21.5	21.4	23.2	24.3	24.1	23.0
23:19	15.9	15.6	21.4	22.0	22.1	23.5	23.8	23.3	22.8
23:29	15.8	15.5	21.5	22.3	22.3	23.3	23.1	22.7	22.3
23:39	15.7	15.4	21.7	22.5	22.3	23.4	22.5	22.2	21.5
23:49	15.7	15.4	21.2	22.2	22.1	21.9	22.0	21.6	20.9
23:59	15.7	15.4	21.4	21.7	21.5	20.8	21.3	20.9	20.1

Table 0.19. *Daily variation in cell concentration of RUN290817. The experiment was started on August 29,*

Date	**Time**	**Day**	**OD2**			**OD4**			**ODavg.**	**Avg. Cell Conc. (gdcw/Lc)**
			OD2.1	**OD2.2**	**OD2.3**	**OD4.1**	**OD4.2**	**OD4.3**		
29.08.17	17:00	1.5	0.674	0.680	0.709	0.644	0.629	0.634	0.636	0.296
30.08.17	08:30	2.0	0.642	0.624	0.613	0.658	0.655	0.652	0.655	0.305
	18:30	2.5	0.673	0.706	0.701	0.701	0.672	0.704	0.692	0.322
31.08.17	08:15	3.0	0.716	0.713	0.714	0.731	0.733	0.729	0.731	0.340
	18:35	3.5	0.800	0.798	0.804	0.824	0.813	0.800	0.812	0.378
01.09.17	08:30	4.0	0.785	0.784	0.785	0.753	0.743	0.744	0.747	0.348
	19:15	4.5	0.916	0.908	0.915	0.928	0.927	0.931	0.929	0.432

02.09.17	09:25	5.0	1.054	1.037	1.061	1.082	1.062	1.049	1.064	0.496
	18:25	5.5	1.253	1.251	1.216	1.269	1.268	1.280	1.272	0.592
03.09.17	08:15	6.0	1.184	1.178	1.177	1.156	1.184	1.157	1.166	0.543
	19:00	6.5	1.481	1.469	1.454	1.480	1.462	1.451	1.464	0.682
04.09.17	08:30	7.0	1.537	1.515	1.528	1.670	1.671	1.657	1.666	0.776
	18:20	7.5	1.686	1.546	1.670	1.677	1.652	1.670	1.666	0.776
05.09.17	09:30	8.0	1.700	1.540	1.687	1.656	1.668	1.667	1.664	0.775
	18:30	8.5	1.789	1.803	1.773	1.768	1.736	1.763	1.756	0.817
06.09.17	08:30	9.0	2.008	1.998	1.972	1.847	1.923	1.908	1.893	0.881
06.09.17	18:30	9.5	1.768	1.806	1.752	1.509	1.520	1.506	1.512	0.704
07.09.17	09:00	10.0	1.610	1.661	1.658	1.670	1.683	1.600	1.651	0.769
	18:30	10.5	1.610	1.636	1.639	1.621	1.637	1.617	1.625	0.757
08.09.17	09:30	11.0	1.913	1.875	1.856	1.931	1.943	1.963	1.946	0.906
	19:00	11.5	1.312	1.378	1.311	1.616	1.637	1.643	1.632	0.760
09.09.17	09:30	12.0	0.700	0.701	0.724	1.567	1.626	1.664	1.619	0.754

Table 0.20. *Daily variation in pH of RUN290817. The experiment was started on August 29, 2017.*

Date	**Time**	**Day**	**pH2**			**pH4**			**pH**
			pH2.1	**pH2.2**	**pH2.3**	**pH4.1**	**pH4.2**	**pH4.3**	
29.08.17	17:00	1.5	7.04	7.04	7.05	7.11	7.12	7.11	7.11
30.08.17	08:30	2.0	7.03	7.04	7.04	7.07	7.05	7.05	7.06
	18:30	2.5	7.56	7.57	7.56	7.02	7.01	7.03	7.02
31.08.17	08:15	3.0	7.03	7.04	7.04	7.05	7.04	7.04	7.04
	18:35	3.5	7.08	7.07	7.07	7.08	7.07	7.07	7.07
01.09.17	08:30	4.0	7.25	7.21	7.27	7.24	7.24	7.24	7.24

	19:15	4.5	7.35	7.33	7.33	7.42	7.47	7.46	7.45
02.09.17	09:25	5.0	7.25	7.24	7.25	6.95	6.94	6.94	6.94
	18:25	5.5	7.31	7.32	7.33	7.28	7.27	7.27	7.27
03.09.17	08:15	6.0	7.24	7.23	7.24	7.29	7.29	7.28	7.29
	19:00	6.5	7.35	7.34	7.35	7.37	7.39	7.36	7.37
04.09.17	08:30	7.0	7.21	7.21	7.21	7.14	7.14	7.14	7.14
	18:20	7.5	7.12	7.13	7.13	7.14	7.14	7.15	7.14
05.09.17	09:30	8.0	7.38	7.40	7.42	7.15	7.17	7.17	7.16
	18:30	8.5	7.51	7.53	7.54	7.50	7.54	7.54	7.53
06.09.17	08:30	9.0	7.25	7.29	7.31	7.25	7.25	7.24	7.25
	18:30	9.5	7.18	7.19	7.19	7.19	7.19	7.19	7.19
07.09.17	09:00	10.0	7.04	7.05	7.07	7.07	7.06	7.07	7.07
	18:30	10.5	7.07	7.07	7.07	7.06	7.04	7.04	7.05
08.09.17	09:30	11.0	7.22	7.23	7.23	7.01	7.00	6.99	7.00
	19:00	11.5	7.27	7.28	7.28	7.07	7.06	7.06	7.06
09.09.17	09:30	12.0	7.32	7.30	7.30	7.10	7.13	7.13	7.12

Table 0.21. *Daily variation in organic acids and sucrose concentrations of RUN290817. The experiment was started on August 29, 2017.*

Date	**Day**	**Lactic acid (mM)**	**Formic acid (mM)**	**Acetic acid (mM)**	**Total organic acid (mM)**	**Sucrose (mM)**
29.08.17	1.5	0.000	0.039	1.065	1.104	5.000
30.08.17	2.0	0.662	1.758	1.392	3.812	4.084
	2.5	1.324	3.477	1.719	6.520	3.169
31.08.17	3.0	0.000	5.940	9.303	15.243	4.775

	3.5	0.000	7.273	13.257	20.530	4.602
01.09.17	4.0	0.134	1.797	3.362	5.293	0.002
	4.5	0.774	3.535	13.966	18.274	0.003
02.09.17	5.0	0.138	0.898	2.583	3.619	3.921
	5.5	0.199	1.322	0.890	2.411	2.553
03.09.17	6.0	0.969	6.009	19.845	26.823	3.781
	6.5	0.992	5.842	21.491	28.324	2.133
04.09.17	7.0	6.042	14.616	6.288	26.946	3.204
	7.5	0.000	12.400	26.656	39.057	4.790
05.09.17	8.0	4.441	15.842	5.142	25.425	1.925
	8.5	1.140	6.571	28.335	36.045	3.579
06.09.17	9.0	0.000	7.787	30.986	38.773	3.031
	9.5	0.000	5.216	17.533	22.749	3.918
07.09.17	10.0	0.000	7.337	19.135	26.472	3.773
	10.5	2.755	13.226	8.436	24.417	3.785
08.09.17	11.0	0.000	3.813	22.440	26.253	3.812
	11.5	1.144	7.944	3.526	12.614	1.629
09.09.17	12.0	0.000	3.948	6.437	10.385	4.081

Table 0.22. *Daily biogas production and solar radiation of RUN290817. The experiment was started on August 29, 2017.*

Date	**Day**	**Biogas Content**		**Daily produced biogas (ml)**	**H_2 produced (mol)**	**H_2 productivity (mol $H_2/m^3.h$)**	**Daily solar radiation (W/m^2)**
		H2	**CO2**				
29.08.17	1	0.0	0.0	0	0.000	0.000	478.333
30.08.17	2	0.0	0.0	0	0.000	0.000	473.507
31.08.17	3	0.0	0.0	0	0.000	0.000	476.253
01.09.17	4	94.4	5.6	695	0.024	0.085	521.153
02.09.17	5	92.4	7.6	3268	0.109	0.390	525.633
03.09.17	6	90.5	9.5	1260	0.041	0.147	524.953
04.09.17	7	96.7	3.3	1575	0.055	0.197	511.533
05.09.17	8	96.7	3.3	1125	0.039	0.141	484.527
06.09.17	9	0.0	0.0	0	0.000	0.000	219.660
07.09.17	10	0.0	0.0	0	0.000	0.000	507.160
08.09.17	11	0.0	0.0	0	0.000	0.000	458.667
09.09.17	12	0.0	0.0	0	0.000	0.000	491.260

Table 0.23. *Weather station data of RUN290817 for September 5, 2017.*

Time	**Air temperature (^oC)**	**Humidity**	**Dew point (^oC)**	**Wind speed (m/s)**	**Heat Index**	**Pressure (bar)**	**Solar Radiation (W/m^2)**
0:00	21.9	27.0	2.1	1.6	20.1	1007.6	0.0
0:05	21.2	28.0	1.9	1.6	19.1	1007.5	0.0
0:10	20.7	29.0	2.0	0.0	18.7	1007.6	0.0
0:15	20.0	30.0	1.9	1.6	18.0	1007.5	0.0

0:20	19.6	30.0	1.5	0.0	17.6	1007.5	0.0
0:25	19.7	31.0	2.1	1.6	17.8	1007.6	0.0
0:30	19.8	31.0	2.2	1.6	17.9	1007.6	0.0
0:35	19.4	31.0	1.8	0.0	17.4	1007.7	0.0
0:40	18.9	32.0	1.8	1.6	17.0	1007.7	0.0
0:45	18.5	33.0	1.9	1.6	16.6	1007.8	0.0
0:50	18.2	34.0	2.0	0.0	16.3	1007.8	0.0
0:55	17.6	35.0	2.0	0.0	15.8	1007.8	0.0
1:00	17.5	36.0	2.2	1.6	15.8	1007.9	0.0
1:05	17.9	35.0	2.2	1.6	16.1	1007.9	0.0
1:10	18.2	35.0	2.5	1.6	16.4	1007.9	0.0
1:15	18.3	36.0	3.0	0.0	16.6	1007.9	0.0
1:20	18.3	37.0	3.3	0.0	16.6	1007.9	0.0
1:25	18.2	39.0	4.0	0.0	16.7	1008.0	0.0
1:30	18.0	39.0	3.8	0.0	16.4	1007.9	0.0
1:35	17.8	42.0	4.7	0.0	16.4	1007.9	0.0
1:40	17.7	43.0	5.0	0.0	16.4	1007.9	0.0
1:45	17.7	46.0	5.9	1.6	16.6	1007.9	0.0
1:50	18.1	46.0	6.3	1.6	16.9	1008.0	0.0
1:55	18.7	46.0	6.9	3.2	17.6	1008.0	0.0
2:00	19.3	45.0	7.0	1.6	18.2	1008.0	0.0
2:05	19.7	45.0	7.4	3.2	18.6	1008.1	0.0
2:10	20.2	45.0	7.9	3.2	19.2	1008.1	0.0
2:15	20.5	45.0	8.2	3.2	19.4	1008.1	0.0
2:20	20.7	45.0	8.3	1.6	19.6	1008.1	0.0
2:25	20.8	45.0	8.4	3.2	19.7	1008.1	0.0
2:30	21.0	46.0	8.9	3.2	19.9	1008.1	0.0
2:35	21.2	45.0	8.8	1.6	19.9	1008.1	0.0
2:40	21.1	46.0	9.0	1.6	19.9	1008.2	0.0

2:45	21.0	47.0	9.3	3.2	19.9	1008.3	0.0
2:50	20.9	48.0	9.5	1.6	19.9	1008.2	0.0
2:55	20.8	49.0	9.7	1.6	19.9	1008.2	0.0
3:00	20.7	48.0	9.3	0.0	19.7	1008.2	0.0
3:05	20.2	51.0	9.8	1.6	19.6	1008.2	0.0
3:10	20.0	52.0	9.8	1.6	19.4	1008.3	0.0
3:15	19.7	52.0	9.5	0.0	19.0	1008.3	0.0
3:20	19.2	54.0	9.6	1.6	18.6	1008.3	0.0
3:25	18.8	56.0	9.8	1.6	18.2	1008.1	0.0
3:30	18.4	58.0	10.0	1.6	17.9	1008.1	0.0
3:35	18.3	59.0	10.1	1.6	17.8	1008.1	0.0
3:40	18.2	61.0	10.5	1.6	17.8	1008.1	0.0
3:45	18.2	62.0	10.8	1.6	17.8	1008.1	0.0
3:50	18.2	61.0	10.5	1.6	17.8	1008.2	0.0
3:55	18.1	61.0	10.4	1.6	17.6	1008.1	0.0
4:00	17.9	62.0	10.5	1.6	17.5	1008.2	0.0
4:05	17.7	63.0	10.6	1.6	17.3	1008.1	0.0
4:10	17.5	63.0	10.4	0.0	17.1	1008.1	0.0
4:15	17.3	65.0	10.6	1.6	16.9	1008.1	0.0
4:20	17.1	65.0	10.5	1.6	16.8	1008.0	0.0
4:25	16.8	66.0	10.4	1.6	16.4	1008.0	0.0
4:30	16.6	67.0	10.4	0.0	16.2	1008.0	0.0
4:35	16.3	68.0	10.4	0.0	16.0	1008.0	0.0
4:40	16.2	68.0	10.3	0.0	15.8	1008.0	0.0
4:45	16.0	69.0	10.3	1.6	15.7	1008.1	0.0
4:50	15.8	70.0	10.3	0.0	15.4	1008.0	0.0
4:55	15.6	70.0	10.1	0.0	15.2	1008.1	0.0
5:00	15.4	70.0	10.0	1.6	15.1	1008.0	0.0
5:05	15.5	73.0	10.7	1.6	15.2	1008.1	0.0

5:10	15.4	71.0	10.2	0.0	15.1	1008.1	0.0
5:15	15.3	73.0	10.5	1.6	15.0	1008.1	0.0
5:20	15.2	74.0	10.6	1.6	14.9	1008.0	0.0
5:25	15.1	74.0	10.5	1.6	14.8	1008.0	0.0
5:30	15.2	75.0	10.8	1.6	14.9	1008.1	0.0
5:35	15.2	76.0	11.0	1.6	15.0	1008.1	0.0
5:40	15.4	76.0	11.2	0.0	15.2	1008.1	0.0
5:45	15.6	76.0	11.3	0.0	15.4	1007.9	0.0
5:50	15.8	76.0	11.6	1.6	15.7	1008.0	0.0
5:55	16.1	75.0	11.7	1.6	15.9	1008.1	0.0
6:00	16.3	73.0	11.5	1.6	16.1	1008.2	0.0
6:05	16.6	73.0	11.7	1.6	16.4	1008.2	0.0
6:10	16.6	72.0	11.5	1.6	16.4	1008.2	0.0
6:15	16.4	71.0	11.2	0.0	16.2	1008.2	0.0
6:20	16.2	71.0	11.0	0.0	15.9	1008.2	0.0
6:25	15.8	73.0	11.0	1.6	15.6	1008.2	5.0
6:30	15.6	73.0	10.7	0.0	15.3	1008.2	9.0
6:35	15.3	73.0	10.5	0.0	15.1	1008.3	12.0
6:40	15.1	73.0	10.3	0.0	14.7	1008.3	17.0
6:45	14.8	74.0	10.2	0.0	14.6	1008.3	22.0
6:50	14.8	76.0	10.6	1.6	14.6	1008.2	28.0
6:55	14.9	76.0	10.7	0.0	14.7	1008.3	35.0
7:00	15.1	76.0	10.9	0.0	14.9	1008.3	44.0
7:05	15.5	76.0	11.3	3.2	15.3	1008.4	54.0
7:10	15.9	75.0	11.5	1.6	15.8	1008.4	65.0
7:15	16.4	74.0	11.8	1.6	16.3	1008.3	75.0
7:20	16.9	73.0	12.0	1.6	16.7	1008.4	87.0
7:25	17.3	71.0	12.0	1.6	17.2	1008.5	100.0
7:30	17.9	70.0	12.3	0.0	17.8	1008.4	107.0

7:35	18.5	68.0	12.5	0.0	18.4	1008.5	112.0
7:40	19.2	66.0	12.7	1.6	19.2	1008.6	119.0
7:45	19.8	64.0	12.8	1.6	19.8	1008.6	135.0
7:50	20.1	62.0	12.6	1.6	20.0	1008.6	156.0
7:55	20.4	60.0	12.4	1.6	20.2	1008.6	182.0
8:00	20.7	59.0	12.4	1.6	20.3	1008.6	205.0
8:05	21.2	58.0	12.6	0.0	20.6	1008.5	226.0
8:10	21.7	56.0	12.5	0.0	21.2	1008.6	248.0
8:15	22.1	54.0	12.4	0.0	21.7	1008.6	268.0
8:20	22.2	54.0	12.5	1.6	21.9	1008.5	287.0
8:25	22.1	53.0	12.0	3.2	21.6	1008.5	305.0
8:30	22.0	53.0	12.0	1.6	21.5	1008.6	322.0
8:35	22.1	54.0	12.3	1.6	21.7	1008.6	340.0
8:40	22.4	53.0	12.3	1.6	22.1	1008.5	353.0
8:45	22.5	52.0	12.2	3.2	22.2	1008.4	368.0
8:50	22.7	52.0	12.4	1.6	22.6	1008.4	385.0
8:55	23.0	52.0	12.6	1.6	22.9	1008.4	403.0
9:00	22.8	51.0	12.1	3.2	22.6	1008.4	418.0
9:05	22.7	52.0	12.3	3.2	22.4	1008.4	433.0
9:10	22.6	52.0	12.2	3.2	22.3	1008.4	445.0
9:15	22.8	51.0	12.1	1.6	22.6	1008.4	459.0
9:20	23.2	51.0	12.5	0.0	23.1	1008.5	473.0
9:25	24.0	49.0	12.6	1.6	24.0	1008.5	488.0
9:30	24.4	47.0	12.3	1.6	24.3	1008.5	504.0
9:35	24.6	46.0	12.2	1.6	24.4	1008.4	520.0
9:40	24.4	47.0	12.4	3.2	24.3	1008.4	534.0
9:45	24.4	47.0	12.3	3.2	24.3	1008.4	546.0
9:50	24.7	46.0	12.3	1.6	24.4	1008.4	559.0
9:55	24.8	45.0	12.1	3.2	24.6	1008.4	572.0

10:00	25.0	45.0	12.2	1.6	24.7	1008.4	585.0
10:05	25.3	44.0	12.2	1.6	25.1	1008.4	602.0
10:10	25.4	44.0	12.3	1.6	25.2	1008.3	616.0
10:15	25.4	43.0	11.9	3.2	25.1	1008.3	627.0
10:20	25.5	43.0	12.0	3.2	25.2	1008.2	638.0
10:25	25.7	43.0	12.2	1.6	25.4	1008.2	651.0
10:30	25.5	43.0	12.0	3.2	25.2	1008.1	663.0
10:35	25.4	43.0	11.9	1.6	25.1	1008.0	674.0
10:40	25.7	42.0	11.8	0.0	25.3	1008.0	686.0
10:45	26.2	42.0	12.3	1.6	25.9	1007.9	698.0
10:50	26.5	41.0	12.2	3.2	26.1	1007.9	708.0
10:55	26.6	40.0	11.8	3.2	26.0	1007.9	718.0
11:00	26.5	40.0	11.8	1.6	26.0	1007.8	725.0
11:05	26.6	41.0	12.2	3.2	26.1	1007.8	734.0
11:10	26.7	41.0	12.3	1.6	26.2	1007.8	743.0
11:15	27.1	40.0	12.3	3.2	26.5	1007.8	750.0
11:20	27.1	39.0	11.9	3.2	26.4	1007.7	758.0
11:25	27.2	40.0	12.4	3.2	26.6	1007.6	767.0
11:30	27.3	39.0	12.1	3.2	26.7	1007.6	773.0
11:35	27.4	39.0	12.2	3.2	26.8	1007.6	780.0
11:40	27.7	38.0	12.1	3.2	27.1	1007.5	786.0
11:45	27.8	38.0	12.2	4.8	27.3	1007.4	791.0
11:50	28.1	37.0	12.0	3.2	27.6	1007.4	801.0
11:55	28.4	37.0	12.3	1.6	28.1	1007.5	802.0
12:00	28.6	36.0	12.0	3.2	28.1	1007.5	810.0
12:05	28.3	36.0	11.8	4.8	27.7	1007.4	817.0
12:10	28.1	37.0	12.0	3.2	27.6	1007.3	821.0
12:15	28.3	36.0	11.8	4.8	27.8	1007.3	822.0
12:20	28.2	36.0	11.7	6.4	27.6	1007.3	824.0

12:25	28.2	36.0	11.7	4.8	27.6	1007.2	824.0
12:30	28.7	36.0	12.1	3.2	28.3	1007.1	825.0
12:35	28.8	34.0	11.4	6.4	28.3	1007.1	826.0
12:40	29.1	34.0	11.6	3.2	28.6	1007.0	829.0
12:45	29.6	32.0	11.2	3.2	28.8	1007.0	831.0
12:50	29.9	31.0	11.0	3.2	29.1	1006.9	823.0
12:55	29.7	31.0	10.8	4.8	28.8	1006.9	823.0
13:00	29.8	32.0	11.4	3.2	29.1	1006.8	824.0
13:05	29.8	31.0	10.8	4.8	28.9	1006.8	830.0
13:10	29.8	32.0	11.4	3.2	29.1	1006.7	822.0
13:15	30.2	31.0	11.2	3.2	29.3	1006.7	818.0
13:20	30.2	31.0	11.2	4.8	29.3	1006.7	820.0
13:25	30.1	31.0	11.1	6.4	29.2	1006.7	817.0
13:30	29.9	31.0	11.0	6.4	29.1	1006.6	816.0
13:35	29.9	31.0	10.9	4.8	29.1	1006.6	813.0
13:40	30.1	31.0	11.1	3.2	29.2	1006.6	810.0
13:45	30.5	30.0	11.0	3.2	29.5	1006.6	805.0
13:50	30.4	31.0	11.4	6.4	29.6	1006.5	801.0
13:55	30.5	30.0	11.0	3.2	29.5	1006.4	792.0
14:00	30.7	31.0	11.6	3.2	29.7	1006.4	789.0
14:05	30.6	31.0	11.6	6.4	29.7	1006.3	780.0
14:10	30.8	30.0	11.2	3.2	29.7	1006.4	772.0
14:15	30.9	31.0	11.8	4.8	29.8	1006.3	765.0
14:20	30.9	31.0	11.8	4.8	29.9	1006.3	759.0
14:25	31.3	30.0	11.6	3.2	30.1	1006.1	753.0
14:30	31.4	30.0	11.8	4.8	30.3	1006.2	742.0
14:35	30.9	30.0	11.3	6.4	29.7	1006.1	734.0
14:40	30.6	31.0	11.6	4.8	29.7	1006.0	724.0
14:45	30.6	31.0	11.6	4.8	29.7	1006.0	711.0

14:50	30.8	30.0	11.2	4.8	29.7	1005.9	703.0
14:55	30.7	31.0	11.6	4.8	29.7	1005.8	695.0
15:00	30.8	31.0	11.7	3.2	29.8	1005.8	688.0
15:05	31.1	31.0	11.9	3.2	29.9	1005.7	678.0
15:10	31.4	31.0	12.2	3.2	30.3	1005.7	672.0
15:15	31.4	30.0	11.8	3.2	30.3	1005.7	657.0
15:20	31.3	28.0	10.6	6.4	29.9	1005.6	647.0
15:25	31.2	28.0	10.5	8.0	29.7	1005.6	633.0
15:30	30.9	28.0	10.3	6.4	29.6	1005.5	622.0
15:35	30.9	28.0	10.3	8.0	29.6	1005.6	610.0
15:40	30.8	29.0	10.7	9.7	29.6	1005.6	595.0
15:45	30.7	28.0	10.1	6.4	29.4	1005.5	583.0
15:50	30.8	29.0	10.7	4.8	29.6	1005.5	582.0
15:55	30.9	29.0	10.8	6.4	29.6	1005.4	568.0
16:00	30.7	29.0	10.6	6.4	29.6	1005.4	558.0
16:05	30.9	29.0	10.8	4.8	29.7	1005.3	530.0
16:10	31.1	28.0	10.4	8.0	29.6	1005.2	514.0
16:15	31.3	27.0	10.1	6.4	29.8	1005.3	502.0
16:20	31.2	27.0	10.0	4.8	29.7	1005.3	485.0
16:25	31.1	26.0	9.3	9.7	29.4	1005.3	467.0
16:30	30.9	27.0	9.7	4.8	29.4	1005.3	457.0
16:35	30.9	28.0	10.3	1.6	29.6	1005.2	435.0
16:40	31.1	27.0	9.9	4.8	29.6	1005.1	404.0
16:45	31.1	26.0	9.3	6.4	29.4	1005.0	121.0
16:50	30.7	26.0	9.0	4.8	29.2	1005.1	81.0
16:55	30.4	28.0	9.9	4.8	29.3	1005.0	99.0
17:00	30.5	29.0	10.5	4.8	29.4	1005.0	192.0
17:05	30.4	28.0	9.9	6.4	29.3	1005.0	309.0
17:10	30.4	28.0	9.8	6.4	29.2	1005.0	327.0

17:15	30.5	30.0	11.0	3.2	29.5	1005.0	317.0
17:20	30.7	28.0	10.1	1.6	29.4	1005.0	302.0
17:25	30.8	28.0	10.2	3.2	29.5	1005.0	284.0
17:30	30.9	27.0	9.7	3.2	29.4	1005.0	263.0
17:35	30.7	25.0	8.4	4.8	29.2	1005.0	247.0
17:40	30.4	24.0	7.6	6.4	28.9	1005.1	225.0
17:45	30.3	26.0	8.6	4.8	28.9	1005.0	207.0
17:50	30.1	27.0	9.1	6.4	28.8	1005.0	191.0
17:55	29.9	27.0	8.9	4.8	28.7	1005.0	172.0
18:00	29.7	27.0	8.7	4.8	28.4	1005.0	154.0
18:05	29.6	27.0	8.6	4.8	28.3	1005.1	136.0
18:10	29.4	27.0	8.5	3.2	28.2	1005.1	120.0
18:15	29.4	27.0	8.4	3.2	28.1	1005.1	103.0
18:20	29.3	27.0	8.3	3.2	28.0	1005.1	86.0
18:25	28.9	28.0	8.6	4.8	27.8	1005.1	58.0
18:30	28.6	28.0	8.3	4.8	27.3	1005.2	33.0
18:35	28.3	29.0	8.5	3.2	27.1	1005.1	28.0
18:40	28.0	29.0	8.3	1.6	26.8	1005.1	25.0
18:45	27.8	29.0	8.1	0.0	26.7	1005.0	22.0
18:50	27.4	30.0	8.3	0.0	26.3	1005.0	19.0
18:55	27.1	31.0	8.5	0.0	26.0	1005.0	16.0
19:00	26.7	31.0	8.2	0.0	25.7	1005.0	13.0
19:05	26.2	32.0	8.2	0.0	25.3	1004.9	9.0
19:10	25.4	34.0	8.4	0.0	24.7	1004.9	6.0
19:15	24.7	35.0	8.2	0.0	24.1	1004.9	1.0
19:20	23.9	37.0	8.3	0.0	23.3	1004.8	0.0
19:25	23.2	38.0	8.1	1.6	22.5	1004.8	0.0
19:30	22.6	39.0	7.9	1.6	21.7	1004.8	0.0
19:35	21.9	40.0	7.7	1.6	20.7	1004.8	0.0

19:40	21.4	41.0	7.6	1.6	20.1	1004.8	0.0
19:45	21.0	42.0	7.6	1.6	19.7	1004.8	0.0
19:50	20.6	43.0	7.5	1.6	19.4	1004.8	0.0
19:55	20.2	45.0	7.9	1.6	19.2	1004.8	0.0
20:00	20.1	45.0	7.7	1.6	19.1	1004.8	0.0
20:05	19.8	46.0	7.9	0.0	18.9	1004.8	0.0
20:10	19.7	47.0	8.0	0.0	18.7	1004.9	0.0
20:15	19.5	48.0	8.2	0.0	18.6	1005.0	0.0
20:20	19.3	48.0	8.0	0.0	18.4	1005.0	0.0
20:25	19.3	49.0	8.3	0.0	18.4	1005.1	0.0
20:30	19.3	49.0	8.3	1.6	18.4	1005.1	0.0
20:35	19.2	49.0	8.2	1.6	18.3	1005.1	0.0
20:40	18.9	50.0	8.3	0.0	18.1	1005.1	0.0
20:45	18.8	51.0	8.5	1.6	18.0	1005.2	0.0
20:50	18.7	52.0	8.6	1.6	17.9	1005.2	0.0
20:55	18.4	53.0	8.7	1.6	17.7	1005.2	0.0
21:00	18.6	55.0	9.3	1.6	17.9	1005.3	0.0
21:05	18.9	56.0	10.0	1.6	18.4	1005.2	0.0
21:10	19.5	55.0	10.2	1.6	19.0	1005.3	0.0
21:15	19.8	55.0	10.5	0.0	19.3	1005.3	0.0
21:20	19.9	54.0	10.3	1.6	19.4	1005.4	0.0
21:25	19.9	55.0	10.6	1.6	19.4	1005.3	0.0
21:30	19.9	55.0	10.6	1.6	19.4	1005.3	0.0
21:35	19.9	56.0	10.9	1.6	19.6	1005.3	0.0
21:40	20.2	57.0	11.4	1.6	19.8	1005.3	0.0
21:45	20.4	58.0	11.8	3.2	20.0	1005.3	0.0
21:50	20.7	57.0	11.9	1.6	20.2	1005.3	0.0
21:55	20.9	58.0	12.4	4.8	20.4	1005.4	0.0
22:00	21.2	58.0	12.6	4.8	20.6	1005.3	0.0

22:05	21.2	58.0	12.6	4.8	20.7	1005.4	0.0
22:10	21.1	59.0	12.8	4.8	20.6	1005.4	0.0
22:15	21.0	59.0	12.7	4.8	20.5	1005.4	0.0
22:20	20.9	59.0	12.6	4.8	20.4	1005.4	0.0
22:25	20.7	60.0	12.7	3.2	20.3	1005.5	0.0
22:30	20.6	61.0	12.8	4.8	20.3	1005.5	0.0
22:35	20.3	61.0	12.6	4.8	20.1	1005.5	0.0
22:40	20.2	62.0	12.7	1.6	20.1	1005.6	0.0
22:45	20.0	63.0	12.7	3.2	20.0	1005.5	0.0
22:50	19.8	63.0	12.6	1.6	19.8	1005.5	0.0
22:55	19.7	64.0	12.7	3.2	19.7	1005.5	0.0
23:00	19.6	64.0	12.6	3.2	19.5	1005.5	0.0
23:05	19.4	64.0	12.5	3.2	19.4	1005.5	0.0
23:10	19.3	65.0	12.6	4.8	19.3	1005.5	0.0
23:15	19.3	65.0	12.6	4.8	19.3	1005.4	0.0
23:20	19.2	66.0	12.7	3.2	19.2	1005.3	0.0
23:25	19.2	66.0	12.7	3.2	19.2	1005.4	0.0
23:30	19.1	66.0	12.6	3.2	19.0	1005.4	0.0
23:35	18.9	66.0	12.4	1.6	18.9	1005.5	0.0
23:40	18.8	66.0	12.3	1.6	18.7	1005.4	0.0
23:45	18.7	66.0	12.2	0.0	18.6	1005.5	0.0
23:50	18.6	67.0	12.3	1.6	18.5	1005.7	0.0
23:55	18.4	67.0	12.2	0.0	18.3	1005.7	0.0

Table 0.24. *Temperature (oC) data of RUN160818 for September 2017. T1, T2, T3 and T4 show number of tubes counted from bottom.*

Time	**T1**	**T2**	**T3**	**T4**	**Time**	**T1**	**T2**	**T3**	**T4**
0:11	12.5	12.9	12.7	11.7	12:11	34.4	27.7	26.8	29.0
0:26	12.1	12.5	12.4	11.2	12:26	33.8	29.6	26.8	29.8
0:41	11.9	12.3	12.1	11.0	12:41	35.0	28.3	26.8	29.6
0:56	11.5	11.9	11.7	10.6	12:56	35.5	29.8	28.0	29.7
1:11	11.4	11.6	11.5	10.4	13:11	34.8	31.0	28.6	29.5
1:26	11.3	11.6	11.4	10.3	13:26	34.5	29.8	28.4	29.0
1:41	10.9	11.2	11.1	10.0	13:41	38.6	29.4	32.8	31.7
1:56	10.8	11.0	10.8	9.8	13:56	37.4	28.9	29.4	30.9
2:11	10.6	10.9	10.8	9.6	14:11	35.5	27.8	28.7	30.2
2:26	10.5	10.6	10.5	9.4	14:26	34.5	29.3	30.9	30.8
2:41	10.5	10.5	10.4	9.3	14:41	39.0	27.9	29.3	30.1
2:56	10.6	10.5	10.4	9.4	14:56	35.0	30.6	29.0	30.1
3:11	10.6	10.6	10.5	9.5	15:11	38.8	30.3	31.4	30.1
3:26	10.6	10.5	10.5	9.4	15:26	39.0	31.8	29.8	30.1
3:41	10.4	10.5	10.3	9.4	15:41	39.2	29.2	29.3	30.0
3:56	10.1	10.2	10.1	9.0	15:56	36.3	27.5	29.9	29.4
4:11	10.2	10.1	10.0	9.0	16:11	36.4	28.0	32.2	31.7
4:26	10.0	10.0	9.8	8.9	16:26	35.5	27.6	29.6	30.4
4:41	10.0	9.9	9.8	8.9	16:41	35.2	28.1	29.1	30.5
4:56	9.8	9.8	9.7	8.7	16:56	35.6	30.6	28.9	30.5
5:11	9.4	9.6	9.4	8.4	17:11	35.5	30.4	28.5	29.9
5:26	9.4	9.5	9.4	8.3	17:26	37.4	30.2	31.2	30.5
5:41	9.2	9.3	9.2	8.1	17:41	37.2	29.2	29.8	29.6
5:56	9.0	9.1	9.0	8.0	17:56	34.3	30.8	28.8	29.9
6:11	9.2	9.1	8.9	8.0	18:11	35.7	27.9	30.8	29.9
6:26	9.6	9.3	9.2	8.3	18:26	33.3	28.5	30.3	29.2

6:41	10.4	9.8	9.6	8.8	18:41	30.0	27.4	28.5	27.3
6:56	11.1	10.5	10.4	9.5	18:56	27.3	26.0	26.6	25.4
7:11	12.4	11.6	11.5	10.5	19:11	24.8	24.7	24.7	23.5
7:26	16.2	14.1	13.4	11.4	19:26	23.4	24.1	23.0	22.0
7:41	19.2	16.3	16.0	16.0	19:41	21.9	23.8	21.8	20.7
7:56	23.1	20.4	19.8	18.5	19:56	20.7	23.3	21.0	19.8
8:11	24.8	21.5	21.3	20.9	20:11	20.0	22.7	20.2	19.2
8:26	28.3	24.6	23.6	22.6	20:26	19.6	22.0	19.7	18.8
8:41	30.5	27.9	27.1	25.9	20:41	19.3	21.6	19.4	18.4
8:56	26.9	26.7	26.4	26.0	20:56	19.4	21.3	19.3	18.3
9:11	30.5	30.4	28.1	26.1	21:11	19.2	20.9	19.2	18.0
9:26	28.7	30.5	30.8	29.8	21:26	18.8	20.7	18.9	17.7
9:41	29.8	31.2	31.6	30.4	21:41	18.8	20.7	18.8	17.5
9:56	30.1	27.5	28.2	30.7	21:56	19.7	21.1	19.1	17.8
10:11	32.1	24.4	24.3	30.5	22:11	20.4	20.9	19.4	18.3
10:26	34.3	28.7	27.7	29.9	22:26	20.7	20.6	19.8	18.6
10:41	36.3	27.9	26.8	30.2	22:41	21.7	20.0	20.5	19.2
10:56	34.0	25.7	25.4	31.9	22:56	22.0	19.3	21.0	19.7
11:11	36.8	29.1	26.8	30.7	23:11	22.0	18.7	21.2	19.9
11:26	33.0	29.9	28.7	30.7	23:26	22.0	18.2	21.3	20.1
11:41	33.4	26.7	29.0	31.2	23:41	21.7	17.7	21.3	20.0
11:56	33.1	27.5	28.0	31.8	23:56	20.8	17.2	20.7	19.4

L. Indoor Experiments

Table 0.25. *Content and given name to the reactors of RUN150718.*

Name	Reactor #	Molasses (mM)	C/N	Glutamate (mM)
A.1	1 & 2	2	15	2.40
B.1	3 & 4	2	30	0.96
C.1	5 & 6	2	45	0.60
D.1	7 & 8	5	15	6.00
E.1	9 & 10	5	30	2.40
F.1	11 & 12	5	45	1.50
G.1	13 & 14	10	15	12.00
H.1	15 & 16	10	30	4.80
I.1	17 & 18	10	45	3.00

Table 0.26. *OD variation of RUN150718 for 18 reactors.*

Time (h)	**OD (660 nm)**																	
0	0.489	0.580	0.466	0.460	0.517	0.463	0.591	0.564	0.500	0.513	0.484	0.484	0.527	0.560	0.555	0.530	0.568	0.563
24	1.368	1.378	1.015	1.026	0.960	0.934	1.649	1.592	1.477	1.628	1.365	1.374	1.432	1.702	1.543	1.477	1.568	1.696
48	1.335	1.191	0.940	0.958	0.843	0.951	1.832	1.790	1.512	1.607	1.274	1.332	1.412	1.591	1.554	1.607	1.629	1.834
72	0.819	0.815	0.947	0.930	0.867	0.809	1.385	1.530	1.460	1.453	1.243	1.364	1.650	1.651	1.627	1.363	1.254	1.332
96	0.535	0.535	0.887	0.858	0.787	0.684	0.920	0.968	1.390	1.429	1.164	1.225	1.283	1.426	1.359	1.350	1.268	1.031
120	0.602	0.624	0.738	0.648	0.687	0.715	0.858	0.768	0.926	0.962	1.269	1.363	1.301	1.302	1.330	1.233	1.238	1.277
Reactor #	1	2	3	4	5	6	7	8	9	10	11	12	13	14	15	16	17	18

Table 0.27. *Dry cell weight of RUN150718 for 18 reactors.*

Time (h)	**Dry cell weight (g/L)**																	
0	0.228	0.270	0.217	0.214	0.241	0.216	0.275	0.263	0.233	0.239	0.225	0.225	0.245	0.261	0.258	0.247	0.264	0.262
24	0.637	0.642	0.473	0.478	0.447	0.435	0.768	0.741	0.688	0.758	0.636	0.640	0.667	0.792	0.718	0.688	0.730	0.790
48	0.622	0.555	0.438	0.446	0.393	0.443	0.853	0.833	0.704	0.748	0.593	0.620	0.657	0.741	0.724	0.748	0.758	0.854
72	0.381	0.379	0.441	0.433	0.404	0.377	0.645	0.712	0.680	0.677	0.579	0.635	0.768	0.769	0.758	0.635	0.584	0.620
96	0.249	0.249	0.413	0.399	0.366	0.318	0.428	0.451	0.647	0.665	0.542	0.570	0.597	0.664	0.633	0.629	0.590	0.480
120	0.280	0.291	0.344	0.302	0.320	0.333	0.399	0.358	0.431	0.448	0.591	0.635	0.606	0.606	0.619	0.574	0.576	0.595
Reactor #	1	2	3	4	5	6	7	8	9	10	11	12	13	14	15	16	17	18

Table 0.28. *Average dry cell weight of RUN150718.*

Time (h)	**Average dry cell weight (g/L)**								
0	0.249	0.216	0.228	0.269	0.236	0.225	0.253	0.253	0.263
24	0.639	0.475	0.441	0.755	0.723	0.638	0.730	0.703	0.760
48	0.588	0.442	0.418	0.843	0.726	0.607	0.699	0.736	0.806
72	0.380	0.437	0.390	0.679	0.678	0.607	0.768	0.696	0.602
96	0.249	0.406	0.342	0.440	0.656	0.556	0.631	0.631	0.535
120	0.285	0.323	0.326	0.379	0.440	0.613	0.606	0.597	0.585
Reactor name	A.1	B.1	C.1	D.1	E.1	F.1	G.1	H.1	I.1

Table 0.29. *pH variation of RUN150718 for 18 reactors.*

Time (h)	**pH**																	
0	7.30	7.34	7.37	7.37	7.40	7.39	7.43	7.43	7.40	7.24	7.35	7.35	7.33	7.36	7.32	7.33	7.37	7.36
24	7.02	7.05	6.98	6.98	6.99	7.04	6.74	6.68	6.59	6.57	6.53	6.56	5.8	5.72	5.66	5.66	5.71	5.81
48	7.08	7.13	7.01	6.99	6.99	7.04	6.92	6.83	6.62	6.66	6.57	6.56	5.9	5.88	5.79	5.86	5.74	5.76
72	7.19	7.22	7.08	7.07	7.04	7.13	7.00	6.92	6.73	6.69	6.58	6.54	5.89	6.03	5.87	5.88	5.91	5.93
96	6.81	6.83	7.01	7.02	7.05	7.05	6.93	6.87	6.70	6.77	6.58	6.58	6.07	6.18	6.02	6.02	6.03	6.06
120	7.12	7.15	7.08	7.11	7.05	7.15	6.95	6.91	6.78	6.82	6.73	6.68	6.39	6.32	6.28	6.2	6.22	6.31
Reactor #	1	2	3	4	5	6	7	8	9	10	11	12	13	14	15	16	17	18

Table 0.30. *Average pH variation of RUN150718.*

Time	**Average pH**								
0	7.32	7.37	7.40	7.43	7.32	7.35	7.35	7.33	7.37
24	7.04	6.98	7.02	6.71	6.58	6.55	5.76	5.66	5.76
48	7.11	7.00	7.02	6.88	6.64	6.57	5.89	5.83	5.75
72	7.21	7.08	7.09	6.96	6.71	6.56	5.96	5.88	5.92
96	6.82	7.02	7.05	6.90	6.74	6.58	6.13	6.02	6.05
120	7.14	7.10	7.10	6.93	6.80	6.71	6.36	6.24	6.27
Reactor name	A.1	B.1	C.1	D.1	E.1	F.1	G.1	H.1	I.1

Table 0.31. *Hourly average H2 percentage of RUN150718.*

Time	**Average H_2 %**								
0	0.0	0.0	0.0	0.0	0.0	0.0	0.0	0.0	0.0
24	85.4	86.0	85.4	68.9	76.6	78.9	57.2	58.7	59.5
48	63.8	78.0	72.4	65.9	68.7	68.2	33.3	43.0	46.8
72	37.4	77.9	42.2	41.4	68.8	68.6	27.9	38.7	44.9
96	12.0	5.7	13.9	15.0	10.5	43.0	11.7	11.5	12.4
120	6.3	7.9	3.0	6.8	0.8	6.1	6.3	4.2	7.3
Reactor name	A.1	B.1	C.1	D.1	E.1	F.1	G.1	H.1	I.1

Table 0.32. *Hourly average CO2 percentage of RUN150718.*

Time	**Average CO_2 %**								
0	0.0	0.0	0.0	0.0	0.0	0.0	0.0	0.0	0.0
24	14.6	14.0	14.6	31.1	23.4	23.4	42.8	41.3	40.5
48	36.2	22.0	27.6	34.1	31.3	31.3	66.7	57.0	53.2
72	62.6	22.1	57.8	58.6	31.2	31.2	72.1	61.3	55.1
96	88.0	94.3	86.1	85.0	89.5	89.5	88.3	88.5	87.6
120	93.7	92.1	97.0	93.2	99.2	99.2	93.7	95.8	92.7
Reactor name	A.1	B.1	C.1	D.1	E.1	F.1	G.1	H.1	I.1

Table 0.33. *Hourly average produced biogas of RUN150718.*

Time	**Produced biogas (ml)**								
0	0.0	0.0	0.0	0.0	0.0	0.0	0.0	0.0	0.0
24	16.5	15.7	17.4	19.4	18.3	22.1	25.7	24.7	24.5
48	3.9	13.7	10.8	12.3	21.3	24.5	7.6	9.8	16.3
72	0.0	2.7	0.5	1.8	6.1	11.7	2.6	2.2	3.5
96	0.0	1.4	0.0	1.7	1.3	6.3	2.8	4.3	4.1
120	0.0	0.8	0.0	2.1	2.5	2.3	2.2	1.9	5.3
Total (ml)	20.4	34.2	28.7	37.3	49.5	66.9	40.8	42.9	53.6
Reactor name	A.1	B.1	C.1	D.1	E.1	F.1	G.1	H.1	I.1

Table 0.34. *Cumulative average hydrogen and average productivity of RUN150718.*

Time (h)	**Average cumulative H_2 (mmol)**								
0	0.000	0.000	0.000	0.000	0.000	0.000	0.000	0.000	0.000
24	0.567	0.543	0.581	0.532	0.563	0.701	0.593	0.583	0.586
48	0.685	0.973	0.890	0.860	1.152	1.374	0.706	0.749	0.892
72	0.685	1.055	0.904	0.891	1.324	1.697	0.737	0.784	0.955
96	0.685	1.060	0.904	0.901	1.330	1.807	0.752	0.804	0.976
120	0.685	1.062	0.904	0.906	1.330	1.812	0.759	0.807	0.991
Productivity $molH_2/(m^3.h)$	0.228	0.354	0.301	0.302	0.443	0.604	0.253	0.269	0.330
Reactor name	A.1	B.1	C.1	D.1	E.1	F.1	G.1	H.1	I.1

Table 0.35. *Hourly average sucrose variation of RUN150718.*

Time (h)	**Sucrose (mM)**								
0	2.000	2.000	2.000	5.000	5.000	5.000	10.000	10.000	10.000
24	1.372	1.603	1.324	2.647	2.980	2.935	3.273	4.879	4.493
48	1.320	1.963	1.530	2.587	2.763	4.680	4.737	5.078	5.506
72	0.828	1.170	1.318	2.171	1.783	2.358	1.798	2.394	3.637
96	0.830	0.930	0.770	2.141	2.329	2.851	3.022	3.279	3.995
120	1.195	1.354	1.206	2.079	2.167	2.499	3.213	3.970	3.098
Reactor name	A.1	B.1	C.1	D.1	E.1	F.1	G.1	H.1	I.1

Table 0.36. *Hourly average lactic acid variation of RUN150718.*

Time (h)	**Lactic acid (mM)**								
0	0.014	0.014	0.014	0.014	0.014	0.014	0.014	0.014	0.014
24	0.014	0.014	0.014	0.592	1.130	0.866	2.092	2.642	2.230
48	0.014	0.014	0.014	0.014	0.014	0.441	0.975	0.624	1.823
72	0.014	0.084	0.083	0.201	0.014	0.014	0.014	0.014	0.150
96	0.316	0.067	0.227	0.158	0.041	0.235	0.079	0.117	0.184
120	0.188	0.048	0.996	0.014	0.014	0.014	0.014	0.014	0.014
Reactor name	A.1	B.1	C.1	D.1	E.1	F.1	G.1	H.1	I.1

Table 0.37. *Hourly average formic acid variation of RUN150718.*

Time (h)	**Formic acid (mM)**								
0	0.000	0.000	0.000	0.000	0.000	0.000	0.000	0.000	0.000
24	1.688	2.023	1.483	3.457	1.278	2.855	3.650	4.790	3.776
48	1.626	2.852	2.113	4.486	4.808	6.519	5.235	4.741	5.350
72	0.910	1.445	1.589	3.374	3.178	3.395	1.798	2.152	3.193
96	2.398	1.244	0.788	3.021	3.960	4.240	2.858	2.690	3.097
120	1.436	1.520	-0.022	3.014	4.074	4.202	1.896	2.422	1.644
Reactor name	A.1	B.1	C.1	D.1	E.1	F.1	G.1	H.1	I.1

Table 0.38. *Hourly average acetic acid variation of RUN150718.*

Time (h)	**Acetic acid (mM)**								
0	0.000	0.000	0.000	0.000	0.000	0.000	0.000	0.000	0.000
24	0.000	0.000	0.000	0.000	0.001	0.063	2.193	2.260	1.245
48	0.000	0.000	0.000	0.000	0.000	0.000	1.626	2.294	1.890
72	0.000	0.000	0.000	0.000	0.000	0.000	0.000	0.000	0.150
96	0.000	0.000	0.000	0.000	0.000	0.000	1.973	1.145	0.829
120	0.000	0.000	0.000	0.000	0.000	1.205	1.315	1.844	0.652
Reactor name	A.1	B.1	C.1	D.1	E.1	F.1	G.1	H.1	I.1

Table 0.39. *Hourly average propionic acid variation of RUN150718.*

Time (h)	**Propionic acid (mM)**								
0	1.004	0.950	0.945	1.250	1.039	1.261	1.856	1.825	1.702
24	1.027	0.862	1.051	1.207	1.130	1.349	1.791	1.335	1.424
48	0.827	0.447	0.807	1.823	1.905	1.345	8.347	9.553	7.303
72	1.737	1.232	0.987	1.614	2.463	3.497	9.777	9.940	8.029
96	2.016	2.278	2.813	1.258	2.008	1.918	6.576	4.716	5.804
120	1.419	1.056	0.947	1.356	1.023	4.410	1.490	1.519	1.514
Reactor name	A.1	B.1	C.1	D.1	E.1	F.1	G.1	H.1	I.1

Table 0.40. *Hourly average butyric acid variation of RUN150718.*

Time (h)	**Butyric acid (mM)**								
0	0.000	0.000	0.000	0.000	0.000	0.000	0.000	0.000	0.000
24	0.000	0.000	0.000	0.000	0.000	0.000	0.000	0.000	0.000
48	0.000	0.000	0.000	0.000	0.000	0.000	0.577	8.525	6.950
72	0.000	0.000	0.000	0.000	0.000	0.000	0.000	5.560	8.519
96	7.476	0.000	0.000	0.000	0.000	0.000	2.099	14.921	13.717
120	9.405	0.000	0.000	0.000	0.000	0.000	2.130	2.232	0.000
Reactor name	A.1	B.1	C.1	D.1	E.1	F.1	G.1	H.1	I.1

Table 0.41. *Content and given name to the reactors of RUN121118.*

	Reactor #	Molasses (mM)	C/N	Glutamate	L/D Cycle
A.2	1 & 2	5	15	6.0	√
B.2	3 & 4	5	30	2.4	√
C.2	5 & 6	5	45	1.5	√
D.2	7 & 8	5	15	6.0	x
E.2	9 & 10	5	30	2.4	x
F.2	11 & 12	5	45	1.5	x

Table 0.42. *OD variation of RUN121118 for 12 reactors.*

Time (h)	**OD at 660 nm**											
0	0.563	0.553	0.565	0.553	0.567	0.584	0.571	0.553	0.557	0.560	0.570	0.589
24	1.250	1.194	1.196	1.153	1.271	1.312	1.806	1.718	1.685	1.681	1.571	1.662
48	1.669	1.557	1.624	1.586	1.430	1.569	1.952	1.910	2.043	2.163	1.836	2.124
72	1.944	1.890	1.742	1.717	1.588	1.661	2.158	1.766	1.659	1.810	1.722	1.801
96	2.016	1.976	1.818	1.725	1.637	1.748	1.645	1.501	1.655	1.723	1.562	1.584
120	1.741	1.759	1.754	1.549	1.866	1.816	1.206	1.344	0.943	0.985	1.250	1.232
144	1.539	1.535	1.568	1.513	1.404	1.576	1.205	1.215	0.847	0.858	1.250	1.263
168	1.459	1.400	1.438	1.385	1.315	1.424	0.934	0.958	0.765	0.777	1.230	1.231
192	1.415	1.366	1.299	1.315	1.155	1.302	0.876	0.902	0.730	0.750	1.156	1.122
216	1.298	1.283	1.200	1.217	1.081	1.191	0.700	0.745	0.689	0.714	1.130	1.114
240	1.207	1.217	1.115	1.180	0.987	1.095	0.589	0.634	0.655	0.635	1.057	1.056
264	1.173	1.163	1.043	1.082	0.942	0.982	0.556	0.605	0.588	0.597	1.001	0.990
288	1.088	1.095	0.853	0.977	0.888	0.889	0.534	0.559	0.576	0.590	0.910	0.917
312	0.997	1.020	0.878	0.884	0.817	0.845	0.503	0.520	0.538	0.618	0.780	0.784
Reactor #	1	2	3	4	5	6	7	8	9	10	11	12

Table 0.43. *Dry cell weight of RUN121118 for 12 reactors.*

Time (h)	**Dry cell weight (g/l)**											
0	0.262	0.257	0.263	0.257	0.264	0.272	0.266	0.257	0.259	0.261	0.265	0.274
24	0.582	0.556	0.557	0.537	0.592	0.611	0.841	0.800	0.785	0.783	0.731	0.774
48	0.777	0.725	0.756	0.738	0.666	0.731	0.909	0.889	0.951	1.007	0.855	0.989
72	0.905	0.880	0.811	0.799	0.739	0.773	1.005	0.822	0.772	0.843	0.802	0.839
96	0.939	0.920	0.846	0.803	0.762	0.814	0.766	0.699	0.771	0.802	0.727	0.738
120	0.811	0.819	0.817	0.721	0.869	0.846	0.562	0.626	0.439	0.459	0.582	0.574
144	0.717	0.715	0.730	0.704	0.654	0.734	0.561	0.566	0.394	0.399	0.582	0.588
168	0.679	0.652	0.670	0.645	0.612	0.663	0.435	0.446	0.356	0.362	0.573	0.573
192	0.659	0.636	0.605	0.612	0.538	0.606	0.408	0.420	0.340	0.349	0.538	0.522
216	0.604	0.597	0.559	0.567	0.503	0.555	0.326	0.347	0.321	0.332	0.526	0.519
240	0.562	0.567	0.519	0.549	0.460	0.510	0.274	0.295	0.305	0.296	0.492	0.492
264	0.546	0.541	0.486	0.504	0.439	0.457	0.259	0.282	0.274	0.278	0.466	0.461
288	0.507	0.510	0.397	0.455	0.413	0.414	0.249	0.260	0.268	0.275	0.424	0.427
312	0.464	0.475	0.409	0.412	0.380	0.393	0.234	0.242	0.250	0.288	0.363	0.365
Reactor	1	2	3	4	5	6	7	8	9	10	11	12

Table 0.44. *Average dry cell weight of RUN121118.*

Time (h)	**Average dry cell weight (g/l)**					
0	0.260	0.260	0.268	0.262	0.260	0.270
24	0.569	0.547	0.601	0.820	0.784	0.753
48	0.751	0.747	0.698	0.899	0.979	0.922
72	0.893	0.805	0.756	0.914	0.808	0.820
96	0.929	0.825	0.788	0.732	0.786	0.732
120	0.815	0.769	0.857	0.594	0.449	0.578
144	0.716	0.717	0.694	0.563	0.397	0.585
168	0.666	0.657	0.638	0.440	0.359	0.573

192	0.647	0.609	0.572	0.414	0.345	0.530
216	0.601	0.563	0.529	0.336	0.327	0.522
240	0.564	0.534	0.485	0.285	0.300	0.492
264	0.544	0.495	0.448	0.270	0.276	0.464
288	0.508	0.426	0.414	0.254	0.271	0.425
312	0.470	0.410	0.387	0.238	0.269	0.364
Reactor name	A.2	B.2	C.2	D.2	E.2	F.2

Table 0.45. *pH variation of RUN121118*

Time (h)	**pH**											
0	7.43	7.43	7.44	7.43	7.44	7.43	7.43	7.43	7.44	7.43	7.44	7.44
24	7.26	7.33	7.31	7.37	7.33	7.31	7.11	7.09	7.08	7.08	7.04	7.02
48	7.21	7.26	7.23	7.21	7.18	7.14	7.02	6.92	6.70	6.71	6.70	6.68
72	6.95	6.98	6.92	6.92	6.90	6.87	6.90	6.86	6.72	6.70	6.65	6.75
96	6.83	6.81	6.63	6.65	6.63	6.67	6.77	6.74	6.60	6.62	6.44	6.48
120	6.71	6.71	6.65	6.48	6.45	6.57	6.68	6.70	6.55	6.54	6.56	6.51
144	6.61	6.67	6.58	6.52	6.48	6.52	6.58	6.59	6.50	6.50	6.48	6.48
168	6.61	6.61	6.49	6.45	6.39	6.43	6.59	6.59	6.45	6.46	6.50	6.51
192	6.64	6.64	6.49	6.46	6.36	6.47	6.66	6.65	6.46	6.48	6.49	6.51
216	6.62	6.65	6.50	6.42	6.38	6.31	6.56	6.54	6.40	6.41	6.45	6.44
240	6.82	6.72	6.66	6.58	6.52	6.54	6.68	6.70	6.50	6.48	6.57	6.58
264	6.83	6.75	6.65	6.63	6.47	6.50	6.60	6.62	6.50	6.50	6.50	6.51
288	6.72	6.68	6.53	6.49	6.40	6.48	6.49	6.51	6.47	6.46	6.50	6.50
312	6.72	6.71	6.53	6.49	6.42	6.50	6.60	6.62	6.55	6.56	6.57	6.59
Reactor #	1	2	3	4	5	6	7	8	9	10	11	12

Table 0.46. *Average pH variation of RUN121118.*

Time (h)	**Average pH**					
0	7.43	7.44	7.44	7.43	7.44	7.44
24	7.30	7.34	7.32	7.10	7.08	7.03
48	7.24	7.22	7.16	6.97	6.71	6.69
72	6.97	6.92	6.89	6.88	6.71	6.70
96	6.82	6.64	6.65	6.76	6.61	6.46
120	6.71	6.57	6.51	6.69	6.55	6.54
144	6.64	6.55	6.50	6.59	6.50	6.48
168	6.61	6.47	6.41	6.59	6.46	6.51
192	6.64	6.48	6.42	6.66	6.47	6.50
216	6.64	6.46	6.35	6.55	6.41	6.45
240	6.77	6.62	6.53	6.69	6.49	6.58
264	6.79	6.64	6.49	6.61	6.50	6.51
288	6.70	6.51	6.44	6.50	6.47	6.50
312	6.72	6.51	6.46	6.61	6.56	6.58
Reactor name	A.2	B.2	C.2	D.2	E.2	F.2

Table 0.47. *Hourly average H2 percentage of RUN121118.*

Time (h)	**H_2 %**					
0	0.0	0.0	0.0	0.0	0.0	0.0
24	94.5	95.2	91.3	90.6	91.2	90.4
48	88.7	97.3	91.3	86.9	83.0	84.1
72	85.5	86.2	84.2	83.7	80.8	74.5
96	85.0	80.7	90.6	79.7	81.6	73.4
120	86.9	82.7	91.2	78.5	79.6	72.8
144	80.9	77.7	100.0	78.5	79.6	72.8
168	77.8	76.8	75.6	78.5	79.6	72.8
192	75.6	75.5	73.6	78.5	79.6	72.8
216	73.5	75.6	73.6	78.5	79.6	74.2
240	73.7	73.7	73.7	78.5	79.6	75.2
264	69.1	70.5	75.1	78.5	79.6	75.2
288	69.4	64.6	72.1	78.5	79.6	75.2
312	69.4	64.6	72.1	78.5	79.6	75.2
Reactor name	A.2	B.2	C.2	D.2	E.2	F.2

Table 0.48. *Hourly average CO2 percentage of RUN121118.*

Time (h)	**CO_2 %**					
0	0.0	0.0	0.0	0.0	0.0	0.0
24	5.5	4.8	8.7	9.4	8.8	9.6
48	11.3	2.7	8.7	13.1	17.0	15.9
72	14.5	13.8	15.8	16.3	19.2	25.5
96	15.0	19.3	9.4	20.3	18.4	26.6
120	13.1	17.3	8.8	21.5	20.4	27.2
144	19.1	22.3	0.0	21.5	20.4	27.2

168	22.2	23.2	24.4	21.5	20.4	27.2
192	24.4	24.5	26.4	21.5	20.4	27.2
216	26.5	24.4	26.4	21.5	20.4	25.8
240	26.3	26.3	26.3	21.5	20.4	24.8
264	30.9	29.5	24.9	21.5	20.4	24.8
288	30.6	35.4	27.9	21.5	20.4	24.8
312	30.6	35.4	27.9	21.5	20.4	24.8
Reactor	A.2	B.2	C.2	D.2	E.2	F.2

Table 0.49. *Hourly average produced biogas of RUN150718.*

Time (h)	**Produced biogas (ml)**					
0	0.0	0.0	0.0	0.0	0.0	0.0
24	3.1	9.2	6.0	5.1	7.9	10.7
48	3.0	2.1	5.4	0.9	11.4	11.9
72	6.7	10.8	13.1	0.2	2.1	11.2
96	3.9	7.4	7.6	0.3	0.0	0.9
120	4.0	9.4	10.9	0.0	0.0	0.0
144	5.5	13.5	11.1	0.0	0.0	0.0
168	4.5	7.2	9.6	0.0	0.0	0.0
192	4.8	9.6	10.8	0.0	0.0	0.0
216	4.1	10.0	11.7	0.0	0.0	0.0
240	1.8	3.7	5.4	0.0	0.0	0.0
264	1.1	1.9	2.4	0.0	0.0	0.0
288	0.4	0.9	2.0	0.0	0.0	0.0
312	0.9	1.8	2.0	0.0	0.0	0.0
Total (ml)	43.8	87.5	98.0	6.5	21.4	34.7
Reactor name	A.2	B.2	C.2	D.2	E.2	F.2

Table 0.50. *Cumulative average hydrogen and average productivity of RUN121118.*

Time (h)	**Cumulative H_2 (mmol)**					
0	0.000	0.000	0.000	0.000	0.000	0.000
24	0.115	0.354	0.234	0.423	0.291	0.389
48	0.219	0.434	0.434	0.502	0.672	0.791
72	0.449	0.809	0.880	0.518	0.740	1.125
96	0.583	1.050	1.151	0.543	0.740	1.152
120	0.723	1.361	1.549	0.543	0.740	1.152
144	0.898	1.778	1.994	0.543	0.740	1.152
168	1.045	2.000	2.285	0.543	0.740	1.152
192	1.186	2.287	2.605	0.543	0.740	1.152
216	1.309	2.590	2.952	0.543	0.740	1.152
240	1.364	2.700	3.111	0.543	0.740	1.152
264	1.394	2.755	3.182	0.543	0.740	1.152
288	1.405	2.778	3.241	0.543	0.740	1.152
312	1.430	2.823	3.297	0.543	0.740	1.152
Productivity molH2/(m^3.h)	0.358	0.706	0.824	0.181	0.247	0.384
Reactor name	A.2	B.2	C.2	D.2	E.2	F.2

Table 0.51. *Hourly average sucrose and lactic variation of RUN121118.*

Time (h)	**Sucrose (mM)**					
0	5.000	5.000	5.000	5.000	5.000	5.000
24	4.490	4.613	4.449	3.417	3.779	3.311
48	3.630	3.848	2.765	2.360	2.704	2.712
72	3.139	3.605	3.077	1.926	2.551	2.673
96	2.642	3.590	2.460	2.657	2.530	2.480
120	2.561	3.573	1.924	2.307	3.002	2.224
144	2.114	2.784	2.658	2.490	2.698	2.174
168	1.884	2.804	2.446	2.479	2.573	1.998
192	1.895	1.882	1.816	2.097	2.299	1.943
216	1.384	1.694	1.791	1.265	1.944	1.371
240	2.272	1.989	1.956	1.848	1.794	1.868
264	1.523	1.894	1.681	1.665	1.777	1.716
288	1.694	1.577	1.581	1.642	1.510	1.357
312	1.714	1.247	1.469	1.668	1.734	1.389
Reactor name	A.2	B.2	C.2	D.2	E.2	F.2
Time (h)	**Lactic acid (mM)**					
0	0.476	0.449	0.467	0.586	0.541	0.556
24	0.171	0.145	0.238	0.014	0.355	0.210
48	0.014	0.014	0.014	1.195	0.642	2.325
72	2.089	2.992	0.493	1.359	0.388	0.191
96	1.407	1.905	1.438	2.698	0.701	0.390
120	1.082	0.361	0.014	0.332	0.615	0.149
144	0.845	0.264	0.271	0.812	1.265	0.014
168	1.029	0.467	0.368	0.869	0.521	0.293
192	0.910	0.139	0.374	0.424	0.611	0.202

216	0.684	1.980	2.139	1.558	1.996	1.642
240	1.058	2.953	2.822	0.964	0.161	3.301
264	0.783	0.022	0.386	0.460	0.099	0.029
288	0.896	0.086	0.234	0.422	0.143	0.065
312	0.835	0.014	0.014	0.441	0.131	0.039
Reactor name	A.2	B.2	C.2	D.2	E.2	F.2

Table 0.52. *Hourly average formic acid variation of RUN121118.*

Time (h)	**Formic acid (mM)**					
0	0.862	0.912	0.991	1.042	0.946	1.107
24	1.259	1.266	1.271	0.000	2.726	2.670
48	2.076	2.090	1.593	3.518	4.543	4.788
72	3.226	4.288	1.876	3.410	1.755	4.048
96	4.392	4.272	3.647	4.698	3.715	4.913
120	4.193	4.474	4.014	1.612	4.811	4.165
144	2.687	3.548	4.064	3.784	4.725	2.090
168	2.460	3.919	3.347	4.261	4.166	3.122
192	2.446	2.474	2.595	2.648	2.567	2.992
216	1.697	0.000	0.626	0.247	0.549	0.000
240	3.590	0.000	0.000	4.223	4.435	0.350
264	2.386	3.169	2.894	3.200	3.232	3.518
288	2.768	2.599	2.691	2.994	3.425	2.857
312	2.673	1.873	2.311	3.077	3.258	2.795
Reactor name	A.2	B.2	C.2	D.2	E.2	F.2

Table 0.53. *Hourly average acetic acid variation of RUN121118.*

Time (h)	**Acetic acid (mM)**					
0	0.000	0.000	0.000	0.000	0.000	0.000
24	0.000	0.000	0.000	2.254	0.000	0.000
48	0.000	0.000	0.000	0.000	0.000	0.000
72	0.000	3.374	0.000	0.000	0.000	0.000
96	0.000	0.000	0.000	0.000	0.000	0.000
120	0.000	0.000	0.000	3.949	0.284	0.000
144	0.000	0.000	0.000	0.000	0.756	6.541
168	0.000	0.000	0.000	0.000	0.126	0.000
192	0.000	0.000	0.000	0.000	0.000	0.000
216	0.000	0.965	0.000	0.000	0.000	0.000
240	0.000	0.000	0.000	0.000	0.000	0.000
264	0.000	0.000	0.000	0.000	0.000	0.000
288	0.000	0.000	0.000	0.000	0.000	0.000
312	0.000	0.000	0.000	0.000	0.000	0.000
Reactor name	A.2	B.2	C.2	D.2	E.2	F.2

Table 0.54. *Hourly average propionic acid variation of RUN121118.*

Time (h)	**Propionic acid (mM)**					
0	1.185	1.098	1.035	1.138	0.780	1.055
24	1.354	1.182	1.364	0.000	1.243	1.145
48	0.000	0.000	2.619	1.225	0.934	2.252
72	2.624	1.938	0.658	1.025	1.211	0.980
96	7.397	0.388	0.120	5.417	0.465	0.400
120	5.720	0.478	-0.218	3.883	0.233	0.541
144	0.214	0.703	0.362	1.908	0.692	1.133

168	0.098	0.124	0.444	1.972	1.063	1.896
192	7.790	0.087	0.869	2.913	2.245	2.397
216	1.132	0.000	0.000	1.173	0.898	0.835
240	10.313	2.584	0.572	0.000	0.000	4.343
264	9.662	1.892	1.570	0.799	0.570	0.631
288	8.262	2.371	1.342	1.791	1.018	0.714
312	9.211	2.416	2.371	0.703	0.737	0.660
Reactor name	A.2	B.2	C.2	D.2	E.2	F.2

Table 0.55. *Hourly average butyric acid variation of RUN121118.*

Time (h)	**Butyric acid (mM)**					
0	0.000	0.000	0.000	0.000	0.000	0.000
24	0.000	0.000	0.000	0.000	0.000	0.000
48	0.000	0.000	0.000	0.000	0.000	0.000
72	0.000	0.000	0.000	0.000	0.000	0.000
96	0.000	0.000	0.000	0.000	0.000	0.000
120	0.000	0.000	0.000	0.000	0.000	0.000
144	0.000	0.000	0.000	0.000	0.000	0.000
168	0.000	0.000	0.000	0.000	0.000	0.000
192	0.000	0.000	0.000	0.000	0.000	0.000
216	0.000	0.000	0.000	0.000	0.000	0.000
240	0.000	0.000	0.000	0.000	0.000	0.000
264	0.000	0.000	0.000	0.000	0.000	0.000
288	0.000	0.000	0.000	0.000	0.000	0.000
312	0.000	0.000	0.000	0.000	0.000	0.000
Reactor name	A.2	B.2	C.2	D.2	E.2	F.2

Table 0.56. *Content and given name to the reactors of RUN030419.*

Reactor name	**Reactor #**	**Molasses (mM)**	**C/N**	**Glutamate (mM)**	**pH control**
A	1 & 2	5	45	1.5	x
B	3 & 4	10	45	3	x
C	5 & 6	15	45	4.5	x
D	7 & 8	5	45	1.5	√
E	9 & 10	10	45	3	√
F	11 & 12	15	45	4.5	√

Table 0.57. *OD variation of RUN030419 for 12 reactors.*

Time (h)	**OD at 660 nm**											
0	0.563	0.553	0.565	0.553	0.567	0.584	0.571	0.553	0.557	0.560	0.570	0.589
24	1.250	1.194	1.196	1.153	1.271	1.312	1.806	1.718	1.685	1.681	1.571	1.662
48	1.669	1.557	1.624	1.586	1.430	1.569	1.952	1.910	2.043	2.163	1.836	2.124
72	1.944	1.890	1.742	1.717	1.588	1.661	2.158	1.766	1.659	1.810	1.722	1.801
96	2.016	1.976	1.818	1.725	1.637	1.748	1.645	1.501	1.655	1.723	1.562	1.584
120	1.741	1.759	1.754	1.549	1.866	1.816	1.206	1.344	0.943	0.985	1.250	1.232
144	1.539	1.535	1.568	1.513	1.404	1.576	1.205	1.215	0.847	0.858	1.250	1.263
168	1.459	1.400	1.438	1.385	1.315	1.424	0.934	0.958	0.765	0.777	1.230	1.231
192	1.415	1.366	1.299	1.315	1.155	1.302	0.876	0.902	0.730	0.750	1.156	1.122
Reactor #	1	2	3	4	5	6	7	8	9	10	11	12

Table 0.58. *Dry cell weight of RUN030419 for 12 reactors.*

Time (h)	**Dry cell weight (g/l)**											
0	0.114	0.111	0.181	0.177	0.227	0.153	0.121	0.102	0.141	0.155	0.158	0.156
24	0.487	0.469	0.515	0.533	0.616	0.637	0.580	0.521	0.590	0.629	0.649	0.656
48	0.560	0.566	0.564	0.562	0.592	0.676	0.579	0.591	0.675	0.643	0.692	0.646
72	0.526	0.543	0.592	0.560	0.540	0.574	0.538	0.538	0.669	0.657	0.683	0.729
96	0.562	0.554	0.588	0.616	0.505	0.544	0.519	0.538	0.744	0.739	0.728	0.768
120	0.559	0.555	0.636	0.599	0.472	0.506	0.487	0.502	0.736	0.731	0.802	0.804
144	0.516	0.506	0.623	0.598	0.458	0.484	0.454	0.458	0.720	0.708	0.792	0.839
168	0.504	0.494	0.634	0.594	0.436	0.467	0.472	0.388	0.697	0.697	0.788	0.817
192	0.469	0.480	0.565	0.541	0.433	0.433	0.460	0.300	0.612	0.593	0.703	0.757
Reactor #	1	2	3	4	5	6	7	8	9	10	11	12

Table 0.59. *Average dry cell weight of RUN030419.*

Time (h)	**Average dry cell weight (g/l)**					
0	0.112	0.179	0.190	0.111	0.148	0.157
24	0.478	0.524	0.626	0.551	0.610	0.652
48	0.563	0.563	0.634	0.585	0.659	0.669
72	0.534	0.576	0.557	0.538	0.663	0.706
96	0.558	0.602	0.524	0.528	0.741	0.748
120	0.557	0.617	0.489	0.495	0.734	0.803
144	0.511	0.610	0.471	0.456	0.714	0.816
168	0.499	0.614	0.452	0.430	0.697	0.802
192	0.474	0.553	0.433	0.380	0.602	0.730
Reactor	A.3	B.3	C.3	D.3	E.3	F.3

Table 0.60. *Average pH variation of RUN030419.*

Time (h)	**Average pH**					
0	7.29	7.24	7.24	7.34	7.27	7.26
24	6.60	6.01	5.56	7.03	6.95	7.00
48	6.44	5.92	5.34	6.97	6.97	6.97
72	6.52	6.04	5.50	6.96	6.94	7.07
96	6.57	6.22	5.55	6.94	6.93	6.96
120	6.61	6.37	5.59	7.01	6.95	6.95
144	6.47	6.32	5.73	7.00	6.99	6.98
168	6.52	6.38	5.82	6.98	7.04	6.95
192	6.55	6.42	5.83	7.08	7.01	6.99
Reactor name	A.3	B.3	C.3	D.3	E.3	F.3

Table 0.61. *Hourly average H2 percentage of RUN030419.*

Time (h)	**H_2 %**					
0	0.0	0.0	0.0	0.0	0.0	0.0
24	71.5	53.4	26.7	76.4	57.0	17.9
48	67.8	46.4	29.5	80.1	68.8	55.4
72	67.8	50.0	30.7	77.4	73.9	68.4
96	66.7	53.1	27.7	77.0	74.1	72.9
120	60.3	57.9	25.1	80.4	76.3	72.0
144	60.5	60.4	23.3	79.5	77.2	72.1
168	60.1	60.9	23.0	79.7	77.0	71.8
192	58.4	62.1	22.2	79.5	79.7	74.2
Reactor name	A.3	B.3	C.3	D.3	E.3	F.3

Table 0.62. *Hourly average CO2 percentage of RUN030419.*

Time (h)	**CO_2 %**					
0	0.0	0.0	0.0	0.0	0.0	0.0
24	28.5	46.6	73.3	23.6	43.0	82.1
48	32.2	53.6	70.5	19.9	31.2	44.6
72	32.2	50.0	69.3	22.6	26.1	31.6
96	33.3	46.9	72.3	23.0	25.9	27.1
120	39.7	42.1	74.9	19.6	23.7	28.0
144	39.5	39.6	76.7	20.5	22.8	27.9
168	39.9	39.1	77.0	20.3	23.0	28.2
192	41.6	37.9	77.8	20.5	20.3	25.8
Reactor name	A.3	B.3	C.3	D.3	E.3	F.3

Table 0.63. *Hourly average produced biogas of RUN030419.*

Time (h)	**Average daily produced biogas (ml)**					
0	0.0	0.0	0.0	0.0	0.0	0.0
24	7.3	10.9	9.2	13.5	11.0	3.3
48	12.7	11.2	9.3	19.6	19.4	17.0
72	7.2	3.6	4.3	10.4	27.3	20.2
96	1.3	3.7	0.8	2.0	10.3	23.0
120	0.7	1.6	0.2	1.4	6.4	15.4
144	0.4	0.2	0.0	0.0	1.4	8.1
168	0.0	0.0	0.0	1.8	0.0	0.8
192	0.0	0.0	0.0	0.0	0.0	0.0
Total (ml)	29.6	31.2	23.8	48.6	75.9	87.7
Reactor name	A.3	B.3	C.3	D.3	E.3	F.3

Table 0.64. *Cumulative average hydrogen and average productivity of RUN030419.*

Time (h)	**Cumulative average daily produced biogas (ml)**					
0	0.000	0.000	0.000	0.000	0.000	0.000
24	0.215	0.233	0.106	0.415	0.253	0.024
48	0.568	0.443	0.228	1.046	0.790	0.403
72	0.765	0.519	0.284	1.373	1.603	0.960
96	0.801	0.606	0.294	1.435	1.911	1.632
120	0.818	0.642	0.296	1.479	2.109	2.081
144	0.827	0.648	0.296	1.479	2.153	2.315
168	0.827	0.648	0.296	1.536	2.153	2.338
192	0.827	0.648	0.296	1.536	2.153	2.338
Productivity $molH_2/(m^3.l)$	0.359	0.216	0.099	0.512	0.718	0.779
Reactor	A.3	B.3	C.3	D.3	E.3	F.3

Table 0.65. *Hourly average sucrose variation of RUN030419*

Time (h)	**Sucrose (mM)**					
0	5.000	10.000	15.000	5.000	10.000	15.000
24	3.536	3.192	4.623	2.698	4.641	7.699
48	3.015	4.210	5.141	2.683	4.066	5.707
72	3.037	3.268	4.351	2.379	3.667	5.411
96	2.966	3.431	5.190	2.219	4.026	5.019
120	2.718	2.945	4.340	2.178	4.039	4.503
144	2.758	2.884	3.436	2.026	3.097	4.599
168	2.494	3.105	4.483	1.949	3.324	4.838
192	2.331	2.741	4.104	1.797	3.058	3.887
Reactor name	A.3	B.3	C.3	D.3	E.3	F.3

Table 0.66. *Hourly average lactic acid variation of RUN030419.*

Time (h)	**Lactic acid (mM)**					
0	0.477	0.796	1.126	0.743	0.754	0.014
24	2.148	4.705	6.639	2.158	5.071	9.144
48	0.014	2.061	5.068	0.990	1.582	2.152
72	0.014	0.014	0.014	0.014	0.014	0.135
96	0.014	0.014	0.067	0.014	0.014	0.123
120	0.014	3.109	2.990	0.442	0.250	0.014
144	0.132	0.392	2.300	0.103	0.265	0.424
168	0.127	0.422	2.052	0.320	0.248	0.329
192	0.084	0.244	0.827	0.147	0.318	0.309
Reactor	A.3	B.3	C.3	D.3	E.3	F.3

Table 0.67. *Hourly average formic acid variation of RUN030419.*

Time (h)	**Formic acid (mM)**					
0	0.428	0.598	1.092	0.370	0.814	0.000
24	1.042	0.829	0.000	1.978	1.417	0.000
48	2.719	2.064	1.322	3.010	4.298	4.995
72	4.016	1.252	4.538	0.390	0.192	0.614
96	0.000	0.000	4.954	0.000	0.093	0.000
120	0.051	3.286	1.180	2.581	7.646	0.209
144	3.680	3.495	0.610	2.391	6.214	7.795
168	3.416	3.957	0.582	1.528	7.031	9.349
192	3.505	3.523	0.580	0.000	6.552	7.513
Reactor	A.3	B.3	C.3	D.3	E.3	F.3

Table 0.68. *Hourly average acetic acid variation of RUN030419.*

Time (h)	**Acetic acid (mM)**					
0	0.014	1.173	0.000	1.003	0.719	0.000
24	5.076	15.192	20.433	5.858	18.104	0.588
48	0.319	26.970	25.626	5.060	0.000	11.725
72	0.000	0.000	0.000	0.000	0.000	0.000
96	0.000	0.000	0.000	0.000	0.000	0.000
120	0.000	0.000	0.000	0.000	0.000	0.000
144	0.000	0.000	0.000	0.000	0.000	0.000
168	0.000	0.000	0.048	0.000	0.000	0.000
192	0.000	0.000	0.329	0.204	0.000	0.000
Reactor	A.3	B.3	C.3	D.3	E.3	F.3

Table 0.69. *Hourly average propionic acid variation of RUN030419.*

Time (h)	**Propionic acid (mM)**					
0	0.174	0.348	0.606	1.388	1.194	0.000
24	1.310	1.075	0.811	1.121	0.983	1.877
48	1.158	0.000	0.201	0.739	0.883	0.907
72	1.024	0.837	0.545	0.545	0.807	3.502
96	1.242	0.298	0.489	0.000	0.832	1.104
120	1.207	1.092	0.826	0.769	1.006	1.105
144	0.896	1.068	0.963	0.783	1.294	1.073
168	0.000	0.700	0.741	0.902	1.021	0.499
192	0.732	0.729	0.987	0.729	0.987	0.861
Reactor name	A.3	B.3	C.3	D.3	E.3	F.3

Table 0.70. *Hourly average butyric acid variation of RUN030419.*

Time (h)	**Butyric acid (mM)**					
0	0.000	0.000	0.000	0.000	0.000	0.000
24	0.000	0.000	0.000	0.000	0.000	0.000
48	0.000	0.000	0.000	0.000	0.000	0.000
72	0.000	0.000	0.257	0.000	0.000	0.000
96	0.000	0.000	3.686	0.000	0.000	0.000
120	0.000	0.000	2.540	0.000	0.000	0.000
144	0.000	0.000	0.103	0.000	0.000	0.000
168	0.000	0.000	2.112	0.000	0.000	0.000
192	0.000	0.000	1.377	0.000	0.000	0.000
Reactor name	A.3	B.3	C.3	D.3	E.3	F.3

M. Sample Calculation

Sample Calculation for Productivity

Sample calculation was performed for RUN160818 on August 23, 2018. The produced biogas was 2322 ml, and hydrogen percentage was 82.86 %. The pressure was 0.9 atm and the average day time was 12.7 hours for August and September 2018 at Ankara.

$$V_{H_2} = (2322\ ml).\left(\frac{82.86}{100}\right) = 2072\ ml$$

$$n_{H_2} = \frac{P.V_{H_2}}{R.T}$$

$$n_{H_2} = \frac{(0.9\ atm).(2072\ ml)}{\left(82.05\ \frac{atm.ml}{mol.K}\right).303\ K}$$

$$n_{H_2} = 0.075\ mol$$

$$Productiviy = \frac{Hydrogen\ produced}{Reactor\ volume.Time}$$

$$Productiviy = \frac{0.075\ mol}{(20.10^{-3}\ m^3).(12.7\ h)}$$

$$Productiviy = 0.295\ \frac{mol}{m^3.h}$$

Sample Calculation for Substrate Coversion Efficiency

Sample calculation was performed for RUN160818 on August 23, 2018. On August 23, 2018 the sucrose concentration in molasses was measured by HPLC and adjusted to 5 mM by adding molasses in the morning. The sucrose was measured as 2.1 mM by HPLC at night August 23, 2018. Thus, the consumed sucrose was 2.9 mM.

$$Y_{H_2} = \frac{Produced\ hydrogen}{Theoretical\ hydrogen} x100$$

Theoretical hydrogen was calculated by assuming that all the substrate was used for hydrogen production. Theoretically, 24 mol hydrogen could be produced from 1 mol of sucrose.

$$Y_{H_2} = \frac{0.075\ mol}{2.9x10^{-3}\ mol\ x\ 24} x100$$

$Y_{H_2} = 107\ \%$**Sample Calculation for Light Conversion Efficiency**

Sample calculation for the light conversion efficiency for RUN160818 on August 23, 2018. The daily solar radiation was 475 W/m^2. Hydrogen density was 0.0899 kg/m^3 (8.99 x 10^{-5} g/ml). The irradiated area was 2.176 m^2.

$$\eta = \frac{V_{H_2} x \rho_{H_2} x 33.61}{IxAxt_{H_2}} x100$$

$$\eta = \frac{(2322\ ml)\ x\ \left(8.99x10^{-5}\frac{g}{ml}\right) x\ \left(33.61\frac{W.\mathrm{h}}{g}\right)}{(475\ W/m^2) x\ (2.176\ m^2)\ x\ (12.7\ \mathrm{h})} x100$$

$$\eta = 0.043\ \%$$

N. Carbon Balance

Carbon balance between 18th and 23rd days of RUN160818.

Hydrogen production was not observed, although sucrose consumption continued for days between 18-23 of RUN160818 that is outdoor experiment with pH control system. Thus, carbon balance is performed to understand the consumed and produced C amount.

- Sucrose consumption

Table 0.71. *Consumed sucrose of RUN160818.*

Consumed Sucrose (mM)	Consumed Carbon of Sucrose (mM)	Day
3.1	36.92	18
3.2	38.53	19
3.2	38.13	20
3.4	40.30	21
3.3	39.28	22
3.3	39.29	23
Total	232.45	

Total consumed carbon from sucrose is 232.45 · 20 L = 4649 mmol

- Produced Carbon of Organic Acids (mM)

Day 18th day at night 197.02

Day 23th at night 292.55

Accumulated organic acids

(292.55 - 197.02) mM·20L = 1910.6 mmol

- CO2 dissolved

Table 0.72. *Produced carbon dioxide percentage of RUN160818.*

CO_2 %	Day
0.09	18
0.00	19
0.00	20
0.00	21
0.00	22
0.15	23

Average carbon dioxide percentage is 0.04.

Henry's law constants for CO_2 = 1.63 X 10^3 atm (Tosun 2012)

$$y \cdot P = H \cdot x$$

$$0.04 \cdot 0.9 = 1630 \cdot \frac{n_{CO_2}}{n_{CO_2} + \frac{1000}{18}}$$

$$n_{CO_2} + \frac{1000}{18} \cong \frac{1000}{18}$$

$$x_{CO_2} = \frac{0.04\ x\ 0.9\ atm}{1630\ atm}\ x\ \frac{1000}{18}\ \frac{g}{\frac{g}{mol}}$$

$$x_{CO_2} = 0.00123 \frac{mol}{L}$$

$$n_{CO_2} = 1.23\ mM \cdot 20\ L$$

$$n_{CO_2} = 24.6\ mmol$$

Total carbon from CO_2(aq) + HCO_3^- (carbonate ≅ 0):

24.6 mmol CO_2 + 4 mmol HCO_3^-/mmol CO_2 *24.6 mmol $CO_2$5 mmol = 123 mmol

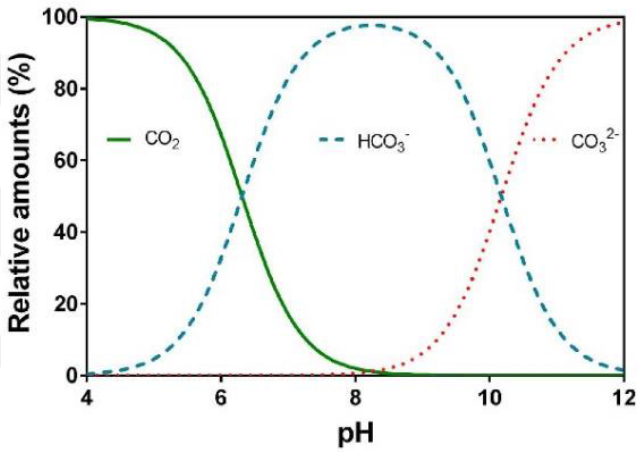

- C from bacteria

Molecular weight of the bacteria according to molecular formula $CH_{1.7}O_{0.45}N_{0.4}$ (Hoekema, 2006) is 22.86 g/mol.

Dry cell weight of the bacteria at 18th day of RUN160818 at night is 0.87 g/l.

Dry cell weight of the bacteria at 23rd day of RUN160818 at night is 1.02 g/l.

$$n_{C_{bacteria}} = \frac{(1.02 - 0.87) g/l}{22.86 \frac{g}{mol}} \cdot 1000 \cdot 20\ L\ mmol$$

$$n_{C_{bacteria}} = 131.23\ mmol$$

- C from CO_2 (gas)

Table 0.73. *Produced carbon dioxide mol of RUN160818.*

C mol of CO_2	Day
0.00	18
0.01	19
0.01	20
0.00	21
0.00	22
0.01	23

Total carbon dioxide at gas phase is 0.03 mol.

$$n_{CO_2(gas)} = 0.03 \cdot 1000 = 30\ mmol$$

As a result, total consumed carbon from sucrose is 4649 mmol and total produced carbon is 2096 mmol. %45 consumed carbon can be calculated and rest is attributed to side product production such as PHB